m p rogers & associates pl ABN 14 062 681 252
creating better coasts and ports

R1518 Rev 0

January 2023

Department of Transport

Tantabiddi Creek
Coastal Processes Study

marinas
boat harbours
canals
breakwaters
jetties
seawalls
dredging
reclamation
climate change
waves
currents
tides
flood levels
water quality
siltation
erosion
rivers
beaches
estuaries

www.coastsandports.com.au

m p rogers & associates pl
creating better coasts and ports

Suite 1, 128 Main Street, Osborne Park, WA 6017
p: +618 9254 6600
e: admin@coastsandports.com.au
w: www.coastsandports.com.au

K1870, Report R1518 Rev 0
Record of Document Revisions

Rev	Purpose of Document	Prepared	Reviewed	Approved	Date
A	Sections 1-4 Issued for DoT Review	M Peterson	L De Lucia	C Doak	24/3/2021
B	Updated with DoT comments on sections 1-4	M Peterson	L De Lucia	C Doak	23/4/2021
C	Sections 5-12 added & issued for DoT Review	L De Lucia	C Doak	C Doak	10/2/2022
D	Updated with DoT Comments on Sections 11 & 12	C Doak	M Peterson	C Doak	1/4/2022
E	Updated to Include Concept C	M Peterson	C Doak	C Doak	14/11/2022
0	Issued to Client	M Peterson	C Doak	C Doak	17/01/2023

Form 035 18/06/2013

Limitations of this Document

This document has been prepared for use by the Client in accordance with the agreement between the Client and M P Rogers & Associates Pty Ltd. This agreement includes constraints on the scope, budget and time available for the services. The consulting services and this document have been completed with the degree of skill, care and diligence normally exercised by members of the engineering profession performing services of a similar nature. No other warranty, expressed or implied, is made as to the accuracy of the data and professional advice included. This document has not been prepared for use by parties other than the Client and its consulting advisers. It may not contain sufficient information for the purposes of other parties or for other uses.

M P Rogers & Associates takes no responsibility for the completeness or form of any subsequent copies of this document. Copying this document without the permission of the Client or M P Rogers & Associates Pty Ltd is not permitted.

Table of Contents

Table of Figures

Table of Tables

Acknowledgment of Country

M P Rogers & Associates and the Department of Transport would like to acknowledge the traditional custodians of the land to which this investigation relates, the Jinigudira people. We pay our respects to Elders both past, present and emerging for they hold the memories, the traditions, the culture and the hope of their people.

1. Introduction

1.1 Background

The Tantabiddi Boat Ramp precinct is of regional significance and is a key asset as a gateway to the Ningaloo Reef tourism and recreational experiences. The Shire of Exmouth (Shire) and the Department of Biodiversity, Conservation and Attractions (DBCA) jointly manage the Tantabiddi land and marine environment under the governance of the Jurabi and Bundegi Coastal Parks and Muiron Island Management Plan 1999. Both agencies manage civil maintenance, environmental maintenance, and preservation programs, though the Shire generally maintains the boat ramp infrastructure. The location of the boat ramp in the context of the North West Cape is shown in in Figure 1.1 below.

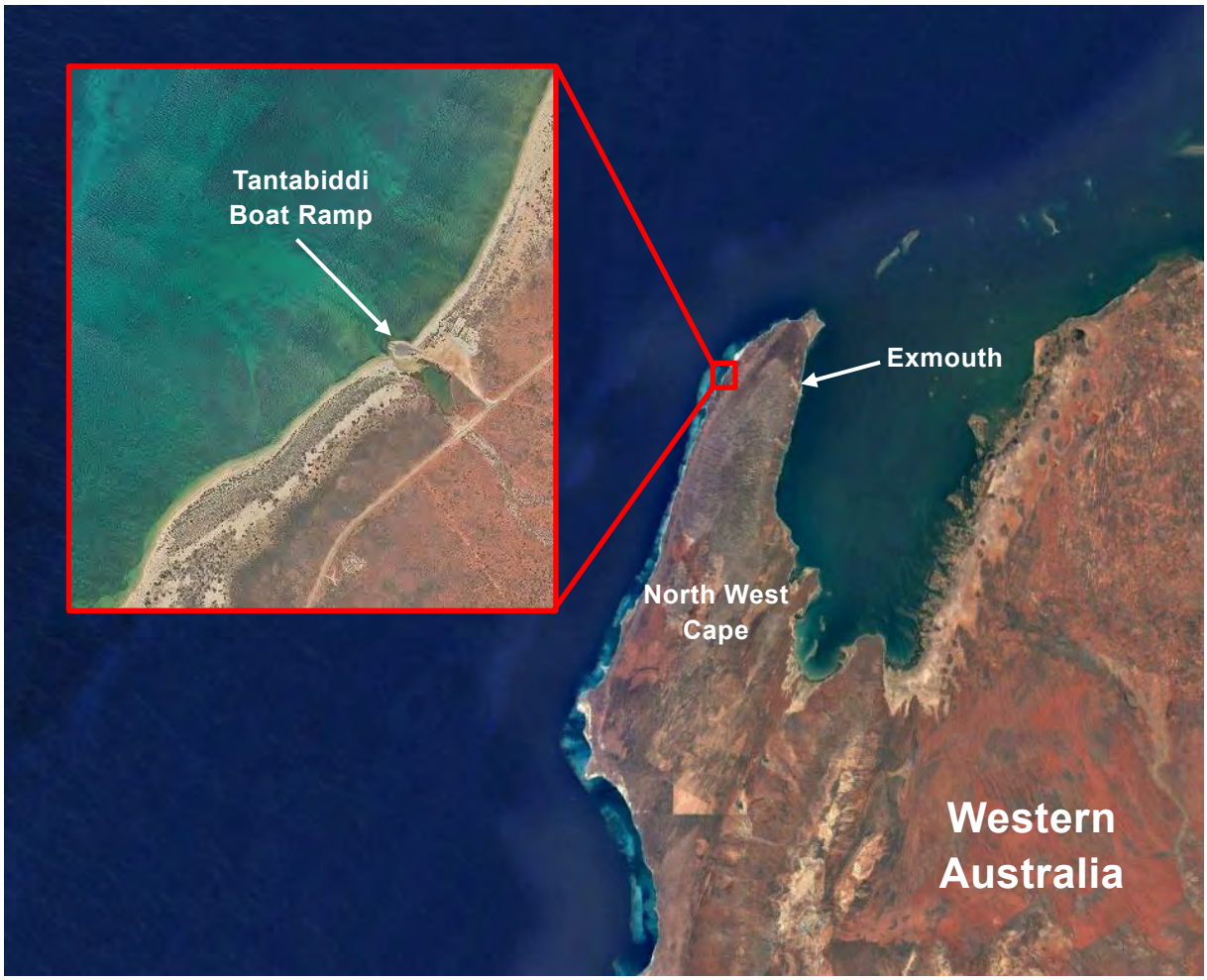

Figure 1.1 Location Plan

To address capacity limitations and maintenance issues associated with the existing Tantabiddi ramp, the Department of Transport (DoT) in collaboration with the Shire, DBCA, Department of Primary Industries and Regional Development (DPIRD), and Tourism WA have resolved to identify the planning, investigations and approvals necessary to develop a new facility at Tantabiddi.

This has involved the development of a preliminary concept for the Tantabiddi Boating Facility (TBF), shown in Figure 1.2, which is known as Concept B.

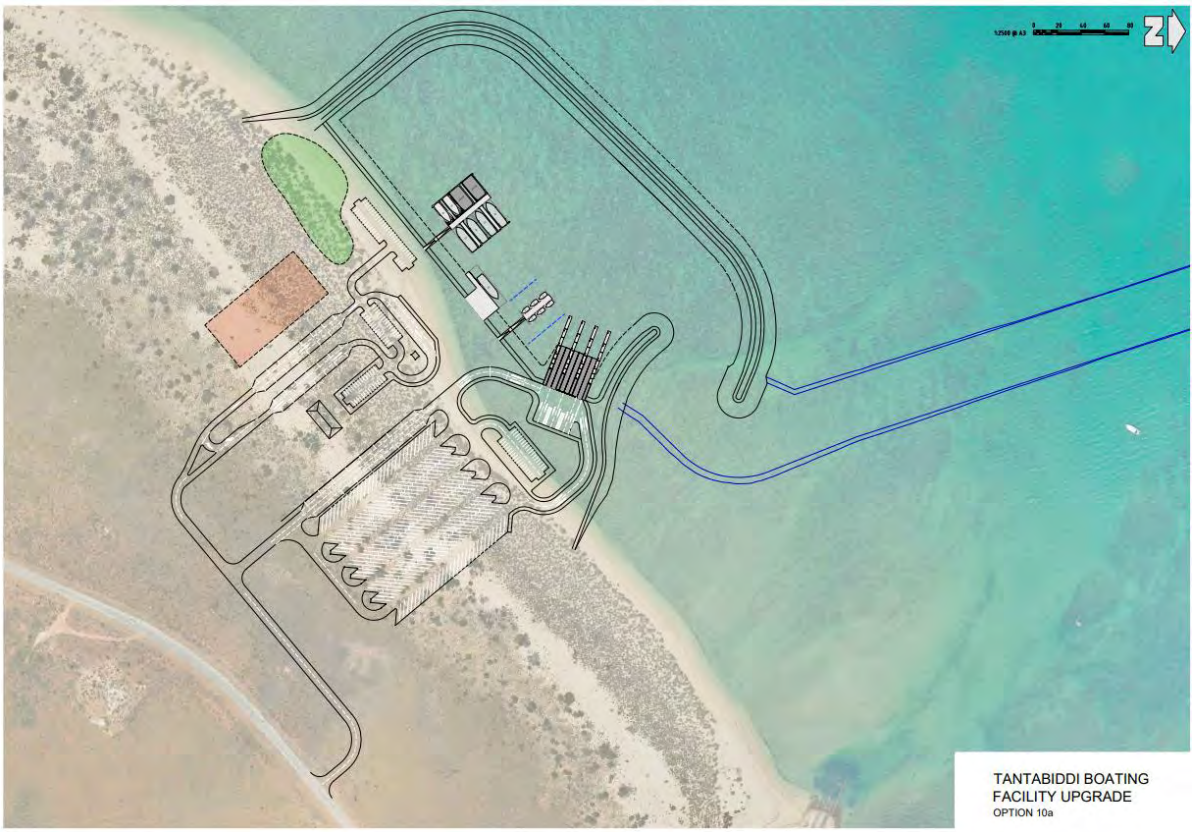

Figure 1.2 Proposed Concept for the TBF – Concept B

In order to investigate the coastal processes at the Tantabiddi site and the impact of the proposed concept, coastal engineers M P Rogers & Associate Pty Ltd (MRA) were engaged by DoT to undertake the Tantabiddi Creek Coastal Processes Study. The outcomes of this study are summarised herein and further detail provided in the attached Appendices.

1.2 Objective

The objective of this study is to perform a comprehensive investigation into the coastal processes, design conditions, potential impacts and risks, mitigation options, and management measures at the proposed TBF. This includes the following.

- Assessment of coastal processes near the proposed TBF.
- Develop an understanding of ambient and extreme Metocean conditions.
- Assess wave, hydrodynamic (coastal currents), and sediment transport impacts.
- Assess expected sedimentation.
- Assess performance in terms of harbour water quality and flushing rate.
- Investigate wave penetration into the harbour and navigability of the entrance channel.
- Develop an understanding of the Long Period Wave (LPW) climate and potential for LPW induced harbour resonance.

- Provide expert advice that will support future detailed design.

The information gained from this study is intended to be used for future planning, consultation, investigations and design work. Additionally, it will be provided as information and background to other project stakeholders including but not limited to the Shire, DBCA, DPIRD and Tourism WA.

1.3 Scope

The scope of this study includes a number of tasks and activities which are detailed below.

- Task 1: Desktop Review, Data Gathering, and Site Visit.
- Task 2: Shoreline Movement Assessment.
- Task 3: Metocean Climate Analysis which includes.
    - Nearshore Ambient Condition Analysis.
    - Offshore Ambient and Extreme Conditions Analysis.
    - Ambient and Extreme Wind Conditions Analysis.
- Task 4: Cyclonic Modelling.
- Task 5: Wave Modelling.
- Task 6: Hydrodynamic Modelling – Impacts and Flushing.
- Task 7: Sediment Transport and Sedimentation Modelling.
- Task 8: Wave Penetration and Long Period Wave Assessment.
- Task 9: Wave Penetration Modelling. Contingent on outcome of Task 8.
- Task 10: Long Period Wave Modelling. Contingent on outcome of Task 8.

The primary deliverable for these tasks is contained herein. Tasks 1, 8, 9 and 10 are wholly contained within sections of this overall Coastal Processes Study report. The outcomes of Tasks 2, 3, 4, 5, 6 and 7 are provided as standalone technical reports included as appendices of this overall Coastal Processes Study report and also briefly summarised herein. For further information on the location of the standalone technical reports refer to Table 1.1.

Table 1.1 Standalone Technical Report Locations

Task	Task Title	Report Number	Location
2	Shoreline Movement Assessment	R1535 Rev 2	R1518 Rev 0 Appendix A
3	Metocean Climate Analysis	R1524 Rev 1	R1518 Rev 0 Appendix B
4	Cyclonic Modelling	R1533 Rev 1	R1518 Rev 0 Appendix C
5	Wave Modelling	R1629 Rev 2	R1518 Rev 0 Appendix D
6	Hydrodynamic Modelling	R1585 Rev 2	R1518 Rev 0 Appendix E
7	Sediment Transport & Sediment Modelling	R1598 Rev 3	R1518 Rev 0 Appendix F

1.4 Project Co-ordinate System

The Coastal Processes study was completed using the Map Grip of Australia Zone 49, based on GDA2020 for the horizontal datum. The vertical datum used for the study was the Tantabiddi Lowest Low Tide 1985 which is 1.01 m below AHD (1989).

1.5 Concept C

Following the work completed by MRA to assess coastal processes and other aspects of Concept B for the TBF, a refinement of the TBF design was completed by DoT resulting in the development of Concept C. This new concept features a refined layout designed to decrease potential infilling of the mouth of the facility and adjacent channel. The layout of Concept C for the proposed TBF is presented in Figure 1.3.

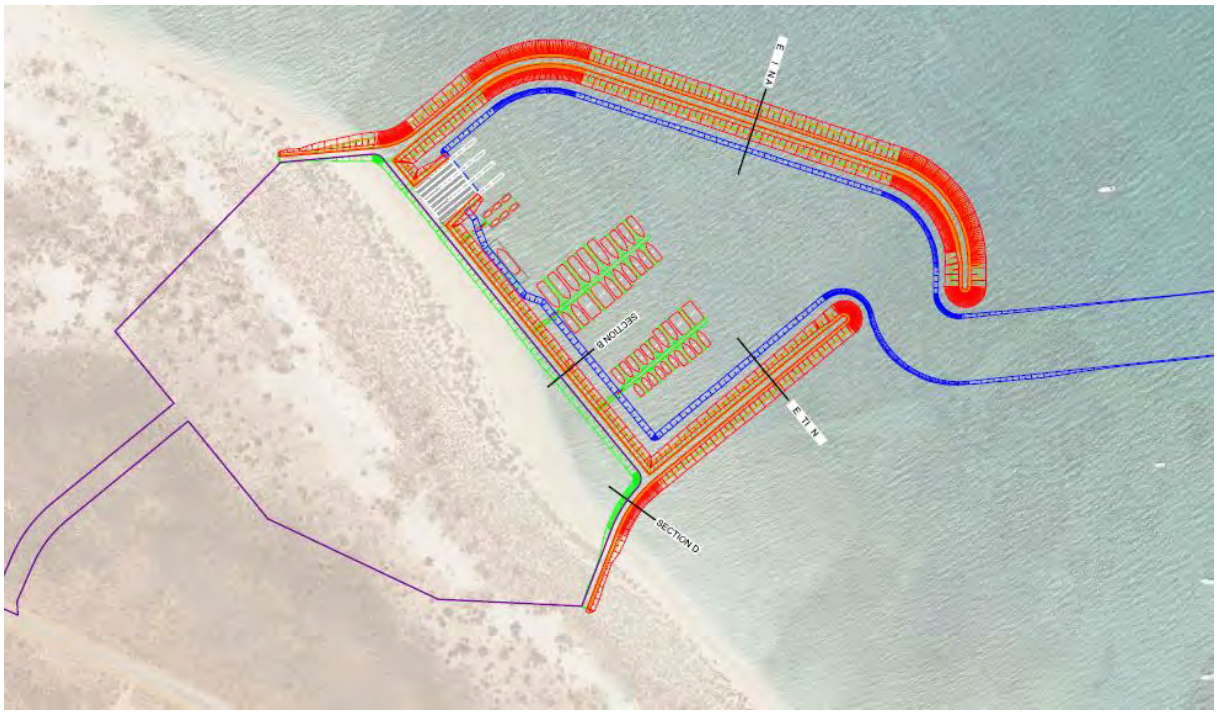

Figure 1.3 Concept C Layout

The previously calibrated models were used to simulate the Concept C layout for the proposed TBF to determine the relevant impacts on all items previously considered for Concept B. The scope of works for the assessment of Concept C was slightly more focused, in an attempt to only cover the main items that required consideration based on the outcomes of the investigations completed for Concept B.

A comparison of the concept layouts, including an earlier Concept A layout, is presented in Figure 1.4.

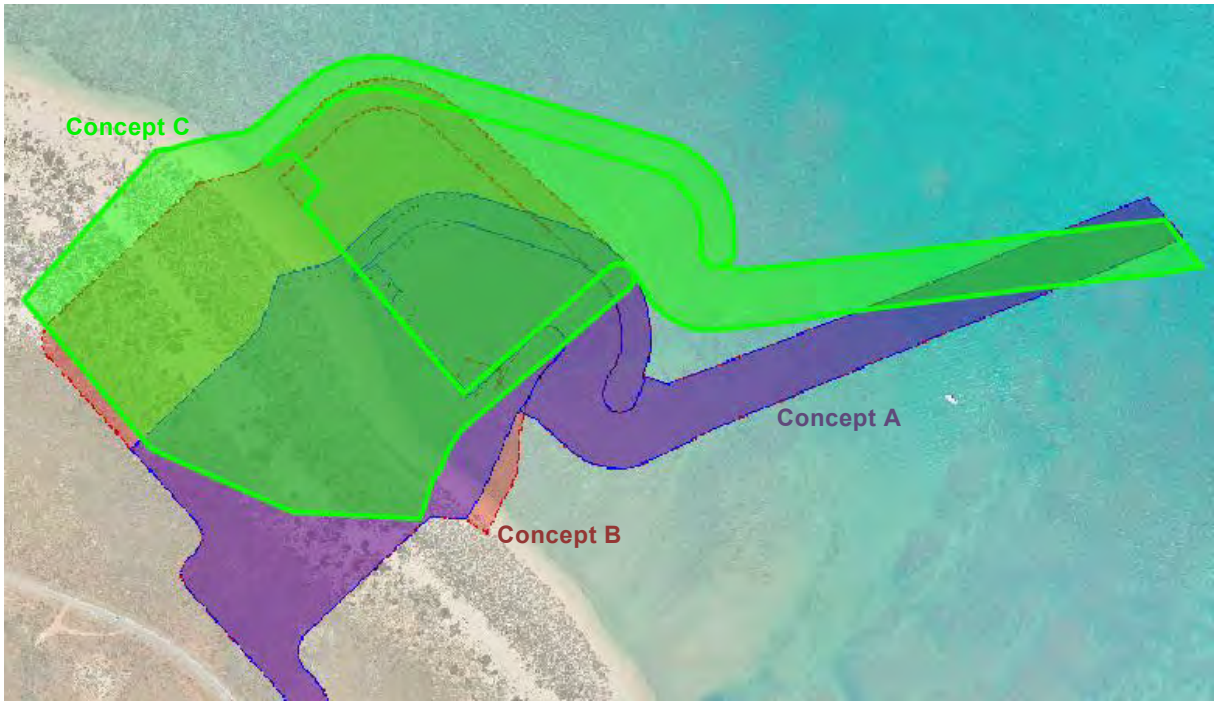

Figure 1.4 Comparison of Concepts A, B & C

2. Data Summary

DoT provided MRA with a range of data and information. Further data was obtained by MRA to complement the provided data. This data can be separated into the seven areas of:

- met-ocean data;
- sediment data;
- survey data;
- drawings;
- imagery
- previous modelling; and
- literature.

A brief review of the data used in the Coastal Processes Study from each of these areas is provided in the sections below.

2.1 Metocean Data

On the Western Australian coastline, DoT and the Bureau of Meteorology (BoM) has historically collected the majority of publicly available metocean data. Metocean data collected in the area includes waves, current, water levels and winds.

For some components of the metocean assessment, the wave datasets were extended using the BoM and CSIRO wave hindcast model. BoM and CSIRO have developed a wave hindcast model that covers the Australian coastline. The hindcast was originally completed for the period from 1979 to 2010. It was later extended to 2013 and BoM now keeps the model updated to present day. The wave hindcast model summary and data can be found at https://data.csiro.au/collections/collection/CIcsiro:39819.

The hindcast model is run on a 0.4° x 0.4° global grid with a series of nested grids of 10 arcminutes (~18km) down to 4 arcminutes (~7km) around the Australian and Western Pacific Island coasts. All grids are forced with Climate Forecast System Reanalysis (CFSR) surface winds at 0.3° spatial and hourly temporal resolution. Further information on this model is provided in Durrant et al (2013) and BoM (n.d.). Results of this model were compared against recorded data to extend the available data record at the Tantabiddi Wave Buoy.

The metocean data sets utilised in the Coastal Processes Study are listed in Table 2.1.

Table 2.1 Metocean Data

Data Type	Description	Location (Lat Long)	Location (GDA 2020 MGA Zone 49)	Source	Data Period
Wind	Yardie Wind Anemometer	21.8883°S 114.0158°E	811641.2328 E 7576477.048 S	DoT	2019 present
	Learmonth Wind Anemometer	22.2406°S 114.0967°E	819213.6397 E 7537274.366 S	DoT	1975-present
Wave	WWIII Hindcast Data	Various	Various	BoM	1979-2021
	Tantabiddi Wave Buoy (Present)	21.8932°S 113.9292°E	802676.2097 E 7576107.526 S	DoT	2019-present
	Tantabiddi Wave Buoy (Historic)	21.8944°S 113.9292°E	802673.673 E 7575974.579 S	DoT	1987-1988
	Exmouth Wave Buoy	21.6994°S 114.0986°E	820624.1193 E 7597236.935 S	DoT	2006-2010
Wave & Current	AWAC	21.0976°S 113.9724°E	807112.0856 E 7574426.253 S	DoT	2019-present
	Aquadopp	21.9104°S 113.9767°E	807550.638 E 7574107.412 S	DoT	2019-present
Wave & Water Level	RBR Pressure Sensor 1 at AWAC	21.0976°S 113.9724°E	807112.0856 E 7574426.253 S	DoT	2019-present
	RBR Pressure Sensor 2 at Aquadopp	21.9104°S 113.9767°E	807550.638 E 7574107.412 S	DoT	2020-present
	RBR Pressure Sensor 3 at Ramp	21.9122°S 113.9776°E	807639.8151 E 7573906.178 S	DoT	2020-present
	Hobo Pressure Sensor at Creek	21.9130°S 113.9793°E	807813.8492 E 7573814.13 S	DoT	2020
Water Level	Exmouth Tide Gauge	21.9123°S 113.9783°E	807711.9699 E 7573893.694 S	DoT	1989-1993

The locations of the respective metocean data sets are displayed in Figure 2.1.

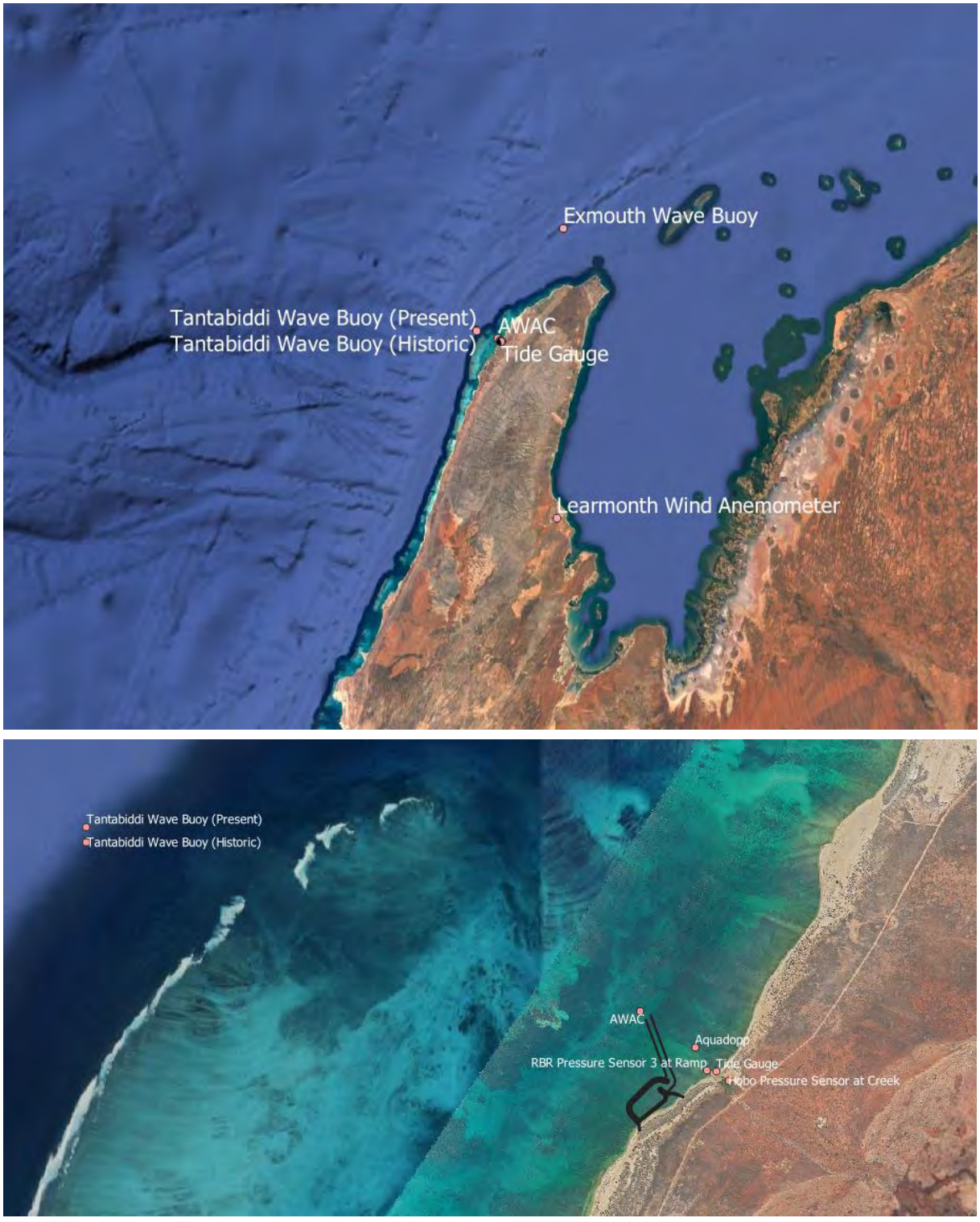

Figure 2.1 Met-Ocean Data Locations

The metocean data will be used for Tasks 3, 4, 5, 6, 7, 8, 9 and 10. The primary use of the metocean data will be as part of the metocean Climate Analysis (Task 3). In addition, the data will also be used for the setup, calibration and validation of the cyclone, wave, hydrodynamic, sediment, wave penetration and long period wave models.

2.2 Sediment Data

The morphology of the Western Australian coastline varies significantly across the state, resulting in large variations of the sediment present along the coast. The composition and size distribution of the site sediment will greatly affect the rates of sediment transport and sedimentation. As such understanding these local sediment characteristics is essential when studying coastal processes.

Three separate recent collections of sediment data have been undertaken at the site to date. The first collection was conducted by DoT in 2019, followed by Advisian in 2020 and then MRA in 2021. Each of these collections involved taking a number of sediment samples which were subsequently analysed to determine the size distributions and compositions.

The Sediment data sets used in this the Coastal Processes Study are listed in Table 2.2.

Table 2.2 Sediment Samples

Sample Date	Source	Name	Description	Location (Lat Long)	Location (GDA2020 MGA Zone 94)
2015	Cuttler et al		75 samples taken north of Tantabiddi Creek	Extent shown in Figure 2.2.	Extent shown in Figure 2.2.
July 2019	DoT	TBSS01	South Beach	21.912741°S, 113.977733°E	807652.4018 E 7573845.972 S
		TBSS02	Estuary	21.912806°S, 113.978462°E	807727.6298 E 7573837.307 S
		TBSS03	North Beach	21.912246°S, 113.978654°E	807748.6846 E 7573898.966 S
		TBSS04	Dredge Spoil	21.912260°S, 113.979806°E	807867.7548 E 7573895.101 S
		TBSS05	Offshore Channel	21.910065°S, 113.974630°E	807337.347 E 7574148.679 S
		AWAC	AWAC	21.0976°S, 113.9724°E	807112.0856 E 7574426.253 S
		Aqua Dopp	Aquadopp	21.9104°S, 113.9767°E	807550.638 E 7574107.412 S
March 2020	Advisian	TS01	Estuary South	21.9139926°S, 113.979611°E	807843.8656 E 7573703.532 S
		TS02	Creek Upstream 1	21.9170933°S, 113.982043°E	808088.6172 E 7573355.107 S
		TS03	Creek Upstream 2	21.920825°S, 113.989911°E	808893.9705 E 7572925.818 S
		TS04	Dredge Spoil	21.9124016°S, 113.980062°E	807893.9168 E 7573878.899 S
		TS05	Estuary Mid	21.9130492°S, 113.97929°E	807812.7094 E 7573808.699 S

Sample Date	Source	Name	Description	Location (Lat Long)	Location (MGA Zone 94)
March 2021	MRA	MRA1	Southern South Beach	21.9250°S, 113.96851°E	806675.9206 E 7572679.79 S
		MRA2	Mid South Beach	21.91913°S, 113.97079°E	806920.7027 E 7573157.47 S
		MRA3	TBF Dune	21.91432°S, 113.97573°E	807442.2183 E 7573678.181 S
		MRA4	TBF Waters Edge	21.914193°S, 113.975598°E	807428.5976 E 7573689.371 S
		MRA5	TBF Nearshore	21.913817°S, 113.975221°E	807390.3492 E 7573731.791 S
		MRA6	North Beach	21.90745°S, 113.98135°E	808037.7288 E 7574425.364 S

The approximate locations of these sampling points are displayed in Figure 2.2.

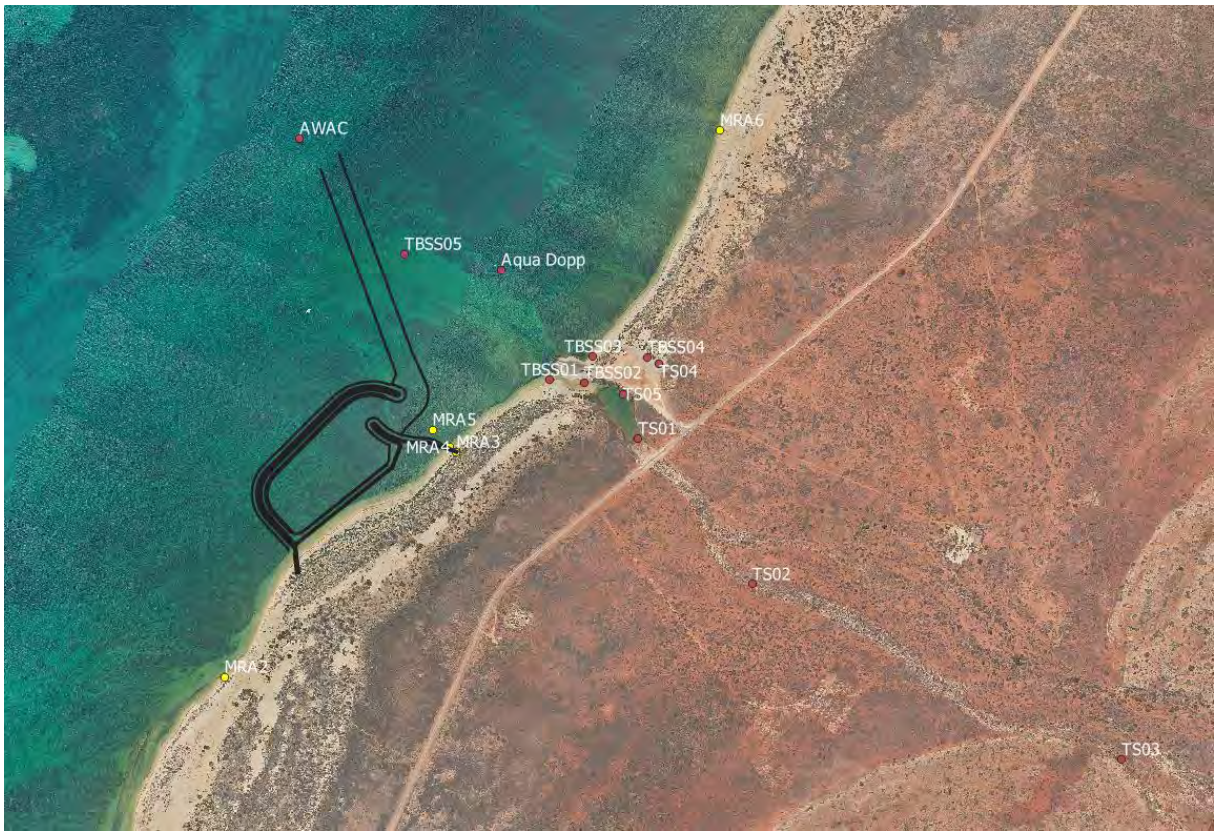

Figure 2.2 Sediment Sampling Locations

Sediment sampling was completed by Cuttler et al in 2015 in the extent shown in Figure 2.3. The specific particle characteristics from this sampling were not available, but the general results will be utilised to provide context for the overall assessment.

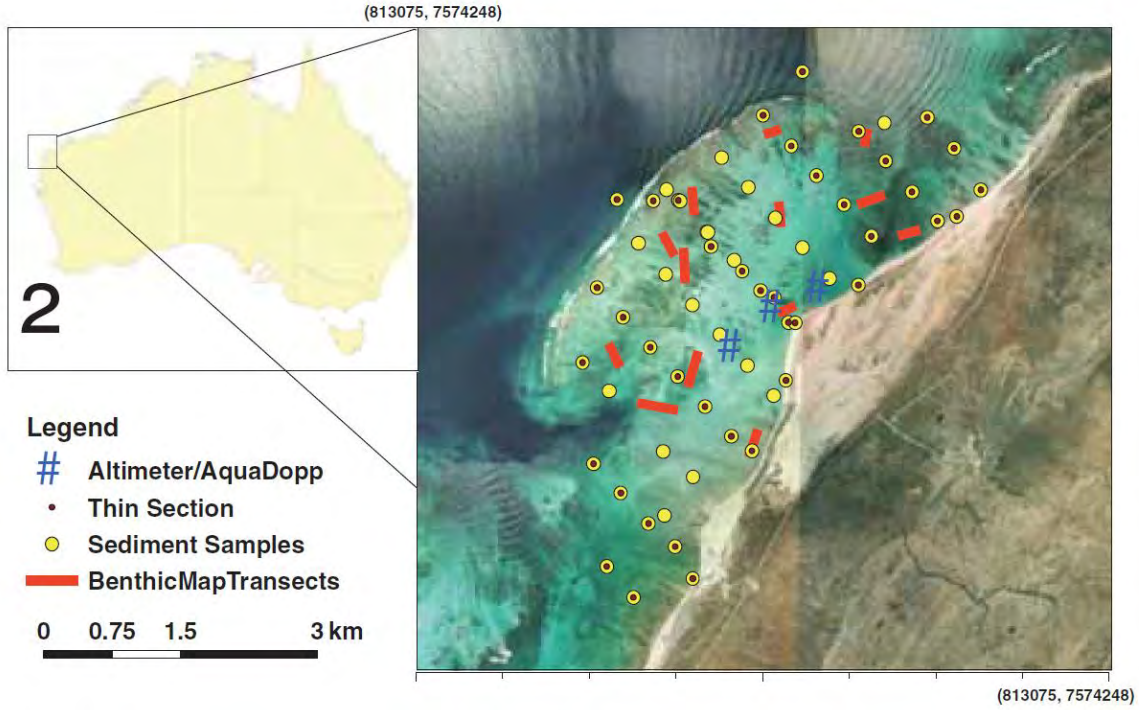

Figure 2.3 Study Area and Sampling Location. Coordinates are given in GDA 1994 UTM Zone 49 (Cuttler et al 2015)

The sediment data will be used for Tasks 4, 5, 6 and 7. The primary use of the sediment data will be in the Sediment Transport and Sedimentation modelling (Task 7). The size distribution of the sediment is critical to the modelling of sediment transport and sedimentation, as such having accurate and up to date sediment data is essential. Additionally, the sediment data will be considered in determining bottom friction factors for the cyclone, wave and hydrodynamic models.

2.3 Survey Data

The majority of the historical survey data of the Tantabiddi area was conducted by/for DoT with more recent survey completed by Platinum Surveys. Survey of the marine area is provided in the form of Multibeam bathymetric survey and a Nautical Chart provided by DoT. Additional terrestrial and marine survey data was also obtained by MRA to complement the DoT data and improve the accuracy of the cyclone, wave and hydrodynamic models.

The Survey data utilised in the Coastal Processes Study is listed in Table 2.3.

Table 2.3 Survey Data

Description	Source	Date	Extent
DoT Planbook 54	DoT	1985	Tantabiddi Creek Nearshore Area
DoT Planbook 54	DoT	2005 – 2019	Tantabiddi Creek Nearshore Area
DoT Planbook 54	DoT	1996 – 1997	Tantabiddi Creek Nearshore Area
RAN Chart 900	DoT	1971 – 1991	North West Cape area.
Multibeam Bathymetric Survey	DoT	2019	Tantabiddi Creek Nearshore Area and Channel.
ex-1006-a-l-1	DoT	**2010**	Tantabiddi Creek Nearshore Area, Shoreline and Channel.
ex_20150925_mean	DoT	2015	Tantabiddi Creek Nearshore Area and Channel.
Creek Survey	Platinum Surveys	2020	Tantabiddi Creek and adjacent road
Bathymetry 50m Multibeam	Geoscience Australia	2018	Offshore areas beyond the coral reef.
25 Metre Intertidal	Geoscience Australia	2019	Water's edge along the coast
1 Second Digital Elevation Model	Geoscience Australia	2011	Land areas immediately surrounding the site.

The survey data will be used to create the bathymetry and topography of all of the models used as part of the Coastal Processes Study. Depth files will be created using the survey data using the Delft3D suite and subsequently checked back against the survey data.

The survey data will also provide context to historical changes in the bathymetry and topography of the site.

2.4 Drawings

DoT provided a number of drawings of both previous works completed on the Tantabiddi Boat Ramp and the proposed Concept A for the TBF. The provided drawings are listed in Table 2.4.

Table 2.4 Drawings

Name	Description	Date
DoT Planbook 54	Tantabiddi Boat Launching Facilities Design Drawings	2005 - 2006
DoT Planbook 1399	Tantabiddi Boat Ramp Civil and Structural Construction Drawings	2011
Tantabiddi_2020-01_Concept6C_3D	Concept A CAD drawing	2020

The concept design drawings provided by DoT are the basis for all works completed as part of the Coastal Processes Study. These drawings will be used to create the depth files for all of the modelling and defining the location and extent of the TBF.

The drawings of the previous works completed on the Tantabiddi Boat Ramp will be used to define and refine the elevations in this area within the models as well as providing general context of the site.

2.5 Imagery

Aerial imagery and field photos of the site have been provided by DoT and additional field photos of the site were also procured by MRA as part of the Site Inspection which is discussed in detail in Section 4. The imagery utilised in the Coastal Processes Study are listed in Table 2.5.

Table 2.5 Imagery

Imagery Set	Date	Description	Source
Aerial Imagery	1969 - 2020	Unrectified aerial photos between 1969 and 1989. Seven rectified aerial photos from 2004 to 2020.	DoT
2003 Field Photos	21/05/03	Field photos of the creek and boat ramp.	DoT
2005 Field Photos	01/01/05 18/07/05	Two sets of field photos of the creek and boat ramp.	DoT
2019 Field Photos	07/06/19	Field photos of the creek and boat ramp.	DoT
2021 Field Photos	14/03/21 15/03/21	Field photos of site inspection, probing and sediment sampling.	MRA

The imagery data will be used to provide context to the works completed as part of the Coastal Processes Study and illustrate the findings and results of the various tasks. The MRA field photos may also be used to assist in the completion of Tasks 2, 3, 4, 5, 6 and 7.

2.6 Vegetation Lines

Vegetation lines mapping the shoreline of the area surrounding the Tantabiddi Boat Ramp were provided by DoT. Ten vegetation lines were provided for the period from 1969 to 2020 covering a period of 51 years. The vegetation lines used in the Coastal Processes Study are listed in Table 2.6.

Table 2.6 Vegetation Lines

Year	Provided By
1969	DoT
1985	DoT
1986	DoT
1989	DoT
2004	DoT
2007	DoT
2010	DoT
2011	DoT
2014	DoT
2018	DoT
2020	DoT

The vegetation lines will be used to conduct the Shoreline Movement Assessment and to provide context to historical changes in the site layout.

2.7 Modelling

Previous modelling of the Tantabiddi area has been completed by Advisian as part of their Hydrology and Geomorphology Study (Advisian 2020). Three separate models were used by Advisian during their study and the results of these models have been provided to MRA by DoT.

Table 2.7 Previous Modelling Results

Model	Author	Date	Program
Wave Model	Advisian	2020	MIKE21
Rainfall Model	Advisian	2020	RORB
Flood Model	Advisian	2020	TUFLOW

Results of the Wave model will be used to provide context for the site. Fluvial discharges from the Flood model will be used as inputs to the hydrodynamic and morphological models. Additionally, the Fluvial Sedigraphs will be used as inputs in the morphological modelling.

The previous modelling results will also provide background information for the site which will be considered throughout the Coastal Processes Study.

2.8 Literature

There has been significant research and investigation into the North West Cape area including Tantabiddi conducted over the last 20 years. DoT provided MRA with a significant amount of literature relevant to the site and the Coastal Processes Study which is listed in Table 2.8. In addition, MRA sourced additional literature to complement the literature provided by DoT which is also included in Table 2.8.

Table 2.8 Utilised Literature

Title	Date	Author	Provided By
Exmouth Floodplain Management Study	2007	Sinclair Knight Merz	DoT
Tantabiddi Boat Ramp, Tantabiddi, Exmouth, Specifications	2007	URS	DoT
Coastal Demarcation Lines For Administrative & Engineering Purposes. Delineation Methodology & Specification	2009	DoT	DoT
Exmouth Hydrological Study	2014	hyd2o Hydrology	DoT
Fact Sheet: Tantabiddi Creek Boat Ramp Sand Bypassing	2015	Shire of Exmouth	DoT
Tantabiddi Boat Ramp Sand Bypassing Environmental Hazard Identification Report	2015	URS	DoT
Tantabiddi Boat Ramp Sand Bypassing Environmental Management Plan	2015	URS	DoT
Response of a fringing reef coastline to the direct impact of a tropical cyclone	2018	Cuttler et al	DoT
Predicting the hydrodynamic response of a coastal reef-lagoon system to a tropical cyclone using phase-averaged and surfbeat-resolving wave models	2018	Drost et al	DoT
Tantabiddi Boat Launching Facility Investigation	2018	MRA	DoT
Spatial Variability of Sediment Transport Processes Over Intratidal and Subtidal Timescales Within a Fringing Coral Reef System	2018	Pomeroy et al	DoT
Design Storms for Western Australian Coastal Planning: Tropical Cyclones	2018	Seashore Engineering	DoT
Source and supply of sediment to a shoreline salient in a fringing reef environment	2019	Cuttler et al	DoT
Tantabiddi Creek Hydrology and Geomorphology Study	2020	Advisian	DoT

Title	Date	Author	Obtained By
Management Plan for the Ningaloo Marine Park and Muiron Islands Marine Management Area. 2005 - 2015	2005	Marine Parks and Reserves Authority, Department of Conservation and Land Management	MRA
Grainsize, Composition and Bedform Patterns in a Fringing Reef System	2015	Cuttler et al	MRA
Ningaloo Coast World Heritage Nomination	2010	Department of Environment, Water, Heritage and the Arts	MRA
Ningaloo Coast World Heritage Nomination – IUCN Technical Evaluation	2011	IUCN	MRA
Nyinggulu (Ningaloo) coastal reserves, Red Bluff to Winderabandi - draft joint management plan.	2019	Department of Biodiversity, Conservation and Attractions	MRA

The literature listed above will form the basis of the literature review completed in Section 3. To keep this report concise only the literature most relevant to the Coastal Processes Study work will be discussed in Section 3. However, all of the literature has been reviewed by MRA and will influence and guide the works completed as part of the Coastal Processes Study.

3. Site Setting & Literature Review

The Tantabiddi Creek site is located on the western coast of the North West Cape within the Ningaloo Coast World Heritage Site. Short (2006) describes this section of coastline as composed of sand beaches paralleled by fringing reefs which extend up to 500 m offshore. Broken sections of coral reef are located further offshore as shown in Figure 3.1. The coral and fringing reef provides significant protection to this area of coast.

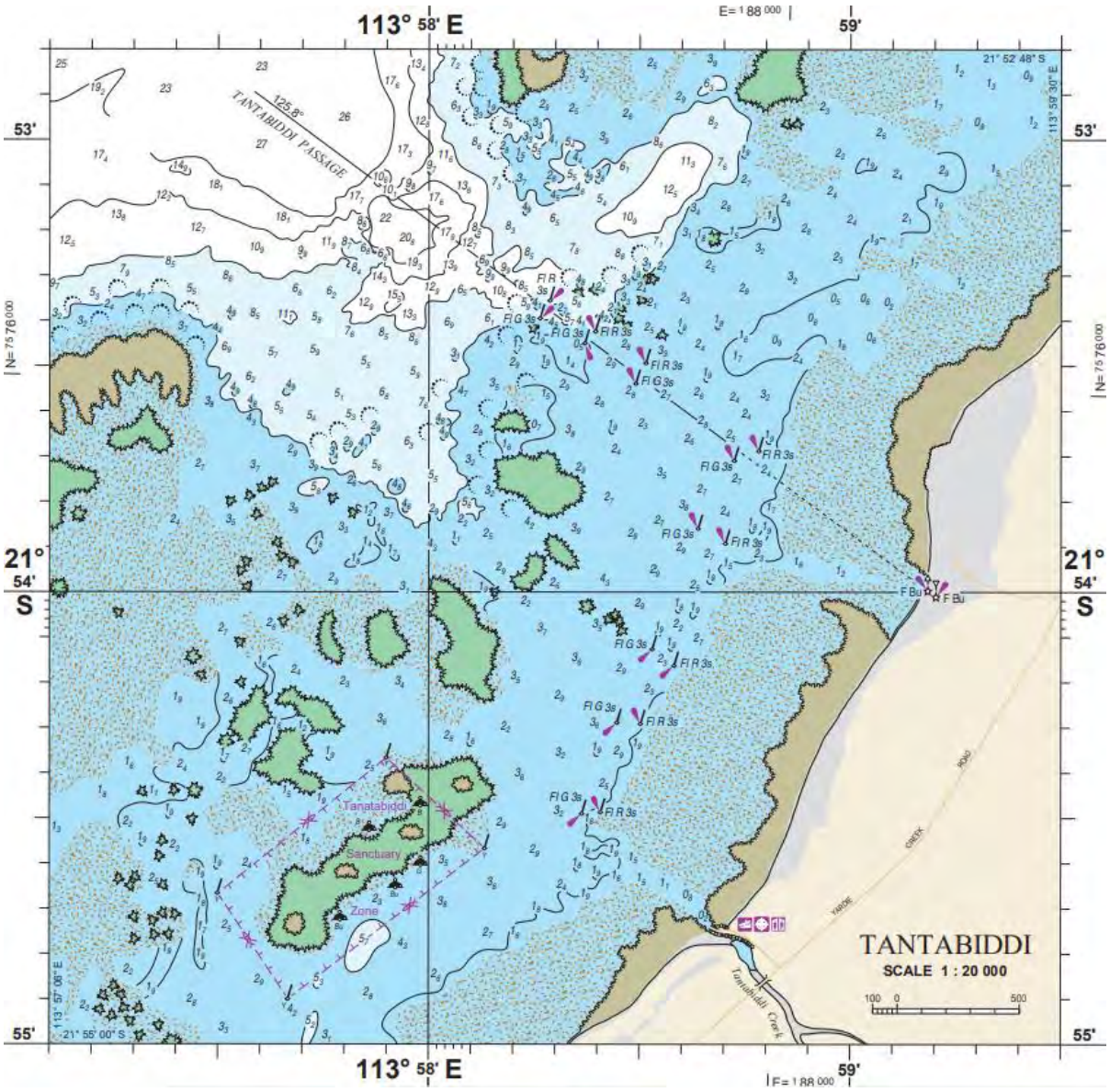

Figure 3.1 Nautical Chart RAN 900 (DoT)

Tantabiddi Creek provides a natural channel through the shallow fringing reef resulting in significant usage of the site for boat launching over the recent decades.

3.1 Existing Facility

The Existing Boat Ramp Facility is located on the northern side of the mouth of the Tantabiddi Creek inlet (refer Figure 1.1). It provides important access for recreational boats and commercial

operators to the Ningaloo Reef and adjacent coastal waters. The use of the Facility by multiple user groups can result in congestion and associated conflicts during peak use periods.

The original single lane boat ramp was constructed adjacent to the Tantabiddi Creek in the 1990s and further upgraded in 2012-2013. The Boat Ramp can however be impacted by creek dynamics during rain events, including tropical cyclones. Previous impacts have resulted in accumulation of sand and creek material, restricting access for boat launching.

This congestion and occasional restriction of access resulted in the creation of the Tantabiddi Task Force. The Task Force subsequently initiated a number of investigations to inform the development of the TBF to address these issues.

3.2 Hydrology

The hydrology of the Tantabiddi Creek area was investigated by Advisian in the *Tantabiddi Creek Hydrology and Geomorphology Study* (Advisian 2020). The North West Cape is dominated by the Cape Range which runs north-south along the peninsula. The crest of this range forms a regional drainage divide with separate drainage systems to the east and west. The Range is characterised by numerous ephemeral creeks draining west and east of the Cape Range ridgeline during significant rainfall events. The upper reaches of these creeks are deeply incised and have steeper bed gradients, while the lower reaches flow onto low lying coastal areas with lower bed gradients before reaching the ocean.

The Tantabiddi Creek Catchment has an area of 27 km^2, however a smaller catchment of 9 km^2 lies to the south west of the Tantabiddi catchment and other minor catchments to the north may contribute flows in more extreme events (Figure 3.2). As these two other catchments are significantly smaller and there would be substantial flow attenuation within them, they are not expected to have a significant influence on the peak flows at the boat ramp.

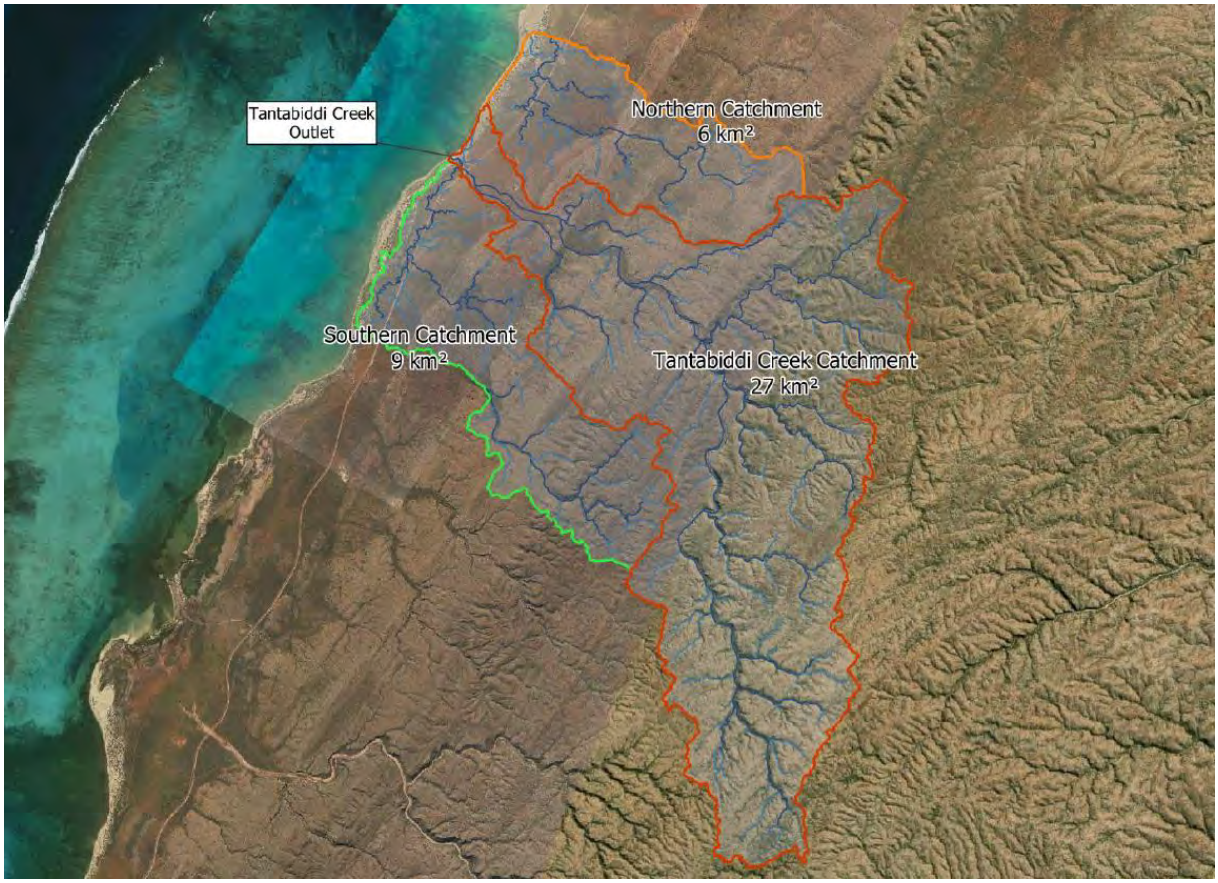

Figure 3.2 Tantabiddi Creek Catchment and other Minor Catchments Contributing Flow to the Study Area (Advisian 2020)

Advisian utilised the TUFLOW model to simulate the distribution of flow and attenuation in the lower gradient area of Tantabiddi Creek. Using this model the peak flows at the Yardie Creek Road floodway (start of the Tantabiddi Inlet) were determined for the 1, 2, 5, 10, 20, 50 and 100 year ARI events. Design rainfalls for these events were taken from the RORB model and used to simulate rainfall on the model domain. The model terrain was developed using survey data provided by Landgate and bathymetric data of the inlet provided by Platinum Surveys. The results of the TUFLOW modelling are displayed in Table 3.1. These will be used in the hydrodynamic and morphological modelling.

Table 3.1 Peak Flow at Yardie Creek Road Floodway (Advisian 2020)

Scenario (ARI)	Peak Flow (m^3/s)
1	13
2	19
5	31
10	53
20	79
50	117
100	146

3.3 Fluvial Geomorphology

In addition to investigating the hydrology of the site, Advisian also investigated the sites geomorphology (Advisian 2020). The geomorphology was separated into two sections which were assessed separately, namely the Fluvial Geomorphology and the Coastal Geomorphology.

Tantabiddi Creek is a significant gully and canyon located on the western side of the Cape Range which flows in a westerly direction from the Range to the ocean. Extending westward from the Cape Range to the ocean is a low, predominantly calcarenite, terrace known as the Tantabiddi Terrace. This terrace was formed by the erosion of the western margin of the Cape Range peninsula by marine processes in the Pleistocene period (Advisian 2020).

The seaward margin of the Tantabiddi Terrace is overlain by coastal deposits which form sandy beaches and coastal dunes. Directly offshore from the site lies Ningaloo reef which parallels the shoreline. The layout of these layers is shown in Figure 3.3.

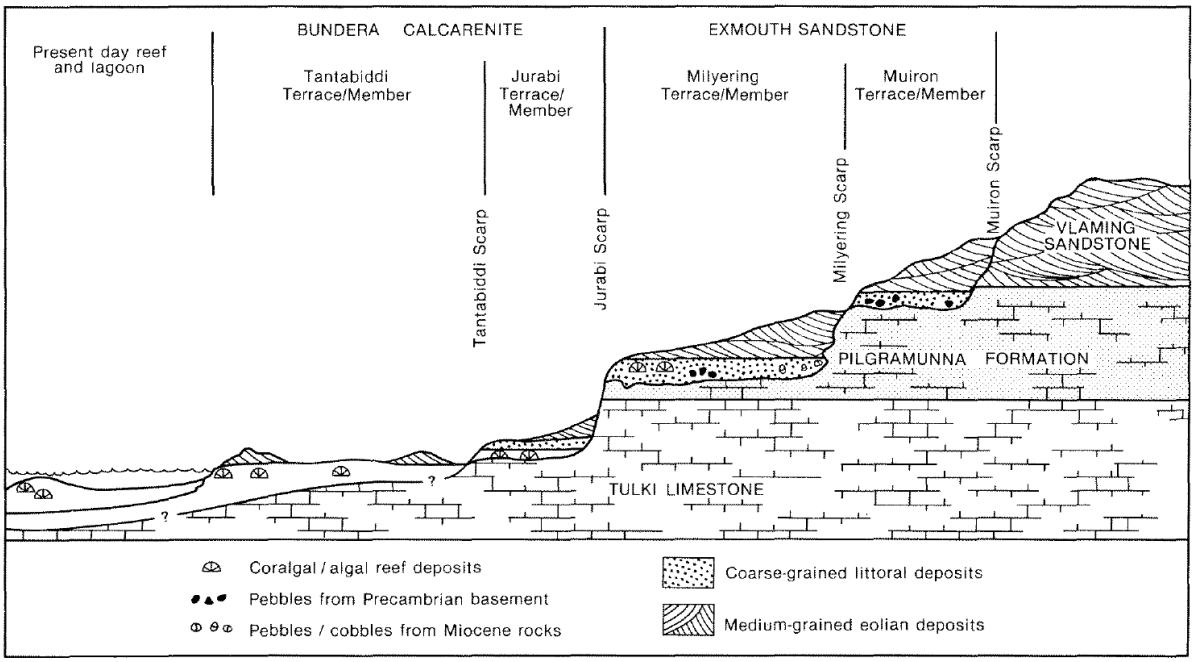

Figure 3.3 Stratigraphic Relationships of the Main Geological Units on the West Side of the Cape Range (Hocking et al 1987)

The Department of Mines and Petroleum (DMP) have completed geological surveys of Western Australia (DMP 1978). Figure 3.4 shows an extract from the Onslow (SF5) tile of the survey covering the study area.

As seen in figure 3.4, the geology surrounding the site can be summarised as follows.

- Offshore consists of the living coralgal Ningaloo Reef.
- The beaches and dunes consist of light grey, unconsolidated and poorly consolidated quartzose calcarenite.
- The Tantabiddi Terrace is classified as calcarenites and calcirudites and shallow marine and minor eolian coralgal reef deposits.
- The Cape Range ridges are classified as redish to yellowish shallow marine partly clayey foraminiferal calcarenitic packstone, known as Tulki Limstone.

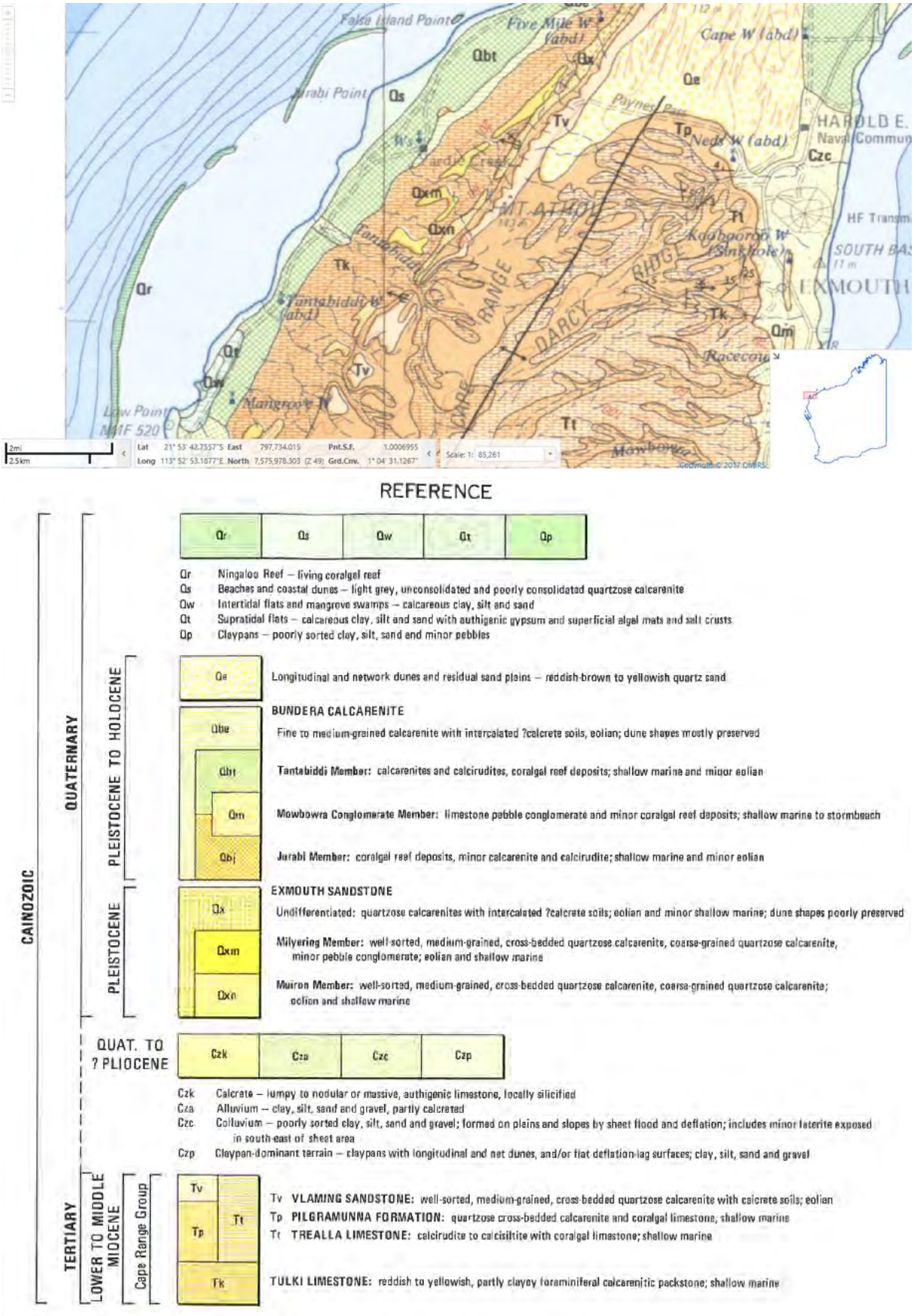

Figure 3.4 Geological Survey of Western Australia (DMP 1978)

The fluvial geomorphology of the area is driven by the transport of sediment from the Tantabiddi Creek catchment to the nearshore area and the alteration of the geomorphic features during flood events. In the Cape Range, Tantabiddi Creek flows over steep stony uplifted coral reefs and aeolian sandstone, flowing down to a relatively flat and low lying Tantabiddi Terrace before reaching the coastal dune system and forming an estuary (Figure 3.3).

The estuary is regularly disconnected from the ocean by a sand bar adjacent to the boat ramp, which is flushed seawards by the creek during high creek flows. Red sediment from the upper catchment is visible in the ramp area in aerial imagery following flood events (like those displayed in Table 3.2), as are the geomorphic changes (eg opening the inlet) resulting from the erosion and deposition of sediment in the ramp area. These flood events can result in major sediment deposition at the creek mouth and through the nearshore area including in the channel.

3.4 Coastal Geomorphology

The Coastal Geomorphology is driven by the wind and wave transport of nearshore sediment along with the fluvial processes previously discussed. The coastal area broadly consists of a living coralgal reef, interspersed with mobile sands, that encloses a sandy bottom lagoon with nearshore reef platforms. The Ningaloo reef is orientated in a north westerly direction and is backed by a relatively narrow reef flat that transitions to a lagoon. There are regular gaps in the main reef line with a relatively large gap 3 km to the north west of the Tantabiddi Boat Ramp known as Tantabiddi Passage. The enclosed lagoon consists of reef covered with sand, and the nearshore area consists of reef outcrops with parts overlain with a shallow layer of sand. The beach is composed of unconsolidated and poorly consolidated quartzose calcarenite which is backed by sparsely vegetated foredunes and relic foredunes.

Sediment is transported across the reef via wave action before longshore transport moves the nearshore sediment to the north east. It is noted that the net sediment transport is to the north east despite seasonal variation in the longshore transport. The boat ramp acts as a barrier to this longshore transport resulting in accretion on the southern side of the ramp (refer Figure 3.5). This often results in a bar at the entrance to the creek disconnecting it from the ocean.

Figure 3.5 Indicative Sediment Transport Pathways (MRA 2018)

The fluvial processes previously discussed can impact the accretion at the ramp especially during major flood events. It is likely that a range of deposits from the geological categories discussed in the Fluvial geomorphology section are present in the nearshore area surrounding the creek and the associated entrance channel.

3.5 Sediment Background

The sediment characteristics of the site will influence most of the tasks completed as part of the Coastal Processes Study. The sediment samples collected by Cuttler et al, DoT, Advisian and MRA are discussed below.

Cuttler et al (2015) investigated the sediment properties approximately 4 km to the north of the Tantabiddi Boat Ramp through the analysis of 75 samples taken across the sub reef environments. They found that the sediments were generally medium (0.3 – 0.4 mm), moderately sorted, coarse skewed sands. There was a trend of grainsize decreasing and sorting increasing as you move shoreward from the reef crest. The sediments were dominated by a combination of coral fragments, coralline algae, foraminifera, molluscs and reworked grains with the composition changing depending on the spatial position.

Cuttler et al noted there is a trend of decreasing median grain size from the reef crest (D50 of ~0.5 mm), shoreward through the lagoon (D50 of ~0.35 mm) to the beach (D50 of ~0.25 mm) (Figure 3.6). MRA's sampling is intended to allow augmentation of these findings for the proposed facility's location.

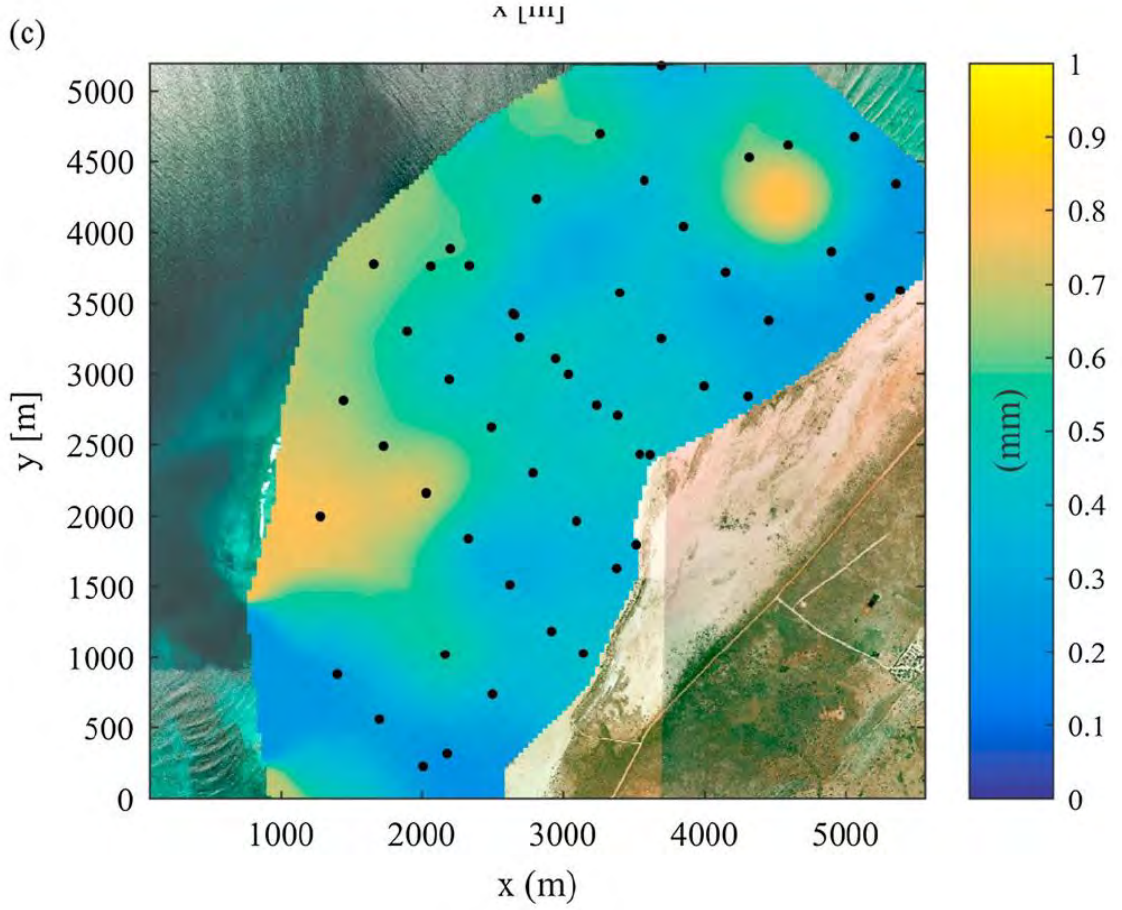

Figure 3.6 Sediment Size Distribution (Pomeroy et al 2018)

The DoT and Advisian sediment samples investigated the sediment properties through Tantabiddi Creek, around the boat ramp and through the channel as shown in Figure 2.2. These samples were used by Advisian to complete their sediment transport modelling (Advisian 2020). The samples and their respective D50's are listed in Table 3.2.

Table 3.2 MRA Sediment Samples

Sample	D50 (mm)
TBSS01	0.35
TBSS02	0.40
TBSS03	0.45
TBSS04	0.45
TBSS05	0.50
AWAC	0.55
Aqua Dopp	0.25
TS01[1]	2.10
TS02[1]	4.30
TS03[1]	4.75
TS04[1]	4.45
TS05[1]	4.10
MRA 1	0.35
MRA 2	0.55
MRA 3	0.35
MRA 4	0.50
MRA 5	0.40
MRA 6	0.45

Note: 1. Samples are fluvial sediments taken from the creek bed or pool. TS04 was taken from the dredge spoil from after a large flood event.

The DoT sediment samples from around the boat ramp have a D50 of around 0.35 mm and the samples from the channel (including sample TBSS04 from the dredge spoil) have a D50 of around 0.55 mm. The Advisian samples from Tantabiddi Creek had a much larger sediment size with a D50 of ranging from 2.3 mm to 4.8 mm. This is likely due to the sediment samples being fluvial sediments as opposed to the coastal sediments assessed by MRA and DoT. There was a significant difference between the sediment sizes of the samples taken by DoT and Advisian from the dredge spoil as shown in Table 3.3.

Table 3.3 Comparison of DoT and Advisian Dredge Spoil Sediment Samples

	D50 (mm)
DoT (TBSS04)	0.4
Advisian (TS04)	4.5

This difference is likely due to the source of the dredged material. The DoT sample was taken from dredge spoil taken from the channel at times that were not associated with flood events and as such is likely coastal sediment. The Advisian sample was taken from the southern side of the dredge spoil stockpile which consists of material dredged following the 2014 flood event and as such is likely fluvial sediment. This fluvial sediment originates from the Cape Range and Tantabiddi Terrace as discussed in section 3.3 and is generally much coarser than the local coastal sediment which leads to the larger D50.

MRA visited the site in March 2021 and collected sediment samples from six locations along the shoreline and in the nearshore area (refer Figure 2.3). These samples were analysed by Mining and Civil Geotest Pty Ltd and particle size distributions for each sample were determined. The resulting D50 of each sample is displayed in Table 3.2.

It appears that the sediment size varies along the coastline from a D50 of 0.35 mm to 0.55 mm, with the larger sediment sizes likely occurring in areas with higher wave energy. The sediment samples from the nearshore area had D50's of 0.4 mm and 0.5 mm and is slightly coarser than the sediment directly on shore (D50 = 0.35 mm).

3.6 Previous Sand Bypassing

Historically the Tantabiddi Boat Ramp has required ongoing maintenance excavation or dredging of sediment that accumulates to the south and offshore of the boat ramp. Typically the excavated material has been removed from the beach or ocean and placed onshore behind the dunes (MRA 2018).

In 2014 a severe rainfall event occurred which resulted in Tantabiddi Creek bursting through the sand dune and depositing a large amount of sand and rubble in the vicinity of the Tantabiddi Boat ramp and the channel. To remove this deposited material, bypassing using a floating dredge was conducted where sediment was dredged from the nearshore area and deposited on the beach to the north of Tantabiddi Boat Ramp (Figure 3.7). Approximately 3,500 m^3 of sand was planned to be bypassed from an area of approximately 14,000 m^2 using a bucket wheel dredger (URS 2015). However due to cost constraints the scope was later reduced (URS 2016). The sand was pumped through a 200 mm polyethylene pipe into the intertidal zone of the beach directly to the north of the boat ramp. This sand was then redistributed through natural coastal processes to renourish this section of beach.

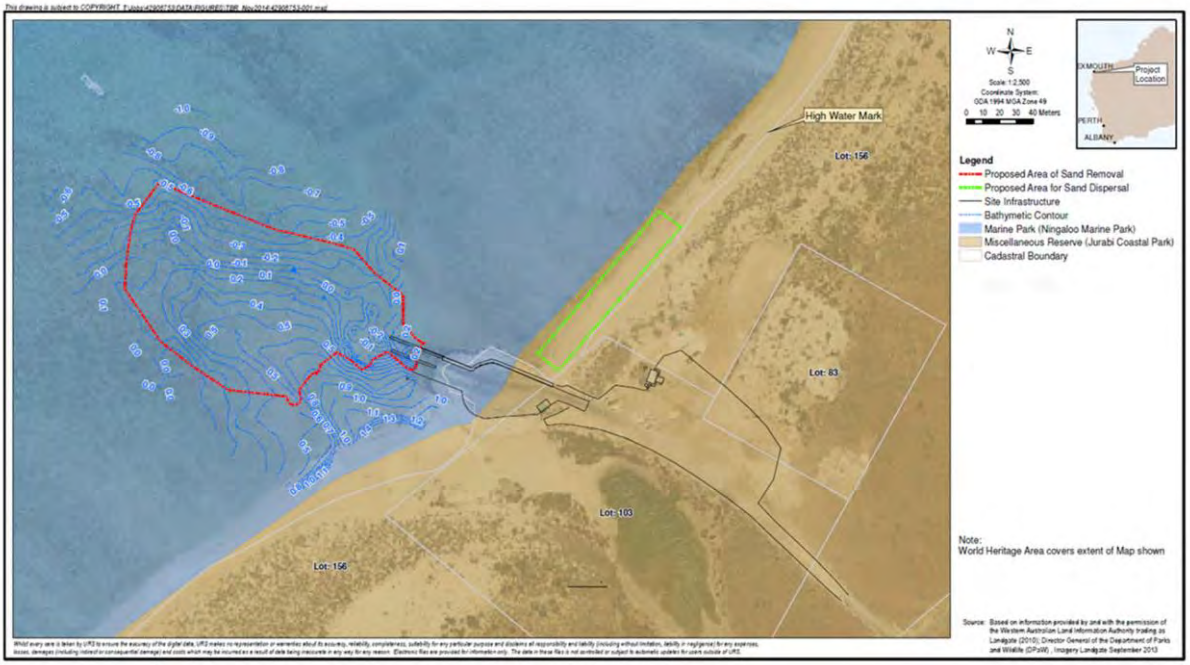

Figure 3.7 Proposed Area of Sand Removal (URS 2015)

3.7 Environmental

The site is located within the Ningaloo Marine Park (Figure 3.8) which is a UNESCO World heritage Site and as such is a very important natural resource. The *Management Plan for the Ningaloo Marine Park and Muiron Islands Marine Management Area 2005 – 2015* (MPRA 2005) details the key environmental values of the Ningaloo Marine Park. These include but are not limited to the following.

- The diverse range of seabed and coastal geomorphology.
- The high water quality of the marine reserves.
- The diverse range of species rich coral communities that occur within the reserves.
- The shoreline intertidal reef communities widely distributed throughout the reserves.
- A range of coastal communities which occur along the terrestrial portion of the park.
- The variety of resident seabirds, shorebirds, and migratory wader species in the reserves.
- The rich and diverse finfish fauna that occur in the reserves.
- The diverse and abundant shark and ray populations which include Whale Sharks and Manta Rays.
- The diverse range of whale, dolphin and turtle species that have been recorded in the reserves.
- The sheltered lagoonal areas of the reserves that provide a habitat for Dugongs.

All of these natural values require monitoring and management to ensure their conservation and to maintain the Ningaloo environment and the tourism industry which it supports.

The Ningaloo Marine park also meets two of the UNESCO World Heritage criteria for outstanding universal value.

- The lush and colourful underwater scenery and its contrast with the arid and rugged land, along with rare and large aggregations of whale sharks meet the criteria for Superlative natural phenomena or natural beauty.

- The hundreds of coral, fish, mollusc and crustacean species along with the diversity and abundance of large marine species meet the criteria for Biodiversity and threatened species.

As such Ningaloo Reef was inducted as a World Heritage Site due to its outstanding environmental and ecological value.

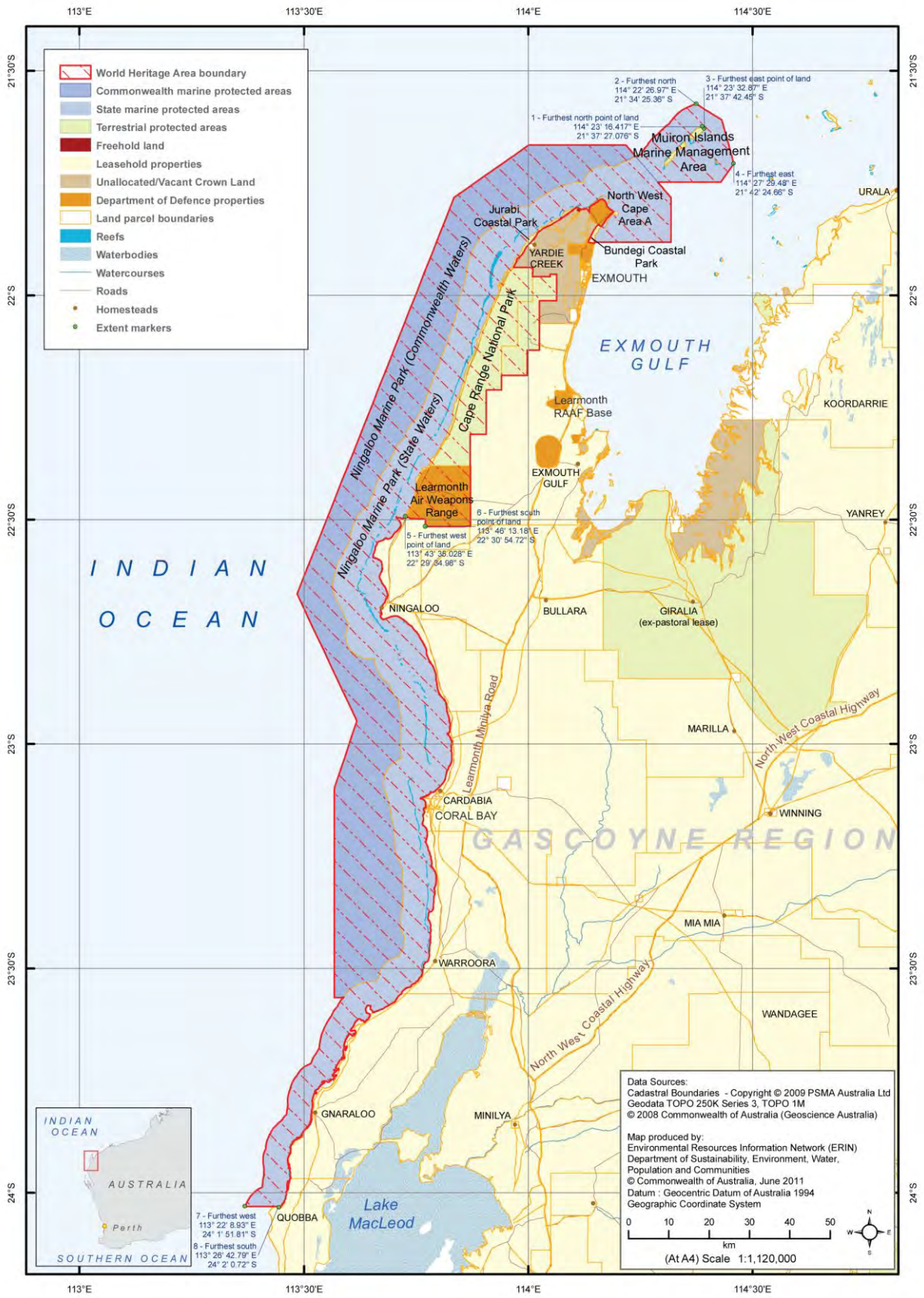

Figure 3.8 Ningaloo Marine Park (Source: Department of Agriculture, Water and Environment 2011)

4. Site Visit & Data Collection

MRA employees visited the project site and surrounding area on the 14th and 15th of March 2021. The objective of the site inspection was to collect sufficient information to ground-truth subsequent assessments. The following item were undertaken as part of the site inspection.

- Review and characterisation of the shoreline surrounding the facility, including for a distance of 1 km either side (as this is the area most susceptible to changes as a result of the TBF its characteristics need to be well known – this also provides flexibility should an alternative option need to be considered).
- Review and characterisation of the sediment properties over the nearshore, berm and dune. This included measurement of sediment depth where thin veneers are present, as well as collection of samples for particle size distribution.
- Review details of Tantabiddi Creek to ascertain potential sediment load and contribution to the nearshore environment.
- Review of the volumes of sediment adjacent to the existing facility. This included inspection of accretion volumes that may help in the preparation of a sediment budget for the area.
- Meeting with local stakeholders including the Shire, DoT and DBCA to discuss current maintenance requirements/observations for the facility with regard to sand management.

The field crew for the inspection included Coastal Engineers Liam De Lucia and Johnson Chen (MRA). The outcomes of the inspection are summarised in the following sections.

4.1 Shoreline Review & Characterisation

The inspection included review and characterisation of the shoreline at the proposed facility and a 1 km extent either side. In addition to inspection 1 km either side of the proposed facility, MRA obtained photographs at access points approximately 2 km north and south of the proposed facility. These items are shown in Figure 4.1 below.

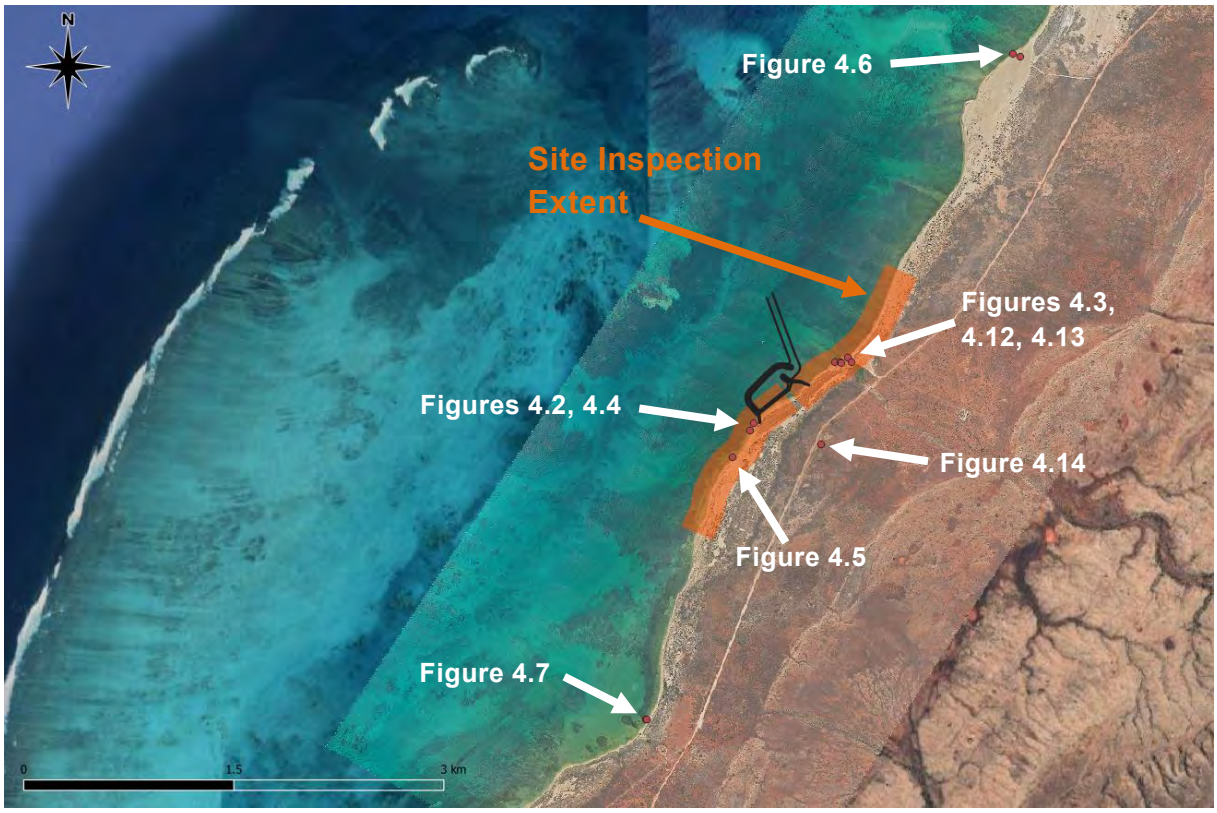

Figure 4.1 Extent of Site Inspection & Photo Locations

The following key shoreline characteristics were identified and confirmed during the inspection.

- The typical beach profile present along much of the shoreline.
- The presence and characteristics of rock in the nearshore and swash zones. This rock is covered in macroalgae making it easily identifiable.
- The presence of gravel and small rock fragments along large portions of the beach berm.
- The varying height of the dune along the shoreline.

These items are discussed and photographs provided in the following sections.

4.1.1 Typical Beach Profile

The typical beach profile at the site consists of the following.

- A beach dune varying in crest elevation from approximately 2 to 6 mCD (estimated visually).
- A debris line present at the base of the dune indicating the approximate high tide level.
- A sandy berm extending from the base of the dune to below low tide at a grade of around 1:20 (estimated visually).

- Nearshore rock (limestone pavement) starting below low tide and gradually sloping down as it extends offshore. This nearshore rock is covered in macro algae, meaning it is easily identifiable in photos and aerial imagery.

These features are shown in Figure 4.2 below.

Figure 4.2 Typical Profile along the Inspection Area

4.1.2 Dune & Shoreline Sections

The dune height was observed to vary between characteristic heights across the approximately 2 km inspection area. In some locations, the dune height was minimal, only around 1 m above the high tide debris line as shown in Figure 4.3. This is indicative of a shoreline with a long-term accretion trend resulting from wave and current driven sediment transport processes.

Waves can only deposit sediment over the elevations across which they act. This is typically up to an elevation around the high tide line. Hence, as a result, accretion caused by wave and current action can result initially in low-lying foreshore areas. As vegetation establishes on the accreted areas, wind-blown sand can be trapped leading to establishment of larger dunes. Large portions of the site appear to be accreting and dune formation is occurring gradually.

Figure 4.3 Typical Accreting Shoreline

At other locations, dunes up to 5 m high were observed with the debris line present at the toe of the dune. At these locations it is possible that a longer-term erosion trend may be present. In this scenario, the waves attack the base of dunes (formed as a result of wind-blown sand) leading to recession of the dune. Small erosion scarps can be observed in some locations.

Figure 4.4 Typical Receding Shoreline

4.1.3 Nearshore Rock & Sandy Pockets

Probing (discussed further in Section 4.2) confirmed the presence of rock in the nearshore and swash zones. This is consistent with observations from aerial imagery and the geomorphological background presented in Section 3. Anecdotally, the elevation and profile of the rock appears fairly consistent across much the site. It is generally visible just below low tide and gradually slopes downwards across the nearshore zone. Probing undertaken on the beach berm confirmed that at some locations this rock also extends onshore.

The nearshore rock is covered in macro algae, meaning it is easily identifiable in photos and aerial imagery. The rock is typically covered by a veneer of sand less than or around 50 mm thick as confirmed by probing. At other locations, there are pockets in the nearshore rock profile where

the veneer of sand is around 100 mm to 200 mm. These locations can also be easily identified from aerial photography and are shown in Figure 4.5.

Approximately 500 m south of the proposed facility, rock can be observed above low tide in the beach berm and protruding from the water surface in the nearshore. The locations of this are also shown in the following Figure 4.5.

Figure 4.5 Nearshore Beach Rock & Sand Pockets

4.1.4 Additional Inspection Points

As shown in Figure 4.1, MRA's site inspection also involved inspection at two access points approximately 2 km either side of proposed facility to allow photographs to be taken along the shoreline and any other items of interest to be inspected. Photographs from each of these inspection points are shown in Figures 4.6 and 4.7 below.

The shoreline characteristics at the northern photo point are quite unique for the inspected shoreline. At this location, highly mobile dunes are present, evidenced by the large expanse of unvegetated sand with visible ripples/waves. North of this open dune expanse, the shoreline resembles the typical accreting shoreline presented in Figure 4.4.

Figure 4.6 Additional Photo Location North of Site, Looking North (top) & South (bottom)

The shoreline characteristics at the southern inspection area were similar to those observed elsewhere along the site. A sandy beach berm, low lying dune, and patches of nearshore rock were identified as shown in Figure 4.7 below.

Figure 4.7 Additional Photo Location South of Site, Looking North (top) & South (bottom)

4.2 Sampling & Probing

MRA collected sediment samples to augment the suite of sediment information already collected, including information obtained by DoT, Advisian (2020) and Cuttler et al (2015). This included collection of 6 sediment samples for particle size distribution testing to assist MRA's review and characterisation of the sediment characteristics over the site.

Samples were collected from the dune, waterline and nearshore to allow MRA to assess the variation in sediment characteristics along the beach profile. Samples were also collected along the 2 km inspection extent to allow MRA to assess the spatial variation in sediment characteristics along the shoreline. The locations of the 6 sediment samples are listed in Table 2.2 and shown in Figure 2.2 along with the samples collected previously by DoT and Advisian (2020).

In addition to collection of sediment samples, MRA undertook hand probing to estimate the thickness of sediment layers along the shoreline. Probing was undertaken to allow MRA to assess the variance in sediment thickness along the profile and shoreline within 1 km. Some probing has been undertaken by DoT. MRA's probing was undertaken to compliment the previously completed works. A total of 50 locations were probed to investigate the depth to rock. The co-ordinates and results of the probing are presented in Table 4.1 and Figure 4.8.

Figure 4.8 Probe Locations

Table 4.1 Probe Results

Probe Number	X	Y	Depth to Rock (mm)
P1	806635.54	7572648.89	0
P2	806589.45	7572657.48	0
P3	806587.77	7572659.67	100
P4	806606.58	7572681.47	100
P5	806609.76	7572682.33	110
P6	806614.54	7572691.79	150
P7	806618.15	7572700.64	150
P8	806619.03	7572701.24	0
P9	806629.39	7572702.27	120
P10	806638.78	7572697.78	160
P11	806735.96	7572909.56	140
P12	806749.68	7572935.78	100
P13	806762.33	7572951.23	70
P14	806767.49	7572950.82	450 (max)
P15	806769.50	7572950.48	80
P16	806792.44	7573007.61	300
P17	806894.50	7573145.40	100
P18	806889.49	7573153.81	90
P19	806880.03	7573154.61	0
P20	806870.40	7573161.57	100
P21	806865.55	7573163.51	0
P22	806849.19	7573164.14	120
P23	806876.49	7573150.06	450 (max)
P24	807162.21	7573514.28	450 (max)
P25	807157.22	7573523.31	100

Probe Number	X	Y	Depth to Rock (mm)
P26	807155.27	7573526.42	0
P27	807150.74	7573529.90	0
P28	807149.35	7573532.70	0
P29	807149.65	7573533.00	450 (max)
P30	807421.21	7573685.36	450 (max)
P31	807426.96	7573700.34	0
P32	807415.94	7573694.70	0
P33	807404.18	7573740.50	290
P34	807743.89	7573925.09	290
P35	807744.45	7573924.16	100
P36	807776.48	7573960.79	0
P37	807769.47	7573969.85	60
P38	807683.64	7574017.70	40
P39	807657.12	7574028.07	30
P40	807708.05	7574002.76	180
P41	807775.87	7573959.26	80
P42	807999.99	7574330.52	200
P43	808035.72	7574439.43	200
P44	808034.87	7574440.06	30
P45	808014.39	7574450.31	90
P46	807939.51	7574485.63	60
P47	807979.83	7574461.14	0
P48	807991.15	7574452.30	250
P49	807778.27	7573831.14	300
P50	807777.95	7573829.30	0

Notes: 1. Max depth indicates that no rock was found at this location within the max probe depth of 450 mm.

The probe results generally align well with what can be observed from aerial photography. At locations where a sand was visible in the nearshore from aerial imagery, typically around 100 mm to 200 mm of sand was present. However, at locations where the limestone reef is clearly visible, either no sand, or pockets of sand less than 50 mm thick were identified. This is demonstrated in Figure 4.9 below. There is sand present in the beach berm along the entire shoreline. At several locations, rock could still be identified below the beach berm. The results of the probe locations will be interpreted further by MRA as required to inform morphological modelling.

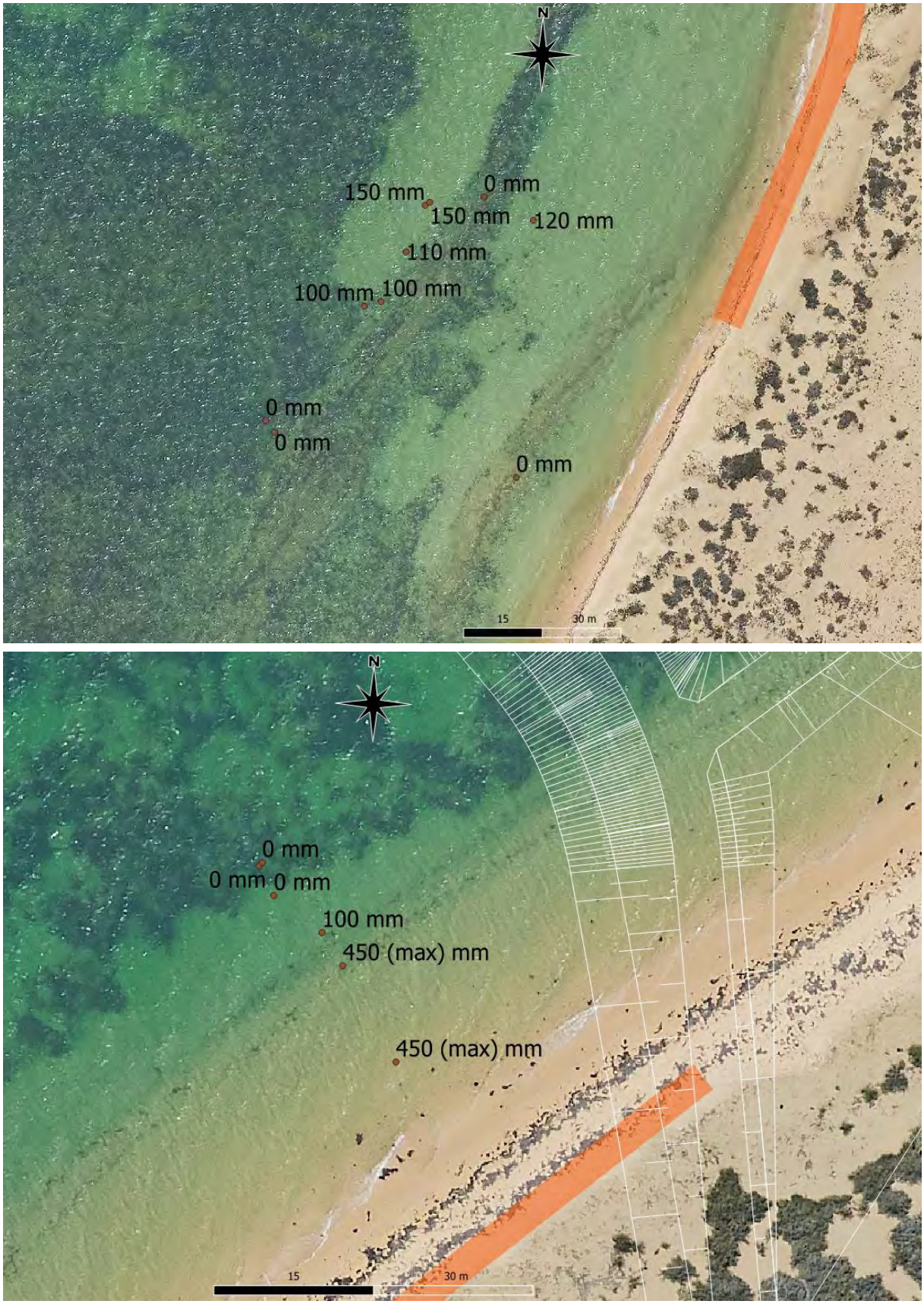

Figure 4.9 Probe Results Expanded

In November 2020 DoT conducted 32 probes of the nearshore area at Tantabiddi (Figure 4.10). The DoT probe results generally align well with what can be observed from the 2018 aerial photo. At locations where rock is clearly visible either no sand or pockets of sand less than 100 mm thick were identified. At locations where the sand is visible, typically around 100 mm to 500 mm of sand was present. The results of the DoT probing support the findings of the MRA results.

Figure 4.10 DoT Probe Locations

4.3 Key Features

Several other key features were inspected as part of the inspection. Including the following.

- The existing Tantabiddi boat ramp.
- Tantabiddi creek located immediately south of the boat ramp.
- The soak located approximately 650 m south of the existing boat ramp.

The locations of these figures are shown in Figure 4.11 and discussed in the following sections.

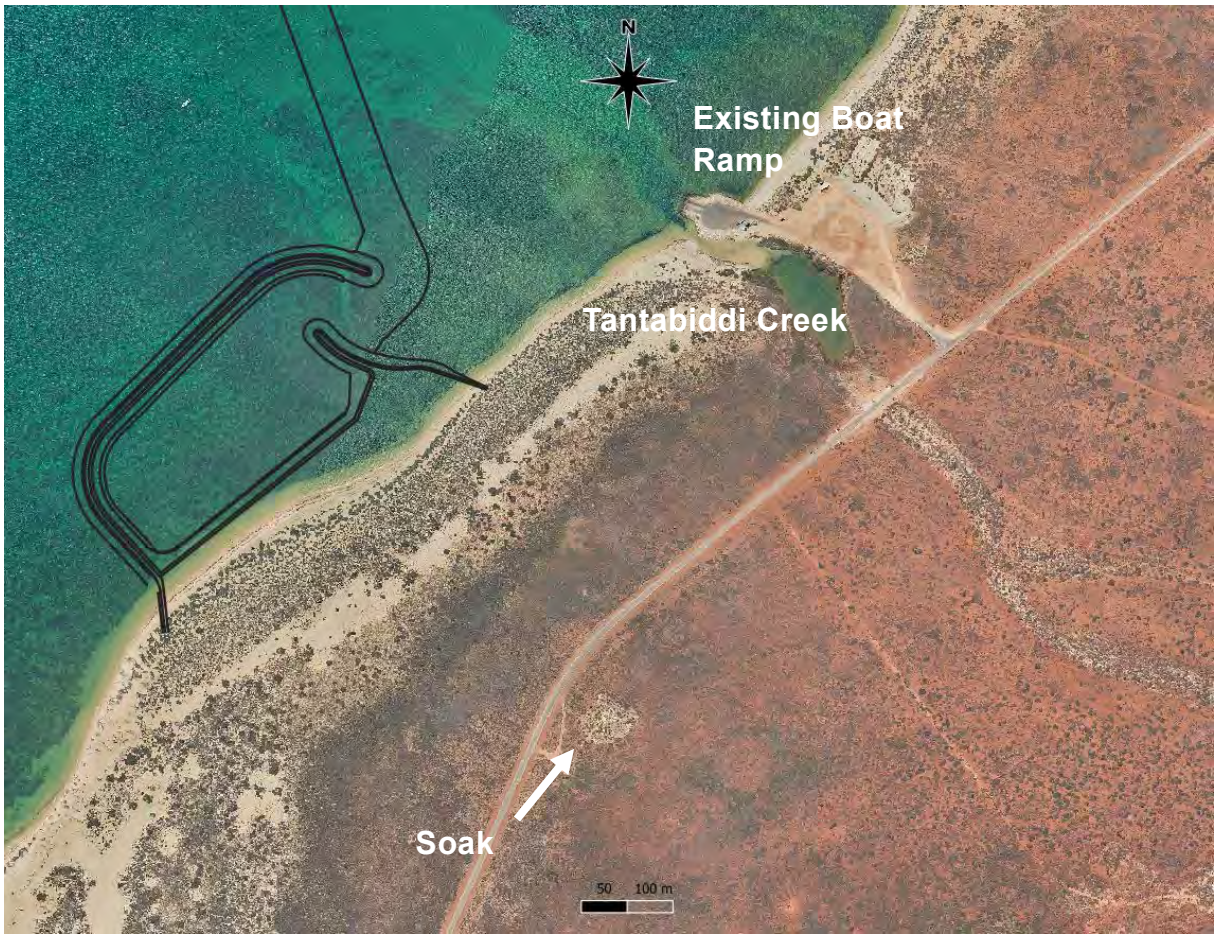

Figure 4.11 Key Features

4.3.1 Tantabiddi Boat Ramp

The existing boat ramp consists of a dual lane precast concrete panel ramp, with two fixed pile finger jetties, and rock revetment on either side. As discussed previously, the ramp acts as a barrier to sediment transport which results in accumulation of sediment on the south-western side of the ramp. The Shire advised MRA that bypassing of the ramp had recently been undertaken, and as such there was no build up on the southern side to observe. Rather, at the time of inspection Tantabiddi Creek was open to the ocean as shown in Figure 4.12 below.

A clear erosion scarp approximately 1 m high was identified on the northern side of the boat ramp. This is likely the result of material recently placed on the northern side being transport away as a result of the net north easterly longshore sediment transport at the site. This is also shown in Figure 4.12 below.

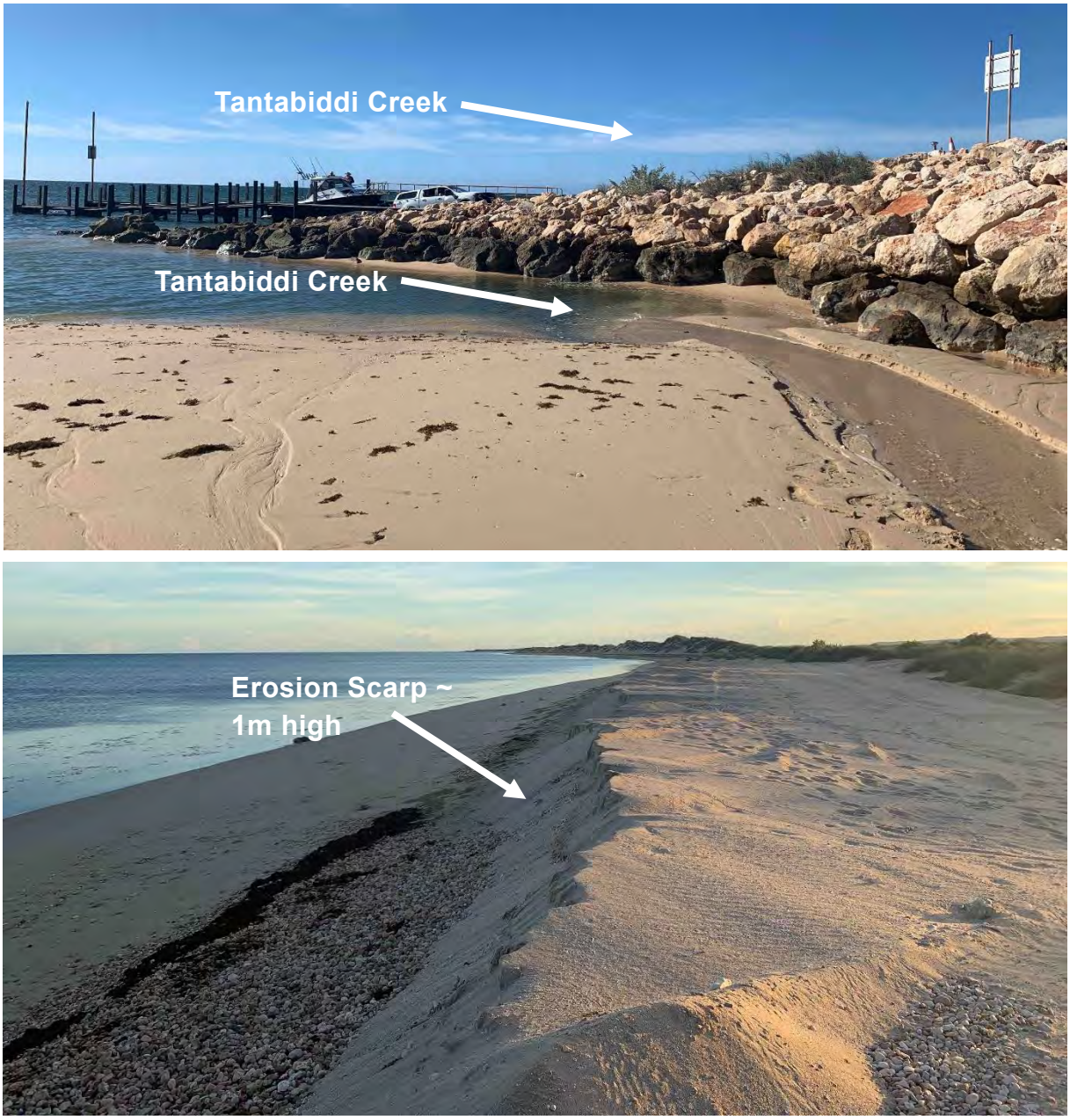

Figure 4.12 South (top) and North (bottom) of the Existing Boat Ramp (March 2021)

4.3.2 Tantabiddi Creek

Tantabiddi Creek is a key contributor to the hydrological and morphological characteristics of the site. Net sediment transport at the site is to the north east which results in accumulation of sediment on the southern side of the existing ramp. During large rainfall events water discharges from Tantabiddi Creek into the ocean washing out sediment from the creek and scouring away the build-up on the southern side of the ramp. At the time of inspection Tantabiddi Creek was open to the ocean as shown in Figure 4.13 below. However, the Shire advised this was a result of bypassing rather than a large discharge event.

Figure 4.13 Tantabiddi Creek (March 2021)

4.3.3 Tantabiddi Soak

The Soak was inspected and photographs obtained for use, if required, for hydrological and environmental purposes. It is understood this soak is of high environmental value and as such, impacts to this feature will need to be considered in the landside design of the TBF. These photographs are shown in Figure 4.14 below.

Figure 4.14 Tantabiddi Soak (March 2021)

4.4 Stakeholder Meeting

A meeting was held with various local representatives of government agencies and key stakeholders in the proposed development. The objective of the meeting was to obtain any information, anecdotal or otherwise, which may be useful in the coastal processes study and to identify any key areas of interest for the agencies when considering the impacts of the TBF. Specifically, the following key items were discussed.

- Key issues at the existing facility.

- Any anecdotal information regarding coastal processes at the site.
- Any key considerations for the coastal processes assessment.
- The key coastal impacts that are likely to be of importance to the relevant government agency.

The following representatives from the government agencies attended meeting.

Table 4.2 Stakeholder Meeting Attendees

Role	Personnel	Organisation
Field Crew (Coastal Engineer)	Liam De Lucia	MRA
Field Crew (Coastal Engineer)	Johnson Chen	MRA
Project Supervisor (Coastal Engineer)	Clint Doak	MRA
Client	Demont Hansen	DoT
Client	Tim Stead	DoT
Client Regional	Tony McCann	DoT
Client Regional	Shannon	DoT
Local Shire	Mike Richardson	Shire of Exmouth
Manager Ningaloo Marina Park	Peter Barnes	DBCA

The key outcomes from the meeting were as follows.

- There are a number of issues at the existing boat ramp. These include the poor condition of the ramp, the operational limitations and the ongoing siltation management requirements.
- The Shire had recently undertaken another bypassing operation from the south to north of the existing facility.
- There are a number of key environmental issues of relevance to DBCA. These are highlighted in documents such as the Ningaloo Marine Park Management Plan. Key environmental values include the local coral, macroalgae and turtle nesting, amongst many others.
- There are a number options being considered for the approach to the existing facility. These include (1) full removal of the ramp, (2) retention as an informal sand launching facility and (3) retention of the ramp its existing form until such a time that dilapidation requires its removal or modification.
- Following the meeting DoT reviewed and advised that the Coastal Processes Study is to be completed on the basis that the existing facility will be removed.

These outcomes will be considered in the coastal processes study.

5. Shoreline Movement Assessment

5.1 Scope

The scope of the Shoreline Movement Assessment is detailed in the following points.

- Obtain and review historical photos of the shoreline from 1969 to 2020.
- Use the historical photos of the shoreline to analyse the shoreline movement over a period of 51 years.
- Review the shoreline movements against significant cyclone events and determine possible impacts of the cyclones.
- Prepare an indicative sediment budget of the study area.
- Estimate future shoreline change based on the outcomes of the shoreline movement and indicative sediment budget.
- Develop a list of considerations and recommendations for the proposed TBF.
- Prepare a standalone report detailing the methods and results of the assessment.

This assessment is detailed in a standalone Shoreline Movement Assessment report attached in Appendix A. Key outcomes are provided in the section below. For detailed methods and outcomes refer to the standalone report.

5.2 Summary

The majority of the study area is comprised of narrow sandy beaches fronted by fringing coralgal reefs and backed by vegetated dunes. However, there are sections of the coast which differ from this including sections of rocky foreshore, a predominantly unvegetated salient, the mouth of Tantabiddi Creek and the Tantabiddi Boat Ramp.

These sections can interrupt and influence the sediment transport across the coast with the rocky foreshores providing a buffer against cross shore transport and the Tantabiddi Boat Ramp presenting an obstacle to the longshore transport.

Large flood events occasionally flush the sandbar at the mouth of Tantabiddi Creek seawards. These events can deposit large amounts of sediment in the nearshore area and effect both the cross shore and longshore transport, for months to years after the event.

The shoreline movement analysis undertaken identified that under existing conditions there is a net sediment transport of on average around 12,000 m^3 to the north each year. Seasonally, this may involve around 16,000 m^3 north and 4,000 m^3 to the south, on average.

To allow projections of impacts to the shoreline and sediment transport induced by the proposed TBF, it is assumed that the majority of seasonal and net sediment transport will be blocked by the facility. This is due to the depth of the facility extending beyond the active depth of sediment transport at the site.

There are a number of considerations for the proposed TBF related to possible future movement of the shoreline, these include the following.

- The facility will likely interrupt the longshore transport of sediment.
- This may result in a long-term accretion trend on the south west side of the facility.
- This may also result in a long-term erosion trend on the north east side of the facility.
- Possible effects of the TBF on Tantabiddi Creek.
- Possible increased rates of erosion to the north east of Tantabiddi Creek as a result of the construction of the TBF.

The following recommendations are proposed for the TBF.

- A modelling campaign to estimate the sediment movement along the coastline under ambient and extreme conditions to determine the likely effect of the TBF on the coastline. This was undertaken as part of Task 7, discussed in Section 10.
- A sediment budget be used for calibration of the sediment transport model. This was undertaken as part of Task 7, discussed in Section 10.
- Further investigation into the possible impact of the TBF on Tantabiddi Creek. This was undertaken as part of Task 7, discussed in Section 10.
- Investigate the feasibility of bypassing sediment in the order of 16,000 m^3/year from the south west side of the TBF to the north east side.

6. Metocean Climate Analysis

6.1 Scope

The scope of the Metocean Climate Analysis was to establish the nearshore and offshore wave climate and wind conditions affecting the proposed TBF. This includes three components of works:

- (1) a Nearshore Ambient Condition Assessment,
- (2) an Offshore Ambient and Extreme Conditions Analysis; and
- (3) an Ambient and Extreme Wind Conditions Analysis. The datasets utilised and analyses outputs are summarised in Table 1.1.

Table 6.1 Metocean Climate Analysis Outputs

Assessment	Datasets	Outputs
Offshore Ambient & Extreme Conditions	■ Tantabiddi Directional Wave Rider Buoy (TDWB) ■ Calibrated BoM WWIII Hindcast Wave (CWWIII)	■ JFTs broken into overall, annual and seasonal Tables. ■ Roses broken into overall, annual and seasonal Tables. ■ Time series plots of key events and periods. ■ Exceedance curves. ■ Extreme Value Analysis (EVA) omni-directional. ■ EVA directional.
Ambient & Extreme Wind Conditions	■ Wind Anemometer ■ Yardie Homestead Wind Anemometer ■ BoM WWIII Hindcast Wind	■ Joint Frequency tables broken into overall, annual and seasonal Tables. ■ Roses broken into overall, annual and seasonal Tables. ■ Time series plots of key events and periods. ■ Exceedance curves. ■ EVA directional. ■ EVA omni-directional.
Nearshore Ambient Conditions	■ Nearshore AWAC (waves) ■ Nearshore AWAC (currents) ■ Nearshore Aquadopp (waves) ■ Nearshore Aquadopp (currents) ■ Tantabiddi Tide Gauge ■ RBR	■ Joint Frequency tables (JFTs) broken into overall, annual and seasonal Tables. ■ Roses broken into overall, annual and seasonal Tables. ■ Time series plots of key events and periods. ■ Exceedance curves.

This assessment is detailed in a standalone Metocean Climate Analysis report attached in Appendix B. Key outcomes are provided in the section below. For detailed methods and outcomes refer to the standalone report.

6.2 Summary

A summary of the three components of this Task is provided below.

6.2.1 Offshore Ambient & Extreme Conditions Analysis

The offshore datasets contain the various metocean information collected offshore from the TBF, in a depth of close to 50 m. Comparison of the two datasets allowed establishment of a 42-year dataset considered appropriately reflective of experienced conditions. This allows the longer term met-ocean context of the region to be established.

These datasets are recorded at (or are representative of) a location outside the nearshore reef. Hence, they are not afforded the protection that the TBF will be. Rather, they provide an indication of the types of conditions experienced offshore from the TBF, that can be translated to the TBF via calibrated modelling. They also provide context for the nearshore assessment.

Predictably, larger wave heights are experienced outside the reef compared to inshore of the reef. Offshore swell waves typically arrive from the WSW through W. When they reach the inshore AWAC they are largely focussed to the WNW through NNW. This is likely and artefact of the refraction of swell waves as they approach the shoreline, combined with the reef passage located to the NNW.

Given these findings, along with the finding that extreme wave events, both cyclonic and non-cyclonic within the data record appear to be dominated by the north westerly conditions, it appears that the most likely cause of severe conditions at the TBF will be associated with north-westerly conditions. This shows that modelling of cyclonic and non-cyclonic events at the site must ensure that the sensitivity of conditions inshore of the reef adequately considers extreme waves arriving offshore from the northwest. This is important for design considerations such as wave penetration, navigability and structural design.

Furthermore, this demonstrates the importance in ensuring the various reef features are adequately resolved in the wave and hydrodynamic models when simulating extreme and ambient conditions at the TBF.

6.2.2 Ambient & Extreme Wind Conditions Analysis

The relevance of wind conditions in design of the TBF is largely related to the waves they may generate during both ambient and extreme conditions. The seasonal variance in sediment transport is largely attributable to the sea breeze wind system which dominates waves generated over spring and summer and lack thereof across the autumn and winter months.

Furthermore, due to the significant protection from swell waves the proposed TBF is afforded by the offshore reef, the largest waves which may be experienced from some directions, may be that which can be locally generated by extreme winds inshore of the reef. Locally generated waves are important for structural design, navigability, wave penetration and harbour tranquillity. Hence, it is important to understand the extreme wind conditions from which these may arise. Such extreme wind conditions have been considered to establish design conditions for the assessment of each of these design considerations.

6.2.3 Nearshore Ambient Condition Analysis

The nearshore datasets contain the various metocean information collected closest to the location of the TBF. Hence, assessment of these datasets provides the most relevant information for the conditions that will actually be experienced at the TBF. However, given the relatively short duration of data collected; less than 2 years for waves and currents and approximately 3.5 years

for water levels, care needs to be taken when considering how representative the assessed data is of the range of conditions that may be experienced during atypical and typical periods. A summary of observations from the assessment of nearshore data over the various data collection period is provided below.

Wave heights at the AWAC during the collection period were fairly benign, with the largest wave height recorded (during cyclone Mangga) of 0.81 m. However, given the sheltering of nearshore reef, wave heights at the site are likely to be highly sensitive to offshore directionality and water levels. Hence, if wind conditions result in wave generation from directions less sheltered by the nearshore reef, or these coincide with a higher tide, the sheltering provided by the offshore reef may be reduced. The sensitivity of wave heights at the TBF to these factors have been considered when establishing design wave heights for structural design.

It is clear that there is directional variance in waves arriving at the site. Hence, given that waves are a key driver of sediment transport at the site, similar seasonality in sediment transport fluxes would be expected. During summer, a larger trend towards northerly sediment transport would be expected due to sea breeze conditions. Whilst in winter, this trend may subside or be reversed. These processes interact with intermittent sediment discharges from the creek to drive sediment change in the area. These outcomes are important in understanding the seasonal and overall response of the shoreline to the proposed TBF. This has been investigated further by a shoreline movement assessment undertaken as part of Task 2 and calibrated sediment modelling undertaken as part of Task 7.

The proposed TBF entrance is largely protected from incident waves from the northwest through southwest. However, the diffraction of waves, particularly swell waves, needs to be considered. This assessment has established that swell waves arrive at the site largely from the WNW through NNW. Some swell waves were recorded from the N and NNE. These were limited to wave heights less than 0.4 m. Due to this, MRA considers the risk associated with penetration into the TBF and entrance to be quite small. However, a more detailed assessment of wave diffraction and penetration from the N, NE and any other relevant conditions has been undertaken as part of Task 8.

As discussed previously, metocean conditions can vary significantly from year to year and during extreme events. Over the short duration of nearshore data collected for this assessment it is unlikely that this range of conditions is captured. The nearshore assessment is useful for establishing the metocean context at the TBF and calibration of the wave and hydrodynamic model.

7. Cyclonic Modelling

7.1 Scope

The scope of the cyclone modelling assessment was heavily influenced by the fact that the length of the reliable cyclone data record is relatively short compared to the severity of the events that need to be simulated. This relative paucity in data means that predictions of statistically reliable extreme cyclonic events require a more detailed analysis and modelling approach. A brief overview of the scope of this assessment is provided below.

- Analyse the historical cyclone database.
- Generation of a 10,000 year synthetic cyclone database through the use of a Markov Chain Multi Carlo (MCMC) model.
- Ranking the simulated cyclones based on predicted surge at Tantabiddi.
- Setup and calibration of the Delft3D model for simulation of cyclonic water levels, wave heights and current speeds.
- Use the Delft 3D model to simulate the most severe cyclone events within the region.
- Conduct extreme analysis using the modelled cyclone events to determine appropriate design conditions for the TBF.

This assessment is detailed in a standalone Cyclone Modelling report attached in Appendix C. Key outcomes are provided in the section below. For detailed methods and outcomes refer to the standalone report.

7.2 Summary

A 10,000 year cyclone record was simulated using the validated MCMC cyclone track model. This resulted in approximately 116,000 cyclones occurring in the Australian region over the simulation. The majority of these cyclones would have little to no effect on the Tantabiddi site and as such the cyclone database needs to be interrogated and the relevant events identified.

When considering the selection of relevant events within the Tantabiddi region, it is important to note that the presence of the fringing reef system at Tantabiddi provides a high degree of sheltering against wave impact at the shoreline, as shown in the Task 3 report. This protection ultimately occurs as the reef system causes depth limitation and frictional wave energy losses as the waves travel onshore. As a result, the primary variate for determining the relative severity of events at the TBF will be the total water levels (including both tide and storm surge) that occur at the site.

For substantial storm surge to occur at a location during a cyclone event a combination of onshore winds, large pressure drop and sizeable waves are required. As tropical cyclones rotate clockwise in the southern hemisphere it stands to reason that the cyclone will need to pass to the south west and reasonably close to Tantabiddi to maximise the onshore winds, waves and pressure drop. This will likely result in significant water level set up at the site. Applying this filter to the overall cyclone dataset reduced the number of cyclones from the initial 116,000 to roughly 6,900.

The filtered cyclone dataset was then ranked using a simplified parametric ranking equation. This ranking was based on the distance (D) and pressure drop (Pd) whilst also considering the local tidal level (T) and the effect that this has upon the overall water level. The simplified form of the parametric ranking equation is presented below.

$$R = 2.5\left(e^{-0.01D+0.0001Pd}\right) + T - 5$$

This equation allowed for the ranking of the filtered cyclone dataset and the selection of 200 cyclone events that were likely to cause elevated water levels at the site. The simplified form of the parametric ranking equation does not consider the bearing of the cyclone as accounted for by the initial filter.

The initial 200 cyclone events were modelled using Delft3D. The results of the modelling were then used to determine the effect that the bearing and direction of approach of the cyclone has upon the total water levels at the site.

The results of the modelling showed that due to the location of Tantabiddi on the northern portion of the North West Cape the direction of approach of the cyclones can have a large impact on the level of surge encountered at the site. Cyclones that approach Tantabiddi from the east and pass through the Exmouth Gulf cause significant water level set down at the site as the cyclone approaches. This set down can then offset any set up that occurs once the cyclone passes to the south west of the site.

Using this information, MRA's previously adopted standard parametric ranking equation was calibrated against the results from the Delft3D modelling of the initial 200 events. The calibrated parametric ranking equation was then used to re-rank the filtered cyclone database. Following this re-ranking a visual inspection of the cyclone tracks was conducted and the top 75 events that had not already been modelled were selected for additional modelling. This provided confidence that the top water level events (i.e. most severe events) have been modelled as part of the assessment.

The results of modelled top 275 cyclone events from the cyclone ranking were utilised to determine design water levels, wave heights, current speeds and wind speeds for the 50, 100 and 500 year ARI cyclone events.

7.2.1 Water Levels & Wave Heights

The output locations for the water levels and wave heights are presented in Figure 7.1.

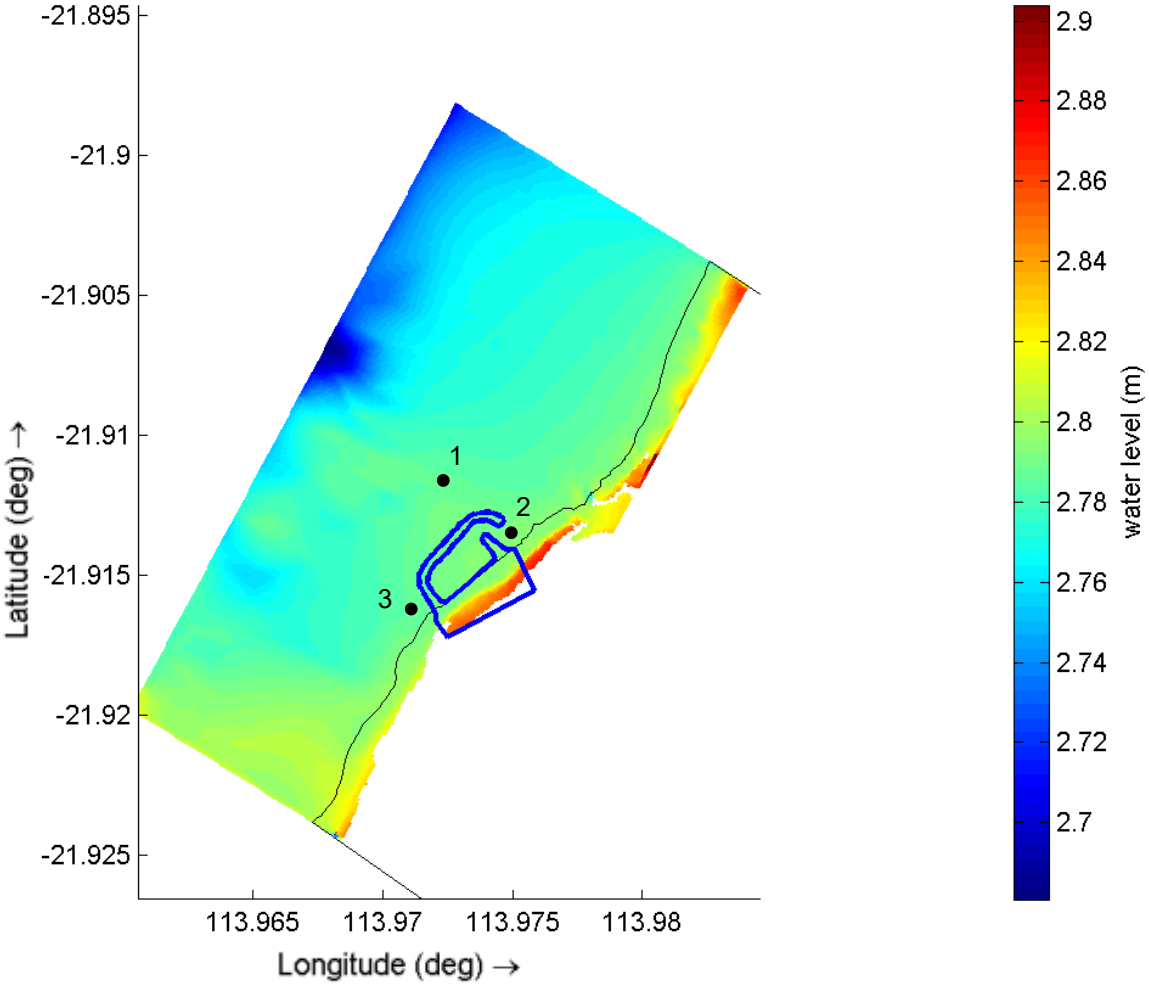

Figure 7.1 Nearshore Water Level Distribution Example with Extraction Locations

The following tables outline the nearshore water levels, shoreline water levels and wave heights at these locations for a number of ARI scenarios and timeframes. It is noted that the shoreline water levels were determined by adding an allowance for wave setup at the shoreline to the previously determined nearshore water levels.

Table 7.1 Design Nearshore Water Levels

ARI		Water level (mAHD)		
		Present Day	2071	2121
50	Location 1	2.3	2.4	3.0
	Location 2	2.3	2.4	3.0
	Location 3	2.3	2.4	3.0
100	Location 1	2.5	2.6	3.1
	Location 2	2.5	2.6	3.1
	Location 3	2.5	2.6	3.1
500	Location 1	2.8	3.0	3.6
	Location 2	2.8	3.0	3.6
	Location 3	2.8	3.0	3.6

Table 7.2 Design Shoreline Water Levels

ARI	Water Level (mAHD)		
	Present Day	2071	2121
50	2.8	2.9	3.5
100	3.0	3.1	3.6
500	3.3	3.5	4.1

Table 7.3 Design Wave Heights

Design Event		Significant Wave Height (m)		
		Present Day	2071	2121
50 year	Location 1	1.4	1.5	1.7
	Location 2	1.2	0.8	1.1
	Location 3	1.2	1.1	1.3
100 year	Location 1	1.5	1.6	1.8
	Location 2	1.2	0.9	1.1
	Location 3	1.2	1.1	1.2
500 year	Location 1	1.6	1.65	1.85
	Location 2	1.3	1.1	1.2
	Location 3	1.2	1.3	1.4

Table 7.4 Corresponding Wave Periods For Design Wave Heights

Design Event		Peak Period (s)		
		Present Day	2071	2121
50 year	Location 1	3.6	3.6	3.4
	Location 2	3.5	3.1	3.1
	Location 3	3.5	3.2	3.5
100 year	Location 1	3.3	3.6	3.6
	Location 2	3.2	3.2	3.5
	Location 3	3.5	3.4	3.5
500 year	Location 1	3.4	3.6	3.6
	Location 2	3.5	3.1	3.5
	Location 3	3.6	3.6	3.7

The range of wave directions at each of the selected output locations that result in significant wave heights during the modelled cyclone events are presented in the following table.

Table 7.5 Wave Direction Ranges

Location	Wave Direction Range (deg)
1	270 – 20
2	10 – 30
3	250 – 340

7.2.2 Depth Averaged Currents

The design currents for each of the ARI events and planning timeframes were determined at the three locations shown in Figure 7.2.

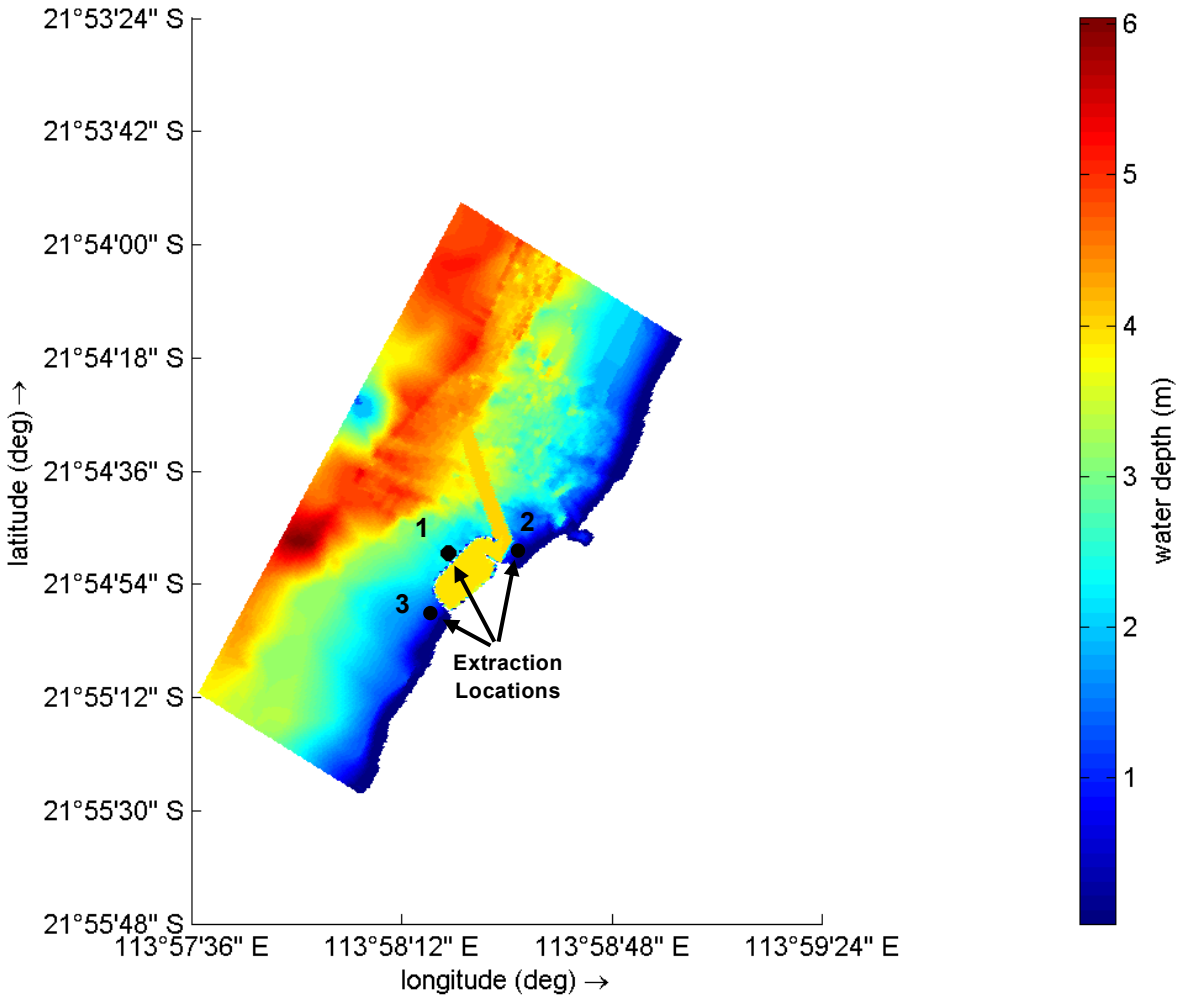

Figure 7.2 Current Extraction Locations Concept B

The resulting maximum current speeds at these locations for each of the ARI scenarios and planning horizons are presented in Tables 7.6.

Table 7.6 Design Current (Depth Averaged) Speeds

Design Event		Depth Averaged Speed (m/s)		
		Present Day	2071	2121
50 year	Location 1	3.4 – 3.6	3.4 – 3.6	3.4 – 3.8
	Location 2	0.9 – 1.4	1.0 – 1.2	1.3 – 1.5
	Location 3	1.0 – 1.1	0.9 – 1.0	0.8 – 1.1
100 year	Location 1	3.0 – 4.2	3.1 – 4.3	3.1 – 4.6
	Location 2	0.5 – 0.8	0.7 – 0.8	0.7 - 2.2
	Location 3	0.9 – 1.0	0.9 – 1.5	1.0 – 1.7
500 year	Location 1	3.4 – 4.0	3.6 – 4.1	3.7 – 4.5
	Location 2	0.7 – 1.5	0.7 – 1.5	0.5 – 1.6
	Location 3	1.0 – 1.2	1.1 – 1.2	1.0 – 1.1

7.2.3 Wind Speeds

To determine the design wind conditions that are applicable for the proposed TBF an EVA of the modelled cyclone wind speeds was conducted. The maximum wind speeds at the site from each of the 275 modelled cyclone events were extracted and used as inputs for the wind speed EVA. The wind direction was not considered in this EVA and as such this analysis presents a omni-directional assessment of the wind speeds.

The results of the EVA of the cyclonic wind speeds are presented in Figure 7.3.

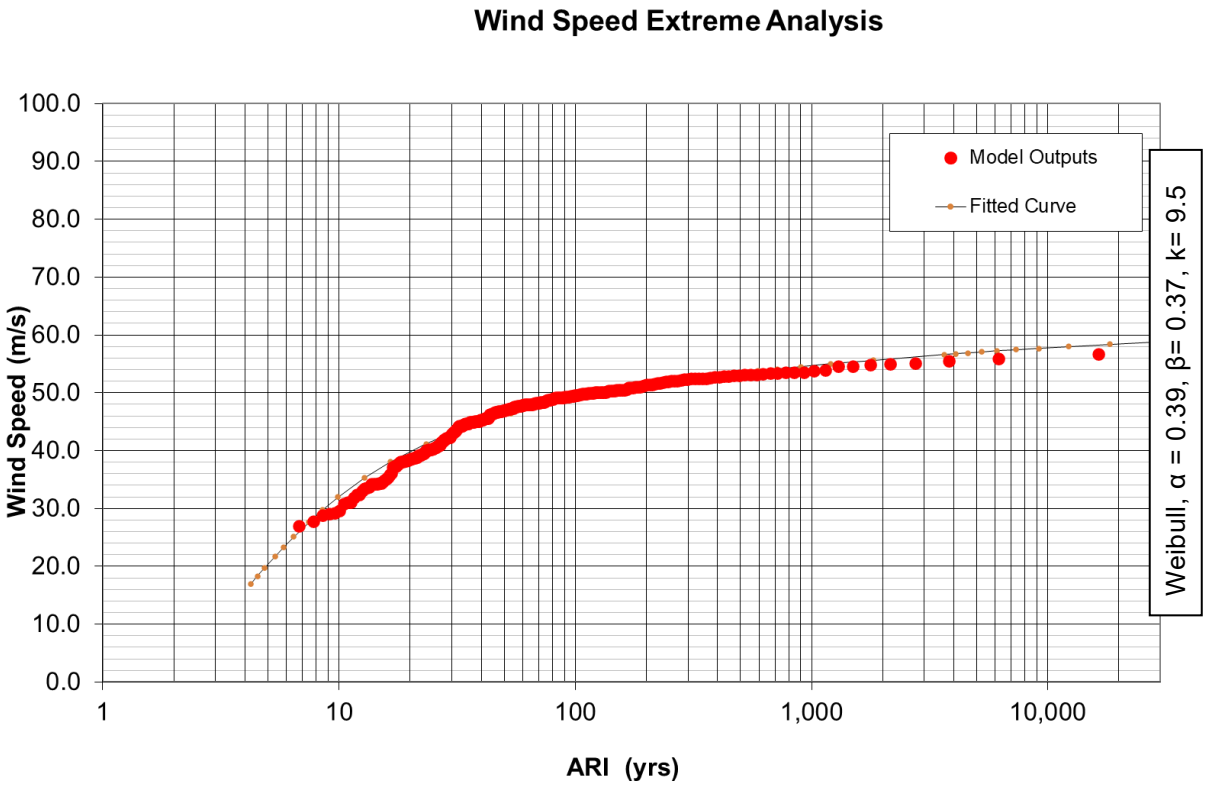

Figure 7.3 Wind Speed EVA

It should be noted that the wind speeds used in the EVA are ten minute averaged. Table 7.7 presents design wind speeds for a range of ARI scenarios taken from the EVA.

Table 7.7 Design Wind Speeds (Ten Minute Average)

ARI	Wind Speed (m/s)
50	47
100	49.5
500	53

Note: These wind speeds are ten minute averages.

7.2.4 Summary

The selected design conditions for each of these ARI scenarios are summarised in Table 7.8.

Table 7.8 Design Conditions Summary

	Present Day			2071			2121		
	50 year Design Event	100 year Design Event	500 year Design Event	50 year Design Event	100 year Design Event	500 year Design Event	50 year Design Event	100 year Design Event	500 year Design Event
Nearshore Water Level (mAHD)	2.3	2.5	2.8	2.4	2.6	3.0	3.0	3.1	3.6
Shoreline Water Level (mAHD)	2.8	3.0	3.3	2.9	3.1	3.5	3.5	3.6	4.1
Wave Heights (m)	1.4	1.5	1.6	1.5	1.6	1.65	1.7	1.8	1.9
Current Speeds (m/s)	3.4 – 3.6	3.0 – 4.2	3.4 – 4.0	3.4 – 3.6	3.1 – 4.3	3.6 – 4.1	3.4 – 3.8	3.1 – 4.6	3.7 – 4.5
Wind Speeds (m/s)	47	49.5	53						

8. Wave Modelling

8.1 Scope

The scope of work completed for this task was as follows.

- Setup the SWAN wave model for the area, including a nested grid framework to provide adequate resolution around the facility.
- Calibrate the SWAN model to available measurement data.
- Review and select appropriate periods for modelling of local wave conditions.
- Use the calibrated SWAN model to simulate the selected periods pre and post construction of the TBF.
- Review the impact of the TBF on the local wave climate.
- Provide recommendations on improvements to the TBF concept if the wave modelling results suggest that undesirable impacts are likely.

This assessment and scope is focused on the more typical wave conditions that will be experienced at the site and does not include assessment of the impacts of severe wave conditions. Severe wave conditions at the site are associated with the passage of tropical cyclone events, so further details regarding extreme conditions are provided in the Task 4 *Cyclone Modelling* report.

This assessment is detailed in a standalone Wave Modelling report attached in Appendix D. Key outcomes are provided in the section below. For detailed methods and outcomes refer to the standalone report.

8.2 Summary – Concept B

The calibrated wave model was used to simulate each of the selected periods. Each period was modelled twice – once based on the existing shoreline and once including the proposed TBF. The different model simulations were then used to directly compare the wave climate in the area surrounding the TBF. As a first pass review of the differences, time history plots of wave conditions were prepared for each of the locations shown in Figure 8.1. The rationale for the selection of these locations is provided in Table 8.1.

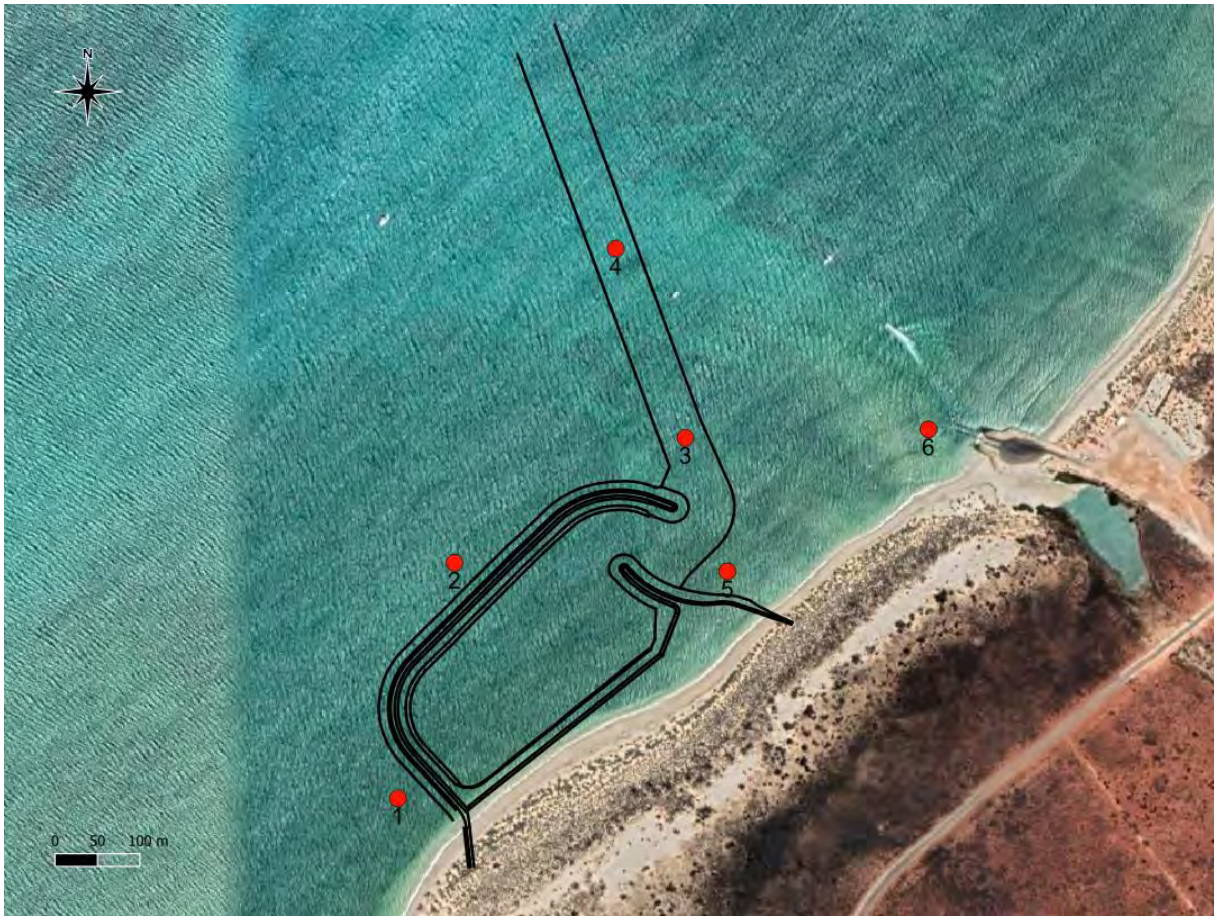

Figure 8.1 Locations used to Review Differences in Wave Conditions

As expected, the time history plots show relatively small differences between the wave conditions at most locations. A summary of the findings from the review of the time history plots is provided in Table 8.1. As part of this review, it should be noted that the SWAN model does not simulate wave reflections off breakwaters or other structures. As a result, the wave conditions presented do not show the full wave climate that could be expected, though it is anticipated that wave reflections would be small due to the characteristics of the incident waves.

Table 8.1 Summary of Differences in Wave Conditions at Each Output Location

Location	Importance of Selection of Location	Observations
1	Assessment of potential wave induced changes on the beach area to the south	Some small reductions in wave heights associated with northerly events, largely during winter and a small amount in autumn. Reductions in wave heights are less than 0.1 m. Slight changes to wave directions occur during these periods with a counter-clockwise change in wave direction.
2	Assessment of potential wave induced changes immediately offshore from the facility	Very minor reductions in wave heights are noted during some periods, largely associated with northerly conditions. Changes are generally well less than 0.05 m.
3	Assessment of any wave changes in the channel adjacent to the breakwaters (to review potential navigation issues)	Reasonably persistent reduction in wave height by between 0.05 and 0.1 m across most periods.[1]
4	Assessment of any wave changes within the approach channel	Very minor changes in wave heights. Most reductions in wave height occur during periods of higher wave periods.
5	Assessment of potential wave induced changes on the beach area in the lee of the entrance	Significant reductions in wave heights during periods with westerly wave conditions combined with a clockwise rotation in wave directions. Much smaller reductions in wave conditions during northerly wave conditions.
6	Assessment of potential wave induced changes on the beach area to the north as a result of the facility and channel	Relatively minor changes to wave conditions, though changes up to around 0.05 m are observed during westerly events.

Notes: 1. The SWAN model does not simulate wave reflection off the breakwaters. Consideration of wave reflections could be completed as part of Task 9.

Not surprisingly, the wave conditions closer to the facility show a greater extent of difference than the sites further afield – largely attributable to the extent of shadowing provided by the facility from different wave directions. To better illustrate the extent of differences across different wave conditions, spatial plots have been prepared for key events which impact the area, including sea breeze, swell and storm events. Spatial plots for these events are presented in Figures 8.2 to 8.4 respectively. These show the magnitude and direction of wave changes resulting from the introduction of the TBF into the wave model.

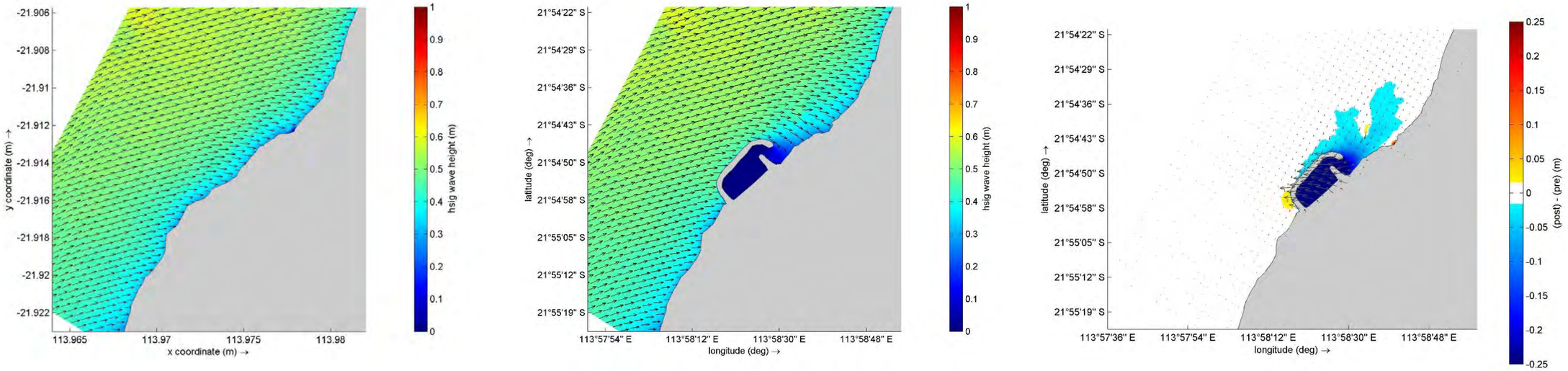

Figure 8.2 Spatial Plots for Typical Summer Sea Breeze Event

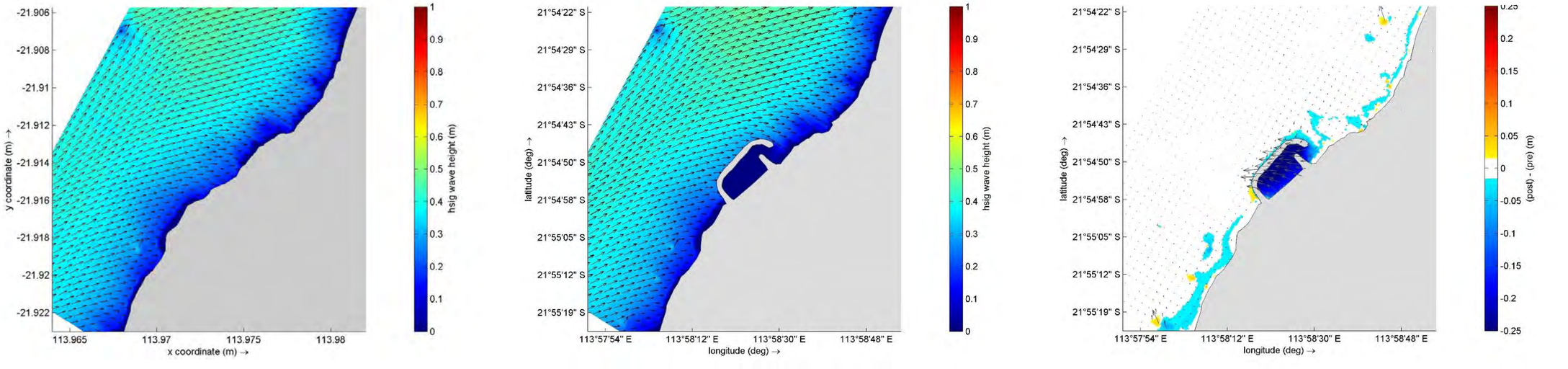

Figure 8.3 Spatial Plots for Typical Swell Event

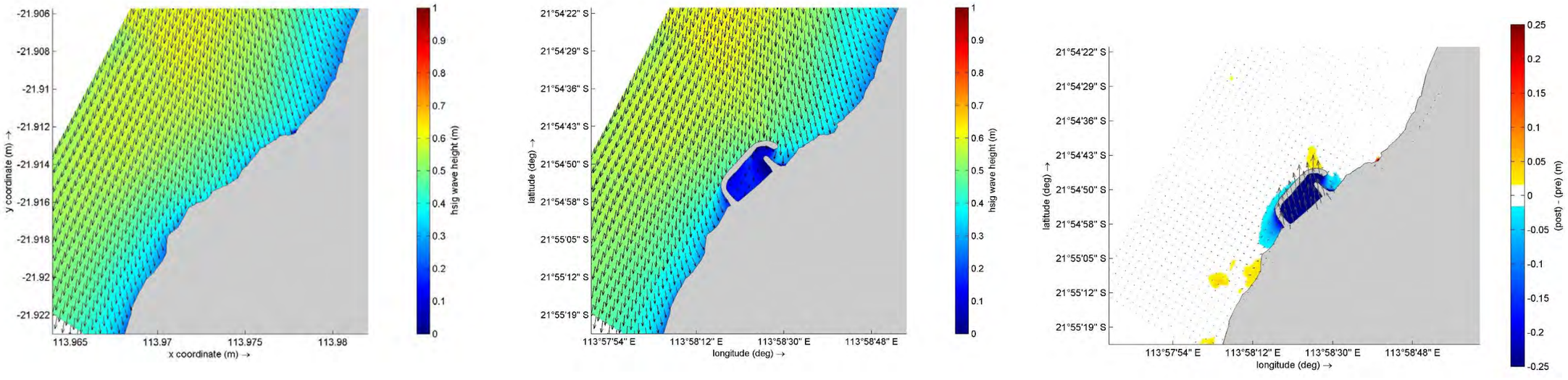

Figure 8.4 Spatial Plots for Typical Storm Event

Based on the review of the modelled wave climate surrounding the TBF, it is clear that the construction of the TBF as proposed would have a highly localised impact on the wave climate. The extent of wave shadowing is limited, though extends slightly further north than south of the facility. This means that the potential for sediment trapping in the shadows of the facility is likely to be as low as practicable, however the one item that will need further review will be the area around the entrance to the facility.

The wave climate near the entrance to the facility has been demonstrated to be quite sheltered, which is a key consideration for safe vessel navigation, however the potential consequence of this is the accumulation of sand in this area over time that will require management to ensure that it does not begin to infill the entrance channel. From review of the wave climate the potential for changes to the local sediment dynamics are quite obvious, though the extent of this change is not as clear. The sediment transport modelling, completed as Task 6, was key to understanding the potential risks associated with the sediment transport in this area and whether the accumulation of sediment on the northern side of the TBF will be problematic.

8.3 Concept C

The wave model was used to simulate each of the selected periods for Concept C. The typical year was modelled for Concept C and the results were then compared to the predevelopment results. As a first pass review of the differences, time history plots of wave conditions pre and post Concept C were prepared for each of the locations shown in Figure 8.5.

Figure 8.5 Time History Output Locations

Similar to Concept B, the time history plots show relatively small differences between the wave conditions at most locations. A summary of the findings from the review of the time history plots is provided in Table 8.2.

Table 8.2 Summary of Differences in Wave Conditions at Each of the Output Locations Concept C

Location	Importance of Selection of Location	Observations
1	Assessment of potential wave induced changes on the beach area to the south. Same location as for Concept B.	Small reduction in wave heights associated with northerly events, largely during winter. Reductions in wave heights are less than 0.1 m. Slight changes to wave direction occur during these periods with a counter clockwise change in wave direction.
2	Assessment of potential wave induced changes immediately offshore from the facility	Very minor reductions in wave heights generally well less than 0.05 m during some periods are noted.
3	Assessment of any wave changes in the channel adjacent to the breakwaters (to review potential navigation issues)	Some small reductions in wave height associated with westerly events. Reductions in wave heights are less than 0.1 m.
4	Assessment of any wave changes within the approach channel	Very minor changes in wave heights. Most reductions in wave height occur during periods of higher wave periods.
5	Assessment of potential wave induced changes on the beach area in the lee of the entrance. Same location as for Concept B.	Significant reductions in wave heights during periods with westerly wave conditions combined with a clockwise rotation in wave directions. Much smaller reductions in wave conditions during northerly wave conditions.
6	Assessment of potential wave induced changes on the beach area to the north as a result of the facility and channel. Same location as for Concept B.	Relatively minor changes to wave conditions, though changes up to around 0.05 m are observed during westerly events.

Notes: 1. The SWAN model does not simulate wave reflection off the breakwaters. Consideration of wave reflections could be completed as part of Task 9.

Similar to Concept B, the wave conditions closer to the facility show a greater extent of difference than the sites further afield – largely attributable to the extent of shadowing provided by the facility from different wave directions. To better illustrate the extent of differences across different wave

conditions for Concept C, spatial plots have been prepared for the same key events as assessed for Concept B. The spatial plots for Concept B have been provided again to allow for easy comparison of the differences between the two designs. It is noted that due to time constraints the wave, hydrodynamic and morphological modelling were completed concurrently for Concept C. As such there may be small differences between the Concept C modelling and that which was completed previously due to the changes in the bathymetry caused by sediment movement within the model. Whilst this can result in minor differences in the plots of the current magnitudes and directions the larger scale changes are what is of interest.

Overall, these plots show that whilst the extent of wave shadowing from Concept C is larger than for Concept B, the extent of influence is relatively minor. The true test of the influence of this wave shadowing will be its influence on the local sediment transport, which is assessed as Task 7.

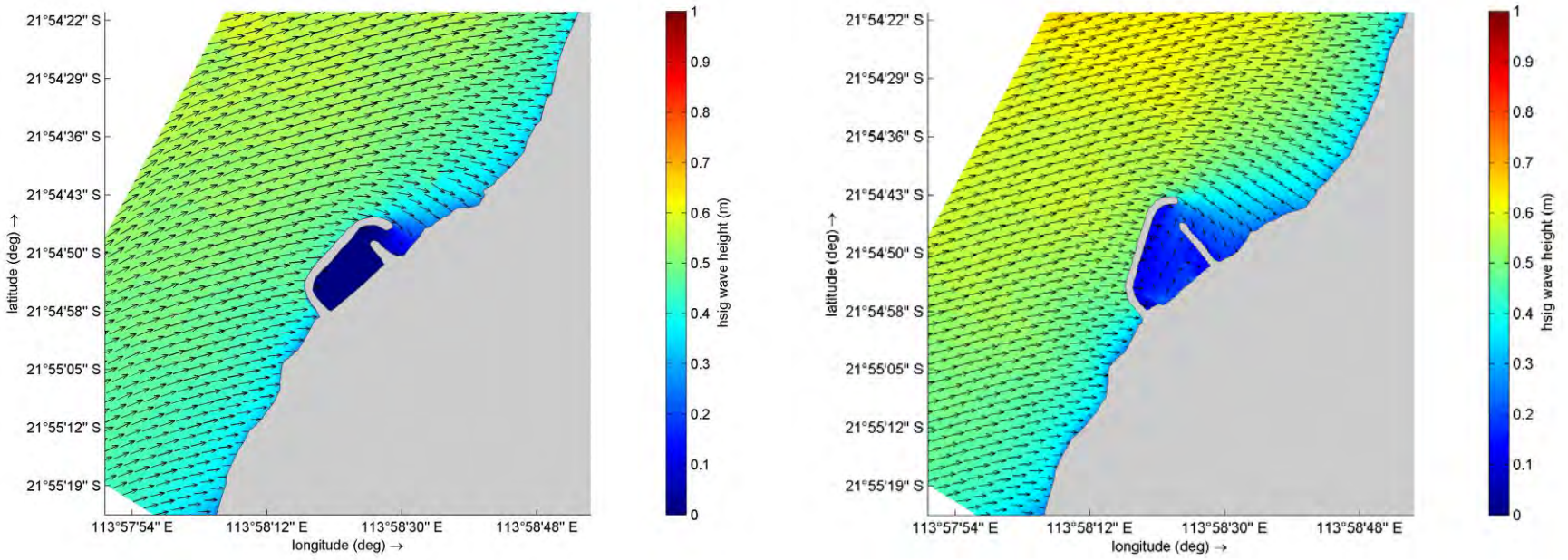

Figure 8.6 Spatial Plots for Typical Summer Sea Breeze Event for Concept B (left) & Concept C (right)

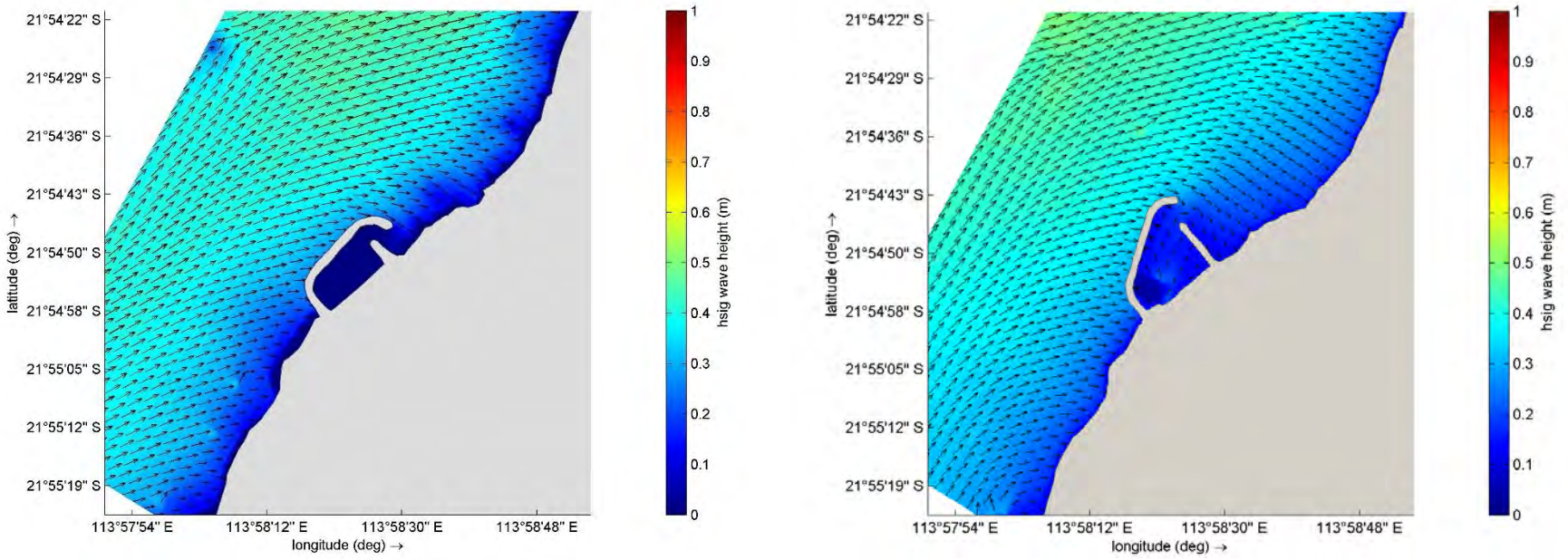

Figure 8.7 Spatial Plots for Typical Swell Event for Concept B (left) & Concept C (right)

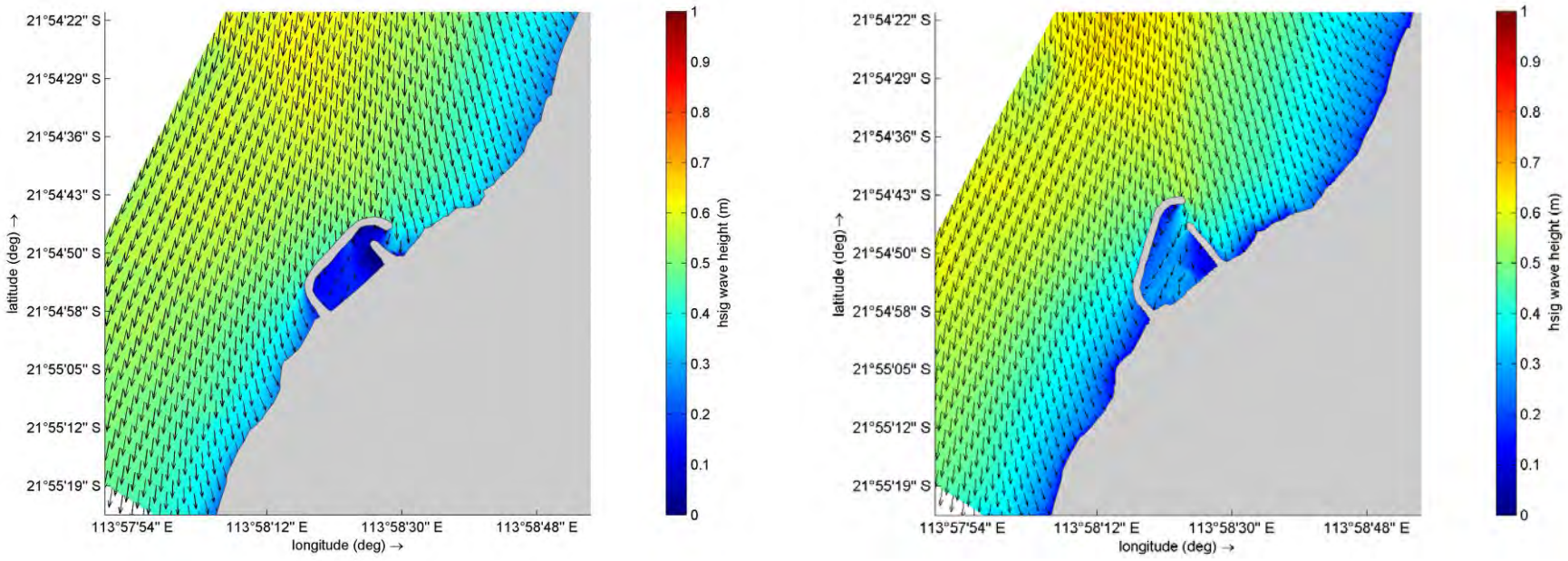

Figure 8.8 Spatial Plots for Typical Winter Storm Event for Concept B (left) & Concept C (right)

9. Hydrodynamic Modelling

9.1 Scope

The scope of work to be completed was as follows.

- Setup the coupled Hydrodynamic and Wave model for the area, including domain decomposition and nested grid frameworks to provide adequate resolution around the facility.
- Calibrate the coupled hydrodynamics and wave model to available measurement data. Calibration of the hydrodynamic model is provided herein whilst calibration of the wave component of the coupled model is provided in the Task 5 report (MRA 2021a).
- Utilise the coupled, calibrated, hydrodynamic and wave model to simulate the representative periods selected in Task 5, pre and post construction of the TBF.
- Review the impact of the TBF on the local hydrodynamics for any undesirable impacts or considerations.
- Configure the coupled, calibrated, hydrodynamic and wave model appropriately for simulation of scenarios relevant to flushing of the TBF. This includes an assessment of groundwater inputs along the coastline (note that MRA engaged Rockwater to complete the groundwater modelling).
- Simulate a selection of periods relevant to flushing from the representative periods to enable a review of flushing and e-folding times.
- Provide recommendations on improvements to the TBF concept if the hydrodynamics or flushing modelling results suggest that undesirable impacts are likely.

This assessment and scope is focused on the more typical hydrodynamic conditions that will be experienced at the site and does not include assessment of the impacts of severe weather conditions. Severe conditions at the site will be associated with the passage of tropical cyclone events, as such further details regarding extreme conditions are provided in the Task 4 *Cyclone Modelling* report (MRA 2021b).

This assessment is detailed in a standalone Hydrodynamic Modelling report attached in Appendix E. Key outcomes are provided in the section below. For detailed methods and outcomes refer to the standalone report.

9.2 Summary – Concept B

9.2.1 Current Dynamics Summary

The calibrated hydrodynamics model was used to simulate each of the selected periods. Each period was modelled twice – once based on the existing shoreline and once including the proposed TBF. The different model simulations were then used to directly compare the hydrodynamic climate in the area surrounding the TBF. As a first pass review of the differences, time history plots of current conditions were prepared for each of the locations shown in Figure 9.1. The rationale for the selection of these locations is provided in Table 9.1.

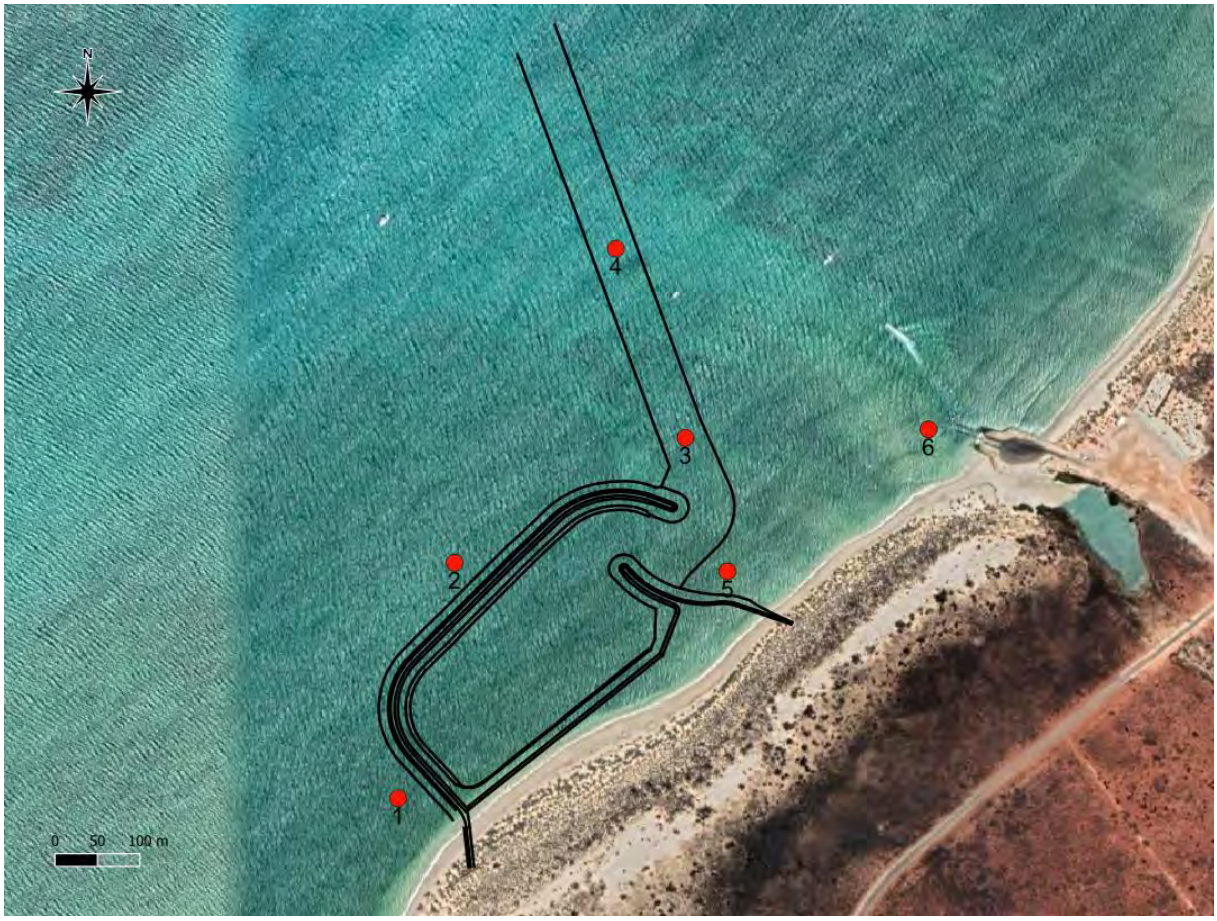

Figure 9.1 Locations used to Review Differences in Hydrodynamics

As expected, the time history plots show relatively small differences between the conditions at some locations and larger differences at other locations. A summary of the findings from the review of the time history plots is provided in Table 9.1.

Table 9.1 Summary of Differences in Hydrodynamic Conditions at Each Output Location

Location	Importance of Selection of Location	Observations
1	Assessment of potential current induced changes on the beach area to the south	Reductions in current magnitudes of typically around 50% are observed. The most significant reductions in current speeds are observed during winter, particularly during storms. Changes to current directions are observed. Where current directions were typically alongshore, they now trend cross shore, likely due to water being forced around the facility.
2	Assessment of potential current induced changes immediately offshore from the facility	Very minor changes in current magnitudes and directions are observed.
3	Assessment of any current changes in the channel adjacent to the breakwaters (to review potential navigation issues)	Significant reductions in current magnitudes are observed. Outside of winter storms, currents are reduced to almost zero. A clockwise rotation of current directions is observed across all periods.
4	Assessment of any current changes within the approach channel	Very minor changes in current magnitudes and directions are observed.
5	Assessment of potential current induced changes on the beach area in the lee of the entrance	Significant reductions in current magnitudes are observed. Outside of winter storms, currents are reduced to almost zero. During northerly conditions this reduction is less significant. A clockwise rotation of current directions is generally observed.
6	Assessment of potential current induced changes on the beach area to the north as a result of the facility and channel	Very minor changes in current magnitudes and directions are observed.

Not surprisingly, the current conditions closer to the facility show a greater extent of difference than the sites further afield – largely attributable to the extent of shadowing provided by the facility from different directions. To better illustrate the extent of differences across different metocean conditions, spatial plots have been prepared for key events which impact the area, including sea breeze, swell and storm events as well as spring and neap typical ebb and flood tides. Spatial

plots for these events are presented in Figures 5.2 to 5.8 respectively. These show the vector of current changes resulting from the introduction of the TBF into the hydrodynamics model.

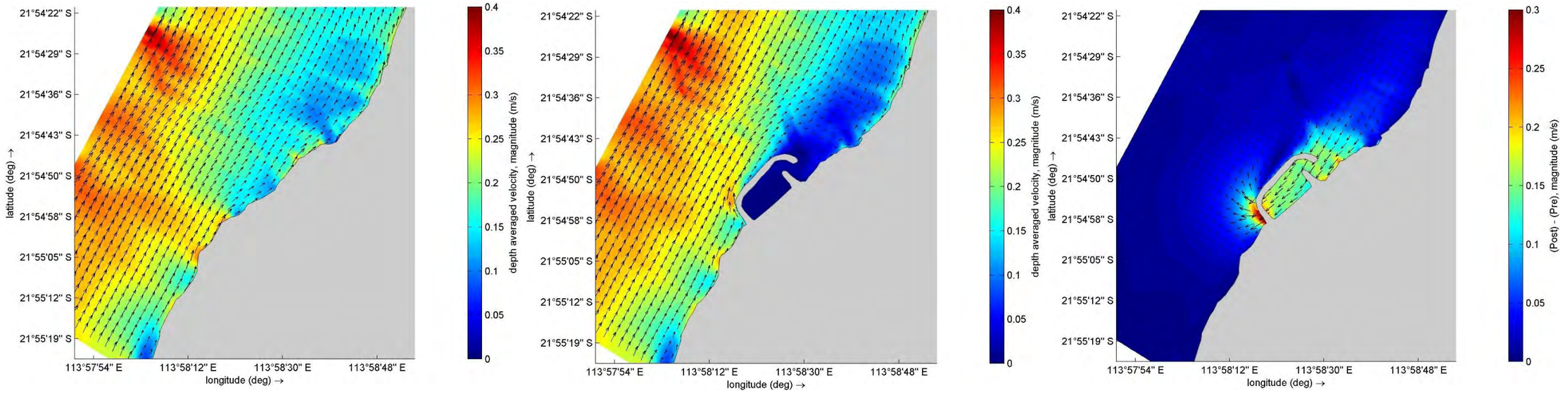

Figure 9.2 Spatial Plots for Summer Sea Breeze conditions (pre – left, post - centre, difference - right)

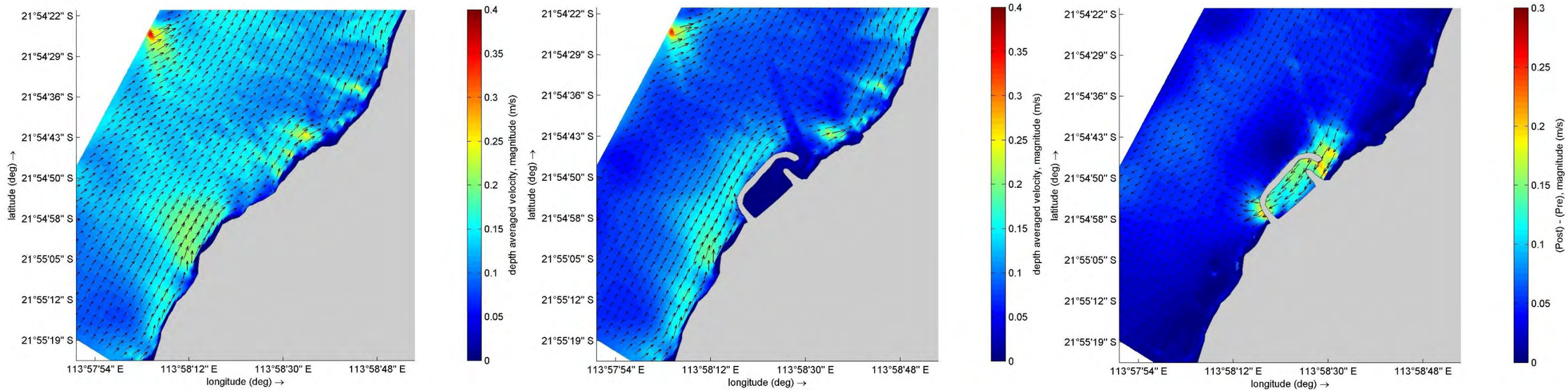

Figure 9.3 Spatial Plots for Calm Conditions with Moderate Background Swell (pre – left, post - centre, difference - right)

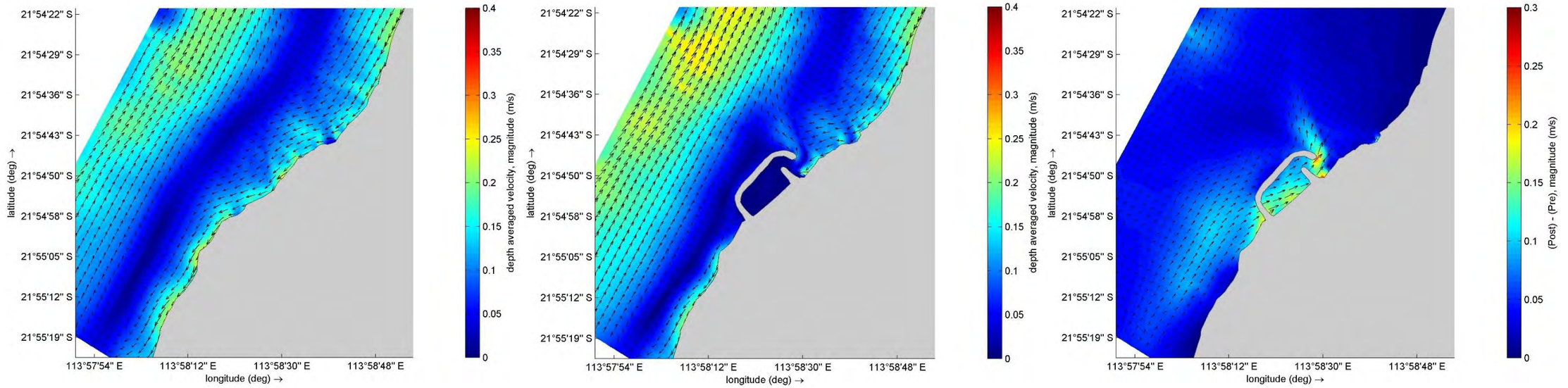

Figure 9.4 Spatial Plots for Typical Storm Conditions (pre – left, post - centre, difference - right)

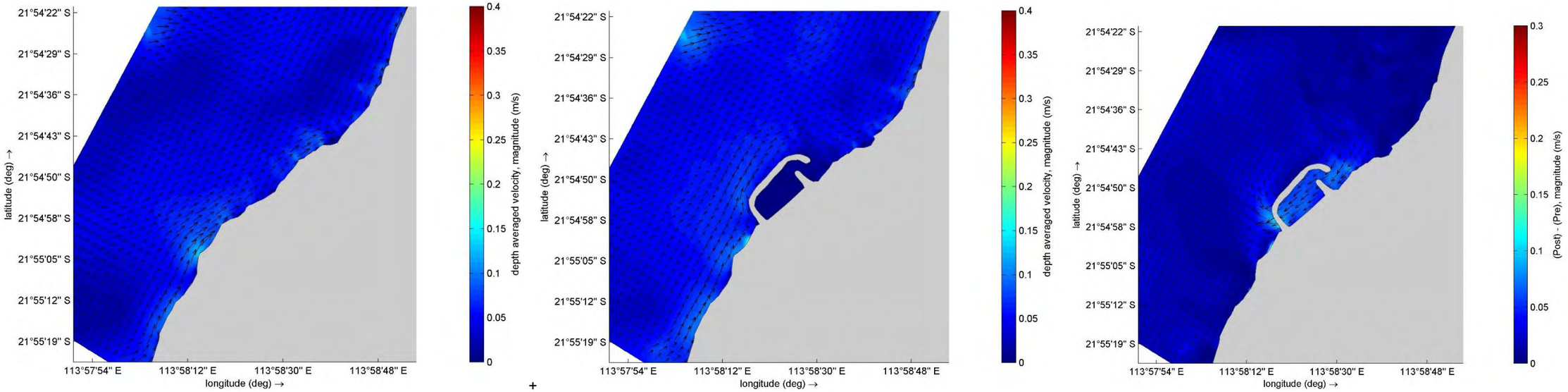

Figure 9.5 Spatial Plots for Spring Flood Tide (pre – left, post - centre, difference - right)

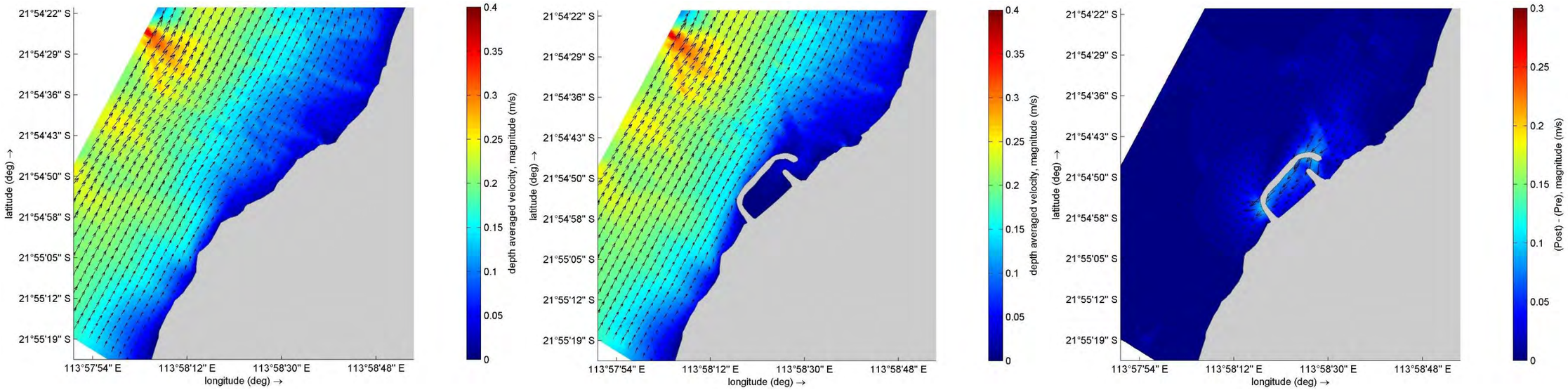

Figure 9.6 Spatial Plots for Spring Ebb Tide (pre – left, post - centre, difference - right)

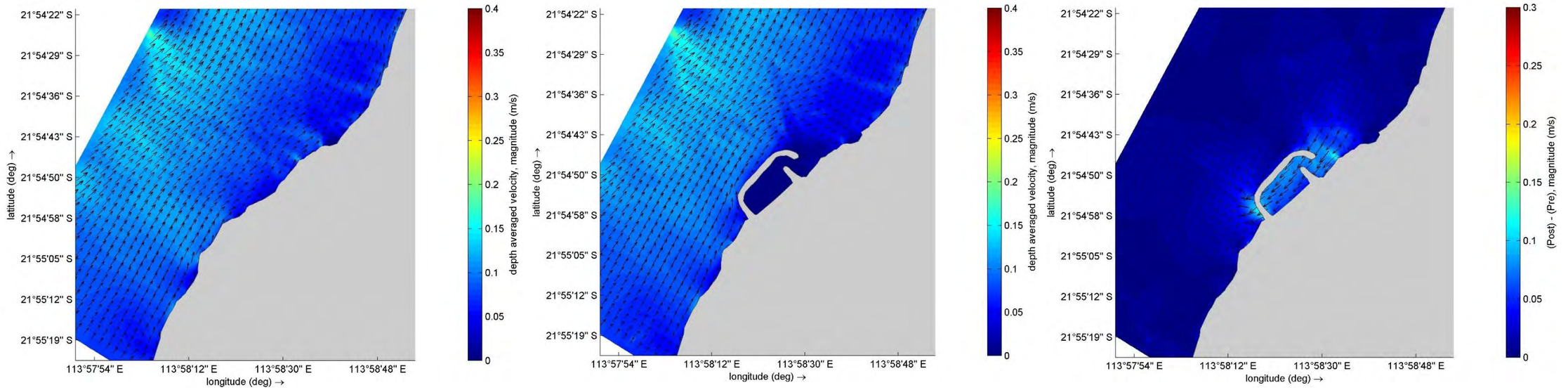

Figure 9.7 Spatial Plots for Neap Flood Tide (pre – left, post - centre, difference - right)

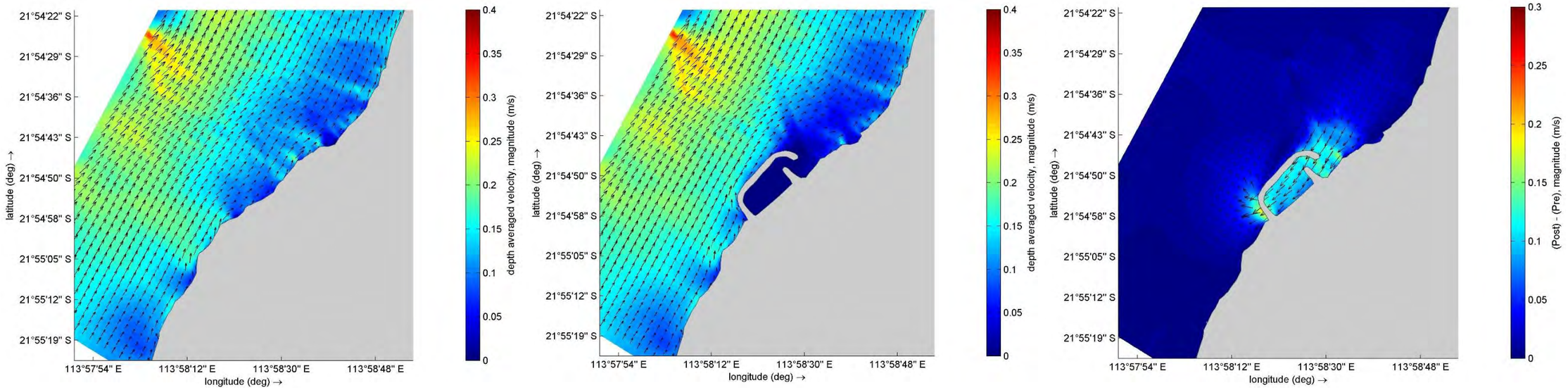

Figure 9.8 Spatial Plots for Neap Ebb Tide (pre – left, post - centre, difference - right)

Observable impacts to currents dynamics extend around 500 m either side of the facility. Beyond this, impacts to currents are negligible. The key observations from the current dynamics assessment are summarised below.

- The introduction of the TBF causes a large reduction in the current magnitudes inside the breakwaters and a few hundred metres to the north and south of the facility. Beyond this, changes to current magnitudes are negligible.

- Changes to current directions extend further than changes to current magnitudes with observable changes present up to approximately 500 m from the proposed facility.

- Changes to the current dynamics likely arise from a combination of the training of flow around the facility and wave shadowing reducing wave generated currents in the lee of the breakwaters. Both of these factors reduce currents immediately adjacent to the facility. The training of flow around the facility also results in a small increase in currents slightly offshore from the southern breakwater during periods dominated by southerly conditions.

Overall, the outcomes of the assessment are reasonably intuitive and expected. At the site, waves are the key driver of sediment transport. Changes to the current dynamics outlined above are unlikely to have any impact to the operation of the facility beyond those impacts already established through the wave modelling assessment presented in Task 5 (MRA 2021a).

9.2.2 Flushing Summary

Flushing is a measure of the rate of renewal of waters within a defined water body. A water body that is efficiently flushed experiences a turnover in water that results in local water quality very near that of the adjacent source water. Assuming that the source water quality meets environmental and aesthetic standards, efficient flushing generally indicates that the adjacent water body will also meet those standards (RPS 2017).

The calibrated hydrodynamics model was configured for the purposes of the flushing study and then utilised to simulate representative periods. Groundwater discharges are an important consideration for flushing and water quality. Average groundwater discharge flows at the site were established by Rockwater (2021).

A total of 8 scenarios were simulated to enable assessment of flushing and water quality. The four typical representative periods were each simulated once with groundwater discharge. These periods are intended to show the likely flushing conditions within the proposed TBF across a typical year. The Autumn (2013) and Spring (2007) were then simulated with no groundwater discharge flows. These are intended to consider the most conservative flushing cases. Additionally, the Autumn 1998 period was also modelled with and without groundwater as this period was specifically selected for modelling of flushing due to its sustained low wind speeds. A summary of the modelled cases is provided in Table 9.2.

Table 9.2 Modelled Cases

Season	Including Groundwater Input	No Groundwater Input
	Case I	Case II
Autumn 2013	✓	✓
Winter 2011	✓	
Spring 2007	✓	✓
Summer 2016	✓	
Autumn 1998	✓	✓

Time varying outputs from the four locations shown in Figure 5.9.9 within the proposed TBF were analysed in further detail to allow assessment of tracer concentrations throughout the facility over the duration of the simulation.

Figure 9.9 Locations used to Track Change in Tracer Concentration

The maximum time taken for the tracer to dilute below the e-folding level (~37%) is shown for each location and for each scenario in Table 9.3. The maximum e-folding time at any site in any of the scenarios was approximately 1.7 days.

The e-folding times can be put into context with measurements undertaken at Hillary's Marina (Schwartz and Imberger 1988). Based on measurements made in the months of April and May 1987, during a period when winds speeds were up to 12 m/s, the flushing time for Hillarys Marina was calculated to be 5 days. This is far greater than the longest e-folding times predicted for the TBF which were based on a wider sample of weather conditions. Further context can be provided by review against modelling undertaken for Ocean Reef Marina (RPS 2017). E-folding times predicted for this facility across a range of weather conditions varied from approximately 3 to 7 days. These times are also longer than the e-folding durations predicted for the TBF.

Based on this assessment, flushing of the proposed TBF is likely to be equal to or better than comparable facilities in Western Australia.

Table 9.3 Summary of e-folding times for a conservative tracer released instantaneously throughout the volume of the proposed TBF

Site	Elevation	Scenario & E-folding Time in Days							
		Summer 2016	Autumn 2013	Autumn 2013	Winter 2011	Spring 2007	Spring 2007	Autumn 1998	Autumn 1998
		Case I	Case I	Case II	Case I	Case I	Case II	Case I	Case II
A	Surface	1.00	1.00	1.00	0.92	0.58	0.63	0.08	0.08
	Bottom	0.13	0.92	0.92	0.88	0.50	0.50	0.08	0.08
B	Surface	1.17	1.54	1.54	1.67	1.04	1.08	1.17	1.17
	Bottom	1.13	1.54	1.54	1.67	1.04	1.08	1.21	1.21
C	Surface	1.08	1.42	1.42	1.50	1.00	1.00	1.00	1.00
	Bottom	1.04	1.42	1.42	1.50	1.00	1.00	0.96	0.96
D	Surface	1.17	1.54	1.54	1.71	1.08	1.08	1.21	1.21
	Bottom	1.17	1.54	1.54	1.71	1.08	1.08	1.21	1.21

Notes: 1. Site Locations are shown in Figure 9.9.
2. Case I refers to with groundwater input. Case II refers to case without groundwater input.

9.3 Concept C

The hydrodynamic model was used to simulate each of the selected periods for Concept C. The typical year was modelled for Concept C and the results were then compared to the predevelopment results. As a first pass review of the differences, time history plots of the current conditions pre and post Concept C were prepared for each of the locations shown in Figure 9.10.

Figure 9.10 Locations used to Review Differences in Hydrodynamics – Concept C

Similar to Concept B the time history plots show relatively small differences between the current conditions at most locations. A summary of the findings from the review of the time history plots is provided in Table 9.4.

Table 9.4 Summary of Differences in Hydrodynamic Conditions at Each Output Location

Location	Importance of Selection of Location	Observations
1	Assessment of potential current induced changes on the beach area to the south	Reductions in current magnitudes of typically around 50% are observed. The most significant reductions in current speeds are observed during winter, particularly during storms. Changes to current directions are observed. Where current directions were typically alongshore, they now trend cross shore, likely due to water being forced around the facility.
2	Assessment of potential current induced changes immediately offshore from the facility	Very minor changes in current magnitudes and directions are observed.
3	Assessment of any current changes in the channel adjacent to the breakwaters (to review potential navigation issues)	Significant reductions in current magnitudes are observed. Outside of winter storms, currents are reduced to almost zero. A clockwise rotation of current directions is observed across all periods.
4	Assessment of any current changes within the approach channel	Very minor changes in current magnitudes and directions are observed.
5	Assessment of potential current induced changes on the beach area in the lee of the entrance	Significant reductions in current magnitudes are observed. Outside of winter storms, currents are reduced to almost zero. During northerly conditions this reduction is less significant. A clockwise rotation of current directions is generally observed.
6	Assessment of potential current induced changes on the beach area to the north as a result of the facility and channel	Very minor changes in current magnitudes and directions are observed.

Not surprisingly, the current conditions showed similar trends to those encountered as part of the Concept B modelling. To better illustrate the differences across different Metocean conditions, spatial plots have been prepared for key events which impact the area, including sea breeze, swell and storm events. Spatial plots for these events are presented in Figures 9.11 to 9.13 respectively. The spatial plots for Concept B have been provided again to allow for easy comparison of the differences between the two designs. It is noted that due to time constraints

the wave, hydrodynamic and morphological modelling were completed concurrently for Concept C. As such there may be small differences between the Concept C modelling and that which was completed previously due to the changes in the bathymetry caused by sediment movement within the model. Whilst this can result in minor differences in the plots of the current magnitudes and directions the larger scale changes are what is of interest.

In addition to the plots for key events, average difference plots have been prepared over the entire duration of the each of the representative periods and are presented in Figures 9.14 to 9.17.

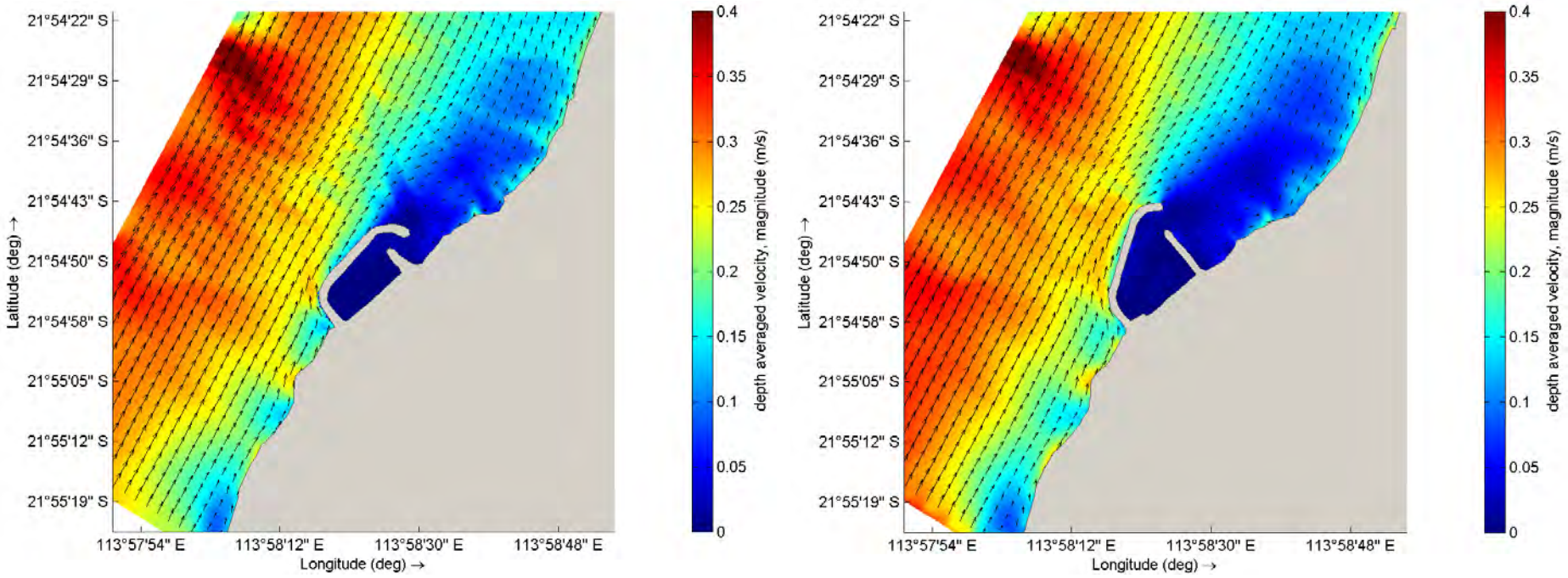

Figure 9.11 Spatial Plots for Typical Summer Sea Breeze Event for Concept B (left) & Concept C (right)

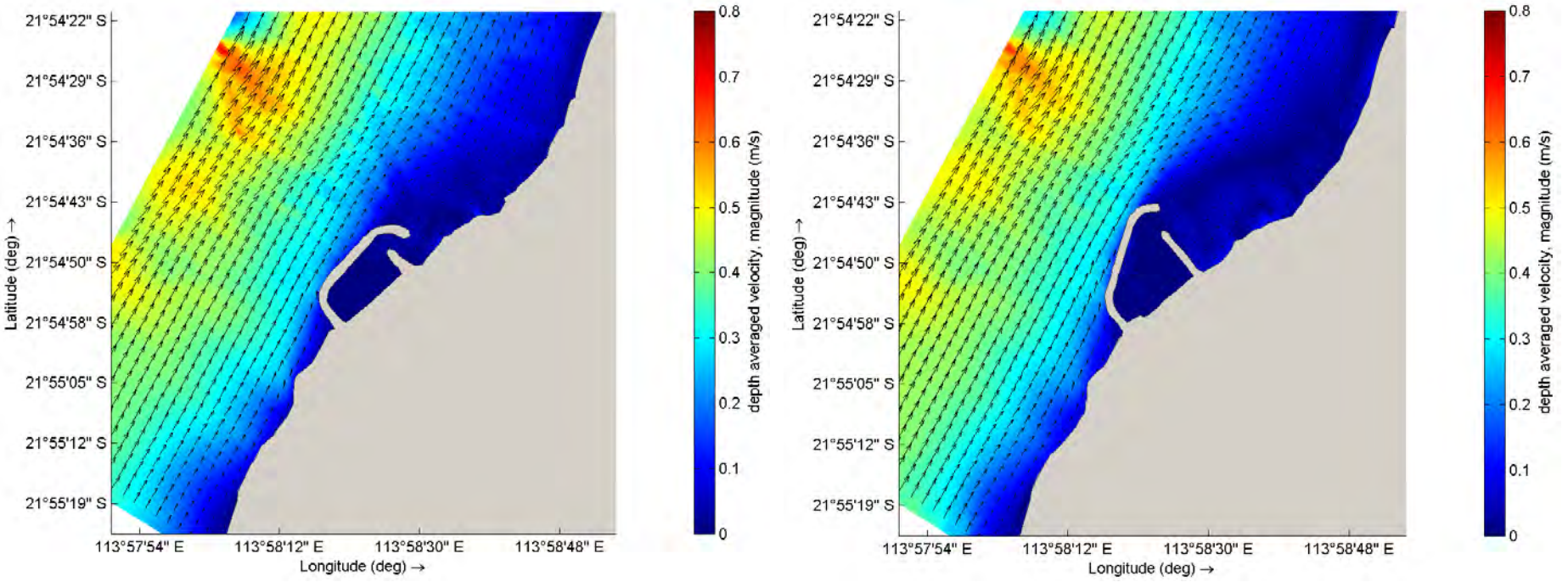

Figure 9.12 Spatial Plots for Typical Swell Event for Concept B (left) & Concept C (right)

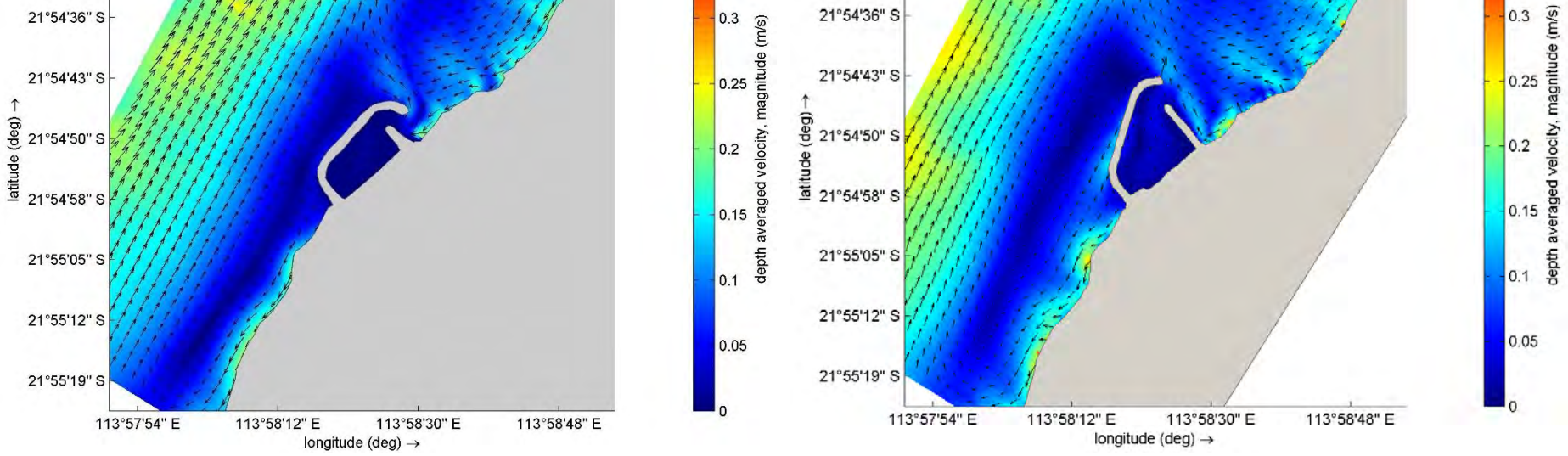

Figure 9.13 Spatial Plots for Typical Storm Event for Concept B (left) & Concept C (right)

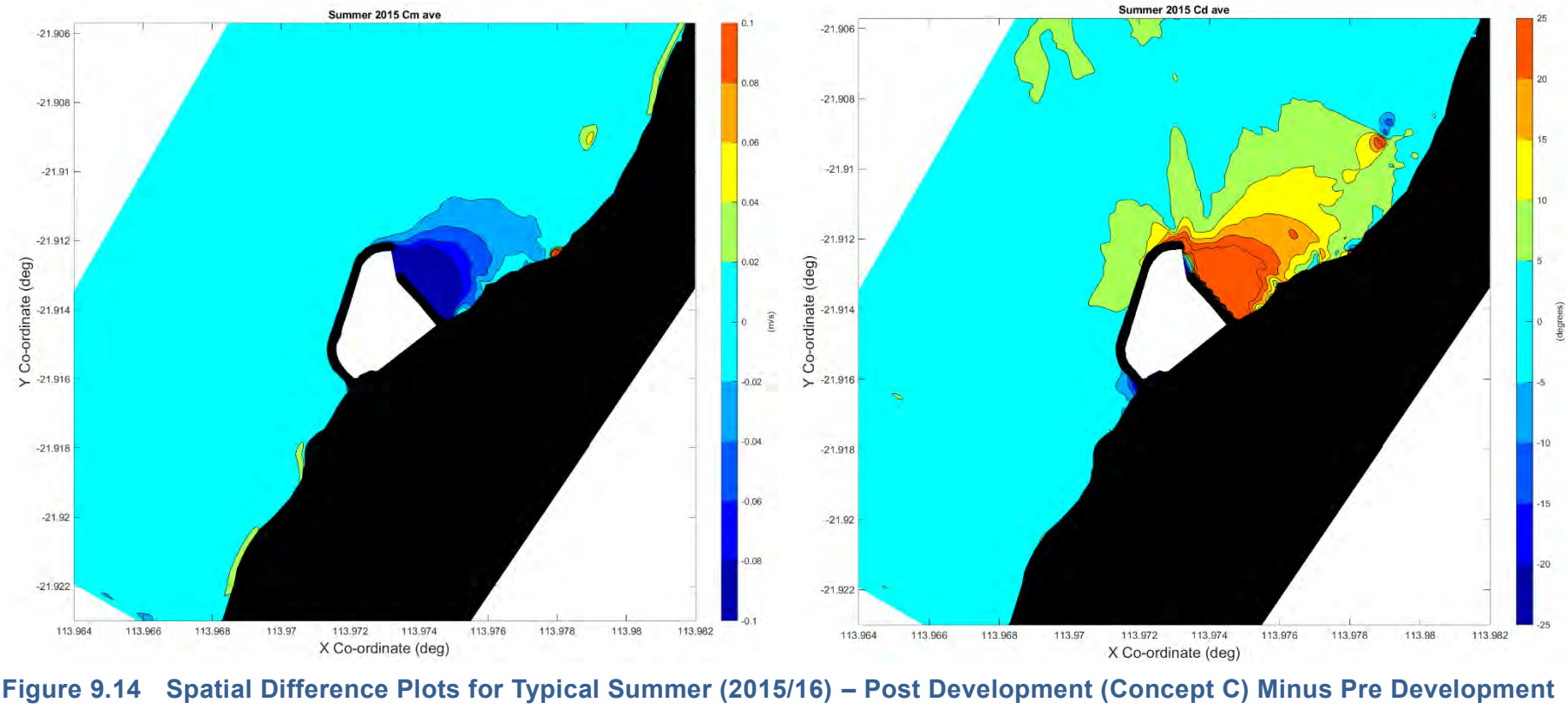

Figure 9.14 Spatial Difference Plots for Typical Summer (2015/16) – Post Development (Concept C) Minus Pre Development

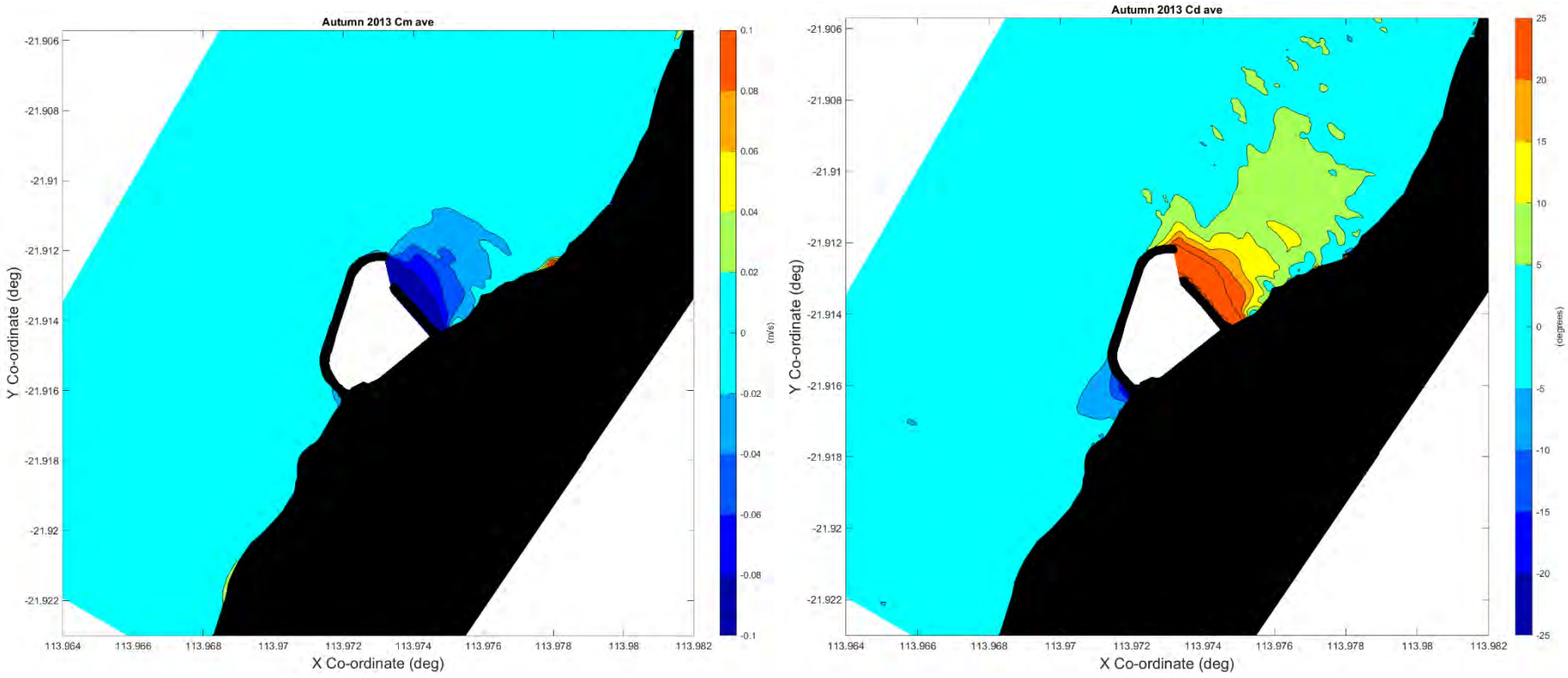

Figure 9.15 Spatial Difference Plots for Typical Autumn (2013) – Post Development (Concept C) Minus Pre Development

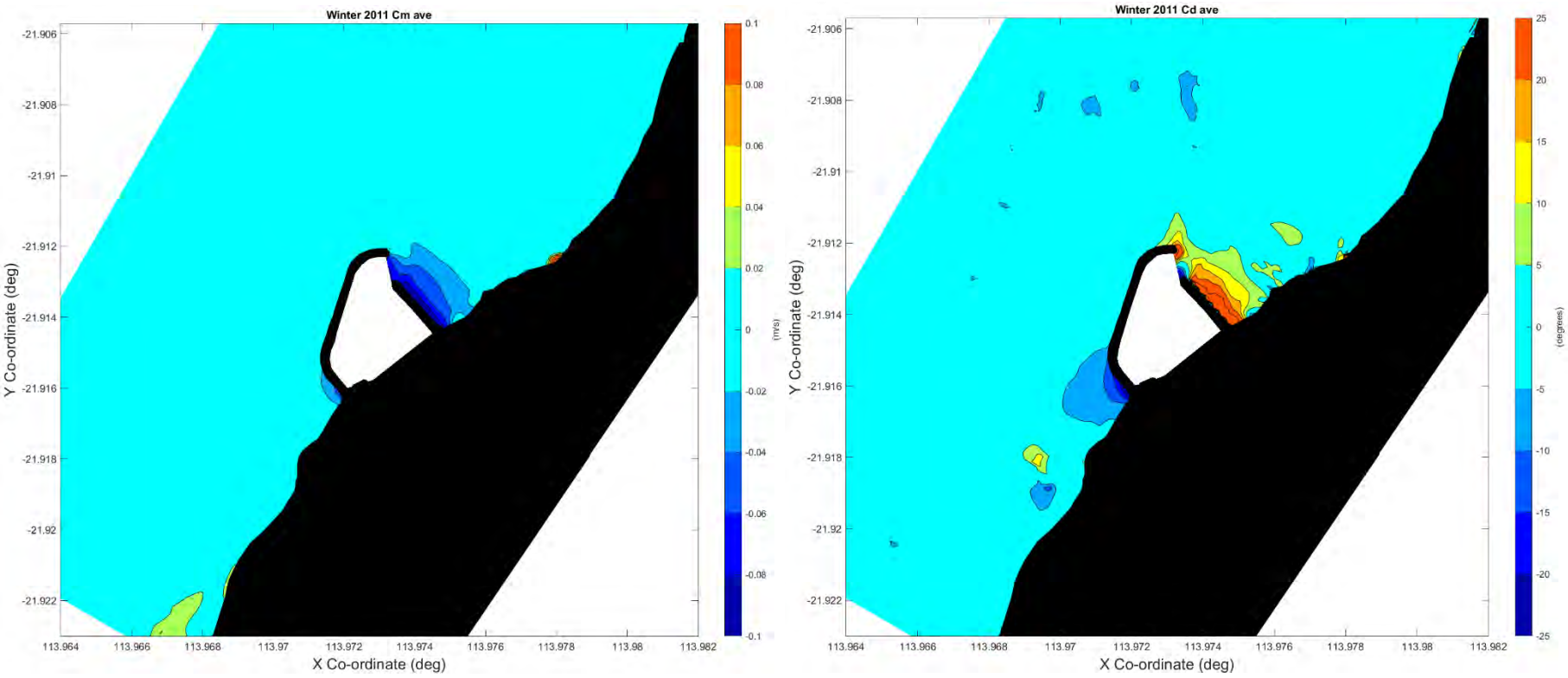

Figure 9.16 Spatial Difference Plots for Typical Winter (2011) – Post Development (Concept C) Minus Pre Development

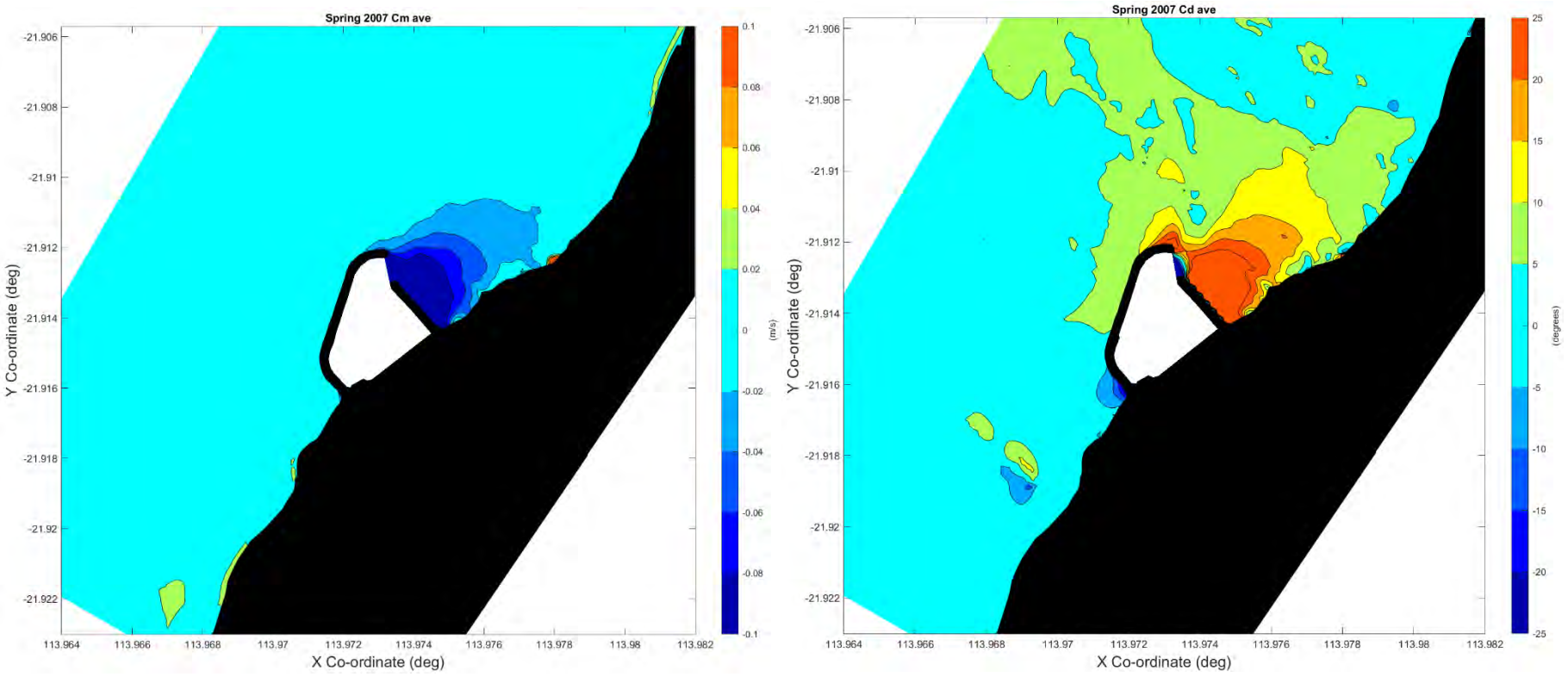

Figure 9.17 Spatial Difference Plots for Typical Spring (2007) – Post Development (Concept C) Minus Pre Development

Observable impacts to current dynamics (approx. -0.02 to -0.1 m/s) extends around 500 m to the north of the facility and around 100 m to the south of the facility. Beyond this, impacts to currents are negligible.

The key observations from the spatial plots are summarised below.

- The introduction of the TBF causes a large reduction in the current magnitude a few hundred metres to the north and south of the facility. There appears to be a slight increase in the extent of the reduction area to the north of the facility compared to Concept B.

- Changes to current directions extend further than changes to current magnitudes with observable changes present up to approximately 500 m from the proposed facility.

- Changes to the current dynamics likely arise from a combination of the training of flow around the facility and wave shadowing reducing wave generated currents in the lee of the breakwaters. Both of these factors reduce currents immediately adjacent to the facility. Unlike Concept B the training of the flow around the southern breakwater does not appear to result in an increase in current magnitude in this area.

Overall, the outcomes of the revised modelling for the Concept C layout of the proposed TBF are reasonably intuitive and expected. As previously discussed for Concept B the changes to the current dynamics outlined above are unlikely to have any impact to the operation of the facility beyond those impacts already established through the wave modelling assessment presented in Task 5 (MRA 2022a).

9.3.1 Concept C Flushing

When compared to Concept B, the mouth of Concept C is a little more open and less protected, which may result in a slight improvement of the flushing rate. However, the volume of the enclosed water body within Concept C is slightly larger than for Concept B, which would likely result in a decrease in the rate of flushing. On balance, the rate of flushing for Concept C and B are expected to be in the same order of magnitude. Given the fast e-folding times for Concept B and the likely similarity in the flushing characteristics of the two marina layouts no flushing modelling has been completed for Concept C.

10. Sediment Transport & Sedimentation Modelling

10.1 Scope

The scope of work to be completed for this task, and as outlined within this report, is as follows.

- Set up and calibrate the Delft3D morphological model to replicate the existing sediment budget determined within the shoreline movement assessment (Task 2).
- Use the Delft3D morphological model to simulate sediment movement over the existing shoreline and simulate six sediment transport scenarios, each covering a 3-month duration, plus a cyclone event.
- Set up the Delft3D morphological model for the TBF concept, including the dredge channel, and remodel the sediment transport scenarios.
- Provide recommendations on any changes to the layout that could improve the performance of the maintenance regime.
- Assess the frequency, volume and timing of sand bypassing and the requirement for maintenance dredging of the entrance channel to the facility.
- Assess the required management measures to mitigate the impacts identified.

This sediment transport is ultimately drive by the hydrodynamic, wave and cyclone modelling reports discussed in Sections 7 to 9. For set-up and calibration of these models refer to the relevant Section and Appendix.

Morphological modelling was initially completed for the Concept B marina layout and subsequently for the revised Concept C Layout. This is discussed in Sections 10.2 and 10.3 respectively.

This sediment transport model set-up, calibration and assessment are detailed in a standalone Sediment Transport Modelling report attached in Appendix E. Key outcomes are provided in the section below. For detailed methods and outcomes refer to the standalone report.

10.2 Summary – Concept B

The sediment transport model was calibrated against the estimated sediment budget. Following calibration the model was used to estimate the impacts that the construction of the TBF could have on the local sediment dynamics.

Figure 10.1 shows the potential changes to bed levels over the average year that was modelled. This figure shows that changes to the area south of the TBF are expected, with accumulation of sediment likely to occur to the south of the facility. The figure also shows that transport and accumulation of sediment around the outer breakwater is predicted by the model. This is likely a function of the relatively shallow nature of the area outside the breakwaters.

The model also predicts accumulation of sediment along the edges of the entrance channel. Figure 10.2 provides a zoomed in view of the accumulation around the channel. In total, the model estimates that approximately 2,600 m^3 of material could accumulate in the channel on an average year. As shown in the figure, the majority of this material accumulates on the batters and along the edges of the channel, with the model suggesting that the total accumulation over the

course of the year would generally be less than 0.05 m within the mid sections of the channel. Nevertheless, variability in weather conditions could change this result.

Additionally, due to limitations in the available data, and subsequent limitations in the modelling outputs, it is recommended that possible variance in the average infill rate be considered for facility planning, noting also that seasonal and interannual variability could significantly change the observed rates of infill.

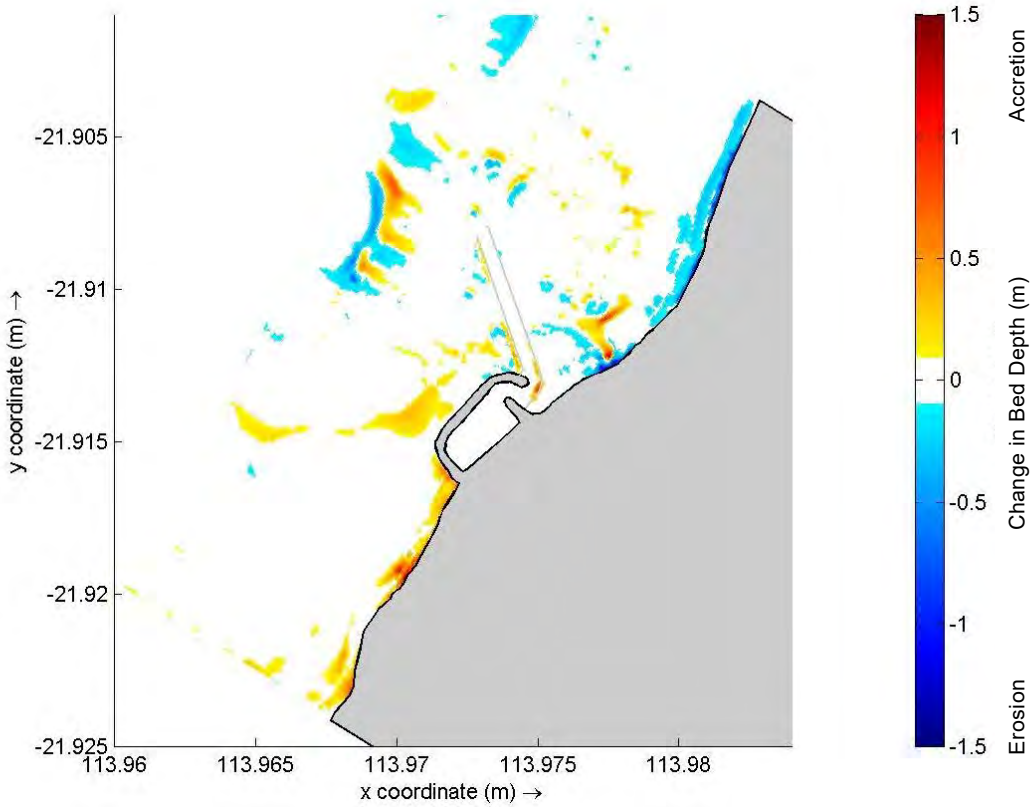

Figure 10.1 Potential Changes to Bed Elevation Over the Course of the Typical Year

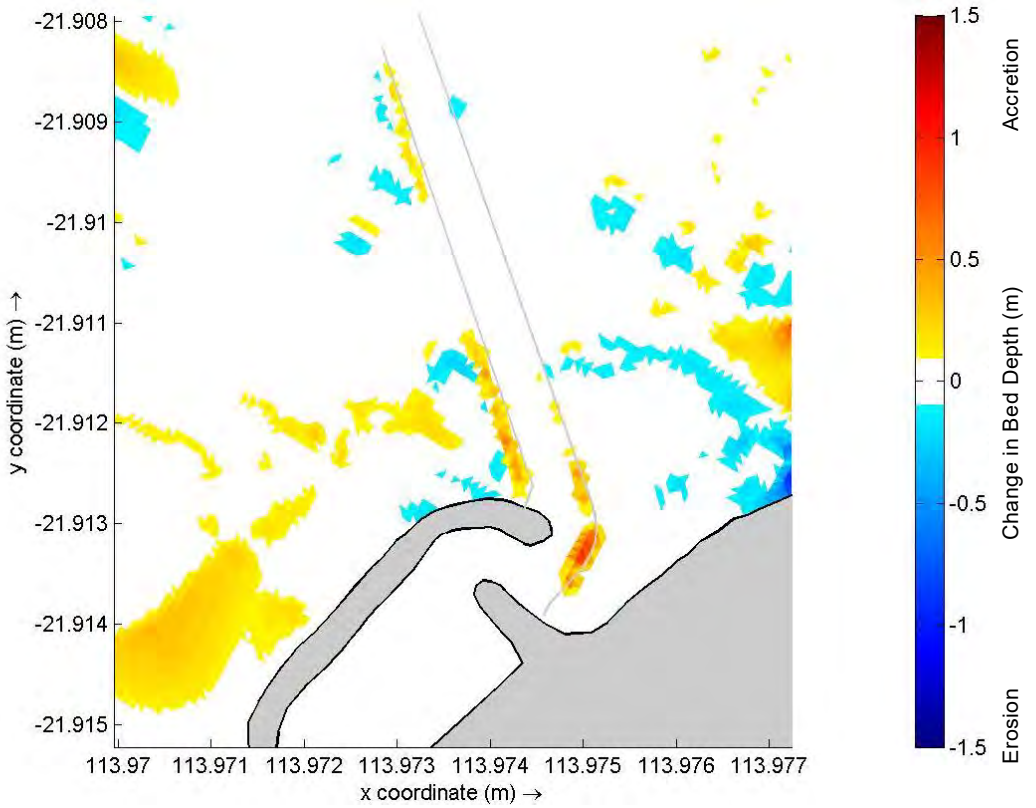

Figure 10.2 Potential Infill of the Entrance Channel over a Typical Year

A key contributor to the variability in shoreline response would be the potential impact of severe tropical cyclones on the coastline. Morphological modelling for a 50 year ARI cyclone event resulted in large scale changes to the nearshore bathymetry surrounding the TBF. Figure 10.3 shows the initial bathymetry prior to the passage of the cyclone, with Figure 10.4 showing the bathymetry after the cyclone has impacted the area. The figures show a clear post cyclone accumulation of sediment in the area surrounding the facility. This includes a significant infill of sediment into the entrance channel.

The infill of sediment into the entrance channel is most significant closest to the shoreline, however the extent of the infill also extends further offshore. Accumulation of sediment also occurs along the coastline to both the north and south of the facility. South of the facility this accumulation is mainly driven by erosion of the beach face and dunes and deposition in the nearshore area. To the north of the facility similar cross shore transport is observed, however a further southerly net transport of sediment is also obvious. These sediment transport changes are illustrated well in the difference plot provided in Figure 10.5.

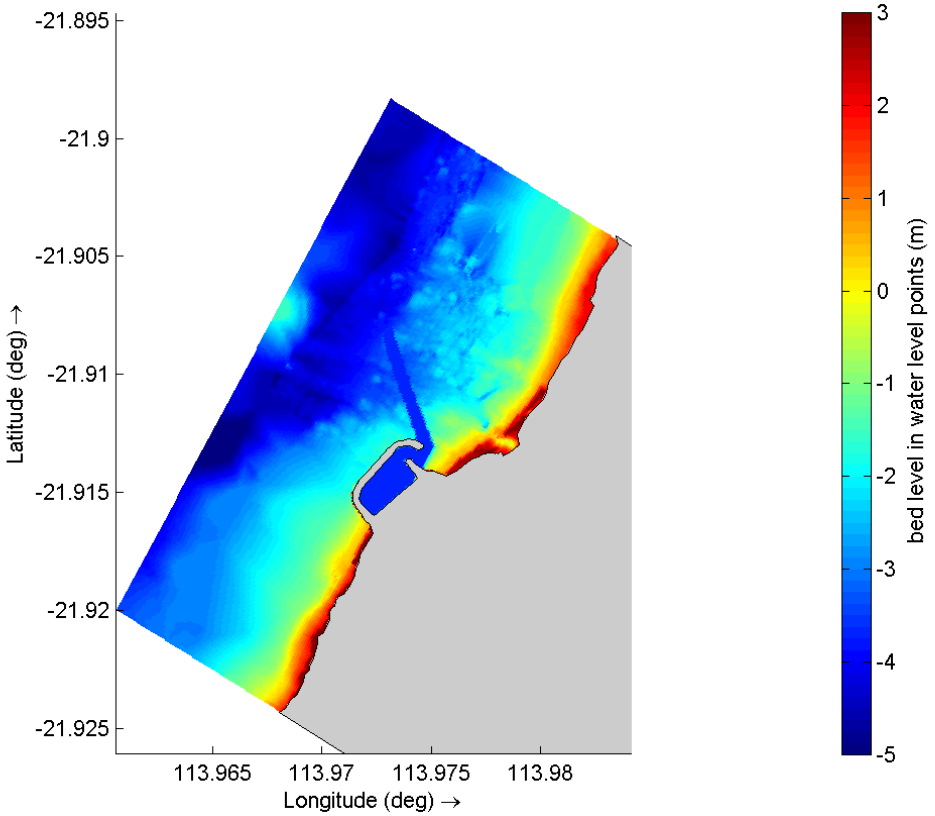

Figure 10.3 Initial Bathymetry prior to Cyclone Impact

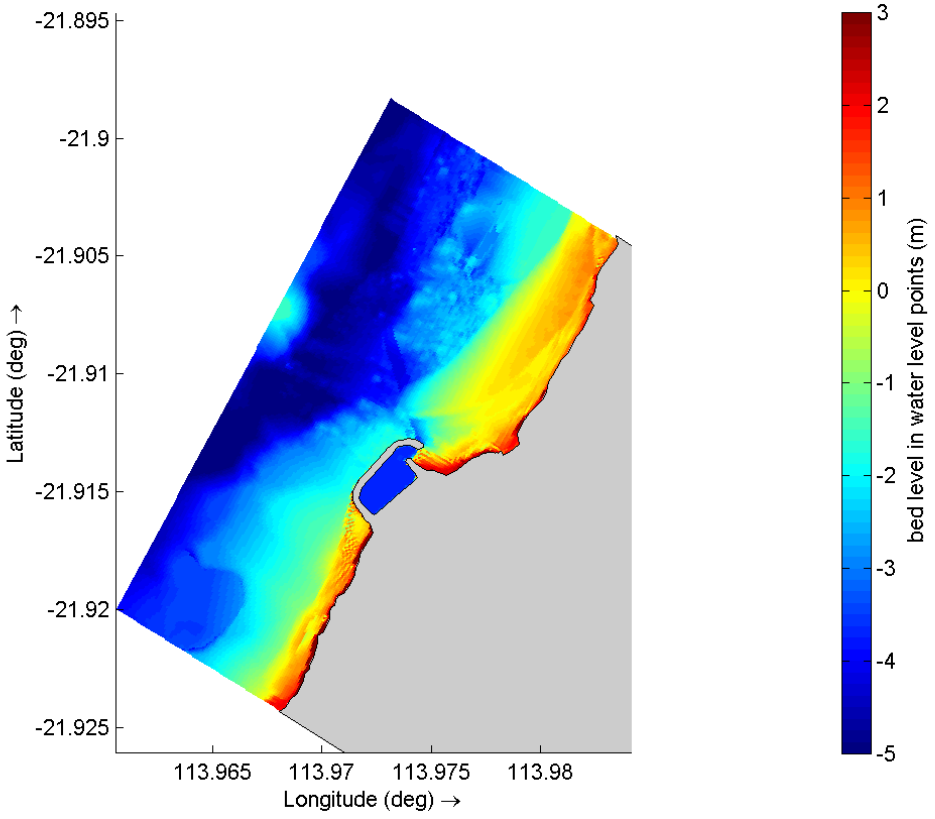

Figure 10.4 Final Bathymetry following Cyclone Impact

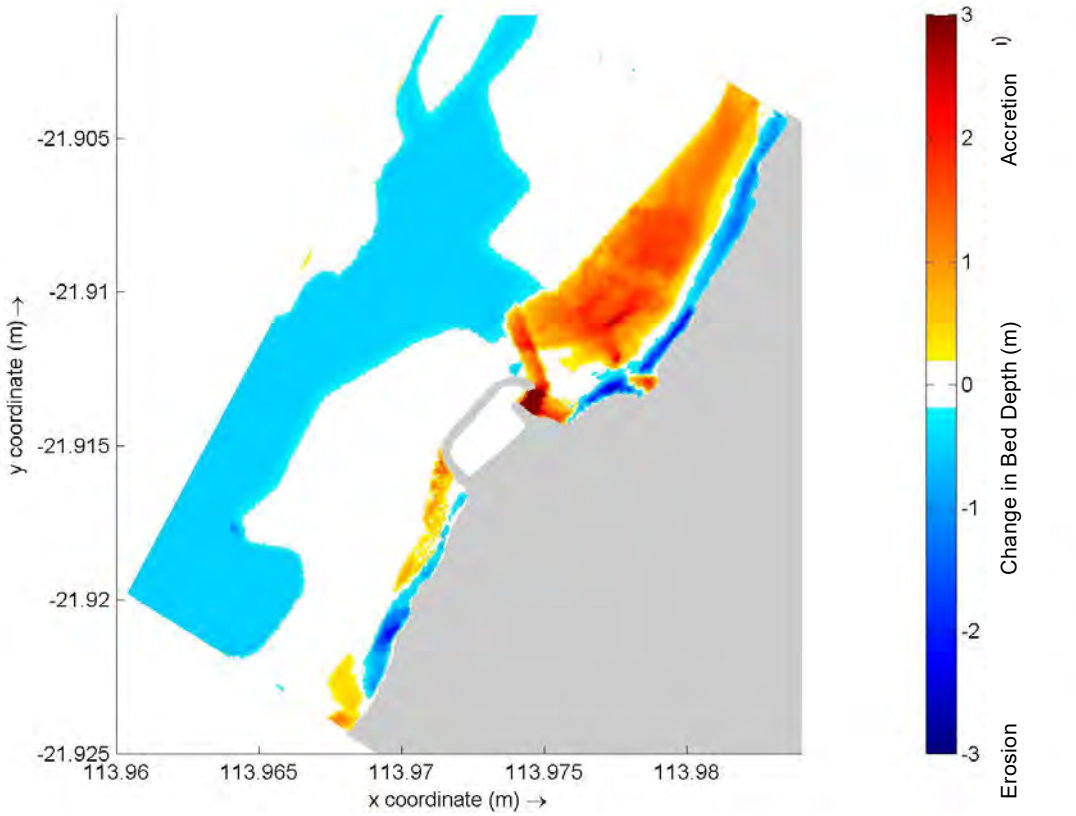

Figure 10.5 Bathymetry Difference Plot Pre Versus Post Cyclone

The volume of material deposited in the channel during the cyclone event is estimated by the model to be approximately 50,000 m^3, which is a substantial volume and would have clear operational impacts for the facility. However, the extent of sediment movement in the nearshore area is impacted by the initial volume of sediment that is included within the model. Without further details on sediment depths, the modelling outcomes will be limited with respect to their potential accuracy.

It must also be noted that the modelled cyclone represents an event with a 50 year ARI. Therefore the modelled morphological changes represent conditions that would only have a 2% chance of being experienced in any given year. The trends in cyclone induced morphological changes would be reasonably consistent across events that follow this track; however the magnitudes of the impact would change. This needs to be considered as part of the planning for the facility.

Based on the results of the modelling, the anticipated impact of the TBF on the local sediment dynamics and shoreline response are presented in Figure 10.6. To manage these potential impacts a high level coastal management regime has been suggested. This management regime would consist of the following operations.

- Bypassing of sediment from the south of the facility to the shoreline north of the facility.
- Management of sediment on the northern side of the facility adjacent to the inner breakwater and entrance channel.
- Dredging of the entrance channel.

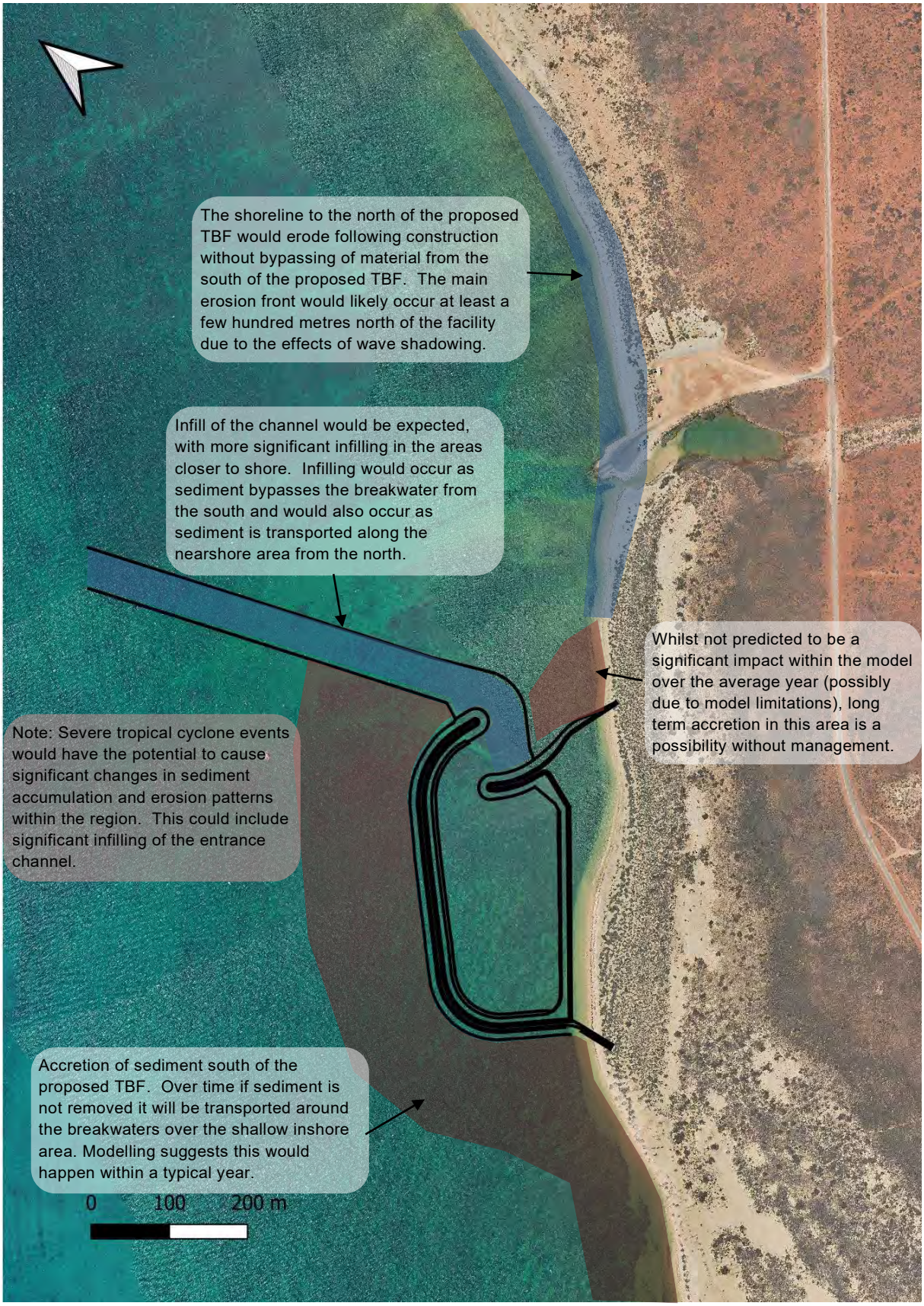

Figure 10.6 Anticipated Shoreline Response Following Construction of the TBF in the Absence of Active Sediment Management

All of these management actions are relatively commonplace, however an exercise in cost optimisation for the ongoing operational costs would be worthwhile. The optimisation could include considerations such as modification to the proposed layout of the TBF to reduce the potential for infill into the entrance channel. There are two primary options that may assist with this approach.

The first option would be to modify the design around the entrance of the proposed TBF to push the entrance channel further offshore. This would reduce the potential for the infill of sediment which has been observed along the shoreward margins and is particularly relevant during cyclone events. There would be many options available to do this and the fact that the wave climate surrounding the facility is reasonably benign removes some of the constraints that would typically apply with respect to sheltering of vessels as they navigate through the entrance. An example of a layout that could achieve better outcomes is provided in Figure 10.7. The main benefits of this example are as follows.

- The dredge channel has been moved from a distance of approximately 90 m offshore in Concept B to a distance of 245 m offshore in the example layout. This provides a much greater sediment trapping volume adjacent to the northern breakwater before sediment would begin to infill within the entrance channel. This is able to be achieved by pushing the marina entrance channel further offshore and also opening up the entrance slightly, which is possible due to the reasonably benign wave climate.

- The potential for sediment to bypass the breakwaters from the south would be reduced given the breakwaters would now extend around 345 m offshore compared to around 245 m for Concept B. This would provide improved trapping on the southern side of the facility before sediment could accumulate within the entrance channel.

- The revised layout could potentially result in a decrease in the volume of capital dredging, as even if the size of the basin remains the same, less dredging would be required for the entrance channel.

- A revised layout such as this may also result in an improved outcome with respect to long waves within the basin.

Further refinements to the example layout would also be possible to further increase the benefits to the project.

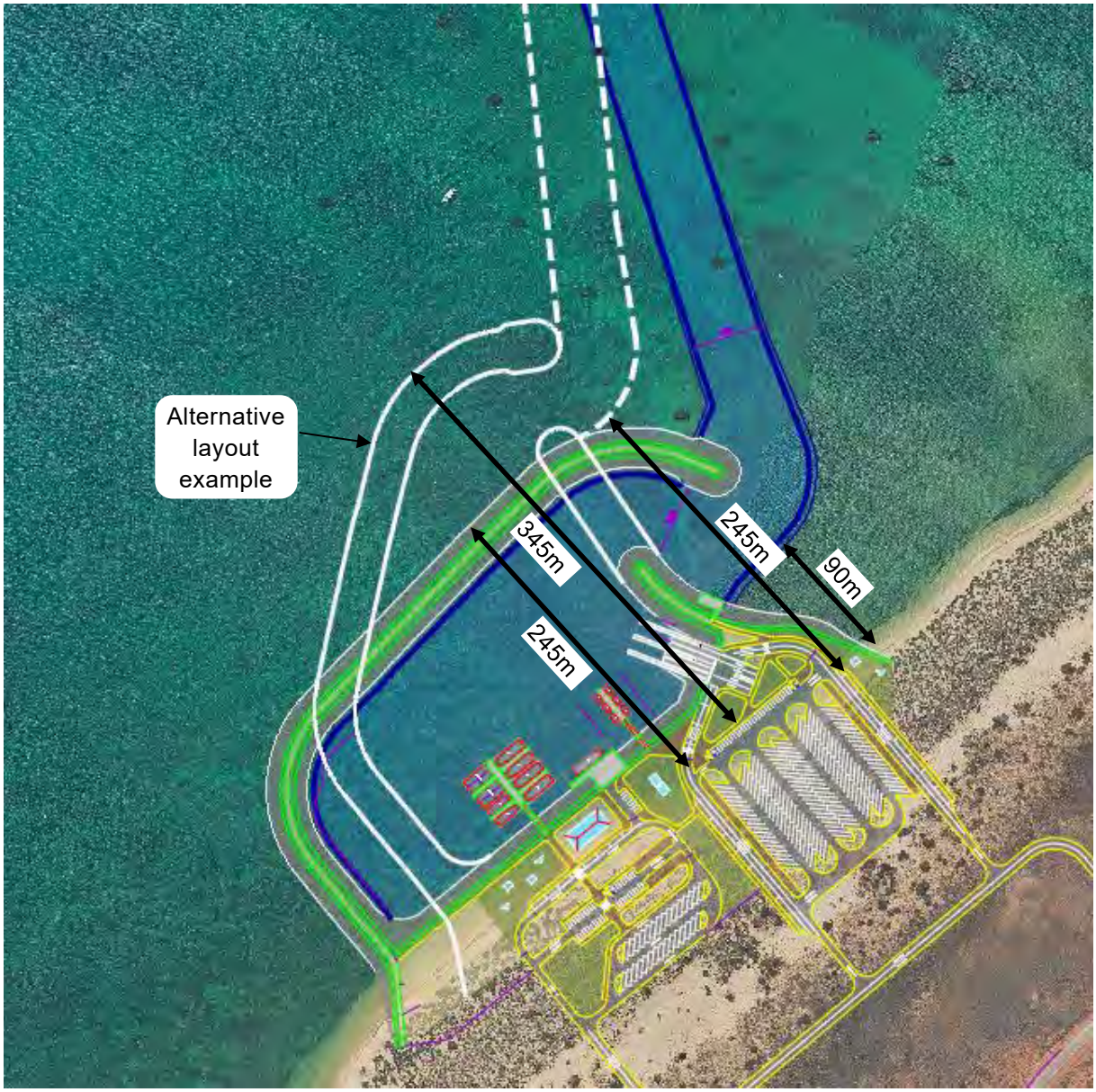

Figure 10.7 Possible Alternative Design for the Marina Layout to Minimise the Potential Impacts of Sediment Transport Processes

The second option would be to add a spur off the southern portion of the breakwater to try to prevent sediment from being transported around the breakwater in the relatively shallow water depths. Whilst there may be merit in this option, as it would potentially stop the bypassing of material, it would perhaps be best to treat this option as a mitigation strategy that could be implemented in the future if the management of sediment on the shoreline is not sufficiently effective.

10.3 Concept C

Modelling was completed for the updated Concept C. Figure 10.8 shows the potential changes to bed levels over the average year that was modelled for this concept. The model shows similar trends around the offshore reefs and existing boat ramp as observed and discussed for Concept B. Closer to shore, the figure shows similar accumulations to the south of the proposed TBF are expected for Concept C as for Concept B, with accumulation of sediment likely to occur to the

south of the facility. The extent of sediment transport around the breakwaters is slightly different, with some accumulation happening offshore from the breakwaters, however within the simulated period this accumulation does not occur to the extent that it would begin to significantly accumulate within the entrance channel.

The overall extent of sediment accumulation within the entrance channel is noticeably less than that predicted by the modelling for Concept B. Some small areas of accumulation are observed on the batters along the northern side and southern side of the channel around the breakwaters. The total volume of accumulation within the channel over the modelled period was approximately 1,000 m^3 of material for Concept C, compared to around 2,600 m^3 for Concept B – a significant improvement.

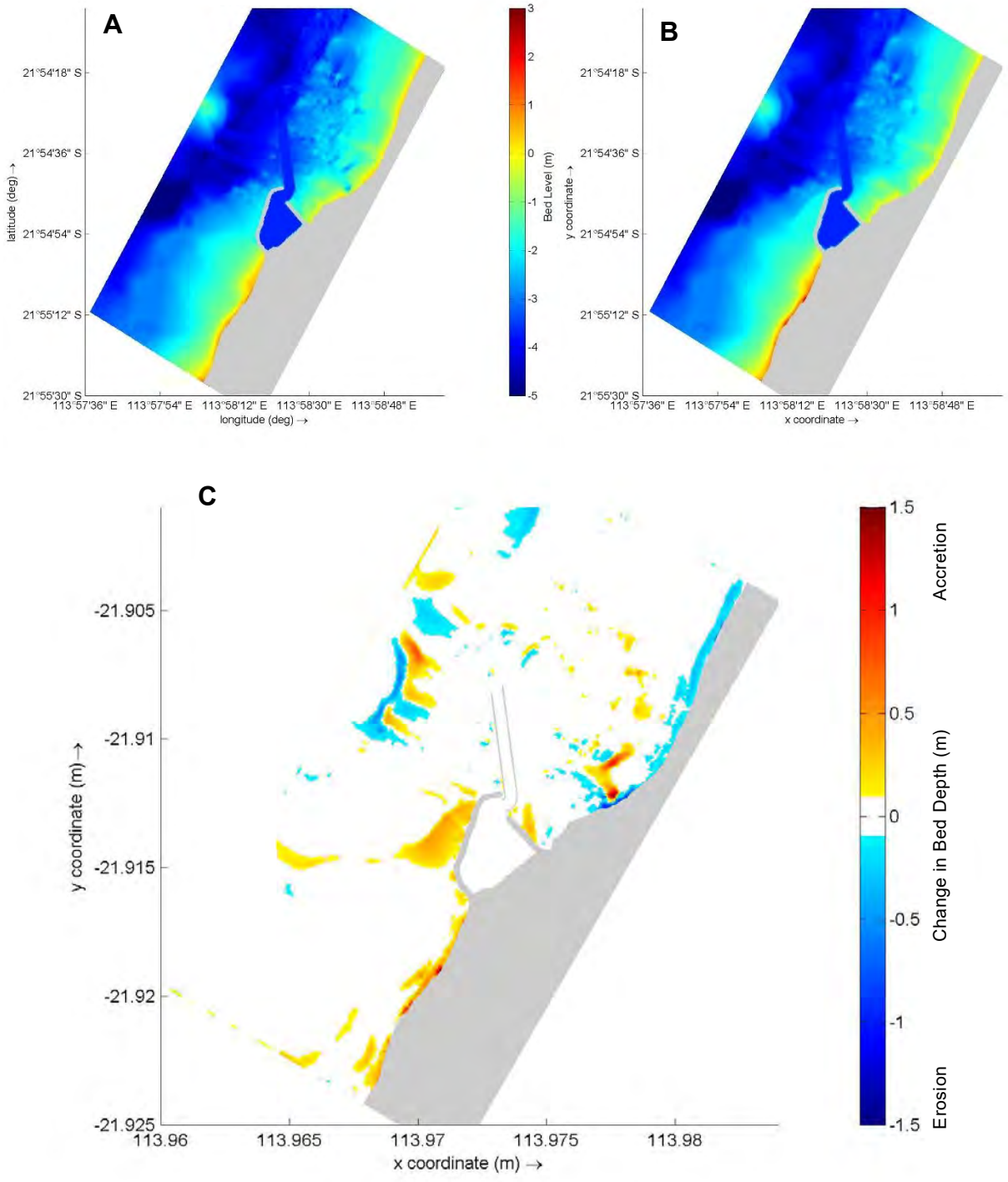

Figure 10.8 Potential Changes to Bed Elevation Over the Course of the Typical Year for Concept C: (A) Initial Bed Level; (B) Final Bed Level; (C) Difference

Based on the outcomes from the modelling, the local average annual sediment budget for the post development case is presented in Figure 10.9. It must be noted that the modelling results match the general expectations regarding sediment transport post development, however the outcomes of the model need to be considered in the context that they present results for the range of

conditions modelled. These changes are therefore indicative of the types of changes that would be expected along the shoreline, but would be subject to fluctuation based on weather conditions, etc.

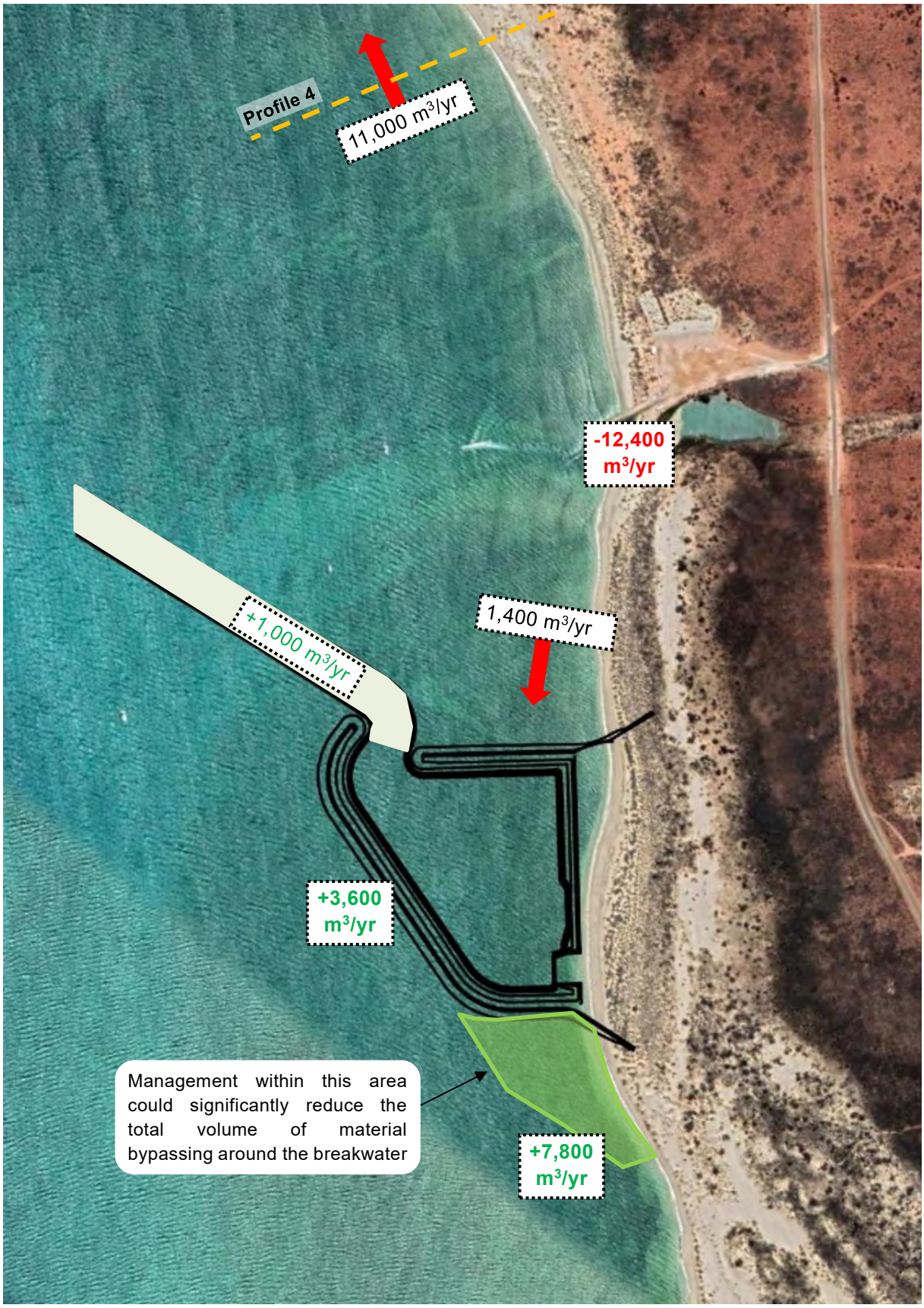

Figure 10.9 Modelled Sediment Budget Post Construction of the Proposed TBF

A key contributor to the variability in shoreline response would be the potential impact of severe tropical cyclones on the coastline. Morphological modelling for a 50 year ARI cyclone event resulted in large scale changes to the nearshore bathymetry surrounding the proposed TBF. Figure 10.10 shows the results from the modelling.

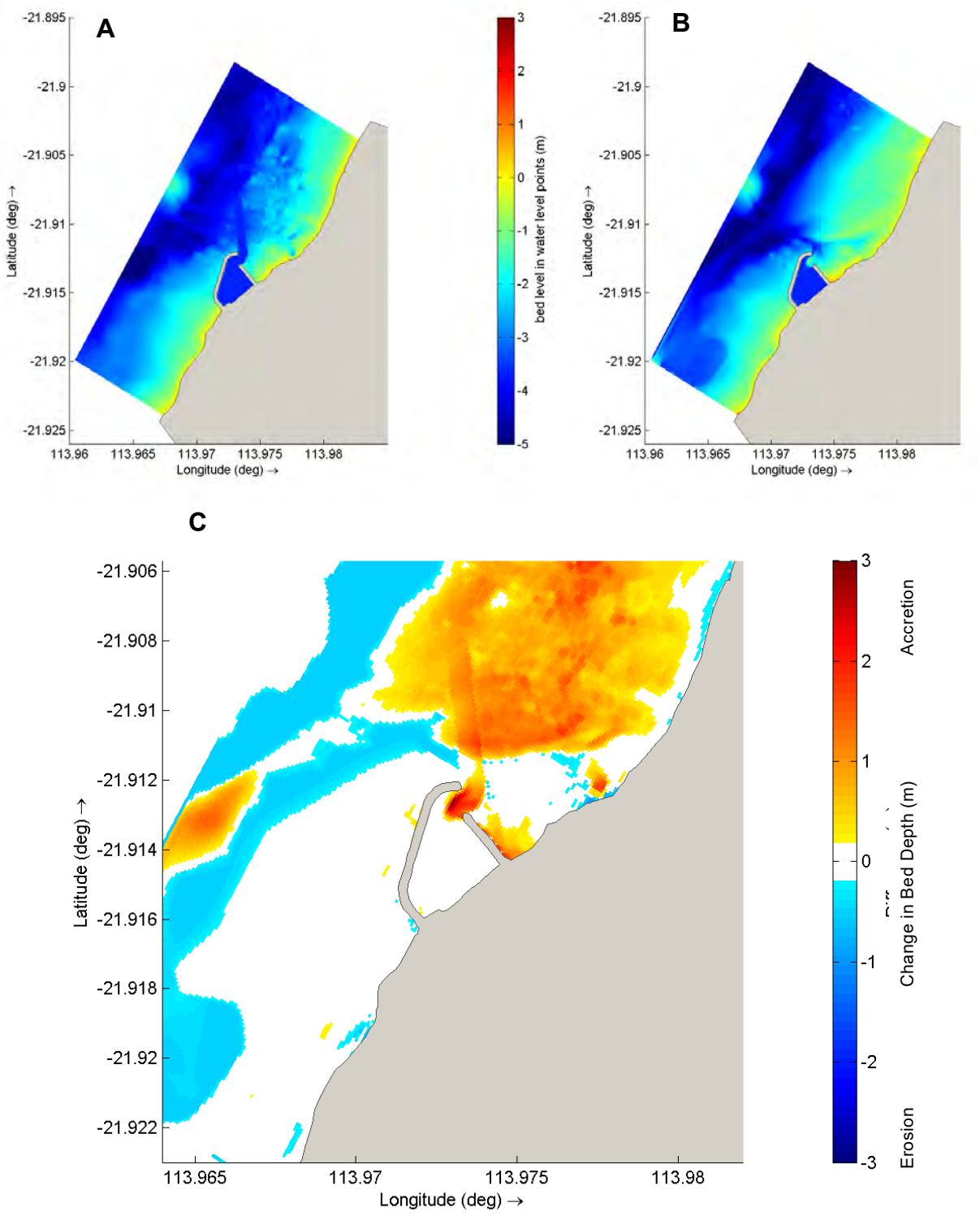

Figure 10.10 Potential Changes to Bed Elevation During a 50 year ARI Cyclone for Concept C: (A) Initial Bed Level; (B) Final Bed Level; (C) Difference

The volume of material deposited in the channel is approximately 50,000 m^3, which is similar to the volume predicted for Concept B. This volume of accumulation results in a significant infill of the channel at the entrance, though would not completely shut off the entrance to the facility as

was predicted for Concept B. Nevertheless, this is a substantial volume of infill and would have clear operational impacts for the facility. As previously stated, the extent of sediment movement in the nearshore area is impacted by the initial volume of sediment that is included within the model. Without further details on sediment depths and composition across the lagoon, the modelling outcomes are limited with respect to their potential accuracy. This reinforces the importance of understanding the actual depth of sediment coverage across the lagoon.

Modelling of the sediment transport around the proposed Concept C layout has shown that there will be similar impacts to those observed for Concept B, albeit the volume of sediment accumulation in the channel will be less during typical conditions. As a result, all of the management recommendations presented for Concept B remain valid for Concept C. The only modification would be that a total channel infill rate under typical conditions of approximately 2,000 m^3 per year should be allowed for in any future planning. This volume is approximately double that predicted by the model to account for limitations in the modelling, as have previously been discussed.

11. Wave Penetration & Long Wave Assessment

The objective of this Task is to identify undesirable wave penetration or excessive basin oscillations that may impact operability of the TBF.

Using the results of the Metocean Climate Analysis, MRA has undertaken a first pass assessment to make recommendations as to whether or not it is anticipated that wave penetration is expected to result in navigability or operability issues for the proposed TBF. This was undertaken via the following methodology.

- Selection of a range of events for wave penetration calculations based on those most likely to be critical for the configuration. A total of 8 events were considered.
- Utilise empirical methods to estimate diffracted wave heights inside the marina under a range of different conditions.
- Assessment of results against design wave criteria for mooring and navigation, providing commentary on risks associated with wave penetration.

MRA has also analysed the data available from nearshore measurement datasets to ascertain the presence of naturally occurring long period wave (LPW) energy in the nearshore environment. MRA has utilised analytical methods to review the expected performance of the TBF concept relative to LPW operability. This was undertaken via the following methodology.

- Analysis of the available pressure sensor data to identify the presence and characteristics of background LPW energy present at each location.
- Undertaking theoretical harbour resonance calculations for a range of length, width and depth inputs to estimate the natural frequencies within the harbour.
- Comparison of the estimated theoretical natural frequencies against background LPW energy to allow commentary on any risks or impacts associated with the operability of the TBF.

11.1 Wave Penetration

11.1.1 Relevant Design Criteria

Wave penetration impacts the wave climate in the entrance and basin of marinas and harbours. ASCE 2020, *Planning and design guidelines for small craft harbours (practice No. 50)*, provides a range of wave climate related criteria which should be considered when designing a small craft harbour.

- Basin agitation caused by diffraction of waves into the entrance.
- Berthing tranquillity – the wave climate that is tolerable for safe mooring of boats.
- Boat Ramp tranquillity – the wave climate that is tolerable for boat ramp and launch areas.
- Entrance navigability – a relationship between the wave climate and geometry of the approach corridor and entrance configuration.

Preliminary design criteria for these considerations have been established to allow selection of design conditions and assessment of risks. These preliminary design criteria, discussed in the following sections, are not intended as final design criteria for the TBF. The design criteria should be developed by the TBF designer in consultation with DoT.

Agitation & Tranquillity

AS3962 provides clear guidance regarding acceptable wave conditions within marina waterways. This guidance is provided in the form of Table 4.2 within AS3962 (reproduced below), which provides a range of criteria for different wave directions and periods. Meeting these criteria would achieve a 'good' wave climate within the marina. It is noted that additional information is provided regarding criteria for 'excellent' (0.75 times the criteria for a 'good' climate) and 'moderate' (1.25 times the criteria for a 'good' climate) wave climates.

Table 11.1 Criteria for a 'Good" Wave Climate in Small Craft Harbours (Table 4.2 from AS3962)

Direction and Peak Period of Design Harbour	Significant Wave Height (Hs)	
	50-year ARI	1-year ARI
Head seas less than 2 s	Conditions not likely to occur during this event	Less than 0.3 m wave height
Head sees greater than 2 s	Less than 0.6 m wave height	Less than 0.3 m wave height
Oblique seas greater than 2 s	Less than 0.4 m wave height	Less than 0.3 m wave height
Beam seas less than 2 s	Conditions not likely to occur during this event	Less than 0.3 m wave height
Beam seas greater than 2 s	Less than 0.25 m wave height	Less than 0.15 m wave height

Note: 1. For an "excellent" wave climate multiply wave height by 0.75, and for a "moderate" wave climate multiply wave height by 1.25.
2. For vessels of less than 20m in length, the most severe wave climate should satisfy moderate conditions. For vessels larger than 20m in length, the wave climate may be more severe.

As shown in Table 11.1, consideration of the wave climate within the marina during the 1 and 50-year ARI events is required to assess harbour tranquillity.

Entrance Navigability

There are no universal codes that apply to small craft harbour design for entrance navigability (PIANC, 2017). This is likely a reflection of the fact that no two locations have the same climate, conditions, constraints or objectives.

Whilst no universal codes are available, there are various documents that provide guidance on the design requirements and are relevant when developing preliminary criteria for the TBF. These guideline documents are as follows.

- Australian Standard 3962 – 2020: Guidelines for design of marinas (AS3962; Standards Australia, 2001).
- PIANC RecCom Report 149/Part II – 2016: Guidelines for marina design (PIANC, 2016).
- ASCE 2020, Planning and design guidelines for small craft harbours (practice No. 50).

Many of the navigability criteria discussed in these documents relate to the specific geometry of the entrance and harbour. The intent of this assessment is to review criteria related to the wave climate generated by wave penetration.

The references above have been reviewed to develop the following preliminary criteria as they relate to wave climate.

Table 11.2 Preliminary Navigability Criteria

Criteria	Origin of Criteria
The final approach to the harbour entrance should be straight, and the portion of the straight approach should be at least 3 to 5 times the length of the largest vessel that uses the harbour. Ideally, the approach to the harbour should meet currents or winds such that the ship drift angle does not exceed 10°-15°, particularly where hazardous navigational conditions are expected.	PIANC & ASCE
The entrance must be designed so that a vessel does not need to make any manoeuvres at the entrance. The craft can start manoeuvres only after it passes the entrance and enters a more protected area.	PIANC
If a straight approach through an entrance is not possible or desirable, then the arrangement of overlapping breakwaters should allow a ship to pass through the restricted entrance and turn and reorient to the sea before it is hit broadside by the waves.	ASCE
For powerboat manoeuvring, the entrance should not cause returning boats to experience a direct following sea, because rudder control may then be lost, especially at low speed.	PIANC
The entrance should also not be such that boats approach the small craft harbour in a beam sea condition, as this may induce broaching of the boat.	PIANC
During storms, when waves are between 1 and 3 m (3–9 ft), the recommended total corridor width increases to 8B. If the waves exceed 3 m (9 ft), the navigational corridor increases to 9B.	ASCE

As shown in Table 11.2, review of the wave climate when navigating the entrance requires consideration of the conditions that may be experienced during typical operation and stormy conditions.

11.1.2 Event Selection

The relevant preliminary design criteria were presented in Section 11.1.1. As shown, these criteria require consideration of different types of met-ocean events.

As shown in Table 11.1, consideration of the wave climate within the marina during the 1 and 50-year ARI events is required to assess harbour tranquillity. Whilst, as Shown in Table 11.2, criteria for entrance navigability require assessment of various operational and stormy conditions.

The outer breakwater affords the entrance significant sheltering against wave events from the south through west. Therefore, the most critical events for tranquillity and navigation are likely to be those with the most northerly direction. This approach was used to select critical wave conditions for testing. The event types selected for the relevant criteria are summarised in Table 11.3.

Table 11.3 Event Selection

Type of Event	Event Description	Relevant Criteria
1 year ARI N Storm Event	This event represents severe north-westerly wave conditions that could be experienced. These conditions are represented by locally generated wind waves which develop during the early stages of a storm system. The severity of the event is such that it would occur approximately once per year.	Agitation & Tranquillity Entrance Navigability
1 year ARI Typical Storm event	This event represents wave conditions that could be experienced during a storm event. These conditions are represented by a combination of swell and locally generated wind waves that originate from the prevailing south-west direction during a storm event. The severity of the event is such that it would occur approximately once per year.	Agitation & Tranquillity Entrance Navigability
50 year ARI NE Storm Event	This event represents severe north-westerly wave conditions that could be experienced. These conditions are represented by locally generated wind waves which develop during the early stages of a storm system. The severity of the event is such that it has a 2% chance of occurring in any year.	Agitation & Tranquillity
50 year ARI Typical Storm event	This event represents wave conditions that could be experienced during a storm event. These conditions are represented by a combination of swell and locally generated wind waves that originate from the prevailing south-west direction during a storm event. The severity of the event is such that it has a 2% chance of occurring in any year.	Agitation & Tranquillity
Seabreeze	This event represents wave conditions that could be experienced during a summer seabreeze. The selected event is a typical strong seabreeze. The severity of the event is such that would occur approximately 5 to 10 times per year.	Agitation & Tranquillity Entrance Navigability
Swell	These events represent swell conditions that could be experienced during a stormy or non-stormy period. Three different swell events were selected to test the impacts of different wave directions. These were the most severe events identified in the representative periods modelled from a range of directions.	Agitation & Tranquillity Entrance Navigability

Test cases in line with the events presented in Table 11.3 were extracted from the wave modelling completed in Task 5. Conditions were extracted at the entrance to the proposed TBF. The details of the selected test cases are presented in Table 11.4.

Table 11.4 Wave Penetration Test Cases

Name	Date	Hm0 (m)	Tp (s)	Dir Peak (°)
1 year ARI NE	10/7/2014 2:00	0.3	15	15
1 year ARI storm	11/7/2014 02:00	0.5	3	360
50-year ARI NE	Synthetic Cyclone	0.9	3	45
50-year ARI storm	Synthetic Cyclone	1.5	4	320
Seabreeze	19/12/2015 10:00	0.4	3	270
Swell – WNW	5/6/2014 10:00	0.3	19	300
Swell – N	28/06/2014 3:00	0.4	16	360
Swell - NE	24/11/2007 0:00	0.1	15	45

11.1.3 Empirical Calculations

Wave penetration into the marina is ultimately a function of wave diffraction through the entrance. Wave diffraction is the bending of wave energy around an obstacle. The diffracted waves contain less energy than the originally supplied waves as it is distributed throughout the shadowed zone behind the obstacle. Depending on the object with which the waves collide and at what angle, the wave energy will react differently. The resultant diffracted energy is a function of the original wave's wavelength.

Empirical methods have been used to estimate wave diffraction into the TBF entrance and basin. This involves the utilisation of diffraction diagrams to estimate how waves with certain periods and approach angles propagate through the breakwater entrance. Diffraction diagrams are utilised by engineers during initial risk assessments and preliminary stages of design. Direct application of any diffraction diagram to real situations for the purpose of final design is not recommended.

The most commonly used set of irregular wave diffraction diagrams were produced by Goda (1978). Goda's study focused on both wind generated waves with large directional spreading and short attenuation lengths, and swell waves with small directional spreading and long attenuation lengths. These drawings were based on scenarios where waves approach either a single thin, straight, fully reflecting semi-infinite breakwater or a gap between two of these structures at an angle normal to the structures.

Examples of the diagrams produced by Goda (1978) are shown in Figure 11.1. Goda notes that for the case of wave diffraction by a semi-infinite breakwater, the problem of oblique incidence can be treated by rotating the axis of the breakwaters in the diffraction diagrams while keeping wave direction and the co-ordinate axis at their original positions.

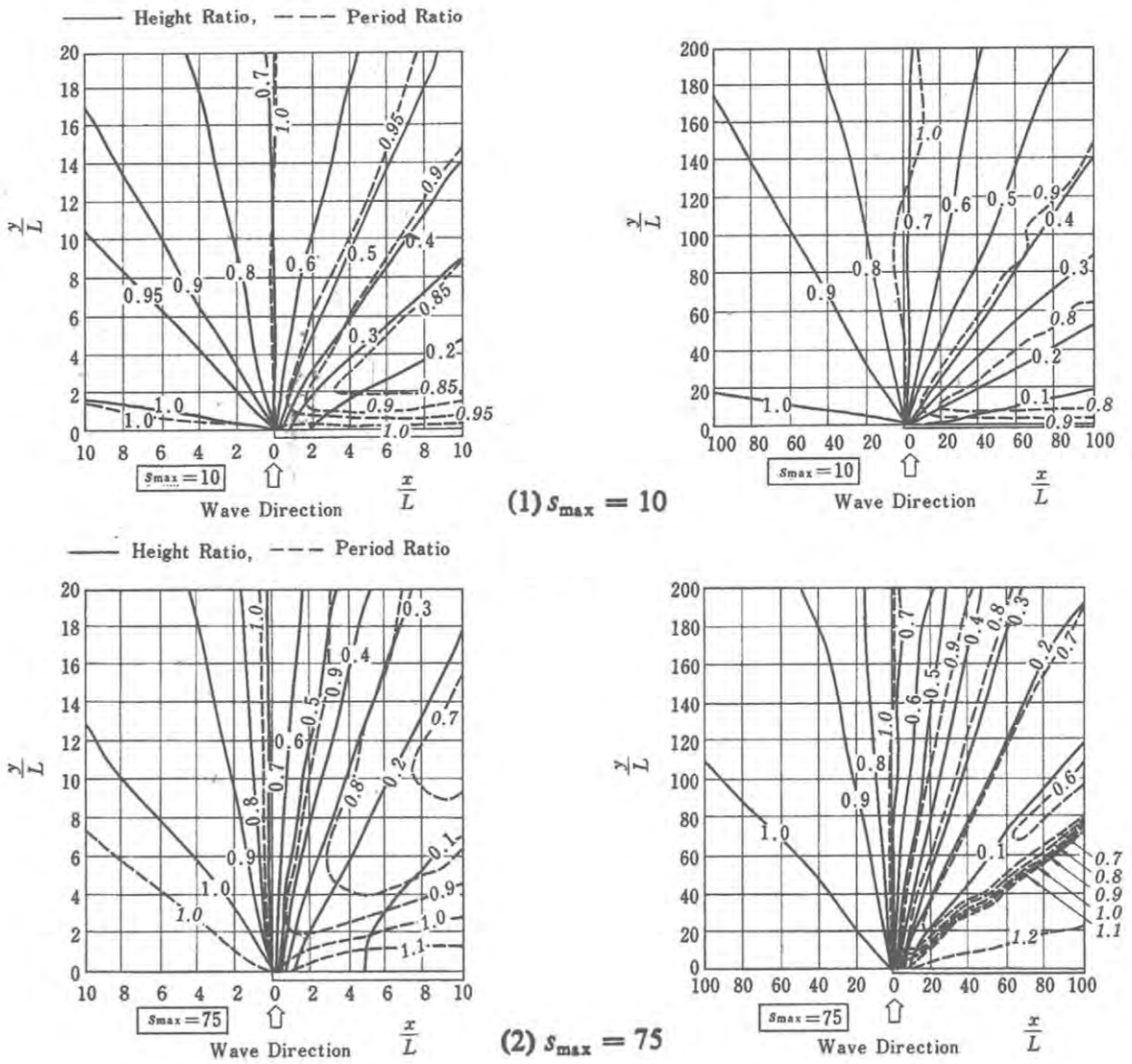

Figure 11.1 Wave Diffraction Diagrams Goda (1978)

11.1.4 Wave Penetration Methodology

Estimates of wave diffraction for the test cases presented previously have been prepared by utilising simplified schematizations of the TBF breakwater configuration. MRA has completed this wave penetration assessment for Concept B and has also completed an updated assessment for Concept C. The points of interest were initially chosen at the entrance of the harbour. This is considered a conservative assumption as it only considers diffraction around the outer breakwater. Ultimately waves will have to diffract around both the outer and inner breakwaters before they penetrate into the harbour, hence the conservative nature of this assessment. One of the 50-year ARI events maintained a reduced wave height above the threshold for a good wave climate at the entrance to the harbour and therefore required a diffraction calculation around the inner breakwater to check the wave climate where boats would be penned. Figure 11.2 demonstrates the empirical approach to calculating wave diffraction with the simplified schematic (indicative figure shows Concept B layout).

One of the limitations of the empirical approach is that it only considers diffraction around an infinitely long breakwater of nominal thickness normal to the incident wave orthogonal. It does not consider curved breakwaters or continuous diffraction around the head of a breakwater. The diffraction diagrams also do not allow for diffraction beyond 90°. Although minor, this may occur particularly around curved structures such as the breakwater heads. For this reason, three different points of interest were chosen at the entrance to, and within, the harbour (refer Figure 11.3).

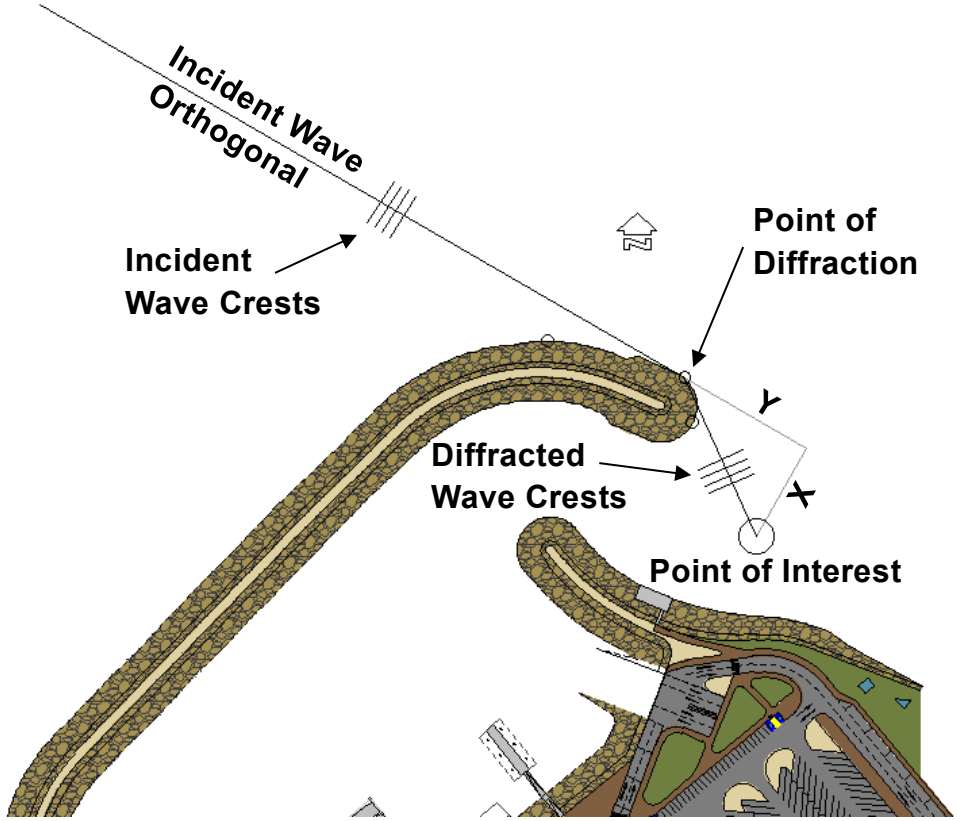

Figure 11.2 Indicative Diffraction Calculation Approach

Figure 11.3 Wave Penetration Diagram for Concept B

Despite the limitations in the empirical approach, the assumptions made in this assessment are considered conservative and yield a reasonable output of what would be expected during real events. A more detailed wave penetration assessment could be produced through Boussinesq type numerical modelling around the structures. This is thought to be excessive for a design that is already conservative and at low-risk of significant wave energy penetration. The results of the assessment for Concept B are presented and discussed in Tables 11.5 to 11.7, and discussed later in this section.

Table 11.5 Wave Penetration Overview for Concept B at Point A

Event Name	Hm 0 (m)	Tp (s)	L (m)	Dp (o)	Smax	X (m)	Y (m)	x/L	y/L	Height Ratio
50-year ARI storm	1.5	4	20	320	10	23	82	1.77	6.31	0.55
Seabreeze	0.4	3	13	270	10	102	96	7.38	7.85	0.3
Swell – WNW	0.3	19	114	300	75	69	50	0.61	0.44	0.4

Table 11.6 Wave Penetration Overview for Concept B at Point B

Event Name	Hm0 (m)	Tp (s)	L (m)	Dp (o)	Smax	X (m)	Y (m)	x/L	y/L	Height Ratio
1 year ARI NE	0.3	15	90	15	75	76	50	0.84	0.56	0.3
1 year ARI storm	0.5	3	13	360	10	90	30	6.92	2.3	0.2
50-year ARI NE	0.9	3	13	45	10	40	80	3.15	6.23	0.5
Swell – N	0.4	16	95	360	75	90	30	0.95	0.32	0.2
Swell - NE	0.1	15	90	45	75	40	80	0.45	0.9	0.5
50-year ARI storm[1]	1.5	4	20	320	10	96	-35	4.80	-1.75	<0.2
Seabreeze[1]	0.4	3	13	270	10	68	-86	5.23	-6.62	<0.2
Swell – WNW[1]	0.3	19	114	300	75	85	-61	0.75	-0.54	<0.1

Note: 1. These events were calculated at Point A, and additionally estimated here for completeness.
2. Negative values of Y denote diffraction past 90°, which is a limitation in the methodology. Despite being very minor in magnitude, the height ratios for these events represent a best fit approximation.

Table 11.7 Wave Penetration Overview for Concept B at Point C

Event Name	Hm0 (m)	Tp (s)	L (m)	Dp (o)	Smax	X (m)	Y (m)	x/L	y/L	Height Ratio
Diffracted 50-year ARI NE	0.45	3	13	45	10	83	100	13	6.38	0.4

A revised wave penetration assessment was completed for the Concept C layout of the proposed TBF using a single point of interest.at the mouth of the marina (refer Figure 11.3). This point was selected based on the results of the previous wave penetration assessment for Concept B and the changes to the marina entrance for Concept C. Results of the assessment are presented in Table 11.8.

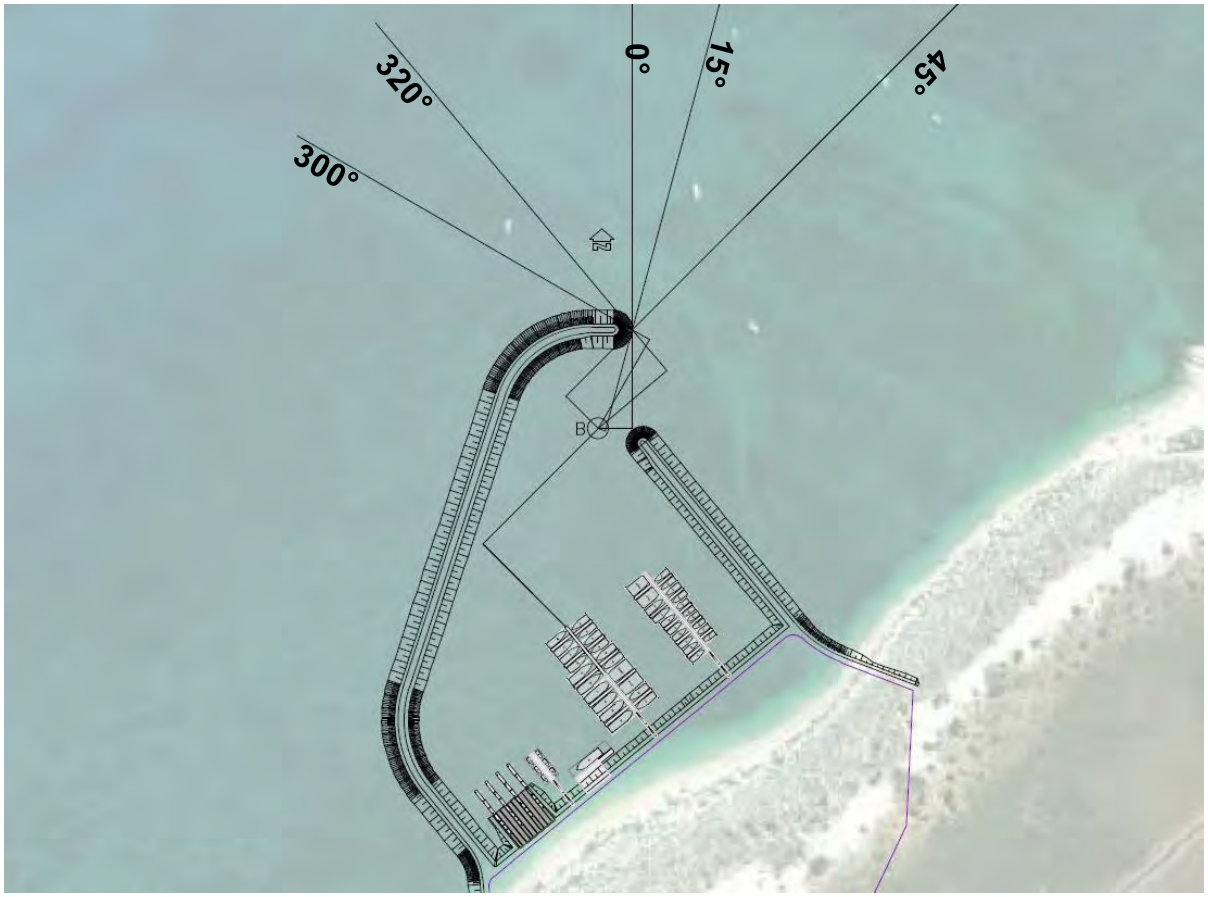

Figure 11.4 Wave Penetration Diagram for Concept C

Table 11.8 Results of Wave Penetration Assessment Concept C

	Event Name	Hm0 (m)	Tp (s)	L (m)	Dp (o)	Smax	Height Ratio	Hm (m)
Point B	1 year ARI NE	0.3	15	90	15	75	0.6	0.18
	1 year ARI storm	0.5	3	13	360	10	0.55	0.275
	50-year ARI NE	0.9	3	13	45	10	0.9	0.81
	50-year ARI storm	1.5	4	20	320	10	0.25	0.375
	Seabreeze	0.4	3	13	270	10	<0.1	<0.04
	Swell – WNW	0.3	19	114	300	75	0.3	0.09
	Swell – N	0.4	16	95	360	75	0.55	0.22
	Swell - NE	0.1	15	90	45	75	1.0	0.1
Pens	Diffracted 50-year ARI NE	0.81	3	13	-	10	0.4	0.31

11.1.5 Internal Basin Wave Generation

It is prudent to also consider the wave climate arising from wind generated waves inside the marina. The prediction of wind waves within fetch limited areas, such as within a marina can be accomplished by conducting a Wave Hindcast Analysis. There are a number of different methods for the estimation of wave heights using a wave hindcast analysis. Wilson's Method, as revised by Goda (2010), was utilised.

The Wilson Method predicts the significant wave height and period of wind waves generated by a constant wind over a fetch. This is accomplished using the two following equations.

$$\frac{gH_{\frac{1}{3}}}{U^2} = 0.30(1 - (1 + 0.004(g\frac{F}{U^2})^{\frac{1}{2}})^{-2})$$

$$\frac{gT_{\frac{1}{3}}}{2\pi U^2} = 1.37(1 - (1 + 0.008(g\frac{F}{U^2})^{\frac{1}{3}})^{-5})$$

Where:

F = Effective Fetch Length (m).

U = Wind Speed (m/s) measured at an elevation of 10 m above the sea surface.

g = Gravitational Acceleration (9.81 m/s)

These equations assume a uniform wind field over the area of wave generation and a sufficiently long duration of wind forcing. Design wind speeds were determined using *AS/NZS 1170.2:2021* (Standards Australia, 2021) based on the Wind Region D. It is unlikely that these temporally and spatially constant wind speeds will occur. However, the assumption of these constant conditions

allows for the calculation of reasonably conservative estimates of the significant wave height and period.

The effective fetch length used in the above formulas was calculated using Saville's Method (Etemad-Shahidi & Mahjoobi, 2009). This calculation determines a total effective fetch length by taking fetch lengths radial from the point of interest up to 45° either side of the desired wind direction as shown in Figure 11.4. These radial fetch lengths are then used to compute the effective fetch with the following equation.

$$X = \frac{\sum_{i=1}^{19} X_i cos^2\theta_i}{\sum_{i=1}^{19} cos\theta_i}$$

Where:

X_i = Individual Fetch length (m)

X = Effective Fetch (m)

The hindcast was conducted for the largest fetch lengths within the marina to provide a conservative estimate of design conditions at the extremities of the basin. Given the TBF is in a cyclonic region, the wind speeds within *AS/NZS 1170.2:2021* do not vary with direction, so the calculated wave heights could occur at both ends of the basin.

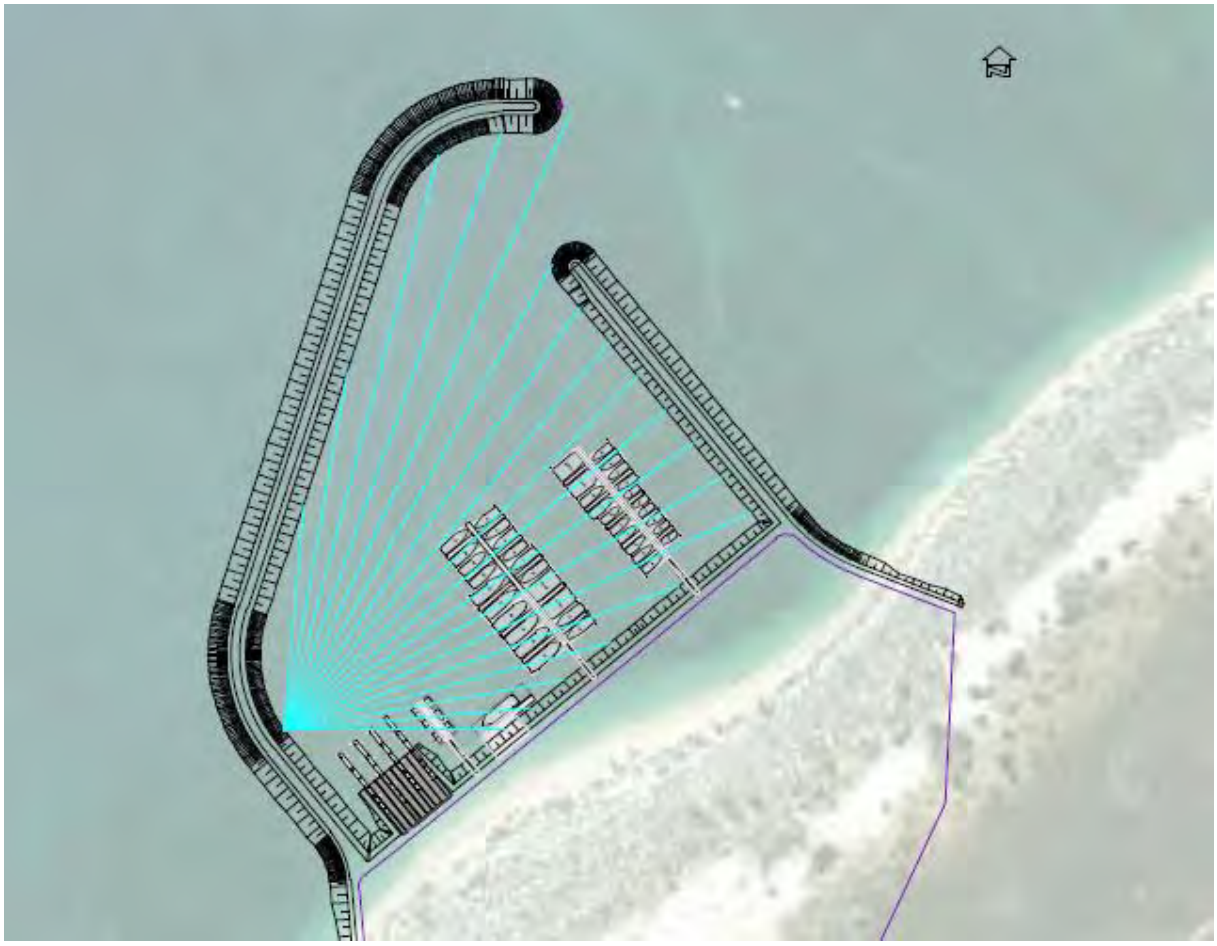

Figure 11.5 Example of Radial Fetch Length Calculation Concept C

The calculated effective fetch was used to estimate significant wave heights and peak periods using the previously discussed equations for both Concept B and Concept C. The results of these calculations are displayed in Tables 11.9 and 11.10 respectively. During periods of more north westerly or south easterly wind conditions, locally generated wave heights would be smaller than those presented in the tables below. Additionally, once boat pens are constructed within the marina any waves generated within the marina would be attenuated.

Table 11.9 Local Wave Generation within the Basin of the TBF (Concept B)

Event	Hs (m)	Tp (s)
1 year ARI	0.1	1.0
50 year ARI	0.4	1.4

Table 11.10 Local Wave Generation within the Basin of the TBF (Concept C)

Event	Hs (m)	Tp (s)
1 year ARI	0.2	1.0
50 year ARI	0.4	1.5

11.1.6 Review & Recommendations

Basin Tranquillity Concept B

The orientation of the seaward breakwater allows for minimal wave penetration from the south-west through to north directions. Table 11.8 shows diffracted wave heights at the selected points. Point A can be considered mostly sheltered from waves with any westerly aspect and slightly exposed to north to north-east waves. Point B can be considered almost entirely sheltered from westerly waves and only receives a small amount of penetration from north-easterly waves. Further inside of the harbour basin (Point C) the wave energy is reduced again. With the exception of one event, most of these initial penetration estimates did not require the diffraction around the inner breakwater to be checked as the height reduction around the outer breakwater was sufficient to demonstrate achievement of tranquillity criteria. The event which maintained a residual wave height of 0.45 m (50-year ARI NE) exceeded the threshold for a good wave climate for beam seas at Point B. An additional diffraction calculation was performed for this scenario to find the wave height closer to the boating facilities (Point C). All other wave events are expected to experience further reduction in wave height about the inner breakwater by similar ratios to the above.

Further to this, a review of the wave climate generated within the basin itself has shown that during the 50 year ARI wind event the maximum wave height generated at the northern or southern (depending on wind direction) extremities of the basin would be around 0.4 m. These wave directions will essentially be head seas, and so will still meet the criteria presented in Table 11.1.

In accordance with Table 11.1, the TBF Concept B appears to exhibit an “excellent” wave climate for small craft exposed to beam, head and oblique seas in the basin protected by both of the breakwaters.

Basin Tranquillity Concept C

The basin tranquillity for the Concept C layout of the proposed TBF was very similar to the basin tranquillity for Concept B. However, Concept C appears to exhibit an "excellent" wave climate for small craft exposed to beam seas in all cases except for the 50 year ARI north easterly, which exhibits a "moderate" wave climate.

Navigability Criteria Concept B

An assessment of navigability criteria was also completed. The results of this review are presented in Table 11.11.

Table 11.11 Addressed Navigability Criteria

Criteria	Comment
The final approach to the harbour entrance should be straight, and the portion of the straight approach should be at least 3 to 5 times the length of the largest vessel that uses the harbour. Ideally, the approach to the harbour should meet currents or winds such that the ship drift angle does not exceed 10°-15°, particularly where hazardous navigational conditions are expected.	Largest design vessel is approx. 25 m in length, the required straight approach would be 75-125 m. The concept design exhibits a straight approach for approx. 75 m. It is recommended that the straight approach to the entrance is reviewed, bearing in mind the wave climate is typically mild, even during 1-year ARI events.
The entrance must be designed so that a vessel does not need to make any manoeuvres at the entrance. The craft can start manoeuvres only after it passes the entrance and enters a more protected area.	The entrance is designed with sufficient space to perform manoeuvres after it passes through the entrance and enters protected water. It is recommended that the entrance configuration is reviewed to ensure that the turning radius for the design vessel is sufficient. The recommended turning radius is 2L.
If a straight approach through an entrance is not possible or desirable, then the arrangement of overlapping breakwaters should allow a ship to pass through the restricted entrance and turn and reorient to the sea before it is hit broadside by the waves.	The breakwaters overlap with sufficient space to allow a small craft to turn before it is hit broadside by waves.
For powerboat manoeuvring, the entrance should not cause returning boats to experience a direct following sea, because rudder control may then be lost, especially at low speed.	The entrance is specifically orientated to avoid boats entering or exiting directly into following seas during typical boating conditions.
The entrance should also not be such that boats approach the small craft harbour in a beam sea condition, as this may induce broaching of the boat.	The entrance is specifically orientated to avoid boats entering or exiting directly into beam seas.
During storms, when waves are between 1 and 3 m (3–9 ft), the recommended total corridor width increases to 8B. If the waves exceed 3 m (9 ft), the navigational corridor increases to 9B.	The navigational corridor at and adjacent to the entrance will not experience waves exceeding 1m during storms (see Table 11.5).

As shown in Table 11.10 navigability of the entrance has been considered under selected wave conditions. It should be noted that only the effects of wave penetration on navigability have been assessed, and that general navigability criteria have not been considered in this section.

Navigability Criteria Concept C

An assessment of navigability criteria for Concept C was also completed. The results of this review are presented in Table 11.12.

Table 11.12 Addressed Navigability Criteria

Criteria	Comment
The final approach to the harbour entrance should be straight, and the portion of the straight approach should be at least 3 to 5 times the length of the largest vessel that uses the harbour. Ideally, the approach to the harbour should meet currents or winds such that the ship drift angle does not exceed 10°-15°, particularly where hazardous navigational conditions are expected.	Largest design vessel is approx. 25 m in length, the required straight approach would be 75-125 m. The concept design exhibits a straight approach for approx. 75 m. It is recommended that the straight approach to the entrance is reviewed, bearing in mind the wave climate is typically mild, even during 1-year ARI events.
The entrance must be designed so that a vessel does not need to make any manoeuvres at the entrance. The craft can start manoeuvres only after it passes the entrance and enters a more protected area.	The entrance is designed with sufficient space to perform manoeuvres after it passes through the entrance and enters protected water. It is recommended that the entrance configuration is reviewed to ensure that the turning radius for the design vessel is sufficient. The recommended turning radius is 2L.
If a straight approach through an entrance is not possible or desirable, then the arrangement of overlapping breakwaters should allow a ship to pass through the restricted entrance and turn and reorient to the sea before it is hit broadside by the waves.	The breakwaters overlap with sufficient space to allow a small craft to turn before it is hit broadside by waves.
For powerboat manoeuvring, the entrance should not cause returning boats to experience a direct following sea, because rudder control may then be lost, especially at low speed.	The entrance is specifically orientated to avoid boats entering or exiting directly into following seas during typical boating conditions.
The entrance should also not be such that boats approach the small craft harbour in a beam sea condition, as this may induce broaching of the boat.	The entrance is specifically orientated to avoid boats entering or exiting directly into beam seas.
During storms, when waves are between 1 and 3 m (3–9 ft), the recommended total corridor width increases to 8B. If the waves exceed 3 m (9 ft), the navigational corridor increases to 9B.	The navigational corridor at and adjacent to the entrance will not experience waves exceeding 1m during storms (see Table 11.8).

As shown in Table 11.12 navigability of the entrance for Concept C is essentially the same as for Concept B. It should be noted that only the effects of wave penetration on navigability have been assessed, and that general navigability criteria have not been considered in this section.

11.2 Long Period Waves

11.2.1 Available Pressure Data

Data utilised in the assessment was collected and provided by DoT. Due to the significant wave lengths associated with LPW energy, surface tracking devises are unable to provide meaningful details of the wave climate. Pressure sensor data, such as that collected by the RBR's were used to investigate the characteristics of the local LPW climate.

A summary of the RBR data available for the assessment is provided in Table 11.13. The location of each dataset is shown in Figure 11.6.

Table 11.13 Summary of Data Collected by RBRs

Dataset	Location Description	Duration	Data Frequency (Hz)	Location (°) (Lat Long)	Location (m) (GDA 2020)	Water Depth (m)
TAN01	Deployed with AWAC	20/3/2019 to 3/8/2021	1	21.9076 S 113.9724 E	807112.09 E 7574426.25 S	~3 m
TAN02	Deployed with Aquadopp	26/7/2019 to 3/8/2021	1	21.9104 S 113.9767 E	807550.64 E 7574107.41 S	~ 3 m
TAN03	Deployed at Boat Ramp	15/8/2020 to 5/8/2021	1/60	21.9122 S 113.9776 E	807639.8151 E 7573906.178 S	~1.5

Data was provided in raw pressure format at the frequencies shown in Table 11.13. The RBR from TAN03 was set-up to measure tidal averaging rather than assessment of long period waves and as such measurements were collected at a frequency of 1/60 Hz. Data from this RBR was not utilised in the assessment as it would not adequately resolve the LPW characteristics. The data from RBRs TAN01 and TAN02 was extracted and analysed as discussed in Section 11.2.2.

Figure 11.6 RBR Locations

11.2.2 Data Analysis & Review

The RBR datasets were analysed to identify the presence (or lack therefore) and bands of LPW energy at each location. This included the following.

- Correction of the data to account for the pressure loss in the water column.
- Calculation of time varying welch spectral densities over a selected number of samples (NFFT) to allow identification and visualisation of key long period bands.
- Integration of the welch spectral densities over the bands to estimate the zero moment wave heights representative of each bands.

Dynamic pressure generated by waves will attenuate from the water surface to the seabed. Therefore, short period wave data collected by a pressure sensor will have lower magnitudes compared to the actual pressure values. Pressure data collected by a pressure sensor must be corrected to account for pressure loss in the water column.

The NFFT is the number of samples utilised for the Fourier Transform to calculate the power spectral density. The generated power spectral density is reported with the following characteristics.

- A frequency range of 0 to sampling frequency/2; with

- NFFT/2+1 data points.

Given the sampling frequency of the TAN01 and TAN02 RBRs, the maximum frequency that can be resolved by the analysis is 0.5 Hz (2s). The NFFT must be selected to sufficiently resolve the waves of interest in the spectrum. Selection of a larger NFFT will smooth data in shorter period bands such that in may not be an appropriate reflection of observations, whilst selection of a smaller NFFT may insufficiently resolve longer period waves. As a result, the sensitivity of the results of the assessment to the NFFT were tested and optimised to best resolve the local LPWs. The time varying spectral densities at each location are shown in Figures 11.7 and 11.8.

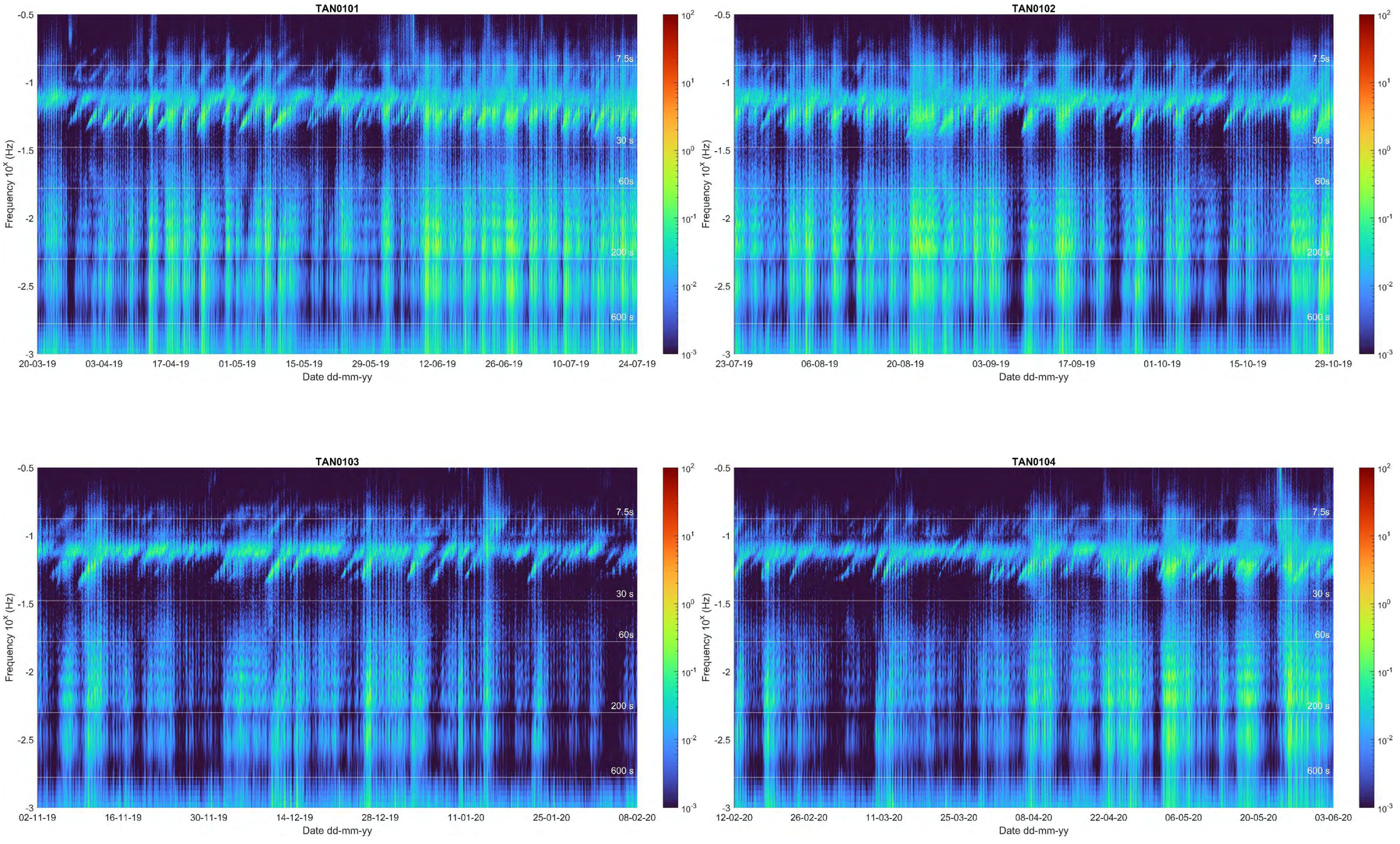

Figure 11.7 Time Varying Spectral Density TAN01

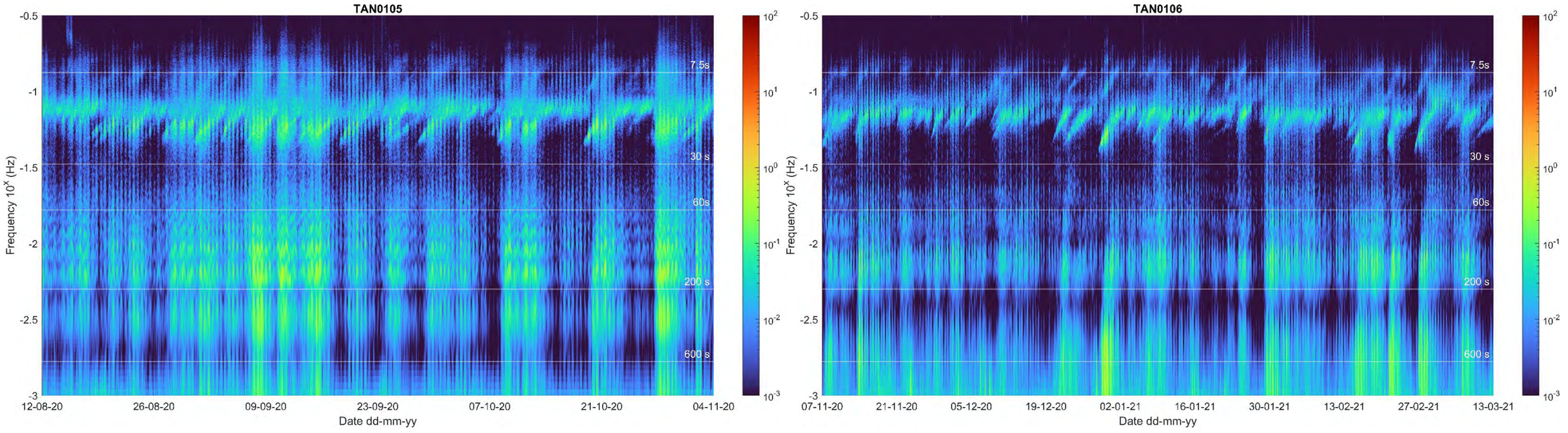

Figure 11.7 (cont.) Time Varying Spectral Density TAN01

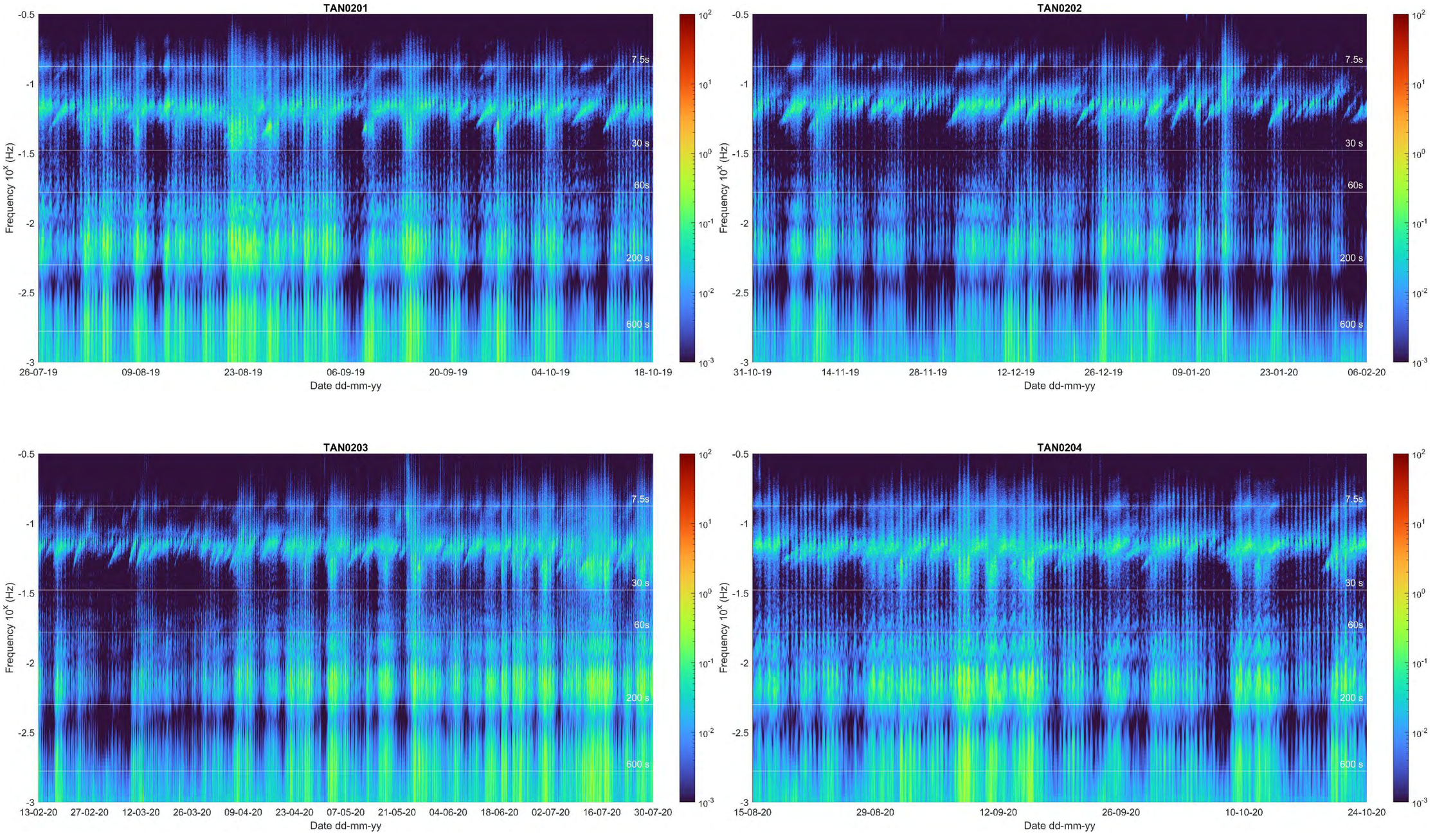

Figure 11.8 Time Varying Spectral Density TAN02

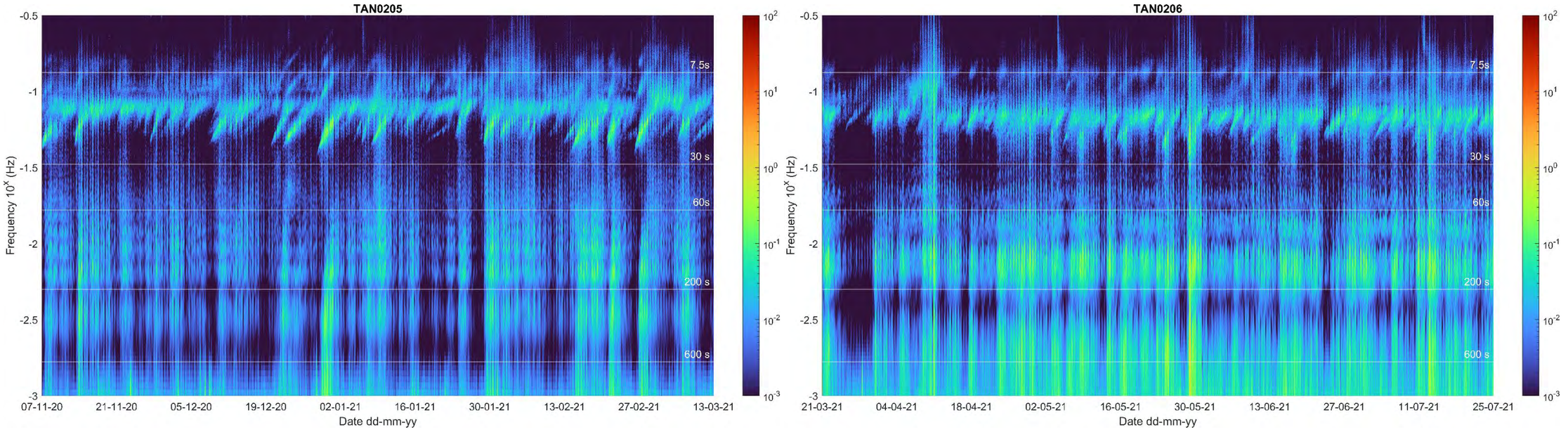

Figure 11.8 (cont.) Time Varying Spectral Density TAN02

Key outcomes of the review of the time varying spectral density analyses are as follows.

- At TAN01 LPW energy can be observed in several bands. This typically includes 3 to 4 bands of LPW energy with periods between 60 and 200s. Greater energy in these bands coincides with greater swell energy with periods of around 15 to 20 seconds.
- At TAN02 long wave energy can be observed in several bands. This typically includes 2 bands of long wave energy with periods between 60 and 300s. Greater energy in these bands coincides with greater swell energy with periods of around 15 to 20 seconds.
- At both locations there is minimal wave energy in the 30 to 60s energy band.
- The trends observable from deployments at the same locations are similar. Over Summer months, there is a reduction in overall wave energy, including long wave energy.

Utilising this assessment, bands were selected visually from the time varying spectral density. The spectral densities were integrated across each of the bands to estimate the zero moment wave heights of the relevant bands. The results of this assessment also allow comparison against data collected at the same locations by the AWAC and Aquadopp devices. Plots showing the LPW heights as well as the calculated sea and swell waves are provided in Figures 11.9 and 11.10.

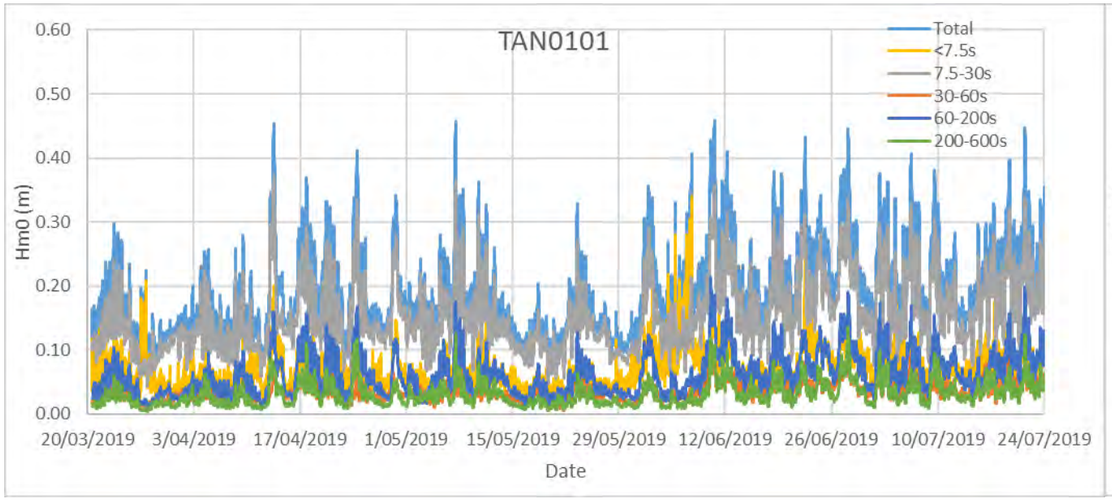

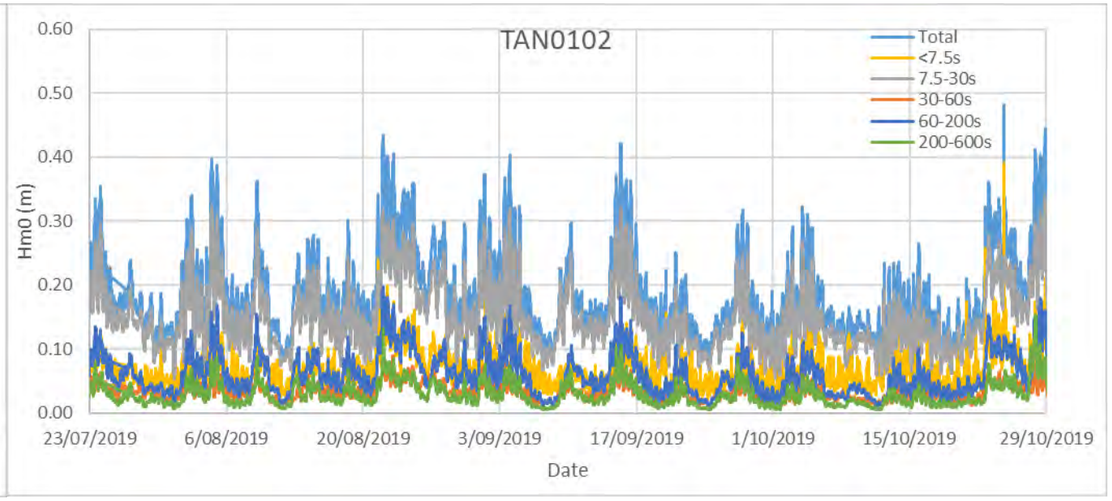

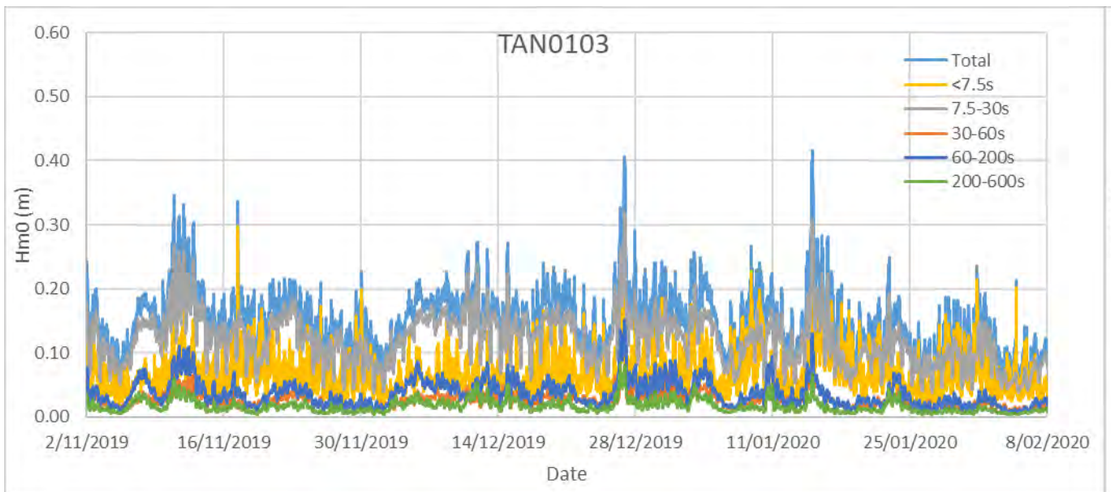

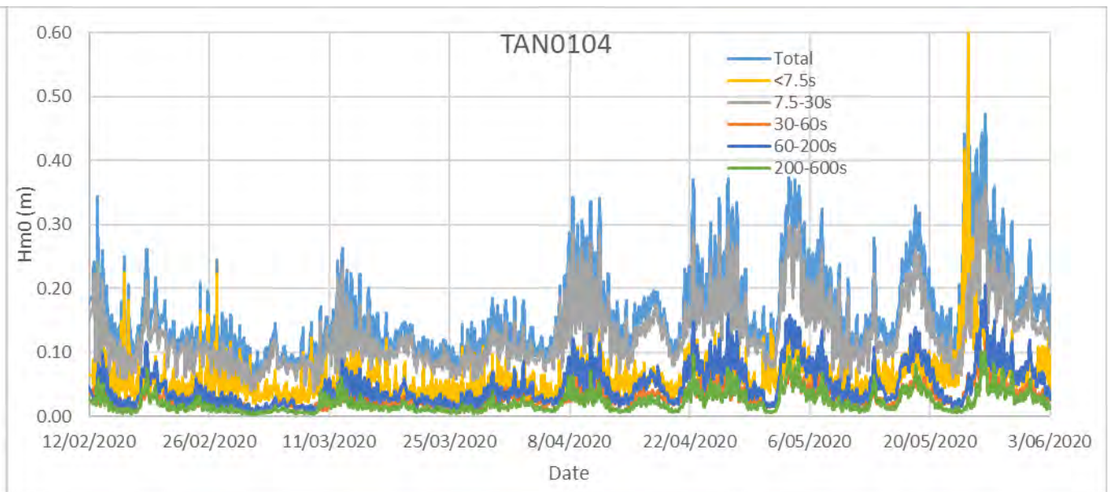

Figure 11.9 Zero Moment Wave Heights of Long Period Wave Bands TAN01

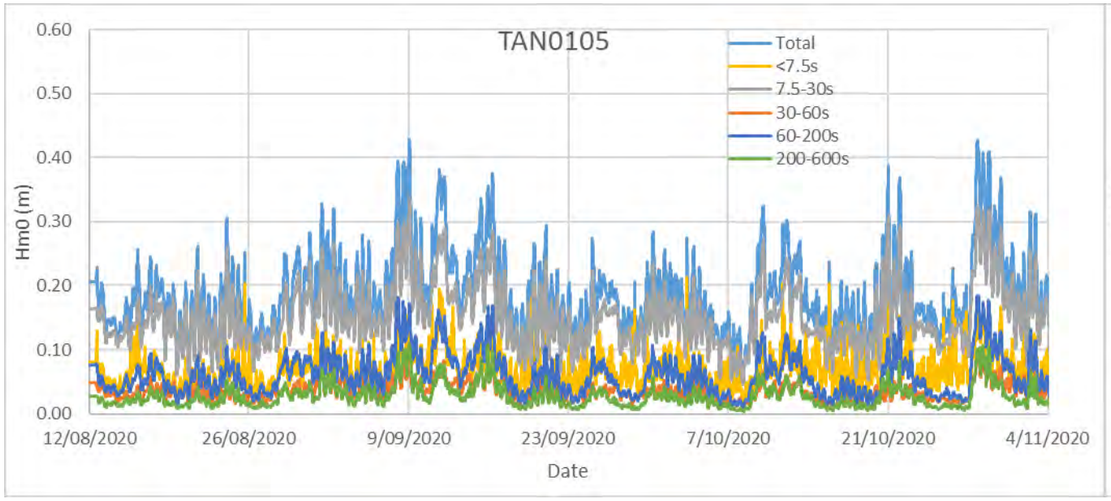

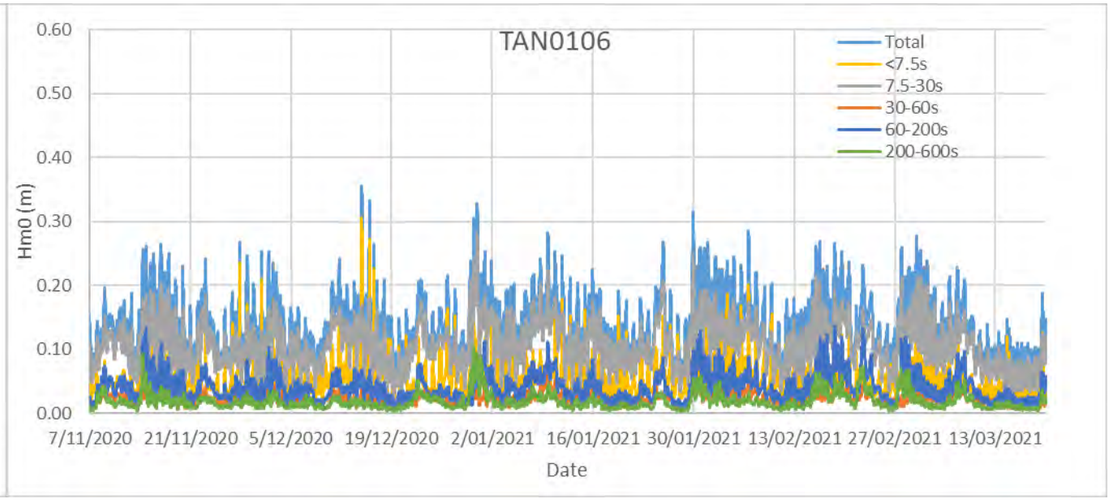

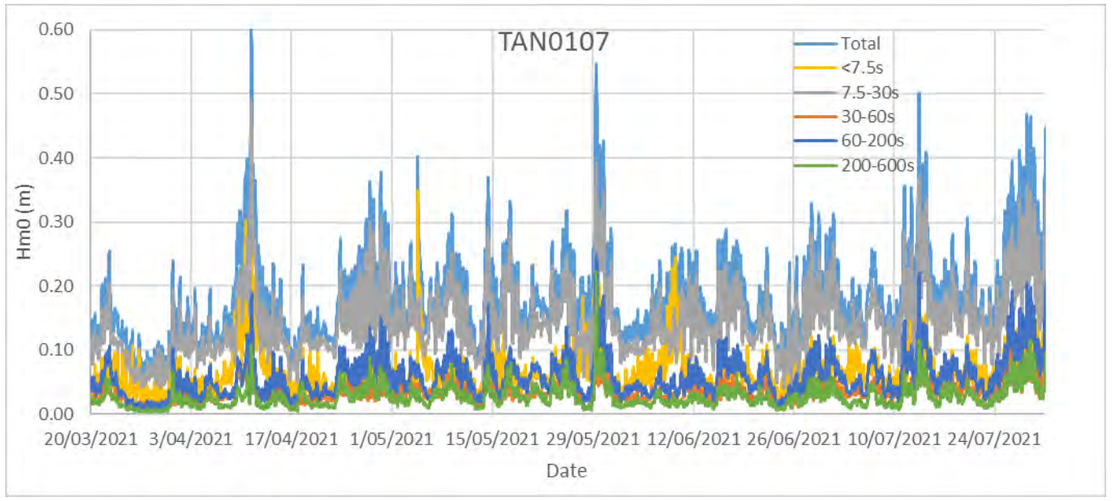

Figure 11.9 (cont.) Zero Moment Wave Heights of Long Period Wave Bands TAN01

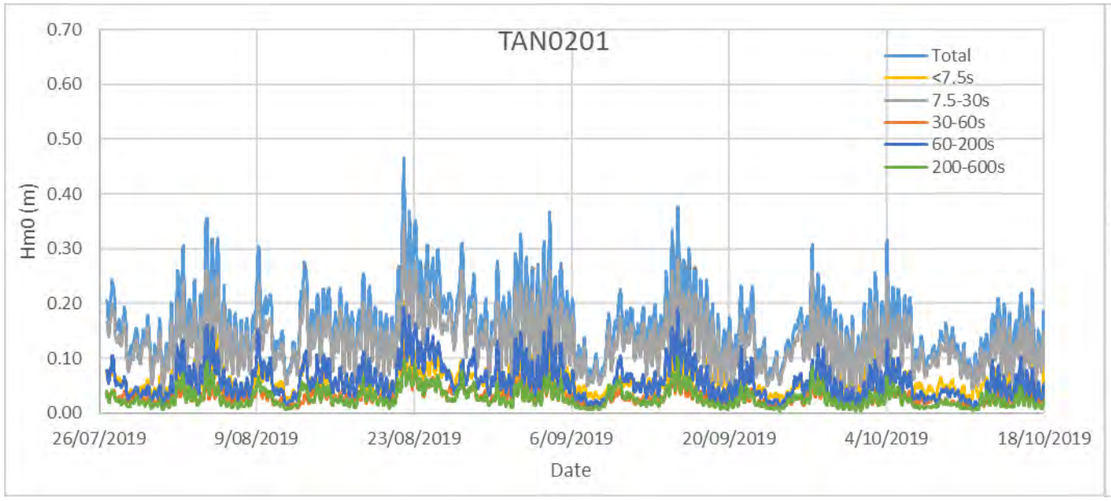

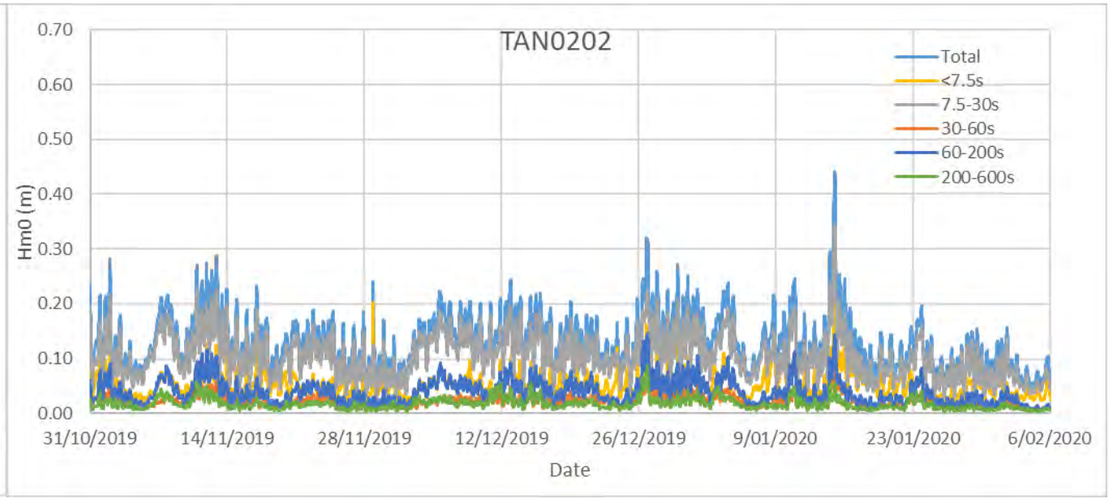

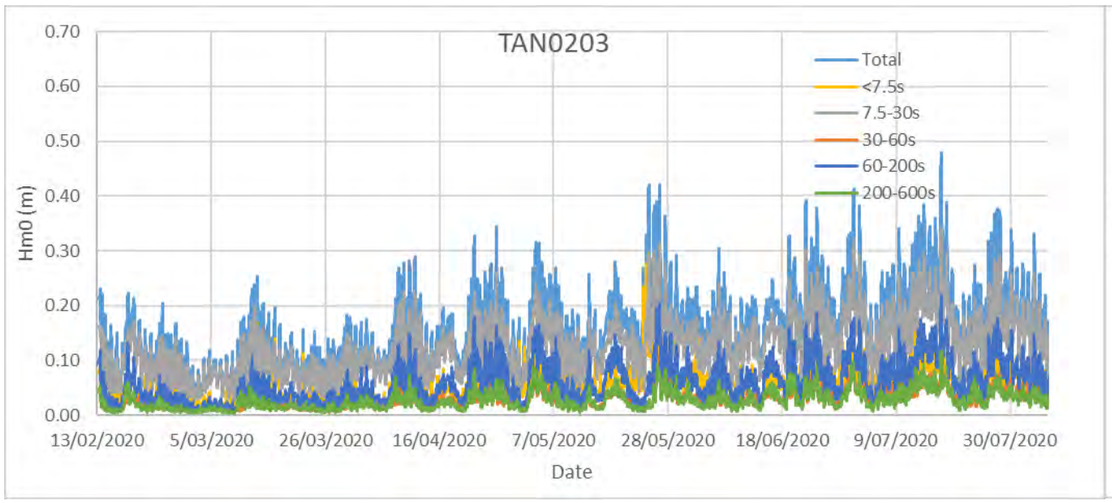

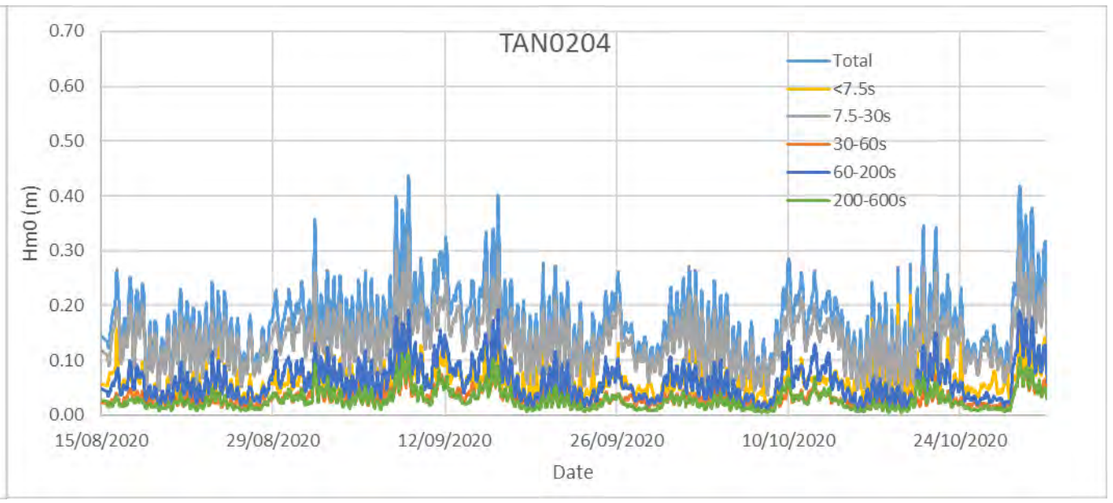

Figure 11.10 Zero Moment Wave Heights of Long Period Wave Bands TAN02

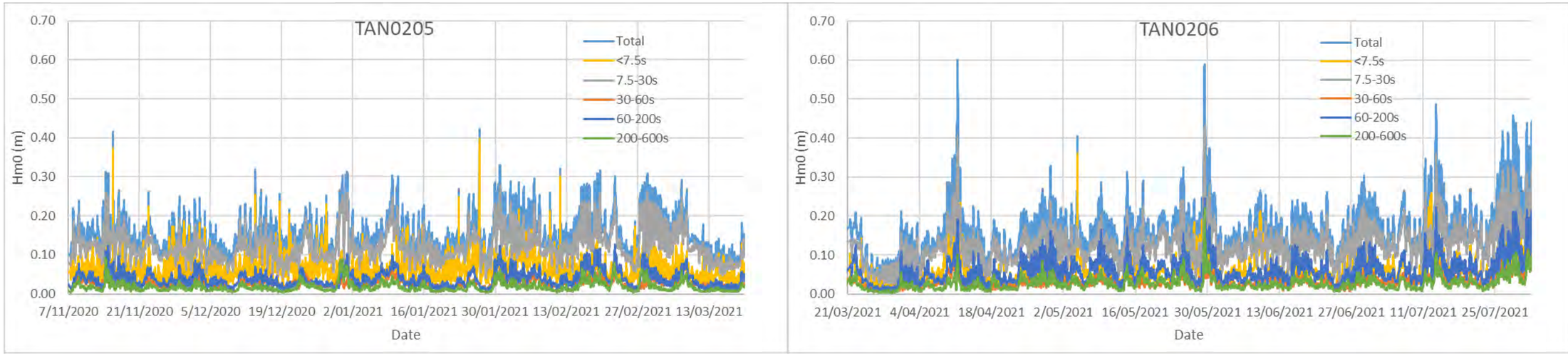

Figure 11.10 (cont.) Zero Moment Wave Heights of Long Period Wave Bands TAN02

In addition to the analysis presented above, a comparison of wave heights obtained through processing of the RBR Data against wave heights from the AWAC and Aquadopp datasets was undertaken. This was undertaken to compare and validate the analysis of the RBR Data.

The plots in Figure 11.11 show a comparison of sea, swell and total wave heights obtained from MRA analysis of the RBR (TAN01) against AWAC data. The RBR (TAN01) and AWAC data are at the same location in approximately 3m of water depth.

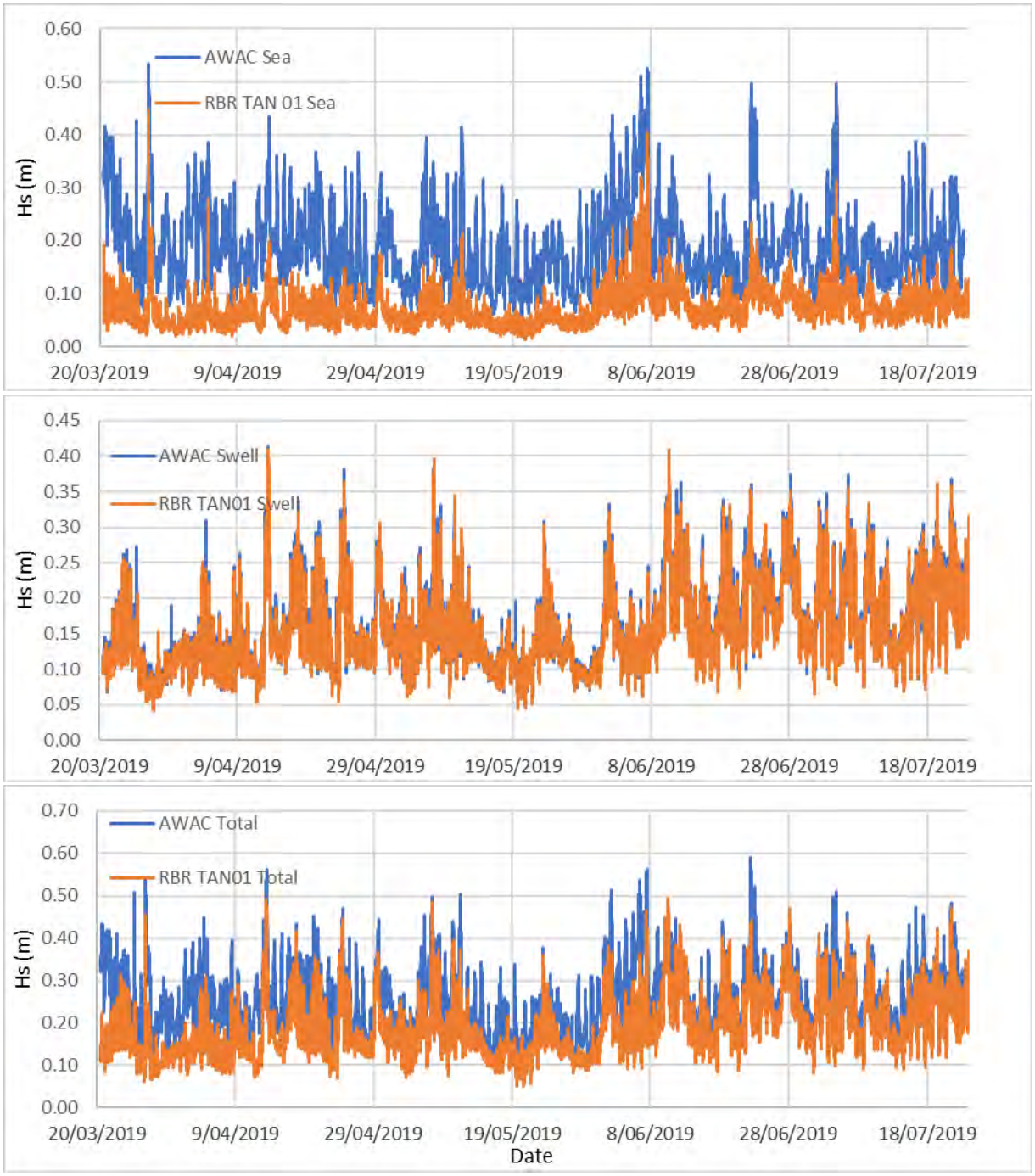

Figure 11.11 Wave Height Comparison TAN01 and AWAC

Key outcomes of this comparison are as follows.

- Predictably, sea wave heights obtained by the RBR are less than those obtained by the AWAC. Given the 1 Hz sampling frequency of the RBR, the shortest period that can be registered by the RBR is 2s. Pressure attenuation also impacts the RBR's capacity to accurately capture waves greater than 2s. Hence, the underestimate of sea wave heights by the RBR is considered justifiable and expected.

- There is good agreement between swell wave heights (7.5s to 30s) obtained by the RBR and the AWAC. This is because the impacts of pressure attenuation on waves greater than 7.5s at the depth of the RBR are minimal. This result provides confidence in the use of both datasets given they are independent instruments with different methods of calculating wave height.

- Total wave heights obtained by the RBR are less than those obtained by the AWAC. This is due to the factors described previously related to the inability of the RBR to accurately capture shorter period waves. Hence, the underestimate of total wave heights by the RBR is considered justifiable and expected.

Figure 11.12 shows a comparison of total wave heights obtained from MRA analysis of the RBR (TAN02) against Aquadopp data. A swell and sea breakdown for the Aquadopp were not available for the assessment. The RBR (TAN02) and Aquadopp data are at the same location in approximately 3m of water depth.

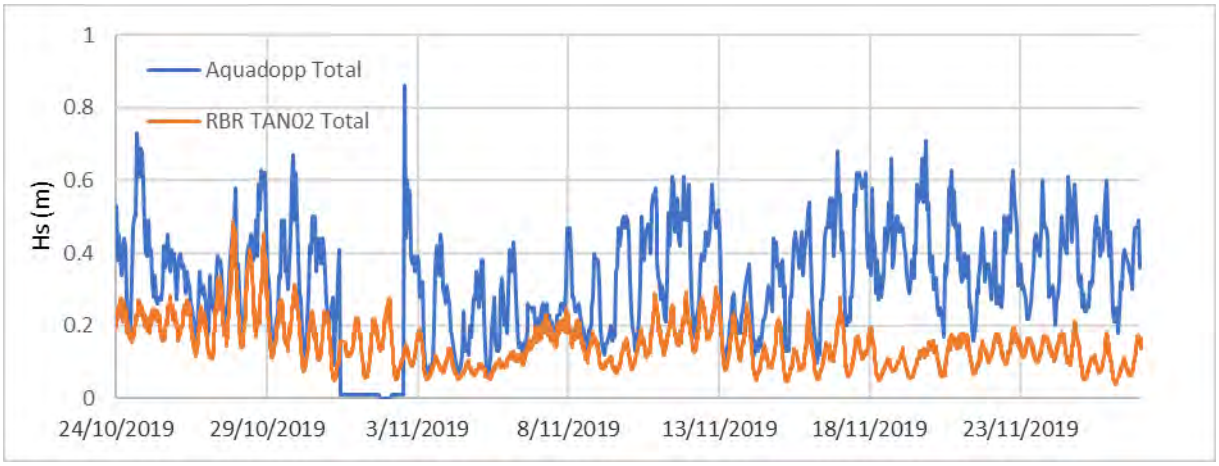

Figure 11.12 Total Wave Height Comparison TAN02 and Aquadopp

The key outcomes of this comparison are as follows.

- The difference in total wave height between the RBR and the Aquadopp is quite significant. It is greater than would be considered the likely contribution of the RBR sea underestimation.

- Based on this, there is limited confidence in the accuracy of wave data provided relating to the Aquadopp. It is suggested that where possible, alternative wave data sources are utilised in preference to the Aquadopp.

11.2.3 Empirical Calculations

Background LPW energy can induce resonance or oscillations within marina or harbour basins. One cause of this can be if the background LPW energy at the site overlaps with the Natural Oscillation Periods of the basin.

Analysis of the available data has been undertaken to identify the presence of background LPW energy at the site. Empirical calculations allow estimation of the Natural Oscillation Periods of the facility and hence whether any such overlaps exist that would require further investigation.

Theoretical Harbour Resonance Calculations were undertaken based on CEM (2002) for open Basins (eq.1) and Sorensen and Thompson (2008) for closed basins (eq.2) as shown in the formulae below. It is known that basins can behave as closed, partially enclosed or open basins depending on the ratio of its entrance width to basin width.

$$T_n = \frac{4L}{(1+2n)\sqrt{gH}} \qquad (eq.1)$$

$$T_{n,m} = \frac{2}{\sqrt{gH}}\left[\left(\frac{n}{L}\right)^2 + \left(\frac{m}{B}\right)^2\right]^{-0.5} \qquad (eq.2)$$

$T = Natural\ Oscillation\ Period$
$L = Basin\ Length\ (m)$
$B = Basin\ Width\ (m)$
$H = Water\ Depth\ (m)$
$n, m = number\ of\ nodes\ along\ each\ axis$

It should be noted that when the n or m term in eq.2 are set to 0, this equation simplifies to eq.1.

At Tantabiddi the depth of the basin can vary due to the tide. It is therefore prudent to review the possible natural oscillation periods (NOPs) of the proposed facility under varying tidal conditions.

Concept B Layout

The results of this assessment for various Nodal Parameters for Concept B are presented in Table 11.14 and Figure 11.13

Table 11.14 Natural Oscillation Periods of Concept B

Nodal Parameters		MLWS		MSL				HAT				Water Depth (m)
n	m	3.15	3.4	3.65	3.9	4.15	4.4	4.65	4.9	5.15	5.4	
0	-	209	201	194	188	182	177	172	167	163	159	Natural Oscillation Period (s)
0	1	50	58	55	53	52	50	49	47	46	45	
0	2	29	28	27	26	25	24	24	23	23	29	
1	0	104	100	97	94	91	88	86	84	82	80	
2	0	52	50	48	47	45	44	43	42	41	40	
1	1	50	49	47	45	44	43	41	40	39	38	
2	2	25	24	23	23	22	21	21	20	20	19	

Notes: 1. NOPs calculated using equations (1) and (2).
2. NOPs highlighted in orange are those which overlap with the background LPW energy in the area.

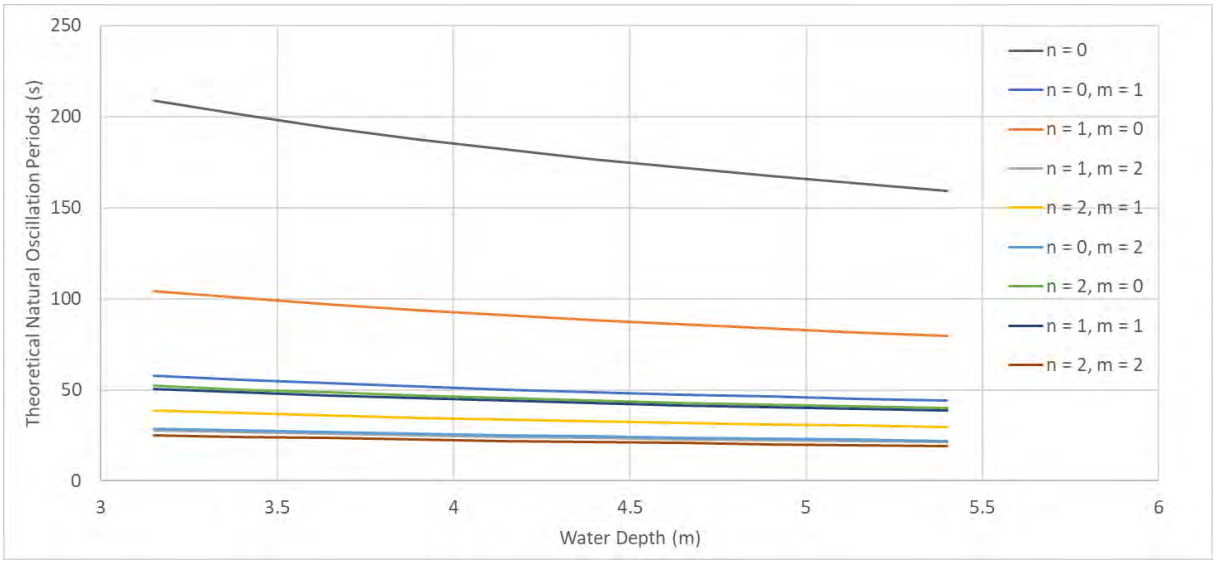

Figure 11.13 Natural Oscillation Periods of Concept B

Concept C Layout

The results of this assessment for various Nodal Parameters for Concept C are presented in Table 11.15 and Figure 11.14

Table 11.15 Natural Oscillation Periods of Concept C

Nodal Parameters		MLWS		MSL				HAT				Water Depth (m)
n	m	3.15	3.4	3.65	3.9	4.15	4.4	4.65	4.9	5.15	5.4	
0	-	209	201	194	188	182	177	172	167	163	159	Natural Oscillation Period (s)
0	1	79	76	74	71	69	67	65	63	62	60	
0	2	40	38	37	36	34	33	33	32	31	30	
1	0	104	100	97	94	91	88	86	84	82	80	
2	0	52	50	48	47	45	44	43	42	41	40	
1	1	63	61	59	57	55	53	52	51	49	48	
2	2	32	30	29	28	27	27	26	25	25	24	

Notes: 1. NOPs calculated using equations (1) and (2).
2. NOPs highlighted in orange are those which overlap with the background LPW energy in the area.

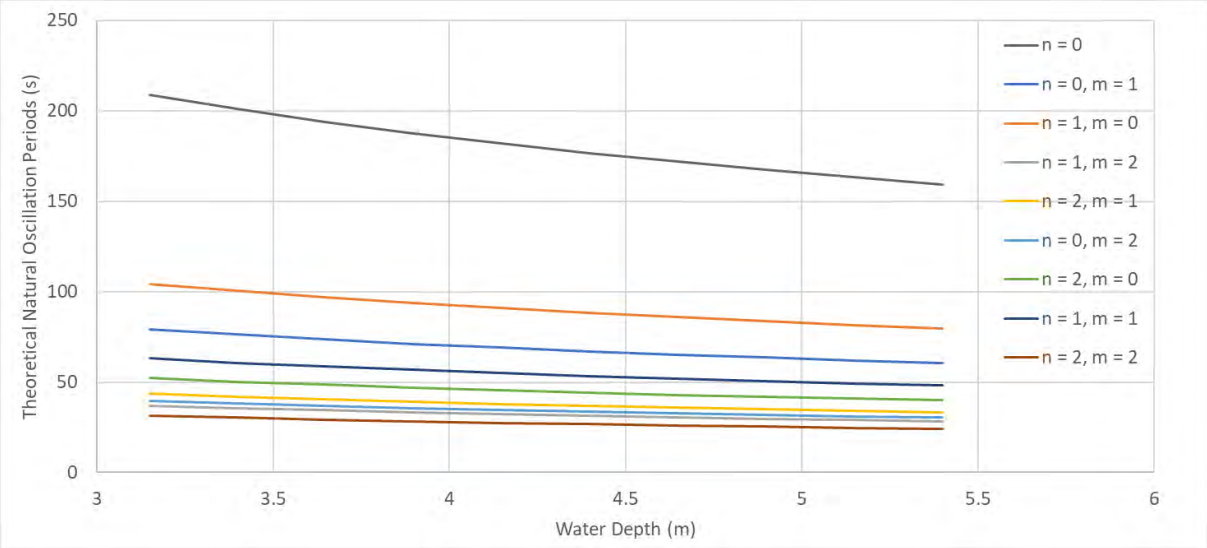

Figure 11.14 Natural Oscillation Periods of Concept C

11.2.4 Review & Recommendations

The key outcomes of the assessment are summarised below.

- Background LPW energy at the site has been identified at both RBRs.
- The most significant LPW energy consists across the 60 to 200s energy band.
- There is an overlap between the most significant LPW energy bands (60-200s) and the free oscillation period (n=0) of Concept B (160-210s).

- There is a clear overlap between this LPW energy band and the NOP (n=1, m=0) of Concept B (80-105s).
- Similarly there is a clear overlap between this LPW energy band and the NOP (n=1, m=0) of Concept C (80-105s).
- The risk of LPW amplification cannot be discounted. As a result, numerical modelling was recommended to further interrogate and define this risk.

12. Long Period Wave Modelling

The analysis and outcomes of the initial LPW assessment were summarised in Section 11. Broadly, the frequencies of background LPW energy identified at the site overlap with natural oscillation periods estimated for the proposed TBF concept. The risk of LPW amplification could not be discounted and numerical modelling has been undertaken to further interrogate and define this risk.

The scope for the Long Period Wave Modelling included the following.

- Selection of a range of forcing inputs for long wave modelling to allow identification of any resonant features. Events are based on the assessment of background LPW energy and empirical calculations to determine the likely resonant frequencies for the harbour. 8 forcings have been tested.
- Setup of the BOUSS2D model grids for the TBF Breakwater Layout and local bathymetry.
- Set-up and simulation of boundary conditions in the BOUSS2D model.
- Extract model outputs and undertake comparison of spectral density at locations within the harbour against locations outside the harbour to identify evidence of a resonant response to any of the forcing functions.
- Visualisation of results for analysis and presentation purposes.
- Consideration of the modelling results to assess potential impacts to mooring, navigation, structures, maintenance and freeboard.

The methods, results and interpretation of the LPW modelling are provided in the following section.

12.1 Selection of Forcing Functions

Forcings for the modelling were selected based on the assessment of background LPW energy and empirical calculations to determine the likely resonant frequencies for the harbour.

The most significant LPW energy consists across the 60 to 200s energy band. There is an overlap between this LPW band and the calculated free oscillation period (n=0) of Concept B (160-210s), this energy band was selected for interrogation. There is also an overlap between this LPW energy band and the calculated NOP (n=1, m=0) of Concept B (80-105s). This background energy band of 60 to 200s was selected for interrogated. The LPW assessment also identified a fairly broad band of background LPW energy across a period range of 200 – 600s. It was assessed as necessary to interrogate any potential impacts of this band also.

A white noise function for numerical simulations is a random signal having equal intensity at different frequencies, giving it a constant power spectral density. White noise functions are computationally intensive and as such, the energy bands of interest were split into a number of smaller white noise functions to achieve viable run times.

Given an infinite number of calculations is required to represent a “true” white noise function, a frequency interval (Hz) is required to define the resolution of the input frequency. The smaller the interval, the more computationally intensive the simulation. A much smaller frequency interval is

required to resolve the longest white noise bands resulting in run times of approximately 10 times those of shorter white noise bands.

Observed LPW amplitudes range from approximately 0.05 to 0.2 m. The amplitudes of the forcing waves are not expected to significantly impact the amplification or resonance response of the facility. The largest change to wave mechanics induced by changes in wave amplitude are wave breaking and reflection and these mechanics would not be expected to be significantly different between a 0.05 m and 0.2 m wave for the purposes of this assessment. This is similar to the fact that Goda's diffraction diagrams are dependant only on wave period and wave length. Based on this, amplitudes for the inputs to the BOUSS2D model were selected to represent typical wave heights observed across the data record. The proportion of amplifications observed in results can therefore be expected to be a reasonable representation of the extent of amplification that would be expected for any wave height corresponding with the same period.

All forcing functions have been simulated as propagating from a direction perpendicular to the shoreline. This is a reasonable assumption given that by the time infragravity waves reach the shoreline they will have refracted sufficiently to have a shore-normal approach.

The selected white noise functions for the assessment are presented in Table 12.1. Results of these simulations are presented in Section 12.3.

Table 12.1 Simulated White Noise Forcing Functions

Function	T Min (s)	L min (m)	T Max (s)	L max (m)	Hs (m)	Df (Hz)
White Noise 1	60	360	200	1200	0.1	1/10,000
White Noise 2	100	600	300	1800	0.05	1/20,000
White Noise 3	30	180	100	600	0.1	1/10,000
White Noise 4	200	1200	400	2400	0.05	1/40,000
White Noise 5	400	2400	600	3600	0.05	1/120,000

Following the simulation of white noise functions, targeted functions were selected for further modelling based on review of the response from the white noise modelling, coupled with a review of the empirical calculations presented in Table 11.12. The selected targeted functions are presented in Table 12.2. Results of these simulations are presented in Section 12.3.

Table 12.2 Targeted Forcing Functions

Function	T Min (s)	T Max (s)	Tp (s)	Hs (m)
Targeted 1	450	530	500	0.1
Targeted 2	90	120	100	0.1
Targeted 3	180	220	200	0.05

12.2 Numerical Model Set-up

12.2.1 BOUSS-2D

BOUSS-2D is a comprehensive numerical model for simulating the propagation and transformation of waves in coastal regions and harbours. It is based on a time domain solution of Boussinesq-type equations, and accounts for 3D wave processes, including, but not limited to the following:

- shoaling;
- refraction;
- diffraction; and
- reflection.

The model was developed by the US Army Corps of Engineers, and is described in detail by Nwogu and Demirbilek (2001).

BOUSS-2D has been validated with a range of coastal and harbour related phenomena and is hence capable of accurately simulating nonlinear generation of long waves by storm waves propagating from deep water to shallow water, diffraction of short and long period waves into harbours and resonant amplification of long waves inside harbours. The model can describe complex wave transformation process such as; changes to wave spectrum due to wave breaking and nonlinear energy transfer to infragravity band (Nwogu and Demirbilek, 2010).

12.2.2 Model Set-up

BOUSS-2D simulates wave propagation over a 2-D Cartesian grid. The computational domain is a rectangular region with uniform grid spacings in the x and y directions. The bathymetric grid represents the seabed elevation at each node of the grid with land points defined as positive while water points are defined as negative. To prepare the grid, the spatial extent and spacing of the computational grid have to be selected. Factors to consider in the selection of the grid boundaries and spacing include the following (Nwogu and Demirbilek (2001).

- The grid axes should be aligned as much as possible with the predominant wave direction.
- Points of interest in the computational domain should be kept at least one wavelength away from the boundaries to minimize the effect of diffraction into the damping layers.
- The water depth should be uniform along the wave generation boundary.
- The grid spacing should be chosen to resolve the shortest wave period of interest (T_{min}) in the shallowest part of the domain (h_{min}). This typically corresponds to having at least eight grid points per wavelength in the shallow regions and 20 to 30 points per wavelength at the peak wave period (T_p) in the deep regions (h_{max}).

Due to the large variation in the characteristics of input conditions, two model grids were prepared for the assessment. Each with varying extent and grid resolution. A 3000 x 3000 m grid with 5 x 5 m resolution was utilised for input waves up to 300 s in period, and an 8000 x 5600 m grid with 10 x 10 m grid resolution was utilised for input waves with periods greater than 300 s. These grids provided an acceptable number of grid cells per wavelength to adequately resolve the propagation of waves. A time step of 0.34 s was selected.

The model utilises real bathymetric data to approximately the -4 mAHD contour and beyond this depth a uniform grid is utilised. Bathymetry data for the grids was sourced from the most recent surveys along the coast as well as the 2005 LiDAR survey data captured by CSIRO (2005). The two grid extents with model bathymetry are shown in Figure 12.1

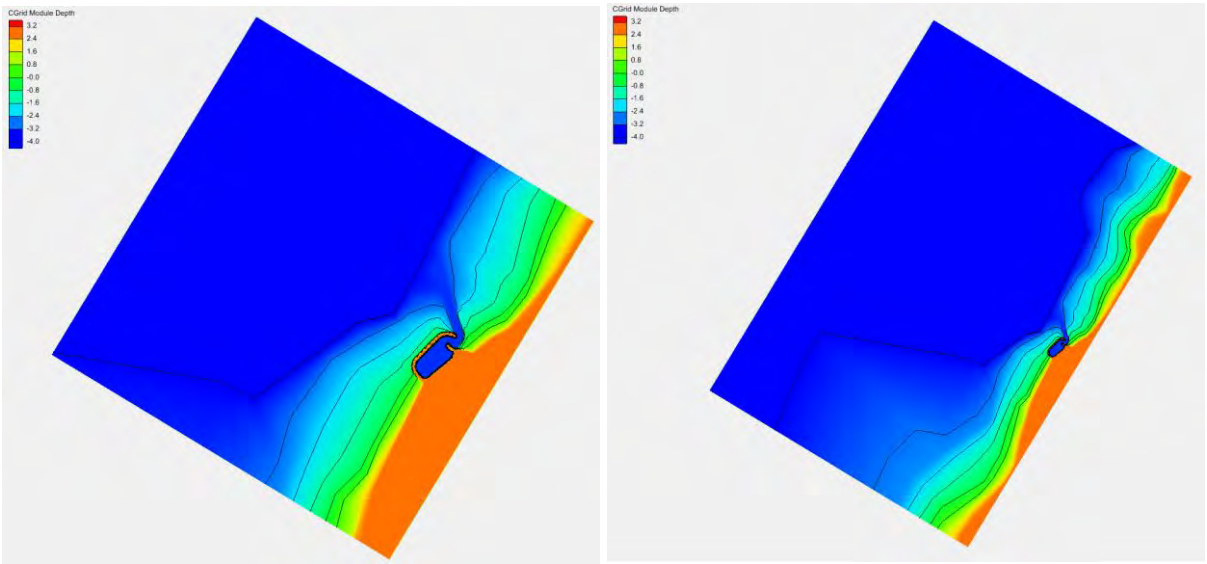

Figure 12.1 Model Grids (3000 x 3000 m left & 8000 x 5600 m right)

Damping layers were utilised around the breakwaters to model the absorption of the waves as they reflect off and diffract around the structures. Damping layers around the breakwaters were conservatively selected to absorb minimal wave energy. As the model boundaries are reflective, damping layers are also utilised around the outside of the model domain to absorb energy reflected off the breakwaters. This minimises the amount of energy that is retained within the model domain throughout the simulation. A wave maker was utilised inside the western boundary to apply wave conditions. A number of probes inside and outside the marina are utilised to continuously track water surface elevation across the simulation. The configuration of the model set-up for the grids is shown in Figure 12.2 below.

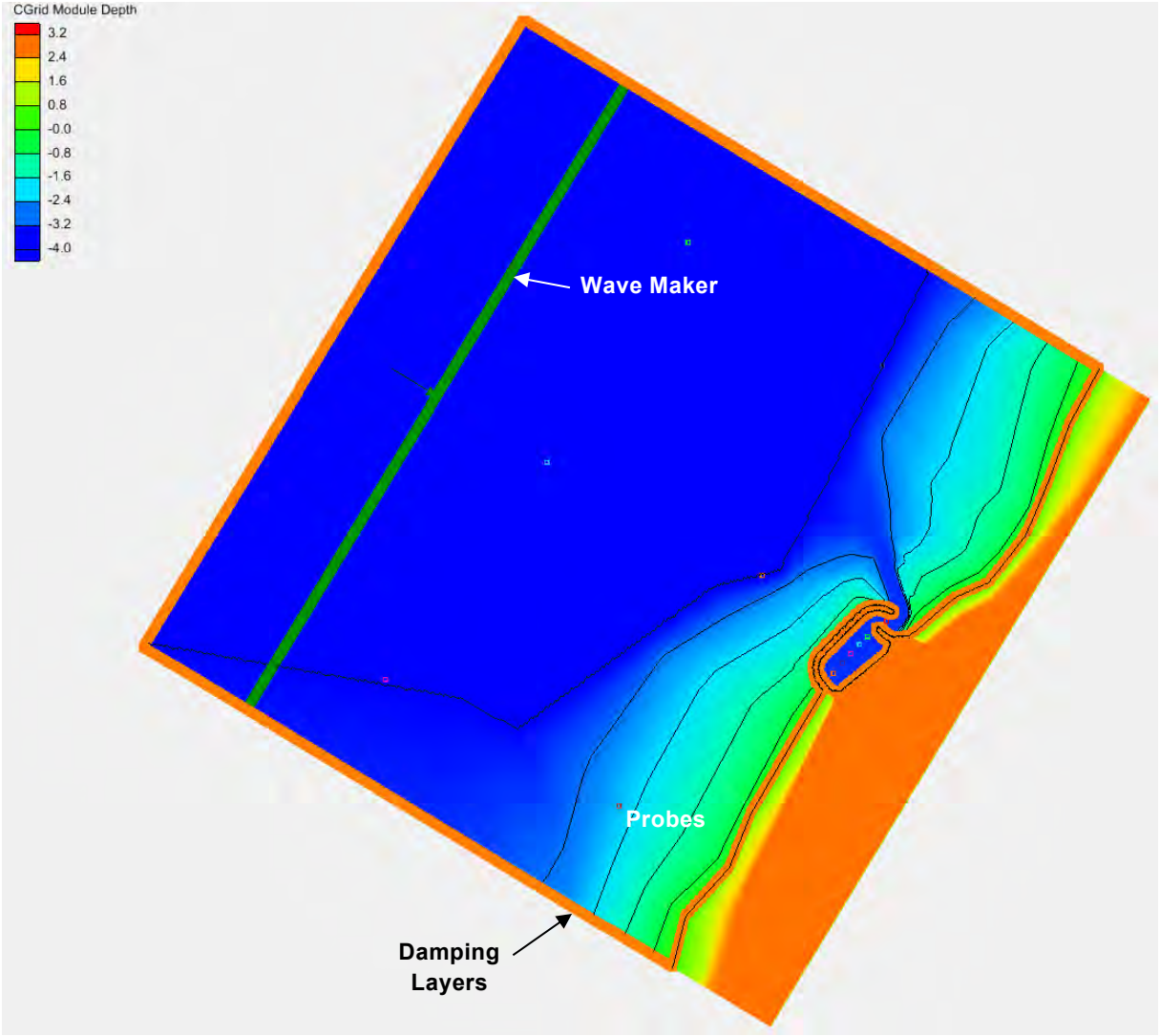

Figure 12.2 BOUSS-2D Model Configuration

12.3 Results – Concept B

Interrogation of the model results was undertaken through review of a number of plots and visualisations. The key plots prepared for each simulation are as follows.

- Spectral Density comparison across probes.
- Time varying water surface elevation comparison across each probe over the simulation.
- Spatial plot of the significant wave height calculated over the entire simulation.

There are 12 probes used to track the water surface elevation across the simulations. The water surface elevation can then be utilised to calculate the power spectral density. The locations of the probes were identical for each of the grids and are shown in Figure 12.3 and Table 12.3.

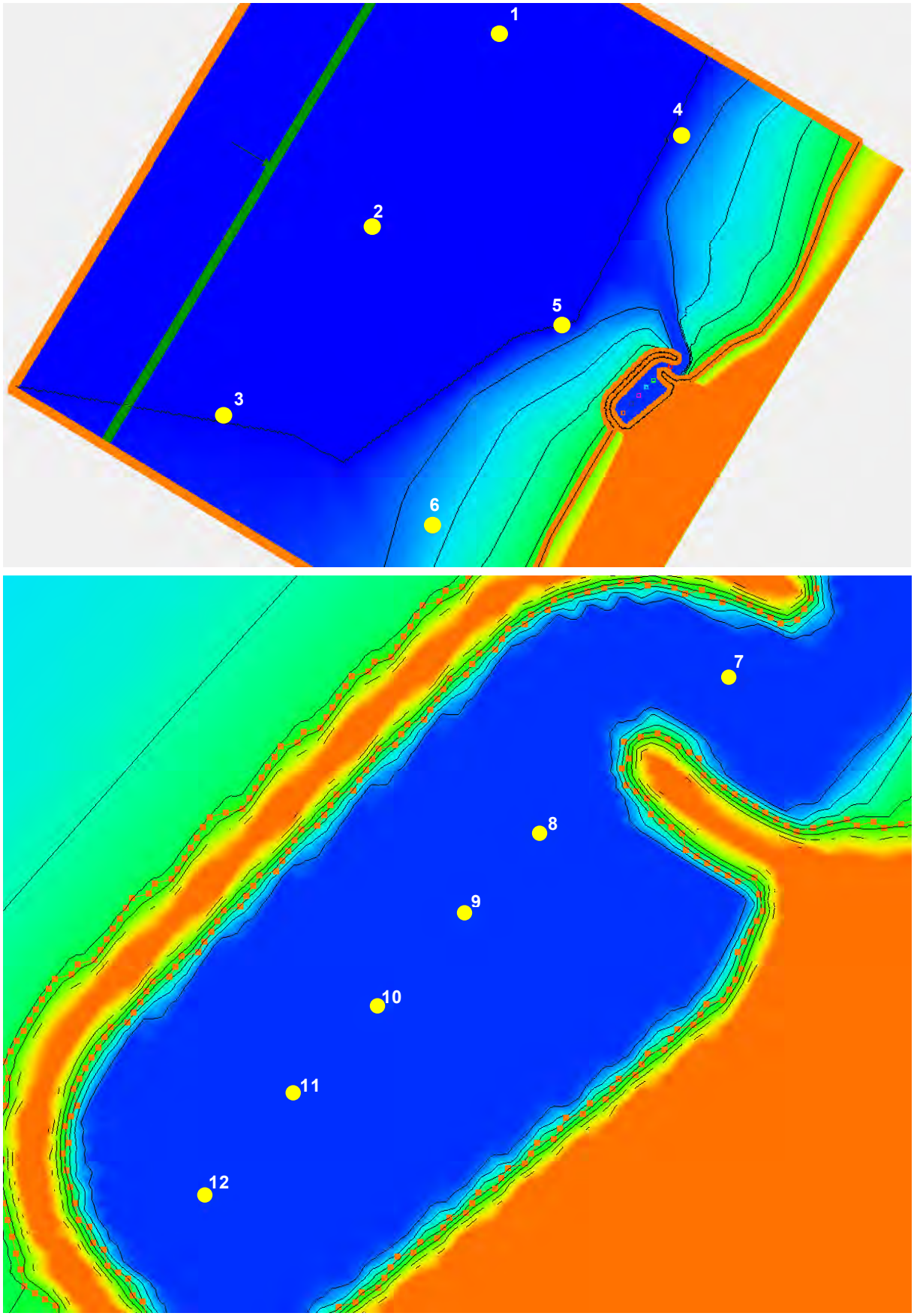

Figure 12.3 Probe Locations

Table 12.3 Probe Locations

Probe	Easting (m)	Northing (m)
1	806,484	7,575,329
2	805,905	7,574,430
3	805,245	7,573,543
4	807,278	7,574,825
5	806,787	7,573,966
6	806,199	7,573,024
7	807,294	7,573,781
8	807,215	7,573,718
9	807,183	7,573,684
10	807,149	7,573,647
11	807,114	7,573,609
12	807,077	7,573,567

Note: 1. Coordinates are in MGA2020 Zone 49.

The results for each of the simulations presented in Tables in 12.2 and 12.3 are discussed in the following sections.

12.3.1 White Noise Function 1

White Noise Function 1 represents an input signal having equal intensity from periods 60 to 200 s with a significant wave height of approximately 0.1 m. This allows testing of an input signal which covers the largest background LPW band observed in the data record at the site. This also covers the theoretical free oscillation period (n=0) of 160-210 s, and the NOP (n=1,m=0) of 80-105 s as calculated for the facility in Section 11.2.

Result visualisations from the simulation of White Noise Function 1 are shown in Figures 12.4 and 12.5. These show a spectral density comparison across probes; time varying water surface elevation comparison across each probe over the simulation; and a spatial plot of the significant wave height calculated over the entire simulation. Black and blue dotted and segmented lines represent results from probes outside the facility, whilst the solid autumn coloured lines represent results from probes inside the facility.

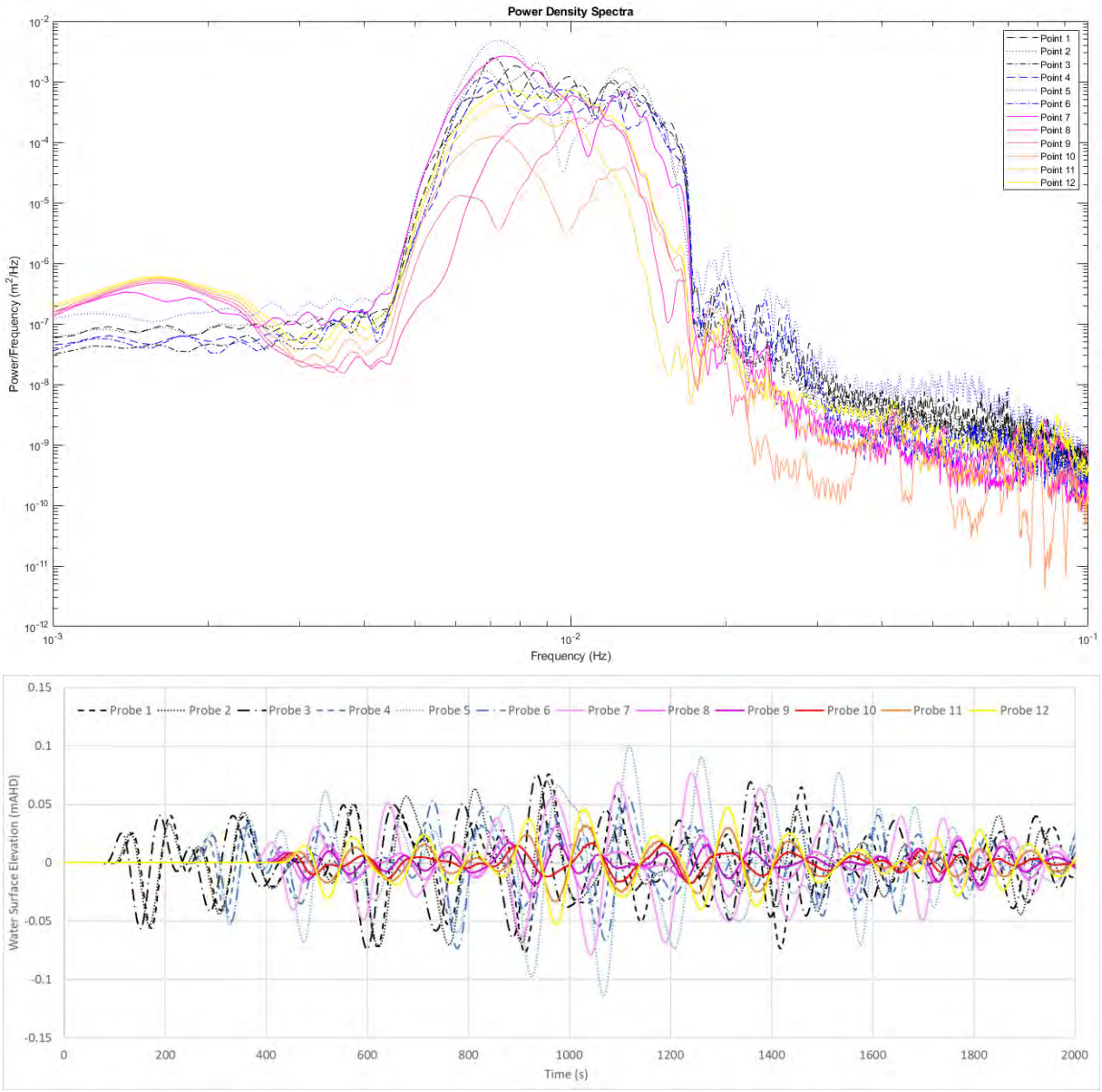

Figure 12.4 Spectral Density Plot (top) & Time series WSE (bottom) for each Probe across White Noise Function 1

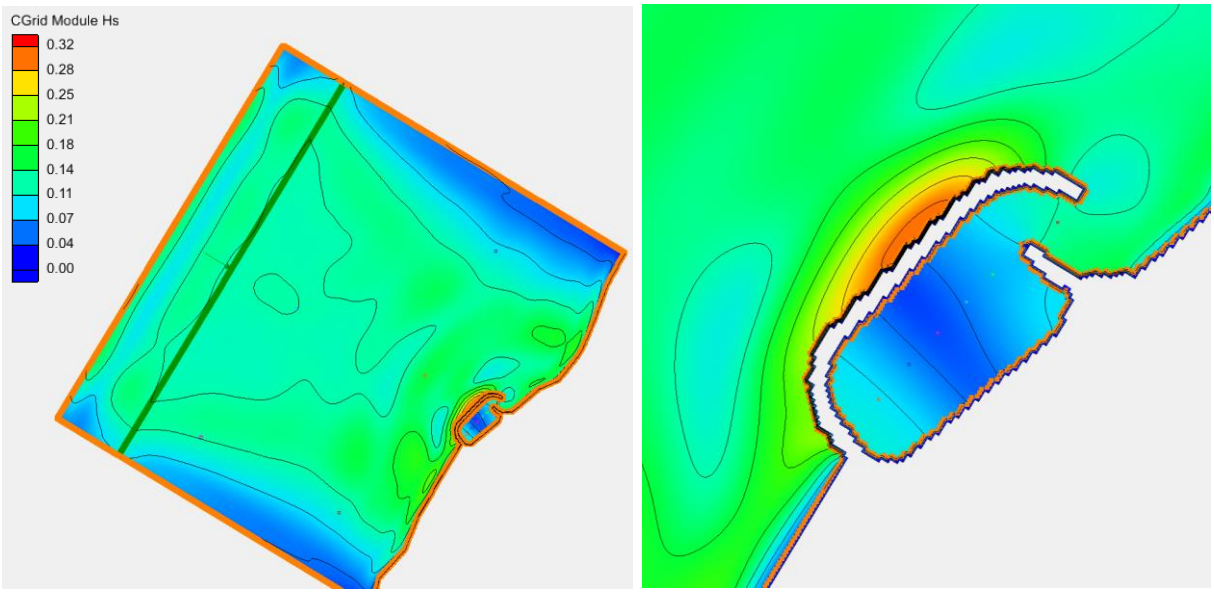

Figure 12.5 Spatial plot of Significant Wave Height across White Noise Function 1

Key outcomes and observations from the plots are discussed below.

- Peaks in the spectral energy density plots allow confirmation of a NOP around 100 s. As shown in Figure 12.5, this results in antinodes at the entrance of the facility and south-western end and a node in the middle. Further targeted testing to interrogate this response has been undertaken.
- The power spectral density shows that the input signal does not result in an amplification of waves at this period. For frequencies corresponding to the input signal; all probes inside the facility show less spectral energy than those outside the facility.
- The response of the facility is confirmed through a review of the spatial plot of significant wave height. This shows that wave heights inside the facility do not exceed the input signal at any location.
- The response of the facility is confirmed through a review of the time varying water surface elevations at each of the probes. This shows that wave heights inside the facility do not exceed the input signal at any location.
- A curious finding is a response identified in the spectral energy plots of frequencies from 0.001 to 0.0025 (Hz) or periods 400 to 1000 s peaking at around 500 s. The mechanism of this response is not entirely clear given the oscillation period is larger than the free oscillation period. It is possible that this is resonance in the grid rather than in the facility itself. Hence, further interrogation has been undertaken with white noise and targeted forcings as well as different grid dimensions.

12.3.2 White Noise Function 2

White Noise Function 2 represents an input signal having equal intensity from periods 100 to 300 s with a significant wave height of approximately 0.05 m. This band was selected to provide an overlap between White Noise Functions 1 and 4. This band partially covers the theoretical free oscillation period (n=0) of 160-210 s as described in Section 11.2.

Result visualisations from the simulation of White Noise Function 2 are shown in Figures 12.6 and 12.7. These show a spectral density comparison across probes; time varying water surface elevation comparison across each probe over the simulation; and a spatial plot of the significant wave height calculated over the entire simulation. Black and blue dotted and segmented lines represent results from probes outside the facility, whilst the solid autumn-coloured lines represent results from probes inside the facility.

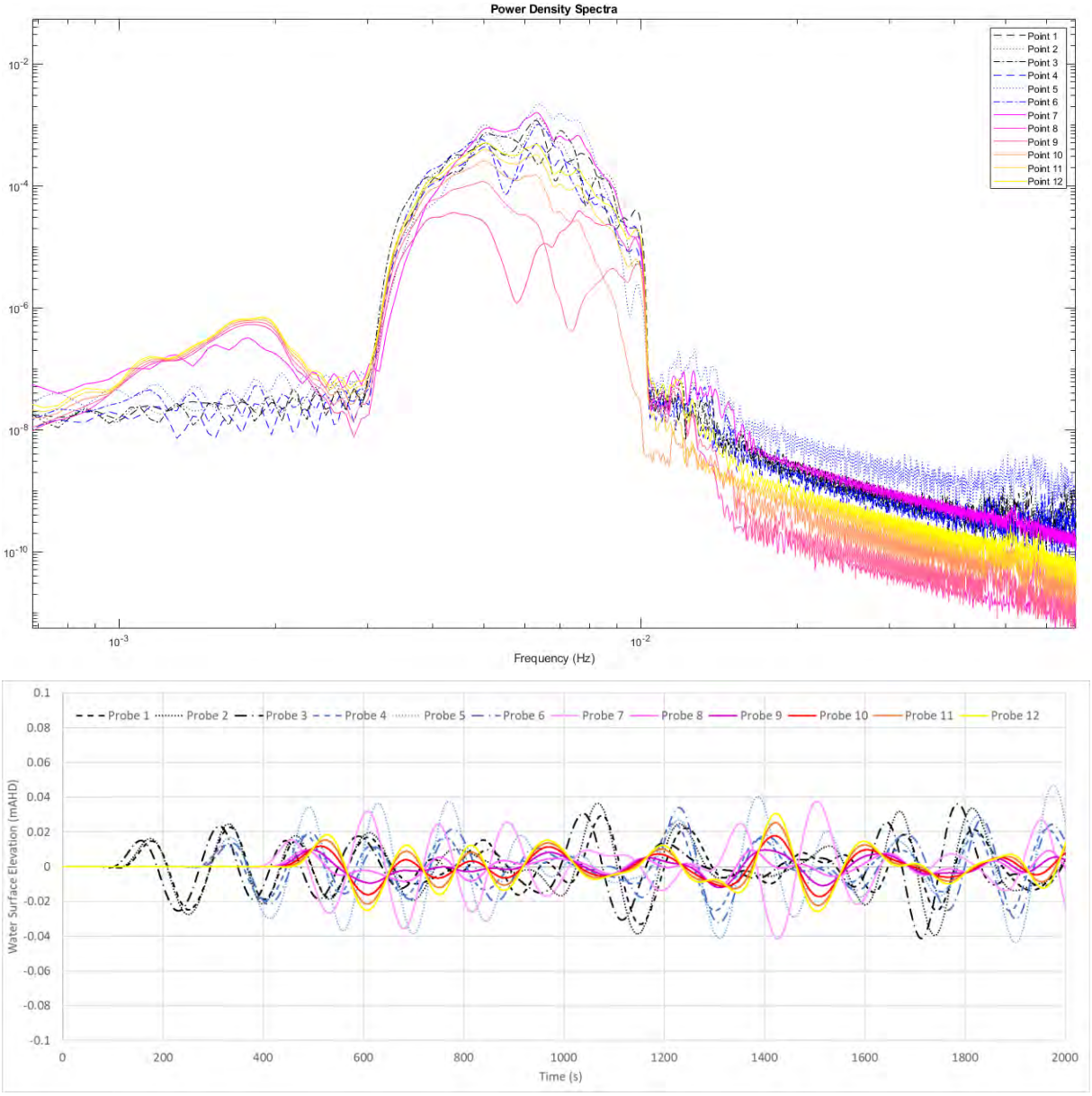

Figure 12.6 Spectral Density Plot (top) & Time series WSE (bottom) for each Probe across White Noise Function 2

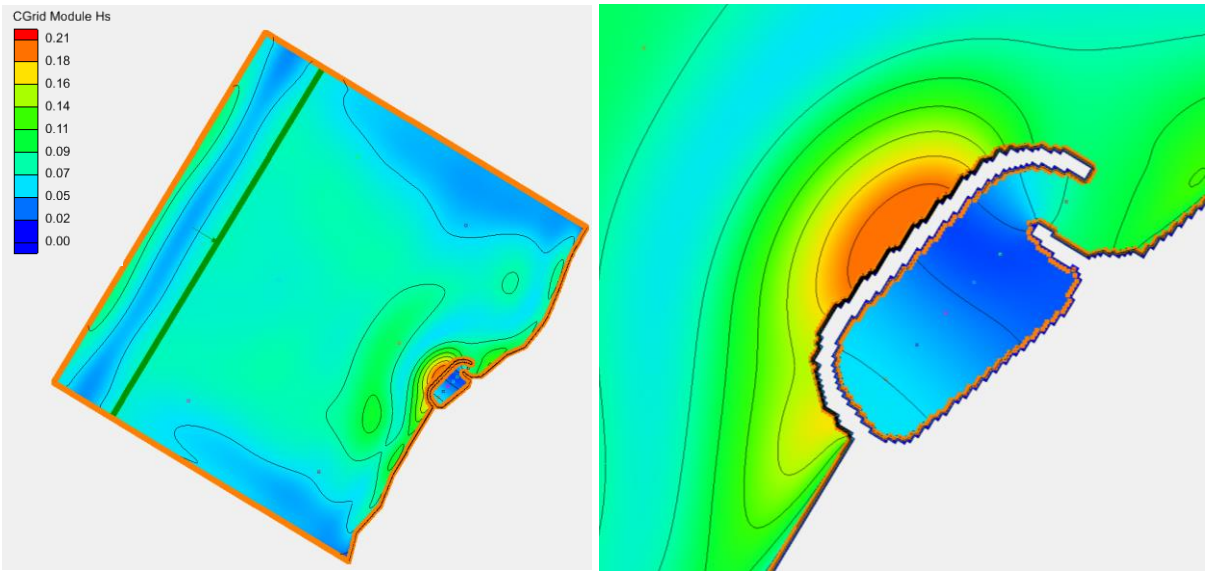

Figure 12.7 Spatial plot of Significant Wave Height across White Noise Function 2

Key outcomes and observations from the plots are discussed below.

- The power spectral density shows that the input signal does not result in an amplification of waves at this period. For frequencies corresponding to the input signal; all probes inside the facility show less spectral energy than those outside the facility.
- The response of the facility is confirmed through a review of the spatial plot of significant wave height. This shows that wave heights inside the facility do not exceed the input signal at any location.
- The response of the facility is confirmed through a review of the time varying water surface elevations at each of the probes. This shows that wave heights inside the facility do not exceed the input signal at any location.
- A similar response to previous modelling results was observed for 0.001 to 0.0025 (Hz) or periods 400 to 1000 s peaking at around 500 s. Further interrogation has been undertaken to assess this observation with white noise and targeted forcings as well as different grid dimensions.

12.3.3 White Noise Function 3

White Noise Function 3 represents an input signal having equal intensity from periods 30 to 100 s with a significant wave height of approximately 0.1 m. This band was selected to cover off the remaining background LPW energy at the lower end of the spectrum and overlap with White Noise Function 1. This band partially covers the NOP (n=1,m=0) of 80-105 s as calculated for the facility in Section 11.2.

Result visualisations from the simulation of White Noise Function 3 are shown in Figures 12.8 and 12.9. These show a spectral density comparison across probes; time varying water surface elevation comparison across each probe over the simulation; and a spatial plot of the significant wave height calculated over the entire simulation. Black and blue dotted and segmented lines represent results from probes outside the facility, whilst the solid autumn-coloured lines represent results from probes inside the facility.

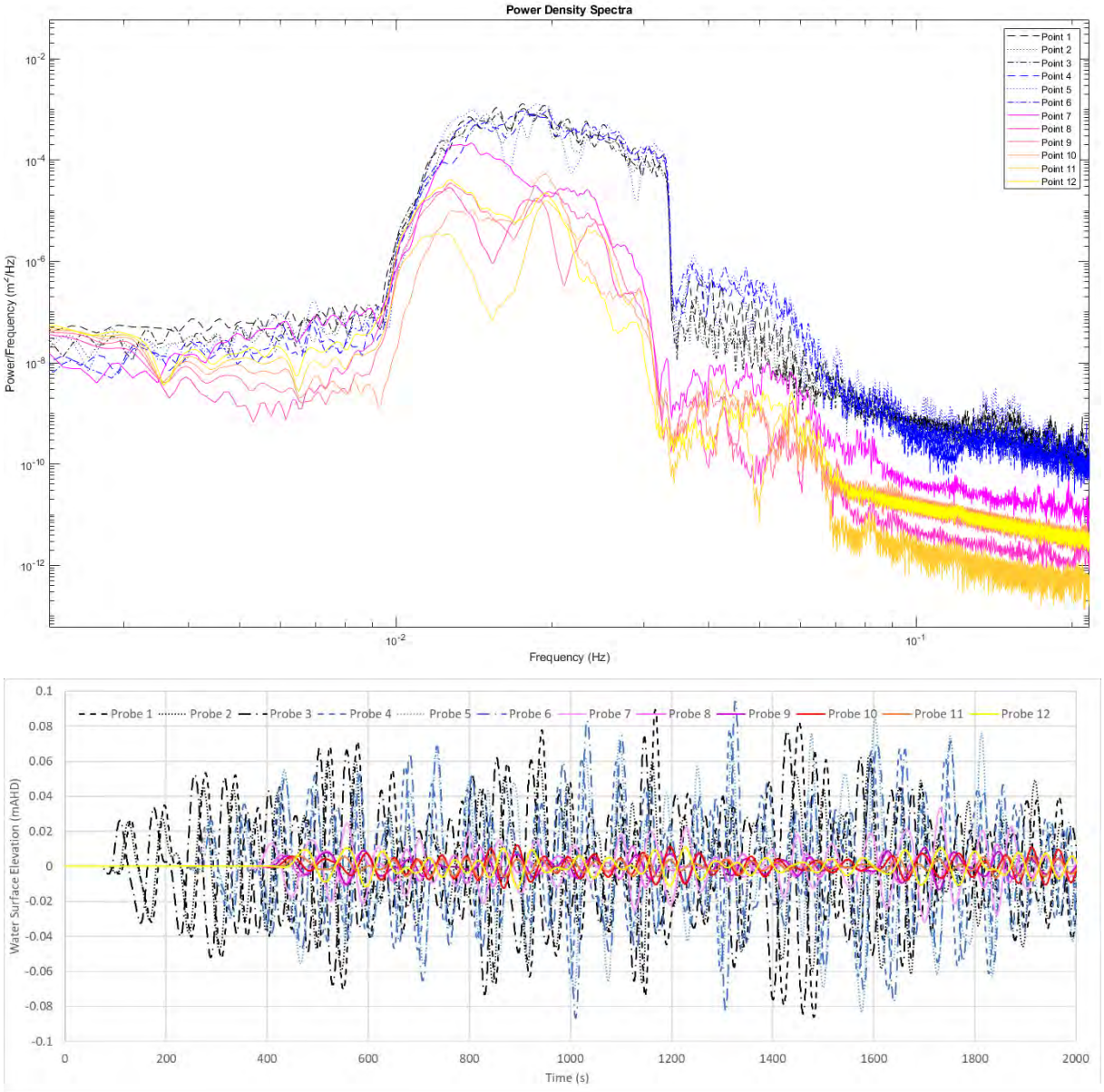

Figure 12.8 Spectral Density Plot (top) & Time series WSE (bottom) for each Probe across White Noise Function 3

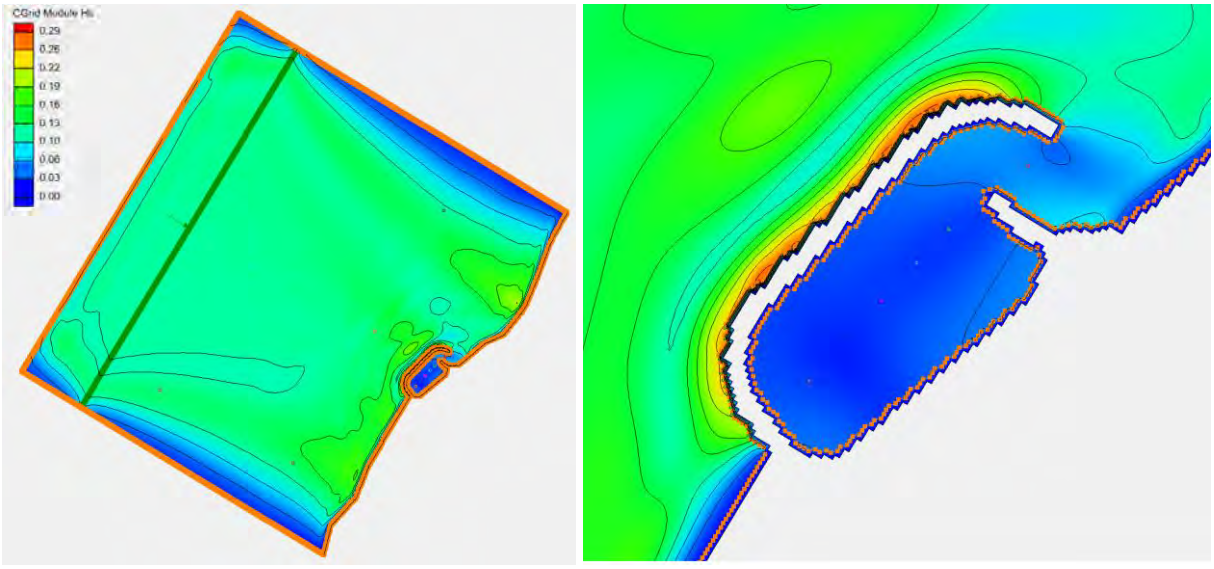

Figure 12.9 Spatial plot of Significant Wave Height across White Noise Function 3

Key outcomes and observations from the plots are discussed below.

- Peaks in the spectral energy density plots allow confirmation of a NOP at around 50 s. As shown in Figure 12.11, this results in antinodes at the entrance of the facility and a node at the entrance. Further targeted testing to interrogate this response has been undertaken.
- The power spectral density shows that the input signal does not result in an amplification of waves at this period. For frequencies corresponding to the input signal; all probes inside the facility show less spectral energy than those outside the facility.
- The response of the facility is confirmed through a review of the spatial plot of significant wave height. This shows that wave heights inside the facility do not exceed the input signal at any location.
- The response of the facility is confirmed through a review of the time varying water surface elevations at each of the probes. This shows that wave heights inside the facility do not exceed the input signal at any location.
- A very small response is identified in the spectral energy plots of frequencies from 0.001 to 0.0025 (Hz) or periods 400 to 1000 s peaking at around 500 s. Further interrogation has been undertaken to assess this observation with white noise and targeted forcings as well as different grid dimensions.

12.3.4 White Noise Function 4

White Noise Function 4 represents an input signal having equal intensity from periods 200 to 400 s with a significant wave height of approximately 0.05 m. This allows testing of an input signal which covers part of the key largest background LPW band of 200 – 600 s observed in the data record at the site.

Result visualisations from the simulation of White Noise Function 4 are shown in Figures 12.10 and 12.11. These show a spectral density comparison across probes; time varying water surface elevation comparison across each probe over the simulation; and a spatial plot of the significant wave height calculated over the entire simulation. Black and blue dotted and segmented lines

represent results from probes outside the facility, whilst the solid autumn-coloured lines represent results from probes inside the facility.

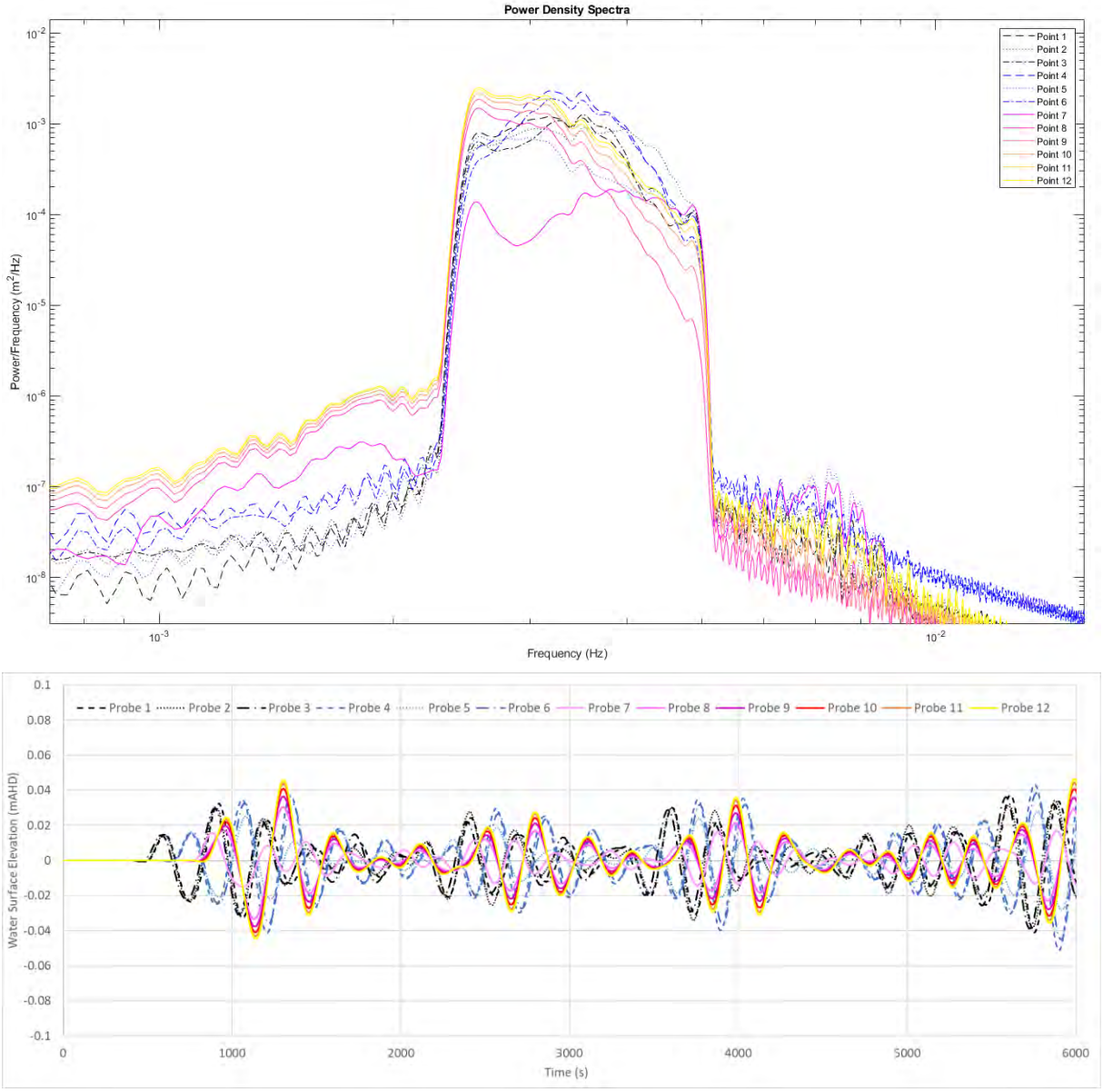

Figure 12.10 Spectral Density Plot (top) & Time series WSE (bottom) for each Probe across White Noise Function 4

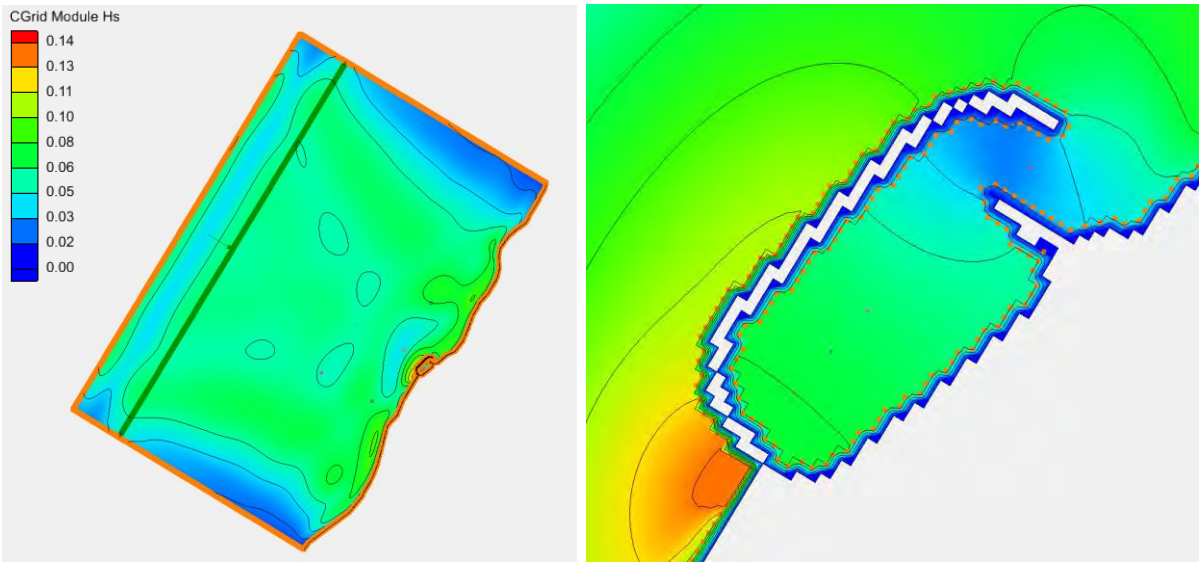

Figure 12.11 Spatial plot of Significant Wave Height across White Noise Function 4

Key outcomes and observations from the plots are discussed below.

- Peaks in the spectral energy density plots allow confirmation of a NOP at around 200 s. As shown in Figure 12.11, this results in antinodes at the entrance of the facility and a node at the entrance. Further targeted testing to interrogate this response has been undertaken.

- A review of the spatial plot of significant wave height shows that wave heights inside the facility do not exceed the input signal at any location.

- The power spectral density shows that as the input signal approaches a frequency of around 0.0025 Hz (400 s) the amplification of wave energy is observed. For a period of around 400 s greater energy is observed at each of the probes inside the facility than outside of the facility. It is possible that this is resonance in the grid rather than in the facility itself. Although the fact that these amplifications are not captured in the probes outside the basin and the feature is present in a grid with different dimensions suggests that the response may not be grid resonance.

- The response of the facility is confirmed through a review of the time varying water surface elevations at each of the probes. This shows that wave heights inside the facility at some locations are larger than those outside the facility.

12.3.5 White Noise Function 5

White Noise Function 5 represents an input signal having equal intensity from periods 400 to 600 s with a significant wave height of approximately 0.05 m. This allows testing of an input signal which covers part of the key largest background LPW band of 200 – 600 s observed in the data record at the site. This also allows further interrogation of the response identified from around 400 to 600 s observed in White Noise Functions 1-4.

Result visualisations from the simulation of White Noise Function 5 are shown in Figures 12.12 and 12.13. These show a spectral density comparison across probes; time varying water surface elevation comparison across each probe over the simulation; and a spatial plot of the significant wave height calculated over the entire simulation. Black and blue dotted and segmented lines

represent results from probes outside the facility, whilst the solid autumn-coloured lines represent results from probes inside the facility.

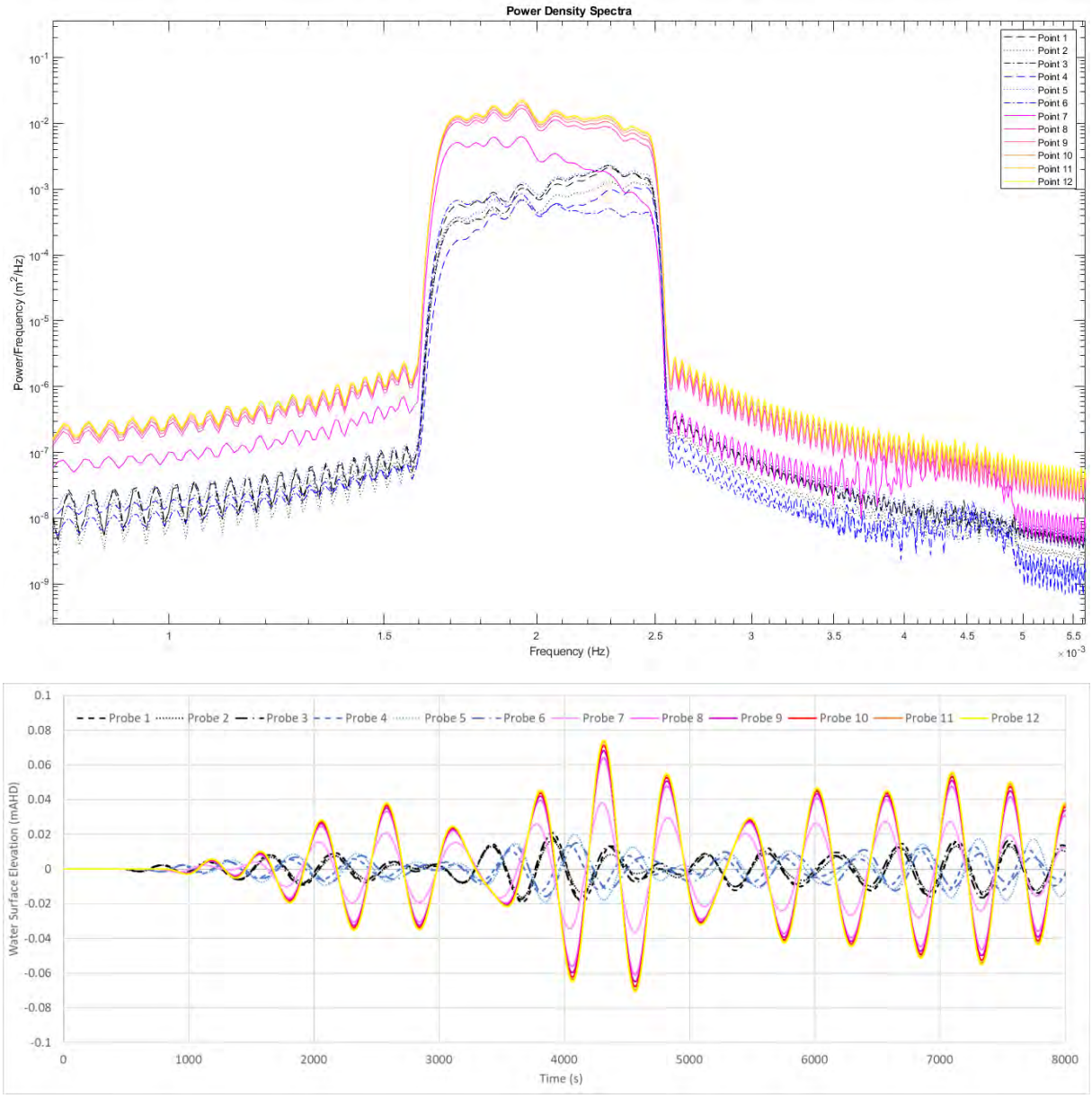

Figure 12.12 Spectral Density Plot (top) & Time series WSE (bottom) for each Probe across White Noise Function 5

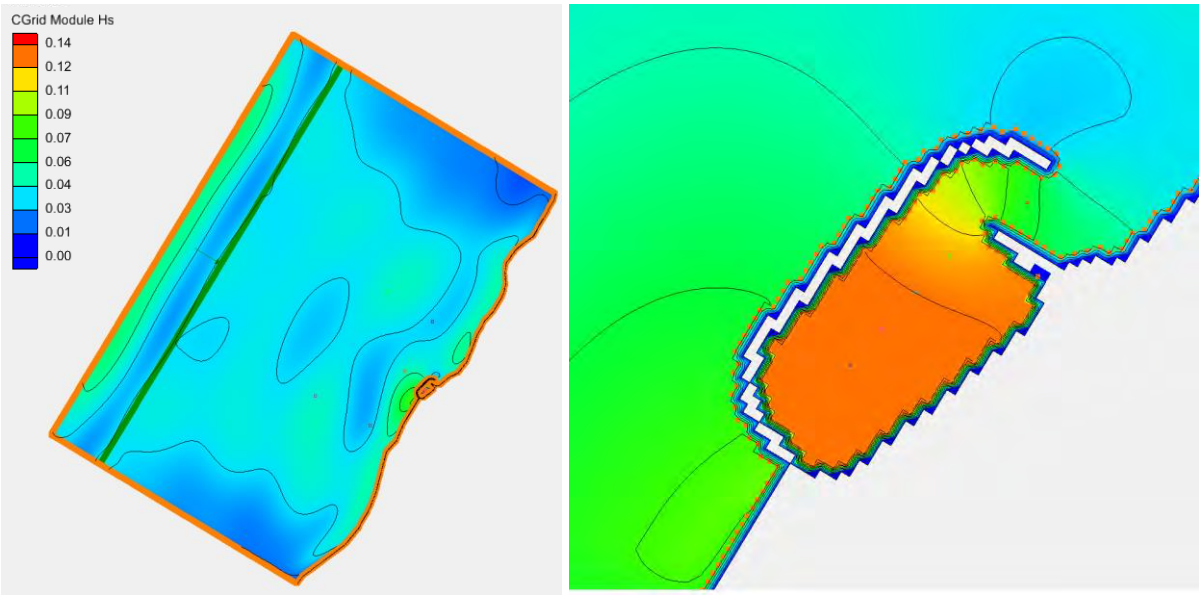

Figure 12.13 Spatial plot of Significant Wave Height across White Noise Function 5

Key outcomes and observations from the plots are discussed below.

- Review of the spectral energy density plots allow confirmation of an amplification response across the entire input white noise band. A peak in the spectral energy density plot outside the input signal allows confirmation of a NOP at around 200 s.
- A review of the spatial plot of significant wave height shows that wave heights inside the facility are approximately a factor of 1.5 to 3 times greater than the input signal. The largest wave heights are observed in the south western end of the basin.
- The response of the facility is confirmed through a review of the time varying water surface elevations at each of the probes. This shows that wave heights inside the facility at some locations are generally larger than those outside the facility.
- It is possible that this is resonance in the grid rather than in the facility itself. Although the fact that these amplifications are not captured in the probes outside the basin and the feature is present in a grid with different dimensions suggests the response may not be grid resonance.
- The representative wave height of background LPW energy across the 400 to 600 s band typically varies from around 0.05 m to 0.1 m. Hence, amplification of 1.5 to 3 times would result in wave heights within the facility of around 0.15 to 0.3 m.
- A water level oscillation of this magnitude over a period of approximately 7 to 10 minutes does not introduce significant orbital currents or rapid water level change. Nevertheless, some addition targeted testing has been undertaken to further interrogate this response.

12.3.6 Targeted Forcing 1

Targeted Forcing 1 represents an input signal with a peak period of 500 s with the spectrum limited to periods from 450 to 530 s and a significant wave height of approximately 0.1 m. This allows testing of an input signal which covers part of the key largest background LPW band of 200

– 600 s observed in the data record at the site. This also allows further interrogation of the response identified from around 400 to 600 s observed in White Noise Functions 1-5.

Result visualisations from the simulation of the Targeted Forcing are shown in Figures 12.14 and 12.15. These show a spectral density comparison across probes; time varying water surface elevation comparison across each probe over the simulation; and a spatial plot of the significant wave height calculated over the entire simulation. Black and blue dotted and segmented lines represent results from probes outside the facility, whilst the solid autumn-coloured lines represent results from probes inside the facility.

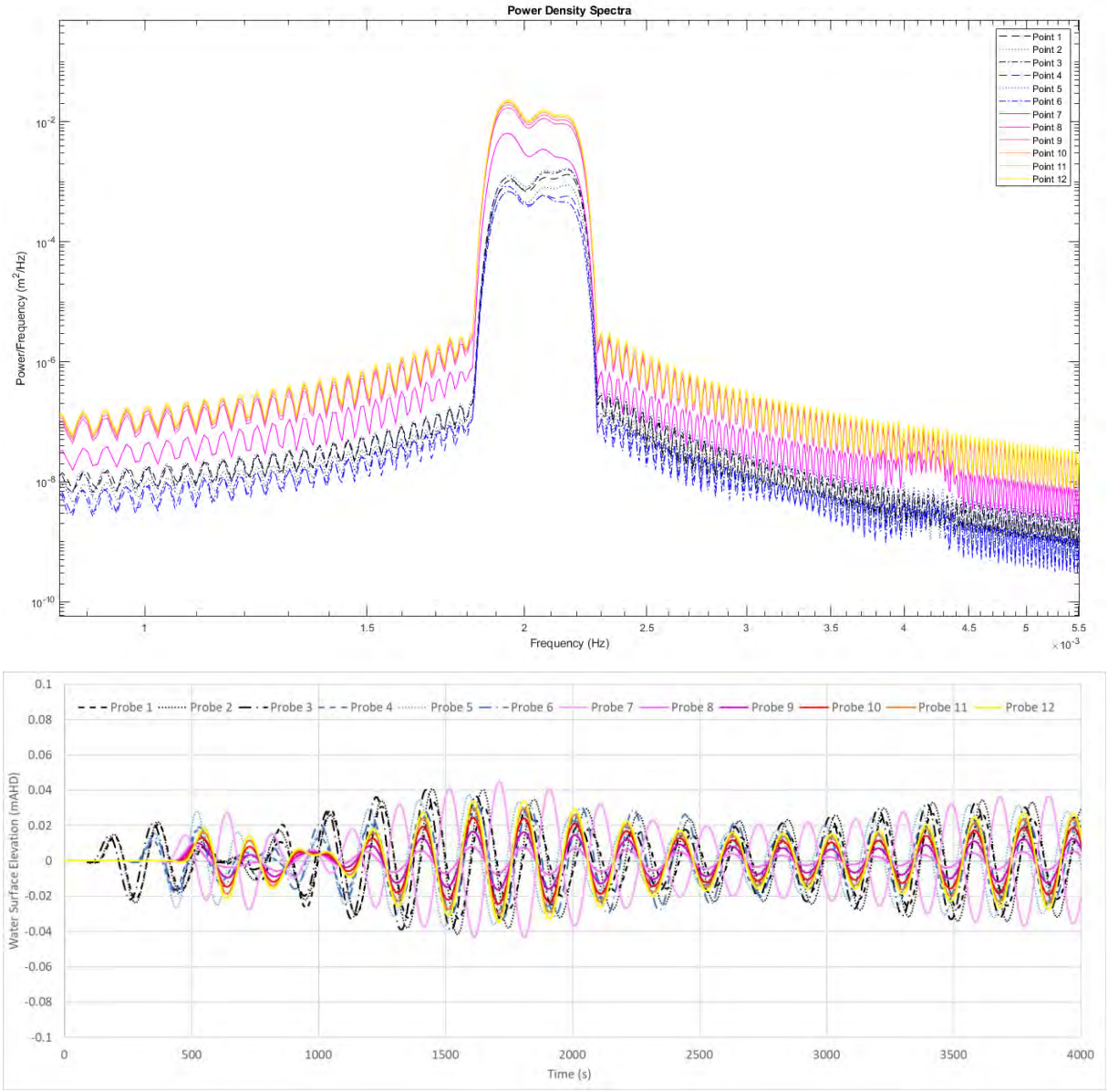

Figure 12.14 Spectral Density Plot (top) & Time series WSE (bottom) for each Probe across Targeted Forcing 1

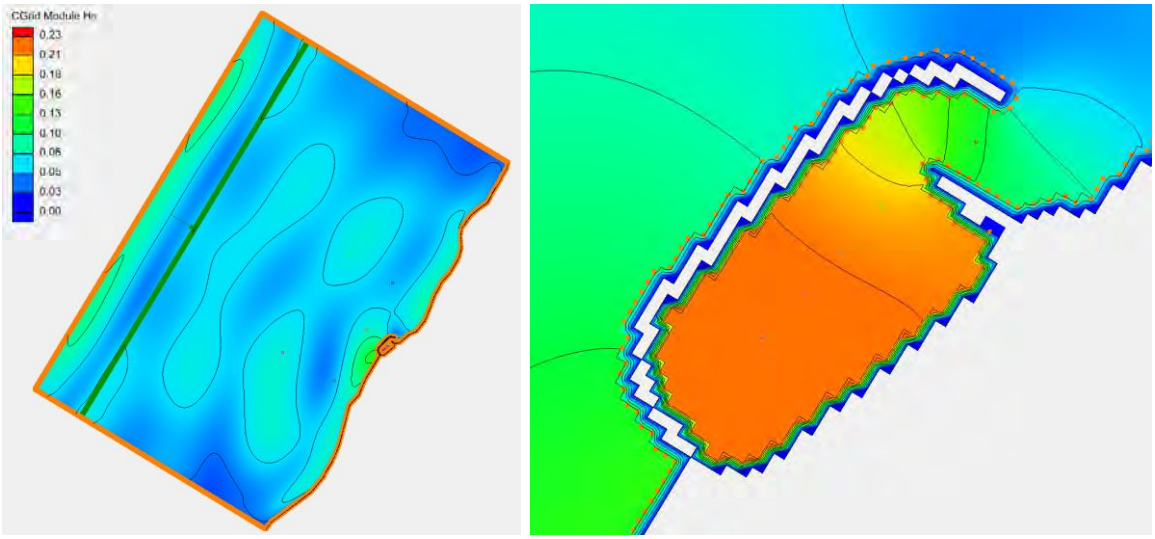

Figure 12.15 Spatial plot of Significant Wave Height across Targeted Forcing 1

Key outcomes and observations from the plots are discussed below.

- Review of the spectral energy density plots confirm the amplification response observed across White Noise Function 5. A peak in the spectral energy density plot outside the input signal allows confirmation of a NOP at around 200 s.
- A review of the spatial plot of significant wave height shows that wave heights inside the facility are approximately a factor of 2 to 3 times greater than the input signal. The largest wave heights are observed in the south western end of the basin.
- The response of the facility is confirmed through a review of the time varying water surface elevations at each of the probes. This shows that wave heights inside the facility at some locations are generally larger than those outside the facility.
- It is possible that this is resonance in the grid rather than in the facility itself. Although the fact that these amplifications are not captured in the probes outside the basin and the feature is present in both grids that have been tested (with different dimensions) suggests the response may not be grid resonance.
- The representative wave height of background LPW energy across the 400 to 600 s band typically varies from around 0.05 m to 0.1 m. Hence, amplification of 2 to 4 times would result in wave heights within the facility of around 0.2 to 0.4 m.
- A water level oscillation of this magnitude over a period of approximately 8 minutes does not introduce significant orbital currents or rapid water level change. Hence, it is not expected to introduce significant risks to the facility. This is discussed further in Section 12.4.

12.3.7 Targeted Forcing 2

Targeted Forcing 2 represents an input signal with a peak period of 100 s with the spectrum limited to periods from 90 to 120 s and a significant wave height of approximately 0.1 m. This allows further interrogation of the NOP identified in the results of White Noise Function 1.

Result visualisations from the simulation of the Targeted Forcing are shown in Figures 12.16 and 12.17. These show a spectral density comparison across probes; time varying water surface elevation comparison across each probe over the simulation; and a spatial plot of the significant wave height calculated over the entire simulation. Black and blue dotted and segmented lines represent results from probes outside the facility, whilst the solid autumn-coloured lines represent results from probes inside the facility.

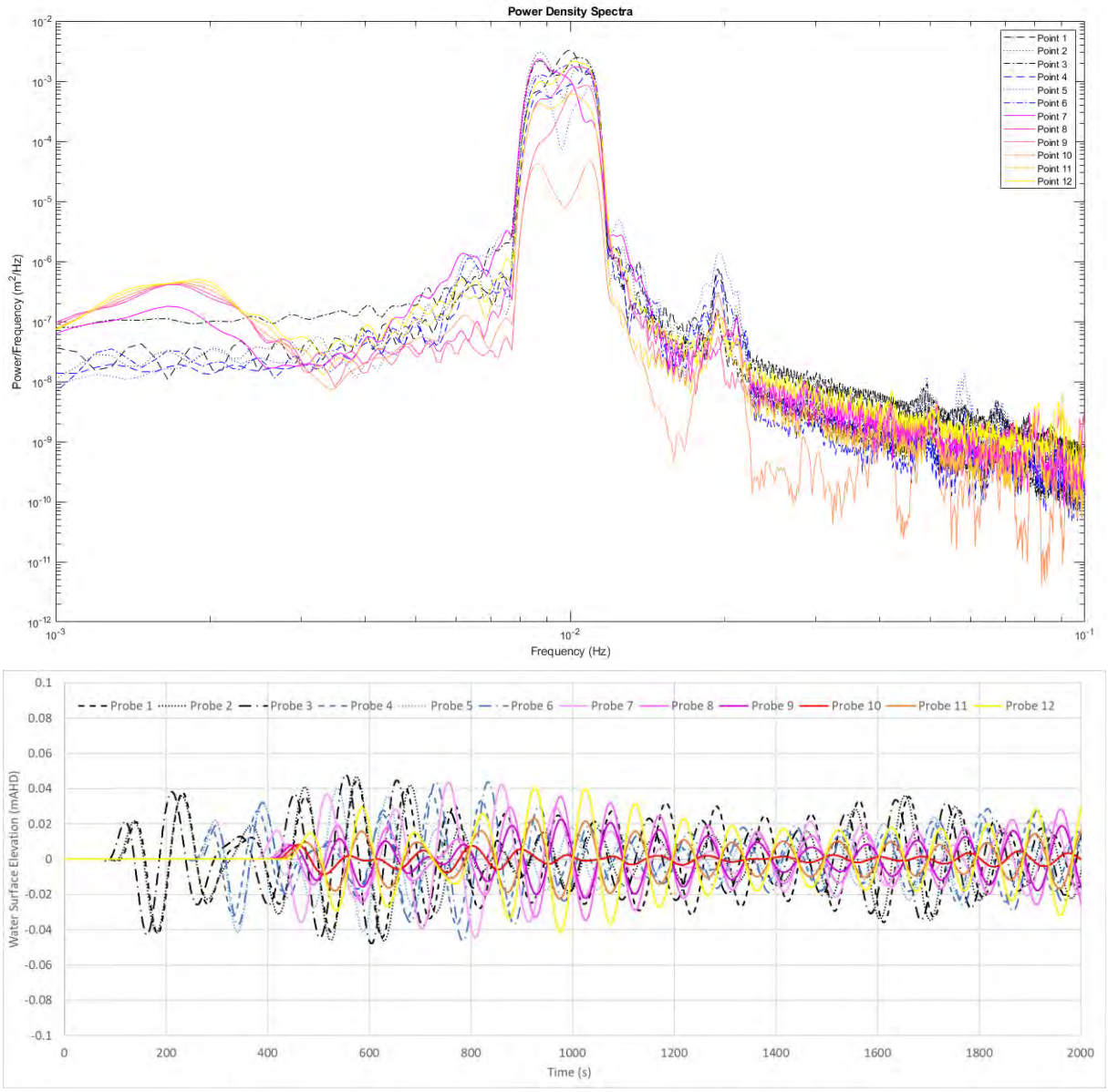

Figure 12.16 Spectral Density Plot (top) & Time series WSE (bottom) for each Probe across Targeted Forcing 2

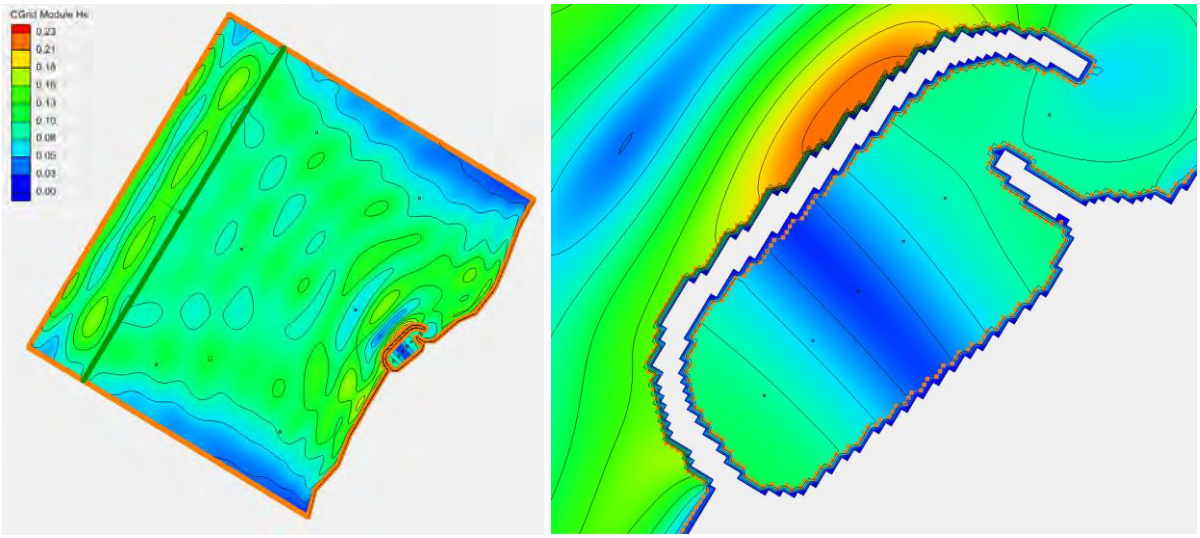

Figure 12.17 Spatial plot of Significant Wave Height across Targeted Forcing 2

Key outcomes and observations from the plots are discussed below.

- Peaks in the spectral energy density plots indicate a NOP at around 50 s.
- Review of the spectral energy density plots confirm the amplification response observed across White Noise Function 5. Peaks in the spectral energy density plot outside the input signal allows confirmation of a NOP at around 200 s and an amplification response at around 500 s.
- The power spectral density shows that the input signal does not result in an amplification of waves at this period. For frequencies corresponding to the input signal; all probes inside the facility show less spectral energy than those outside the facility.
- The response of the facility is confirmed through a review of the spatial plot of significant wave height. This shows that wave heights inside the facility do not exceed the input signal at any location.
- The response of the facility is confirmed through a review of the time varying water surface elevations at each of the probes. This shows that wave heights inside the facility do not exceed the input signal at any location.

12.3.8 Targeted Forcing 3

Targeted Forcing 3 represents an input signal with a peak period of 200 s with the spectrum limited to periods from 180 to 220 s and a significant wave height of approximately 0.05 m. This allows further interrogation of the NOP identified in the results of White Noise Functions 4 and 5.

Result visualisations from the simulation of the Targeted Forcing are shown in Figures 12.18 and 12.19. These show a spectral density comparison across probes; time varying water surface elevation comparison across each probe over the simulation; and a spatial plot of the significant wave height calculated over the entire simulation. Black and blue dotted and segmented lines represent results from probes outside the facility, whilst the solid autumn-coloured lines represent results from probes inside the facility.

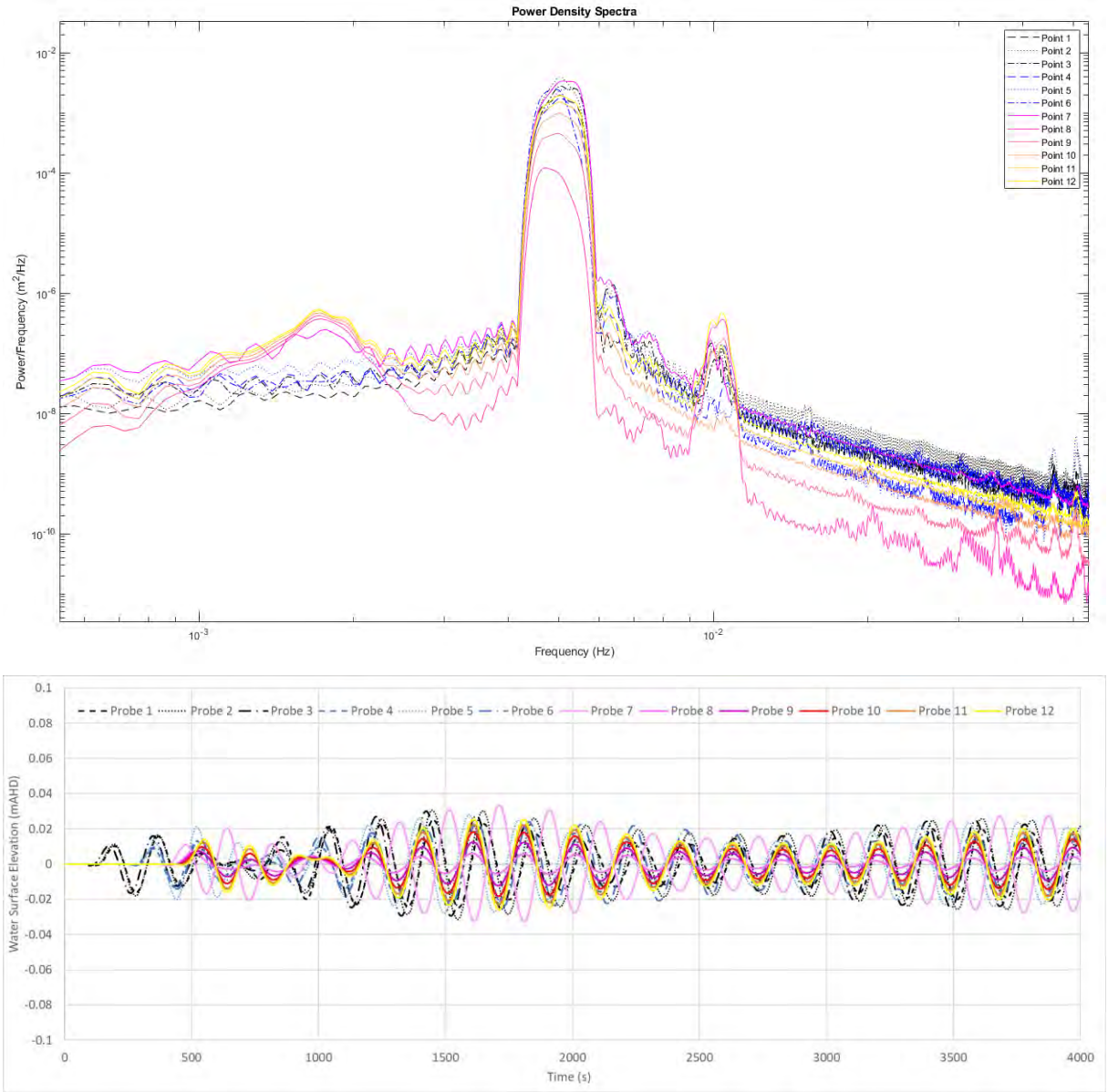

Figure 12.18 Spectral Density Plot (top) & Time series WSE (bottom) for each Probe across Targeted Forcing 3

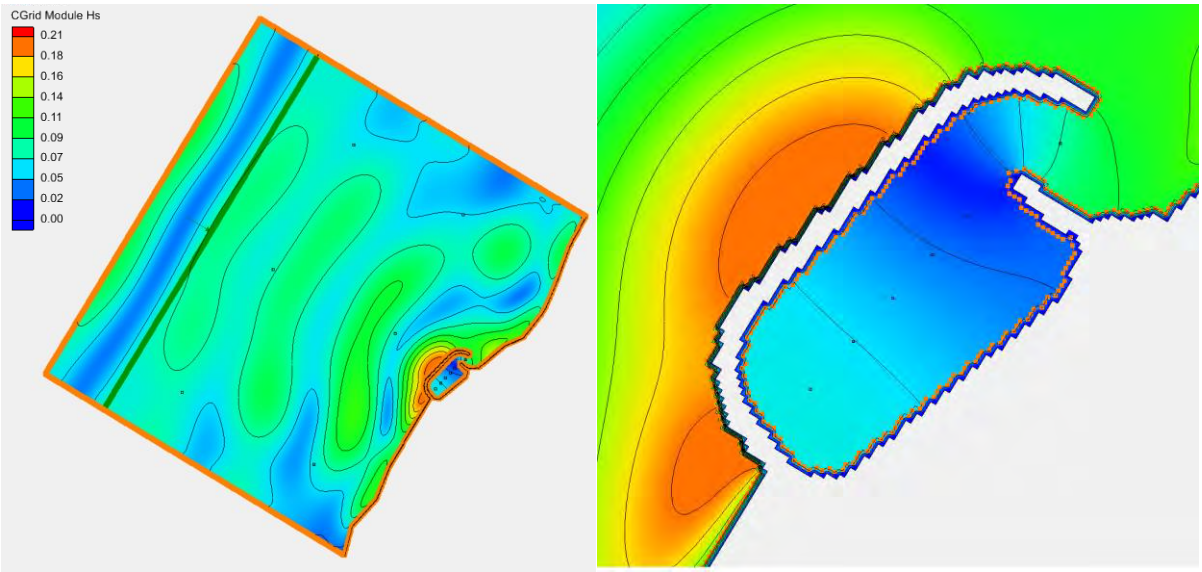

Figure 12.19 Spatial plot of Significant Wave Height across Targeted Forcing 3

Key outcomes and observations from the plots are discussed below.

- Review of the spectral energy density plots confirm the amplification response observed across White Noise Function 5. Peaks in the spectral energy density plot outside the input signal allows confirmation of a NOP at around 200 s and an amplification response at around 500 s.
- The power spectral density shows that the input signal does not result in an amplification of waves at this period. For frequencies corresponding to the input signal; all probes inside the facility show less spectral energy than those outside the facility.
- The response of the facility is confirmed through a review of the spatial plot of significant wave height. This shows that wave heights inside the facility do not exceed the input signal at any location.
- The response of the facility is confirmed through a review of the time varying water surface elevations at each of the probes. This shows that wave heights inside the facility do not exceed the input signal at any location.

12.4 Comparable Facilities

Various marine facilities around the world and in Western Australia are known to have significant LPW oscillations.

12.4.1 Geraldton Port

The presence of long waves at Geraldton is well known and has been studied extensively, particularly with regard to resonance within Geraldton Port Inner Harbour and resultant moored vessel movements and mooring issues (Mid West Ports Authority, 2014). Long waves investigations by McComb et al (2009) and Johnson & McComb (2011) found that long waves in the region occur as a result of wave transformation and wave breaking processes caused by large swell on the reefs adjacent to Geraldton Port. As a result, long waves are not always present. Johnson & McComb, (2011) completed numerical modelling of known long wave events. An output from their modelling is provided in Figure 12.20.

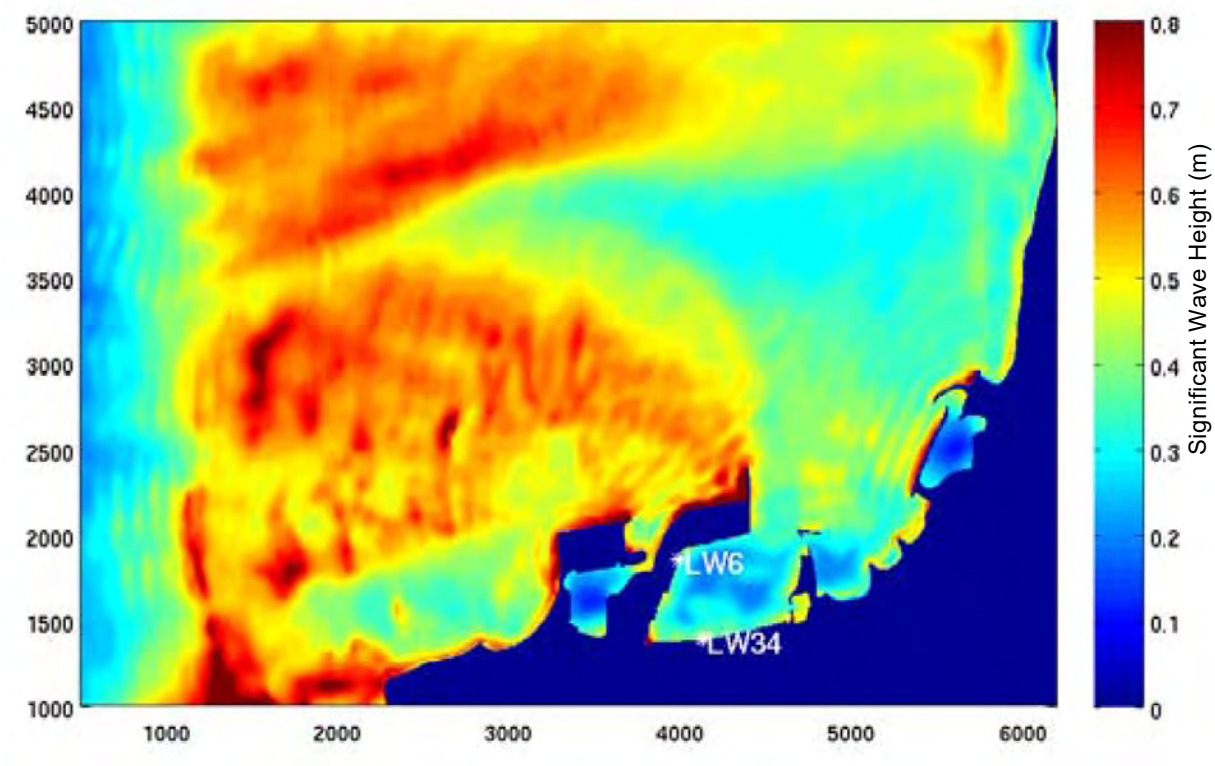

Figure 12.20 Modelled Long Wave Heights in Geraldton Port (Johnson & McComb, 2011)

The presence of long wave energy inside the port, in and of itself, is not evidence of marina seiching or resonance. If long waves are naturally occurring in the ocean close to a marina, then it is unavoidable that some of these long waves will penetrate the marina contributing to oscillations inside. However, these oscillations can still lead to significant horizontal currents and changes in water level.

Within the Batavia Coast Marina the modelling results show that there is node in the centre of the basin, with antinodes at the southern and northern extremities. The wave heights within the marina are smaller than those observed outside of the structure within this example, so this is also not reflective of true resonance, however the amplitude of the LPW within the marina is in the order of 0.4 m.

12.4.2 Two Rocks Marina

Two Rocks marina occasionally experiences significant water level oscillations during storm events. A study undertaken by Thotagamuwage (2014) identified dominant seiche oscillations in the marina, and the marina response to different incident offshore wave conditions. Collection and analysis of field data collected within the Marina identified four infragravity oscillations ranging from 60 to 300 s. Thotagamuwage (2014) concluded that these were generated through excitation of the natural oscillation periods of the marina. The frequency spectrum of the forcing infragravity waves outside the marina consisted of near-constant energy level (no main frequency peaks), and were capable of exciting the NOPs of the marina.

Modelling of a range of input conditions including stormy and calm wave events was undertaken by Thotagamuwage (2014) to interrogate the response of the marina. Time series of water levels predicted by the model for locations inside the marina contained spectral peaks corresponding to

the marina's natural frequencies. Figure 12.21 shows a snapshot of band-filtered water surface elevations corresponding to different infragravity wave bands within the marina.

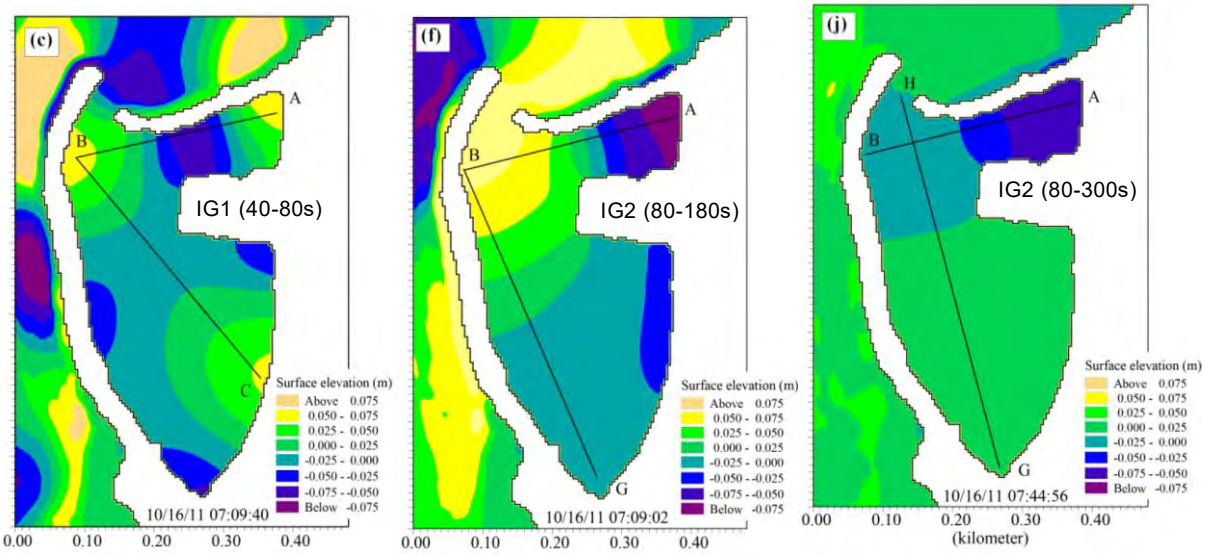

Figure 12.21 Modelled Long Waves in Two Rocks Marina (Thotagamuwage 2014)

Thotagamuwage (2014) found oscillations were continuously present in the marina independent of the offshore conditions. The spectral energy of the oscillations was increased during storm events by a factor ~50 times to that during calm sea conditions. Excessive seiche wave heights in the marina during storm events caused undesirable conditions within the marina.

12.5 Discussion & Recommendations – Concept B

LPW energy can impact various elements of marine facilities during design and operation. Significant LPW energy can result in undesirable water level fluctuations and horizontal currents within a basin. If the harbour oscillation periods coincide with natural period of moored vessels, then damage to pens, mooring lines and fenders can occur. Significant horizontal currents can contribute to increased maintenance requirements by increasing loads on marine infrastructure. Large water level fluctuations can impact navigable depths, boat launching and infrastructure freeboard.

LPW modelling results discussed in Section 12.3 demonstrate the characteristics of oscillations likely to be experienced in the facility during operation. Peaks in the spectral energy density plots indicate key NOPs at approximately 50, 100 and 200 s. White Noise and targeted testing of forcing conditions around these periods did not indicate an amplification response to these conditions. However, the energy associated with these periods is not dampened compared to that of other periods. This means that oscillations of these periods are likely to be experienced within the marina under a range of forcing conditions. These are likely to induce significant horizontal currents and water level fluctuations which should be considered in the design.

LPW modelling also showed an amplification response to wave energy in the 400 to 600 s energy band. It is possible that this response was resonance in the grid rather than in the facility itself. Although the fact that the response was not captured in the probes outside the basin, and that the feature is present across two grids with different dimensions suggests the response may not be grid resonance.

The representative wave height of background LPW energy across the 400 to 600 s band typically varies from around 0.05 m to 0.1 m, and is generally associated with periods of high swell (approaching 2 m offshore), which are more prevalent during winter. Amplification of 1.5 to 3 times would result in wave heights within the facility of around 0.15 to 0.3 m. A 0.3 m significant wave height can result in a reduction or increase in water surface elevation of around 0.15 m about the mean water level over approximately 7 to 10 minutes. A water level oscillation of this magnitude over this period is unlikely to introduce significant orbital currents or rapid water level change impacting moorings or structures. However, these oscillations can reduce the amount of navigable water available for vessels within the marina and increase the still water level during design conditions. Consideration of water level variation induced by LPW activity should be included when designing for these elements.

12.6 Concept C

To assess the potential for long wave resonance within the Concept C layout the three most significant white noise forcing conditions considered previously for Concept B were simulated for the Concept C layout.

12.6.1 Results

Interrogation of the model results was undertaken through review of a number of plots and visualisations. The key plots prepared for each simulation are as follows.

- Spectral Density comparison across probes.
- Time varying water surface elevation comparison across each probe over the simulation.
- Spatial plots of the significant wave height calculated over the entire simulation.

There are 12 probes used to track the water surface elevation across the simulations. The water surface elevation can then be utilised to calculate the power spectral density. The locations of the probes were identical for each of the simulations and are shown in Figure 12.22 and Table 12.4.

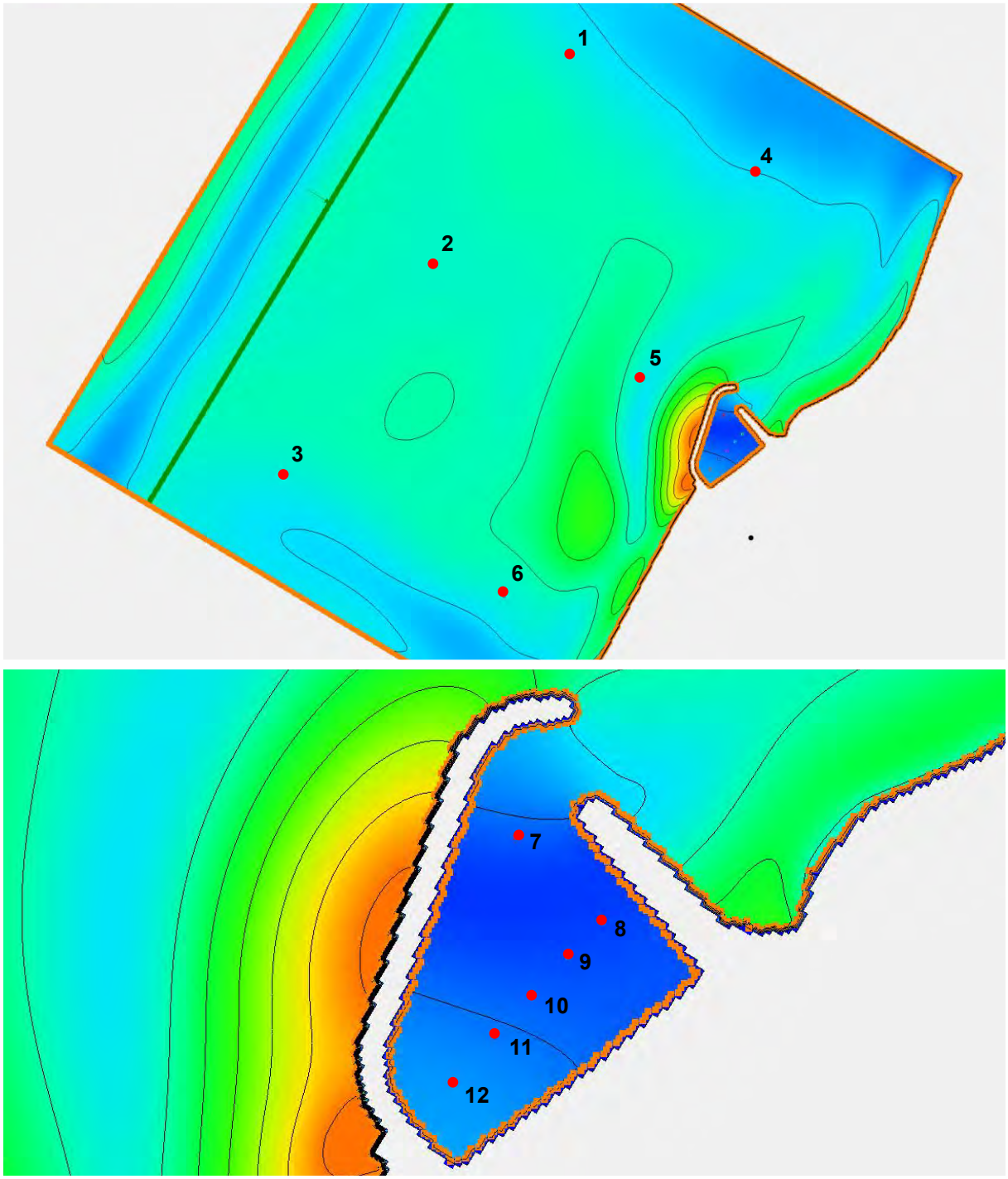

Figure 12.22 Probe Locations Concept C

Table 12.4 Probe Locations Concept C

Probe	Easting (m)	Northing (m)
1	806,484	7,575,329
2	805,905	7,574,430
3	805,245	7,573,543
4	807,278	7,574,825
5	806,787	7,573,966
6	806,199	7,573,024
7	807,134	7,573,796
8	807,215	7,573,718
9	807,183	7,573,684
10	807.149	7,573,647
11	807,114	7,573,609
12	807,077	7,573,567

White Noise function 1

White Noise Function 1 represents an input signal having equal intensity from periods 60 to 200 s with a significant wave height of approximately 0.1 m. This allows testing of an input signal which covers the largest background LPW band observed in the data record at the site

Result visualisations from the simulation of White Noise Function 1 are shown in Figures 12.23 and 12.24. These show a spectral density comparison across probes; time varying water surface elevation comparison across each probe over the simulation; and a spatial plot of the significant wave height calculated over the entire simulation. Black and blue dotted and segmented lines represent results from probes outside the facility, whilst the solid autumn coloured lines represent results from probes inside the facility.

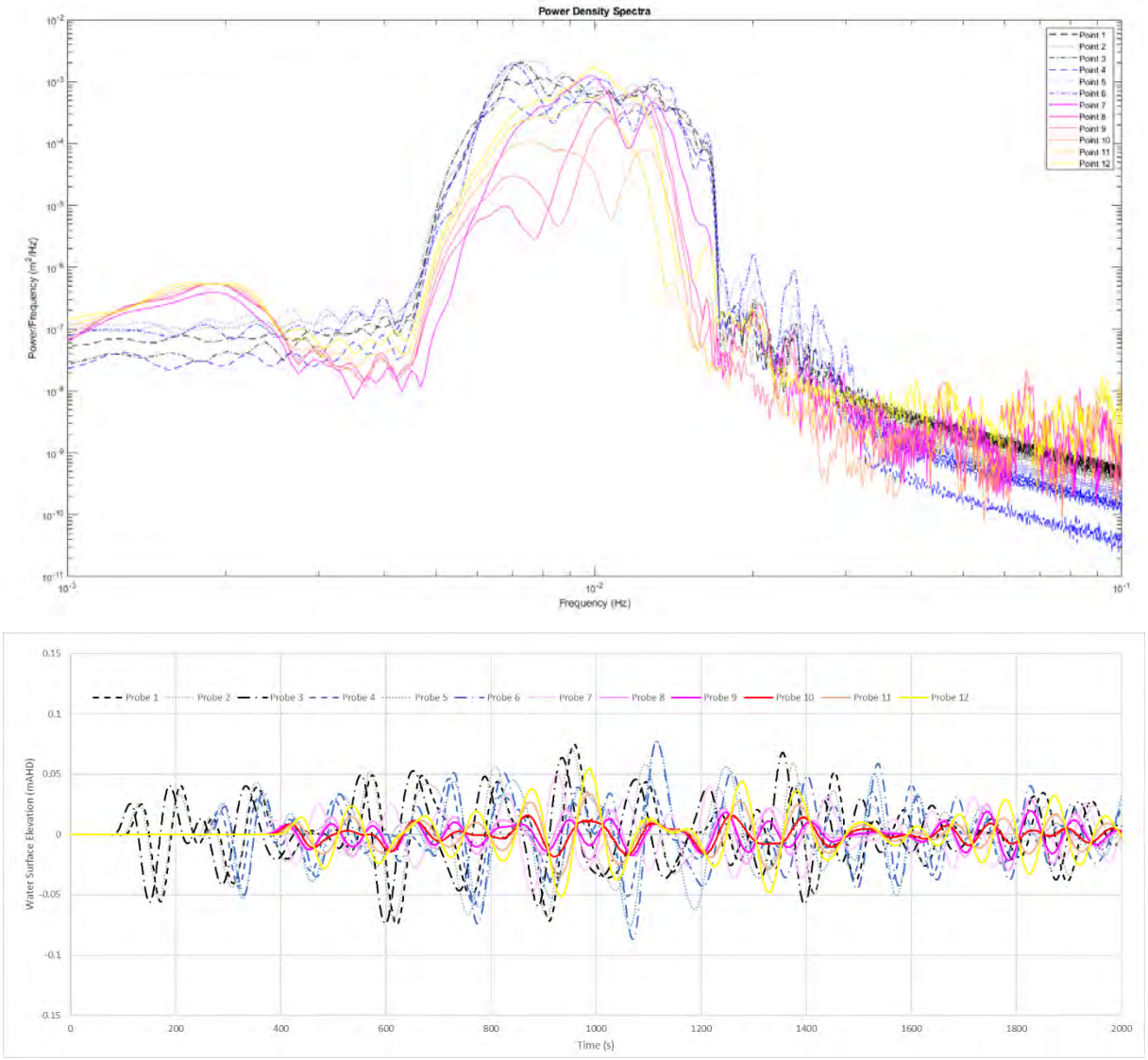

Figure 12.23 Spectral Density Plot (top) & Time Series WSE (bottom) for each Probe across White Noise Function 1

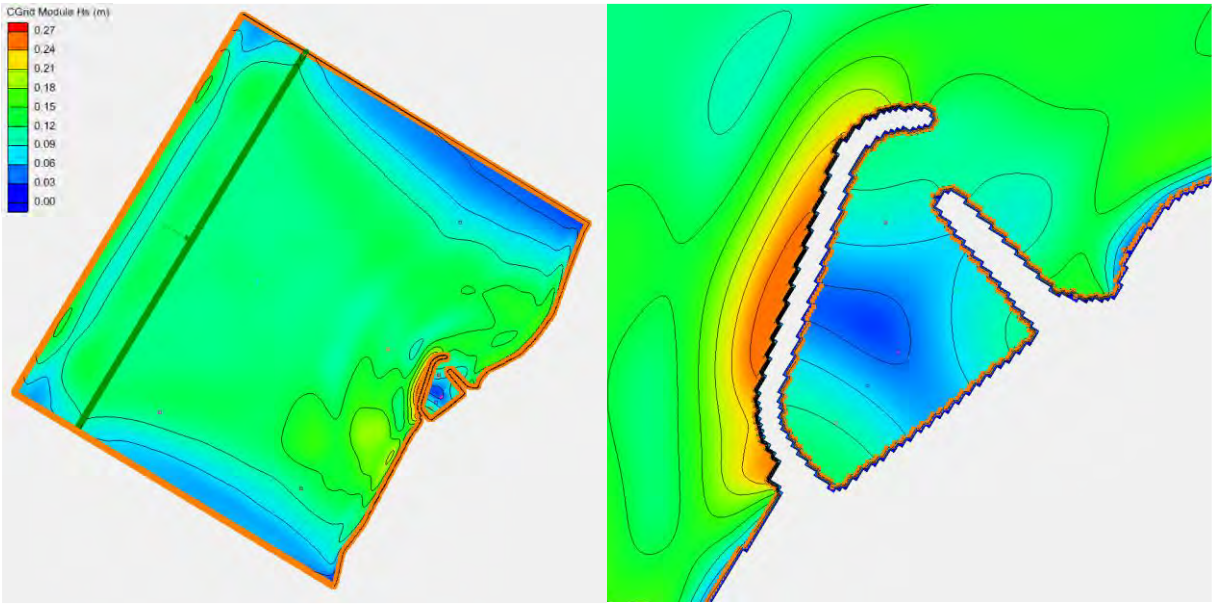

Figure 12.24 Spatial Plot of Significant Wave Height Across White Noise Function 1 Concept C

Key outcomes and observations from the plots are discussed below.

- Peaks in the spectral energy density plots allow confirmation of a NOP around 100 s. As shown in Figure 12.23, this results in antinodes at the entrance of the facility and south-western and eastern ends and a node in the middle.
- The power spectral density shows that the input signal does not result in an amplification of waves at this period. For frequencies corresponding to the input signal; all probes inside the facility show less spectral energy than those outside the facility.
- The response of the facility is confirmed through a review of the spatial plot of significant wave height. This shows that wave heights inside the facility do not exceed the input signal at any location.
- The response of the facility is confirmed through a review of the time varying water surface elevations at each of the probes. This shows that wave heights inside the facility do not exceed the input signal at any location.
- Similar to the modelling for the Concept B marina layout there is a response identified in the spectral energy plots of frequencies from 0.001 to 0.0025 (Hz) or periods 400 to 1000 s. The mechanism of this response is not entirely clear given the oscillation period is larger than the free oscillation period. It is possible that this is resonance in the grid rather than in the facility itself. Hence further interrogation has been undertaken with white noise forcings.
- The long wave modelling results for White Noise Function 1 are very similar for both the Concept B and Concept C marina layouts.

White Noise function 2

White Noise Function 2 represents an input signal having equal intensity from periods 100 to 300 s with a significant wave height of approximately 0.05 m. This allows testing of an input signal which covers the largest background LPW band observed in the data record at the site.

Result visualisations from the simulation of White Noise Function 2 are shown in Figures 12.25 and 12.26. These show a spectral density comparison across probes; time varying water surface elevation comparison across each probe over the simulation; and a spatial plot of the significant wave height calculated over the entire simulation. Black and blue dotted and segmented lines represent results from probes outside the facility, whilst the solid autumn coloured lines represent results from probes inside the facility.

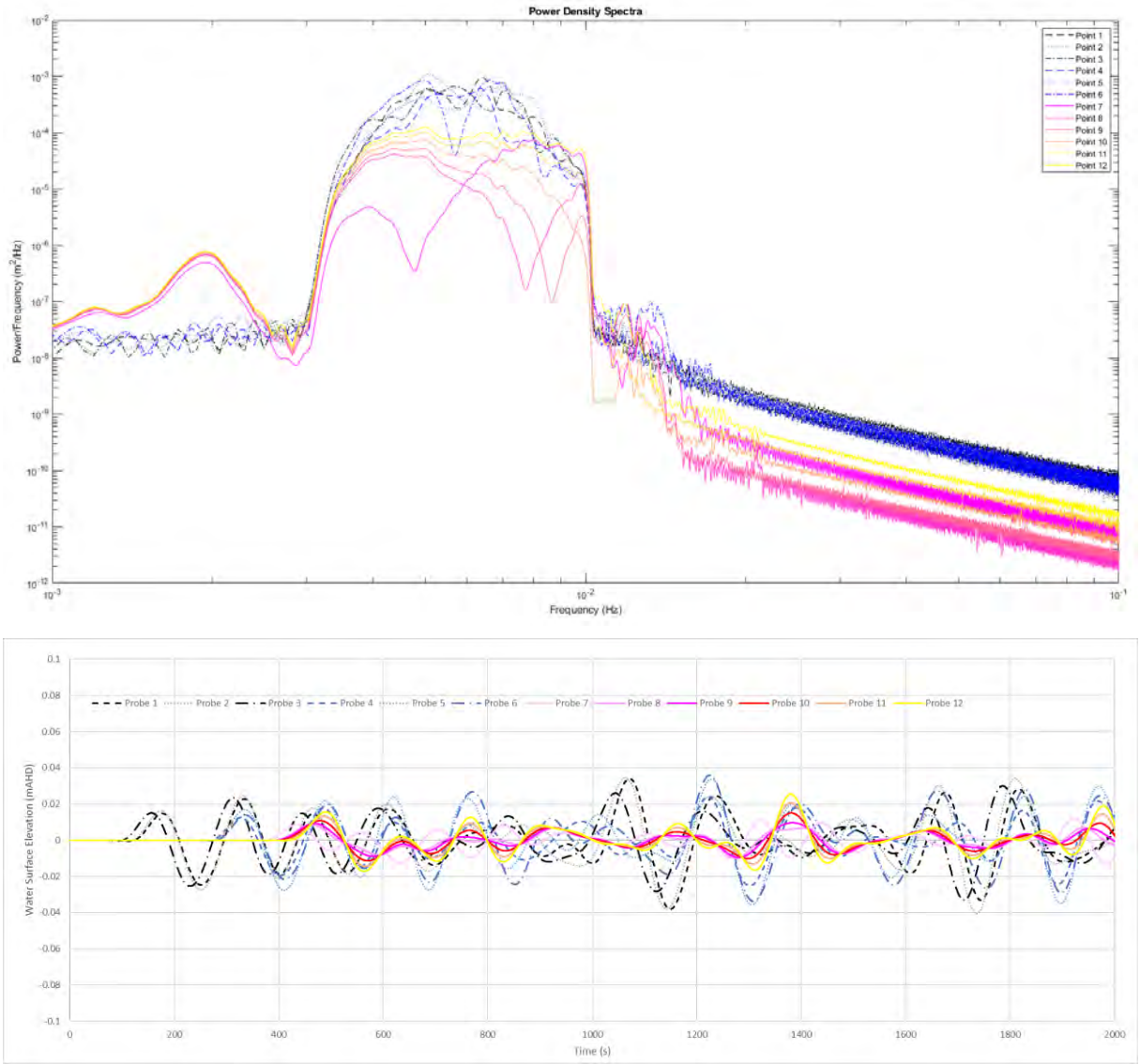

Figure 12.25 Spectral Density Plot (top) & Time Series WSE (bottom) for each Probe across White Noise Function 2

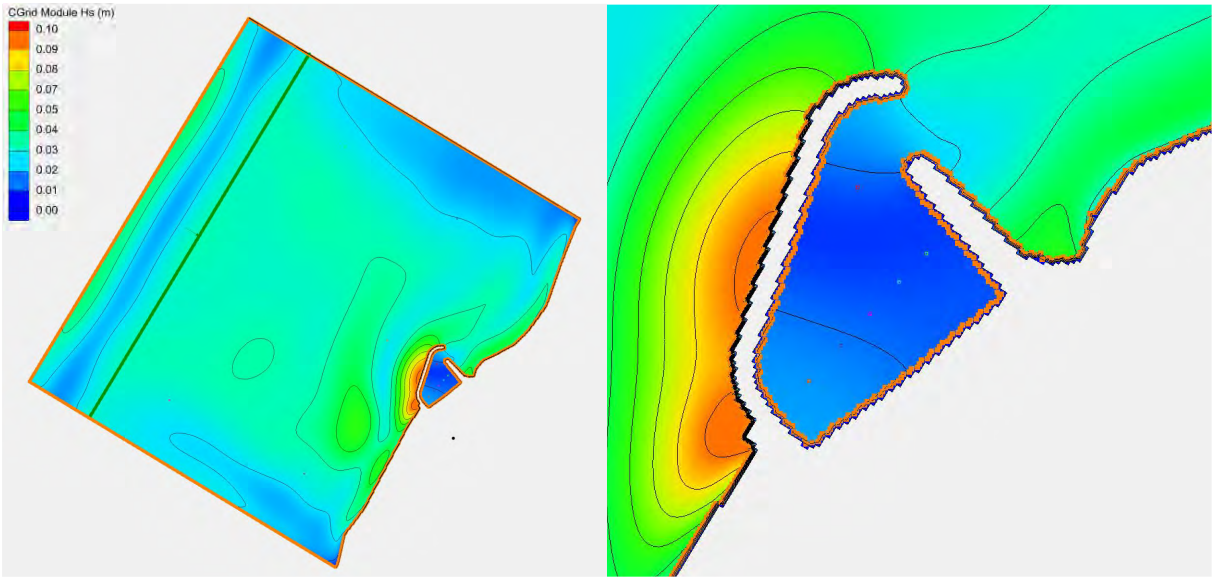

Figure 12.26 Spatial Plot of Significant Wave Height Across White Noise Function 2 Concept C

Key outcomes and observations from the plots are discussed below.

- The power spectral density shows that the input signal does not result in an amplification of waves at this period. For frequencies corresponding to the input signal; all probes inside the facility show less spectral energy than those outside the facility.
- The response of the facility is confirmed through a review of the spatial plot of significant wave height. This shows that wave heights inside the facility do not exceed the input signal at any location.
- The response of the facility is confirmed through a review of the time varying water surface elevations at each of the probes. This shows that wave heights inside the facility do not exceed the input signal at any location.
- A similar response to previous modelling results was observed for 0.001 to 0.0025 (Hz) or periods 400 to 1000 s peaking at around 500 s.
- The long wave modelling results for White Noise Function 2 are very similar for both the Concept B and Concept C marina layouts. However, there appears to be a smaller oscillation in water levels within the marina for the Concept C layout.

White Noise function 3

White Noise Function 3 represents an input signal having equal intensity from periods 30 to 100 s with a significant wave height of approximately 0.1 m. This allows testing of an input signal which covers the largest background LPW band observed in the data record at the site

Result visualisations from the simulation of White Noise Function 1 are shown in Figures 12.27 and 12.28. These show a spectral density comparison across probes; time varying water surface elevation comparison across each probe over the simulation; and a spatial plot of the significant wave height calculated over the entire simulation. Black and blue dotted and segmented lines represent results from probes outside the facility, whilst the solid autumn coloured lines represent results from probes inside the facility.

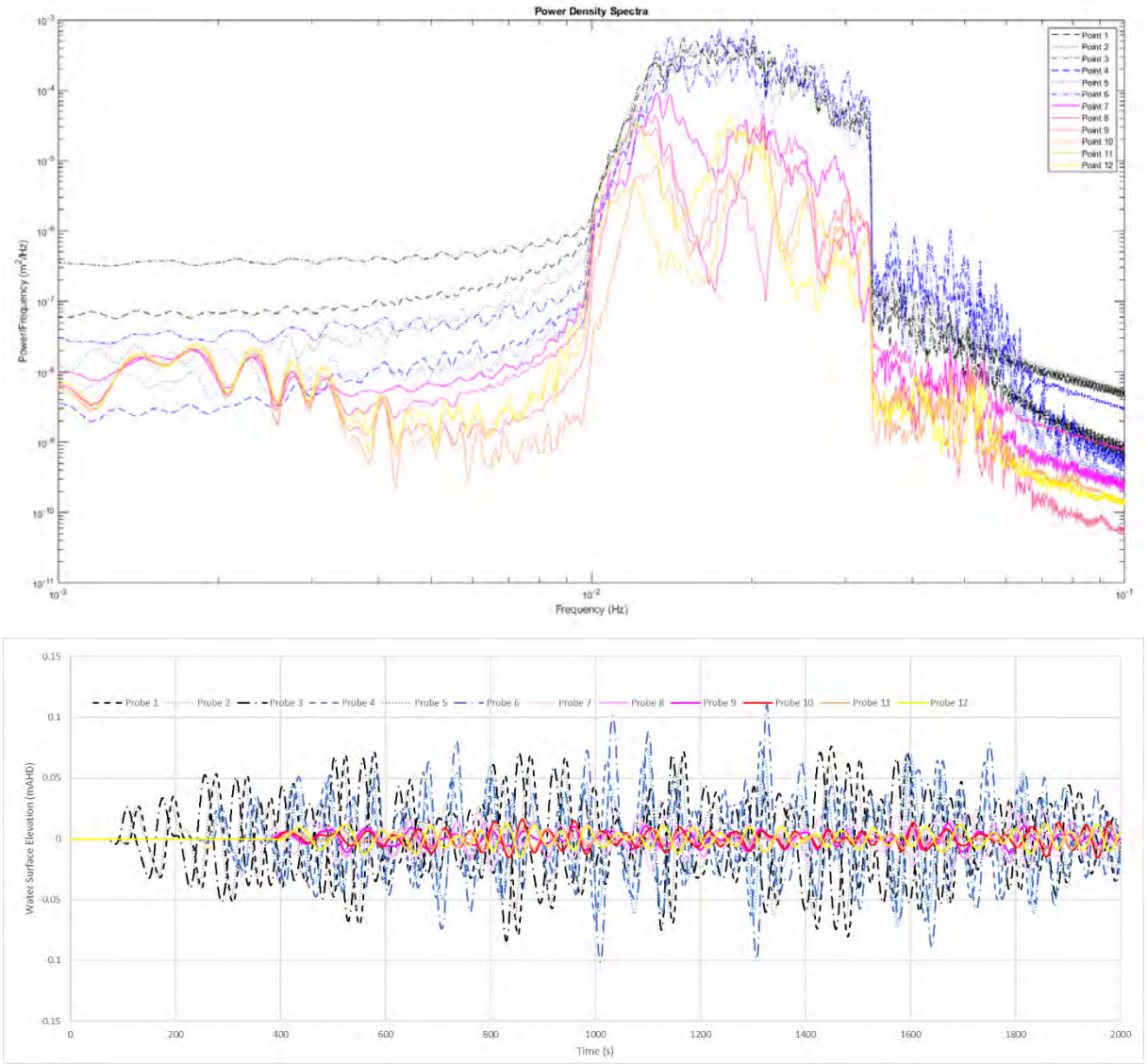

Figure 12.27 Spectral Density Plot (top) & Time Series WSE (bottom) for each Probe across White Noise Function 3

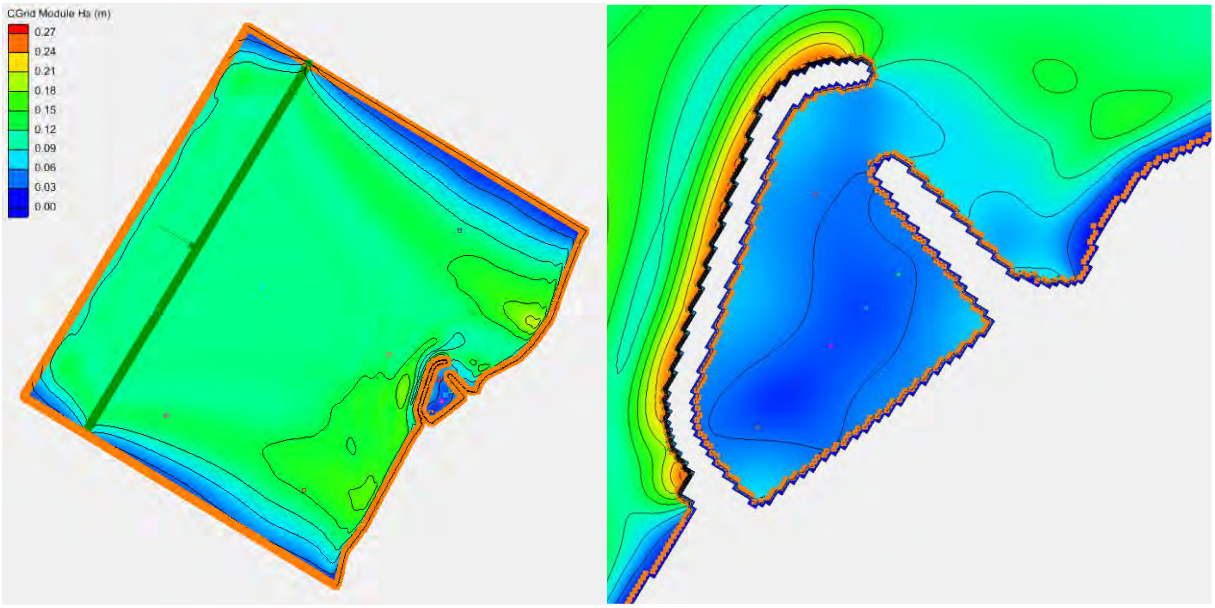

Figure 12.28 Spatial Plot of Significant Wave Height Across White Noise Function 3 Concept C

Key outcomes and observations from the plots are discussed below.

- The power spectral density shows that the input signal does not result in an amplification of waves at this period. For frequencies corresponding to the input signal; all probes inside the facility show less spectral energy than those outside the facility.
- The response of the facility is confirmed through a review of the spatial plot of significant wave height. This shows that wave heights inside the facility do not exceed the input signal at any location.
- The response of the facility is confirmed through a review of the time varying water surface elevations at each of the probes. This shows that wave heights inside the facility do not exceed the input signal at any location.
- A very small response is identified in the spectral energy plots of frequencies from 0.001 to 0.0025 (Hz) or periods 400 to 1000 s peaking at around 500 s.
- The long wave modelling results for White Noise Function 3 are very similar for both the Concept B and Concept C marina layouts.

Comparison with Concept B

Overall the modelling results for Concept C show a slightly improved outcome compared to Concept B. The potential response shown in the simulation of White Noise Function 1 is similar in magnitude, though configured slightly differently, than for Concept B. The overall magnitude of the expected oscillation is not large when compared to other existing facilities. As a result, it is expected that the key consideration of LPW impact would be through reduced under keel clearances or navigable depths. This should be considered in the design.

13. Conclusion

To address capacity limitations and maintenance issues associated with the existing Tantabiddi ramp, DoT in collaboration with the Shire, DBCA, DPIRD, and Tourism WA have resolved to identify the planning, investigations and approvals necessary to develop a new facility at Tantabiddi.

In order to investigate the coastal processes at the proposed site of the new facility coastal engineers MRA were engaged by the DoT to undertake the Tantabiddi Creek Coastal Processes Study. The objective of this study was to perform a comprehensive investigation into the coastal processes, design conditions, potential impacts and risks, mitigation options, and management measures at the proposed TBF. This included the following.

- Assessment of coastal processes near the proposed TBF.
- Develop an understanding of ambient and extreme Metocean conditions.
- Assess wave, hydrodynamic (coastal currents), and sediment transport impacts.
- Assess expected sedimentation.
- Assess performance in terms of harbour water quality and flushing rate.
- Investigate wave penetration into the harbour and navigability of the entrance channel.
- Develop an understanding of the Long Period Wave (LPW) climate and potential for LPW induced harbour resonance.
- Provide expert advice that will support future detailed design.

The information gained from this study is intended to be used for future planning, consultation, investigations and design work. Additionally, it is appropriate information and background for other project stakeholders including but not limited to the Shire, DBCA, DPIRD and Tourism WA. The outcomes of this study were summarised hereto, with further detail provided in the attached Appendices.

14. References

Cuttler et al. 2015. *Grainsize, Composition, and Bedform Patterns in a Fringing Reef System.* World Scientific 2015.

Department of Mines & Petroleum (1978). *Onslow, SF49-5, First Edition*. Geological Survey of Western Australia.

Durrant, Thomas; Hemer, Mark; Trenham, Claire; Greenslade, Diana, 2013. *CAWCR wave hindcast extension Jan 2011 - May 2013*. v5. CSIRO. Service Collection. https://doi.org/10.4225/08/52817E2858340

Etemad-Shahidi, A. and Mahjoobi, J., 2009. Comparison between M5′ model tree and neural networks for prediction of significant wave height in Lake Superior. *Ocean Engineering*, *36*(15-16), pp.1175-1181.

Goda, Y., 2010. *Random seas and design of maritime structures*. World scientific.

Johnson, D. L., and McComb, P. J. (2011). Modelling long wave generation and propagation around and within ports, Proceedings of the 20th Australasian Coastal and Ocean Engineering Conference (28-30 Sep 2011, Perth).

McComb, P., Johnson, D., & Beamsley, B. (2009). Numerical model study to reduce swell and long wave penetration to Port Geraldton. *Proceedings of the Pacific Coasts and Ports Conference 2009*. Wellington, NZ: Engineers Australia.

Mid West Port Authority 2014. Technical Symposium Long Period Wave Mitigation – Geraldton Harbour May 2014 Proceedings and Papers. Geraldton: Western Australia.

MRA 2021a. *Tantabiddi Boating Facility – Shoreline Movement Analysis*. Report R1535 prepared for Department of Transport.

MRA 2021b. *Tantabiddi Boating Facility – Metocean Climate Analysis*. Report R1524 prepared for Department of Transport.

MRA 2021c. *Tantabiddi Boating Facility – Hydrodynamic Modelling.* Report R1585 prepared for Department of Transport.

Nwogu, O., & Demirbilek, Z. (2010). Infragravity Wave Motions and Runup over Shallow Fringing Reefs. *Journal of Waterway, Port, Coastal, and Ocean Engineering, 136*(6),

Rockwater, 2021. *Estimation of Groundwater Flows*. Prepared for M P Rogers & Associates Pty Ltd.

RPS 2017, Ocean Reef Marina Development Phase 2: Water Quality Modelling. Prepared for M P Rogers & Associates Pty Ltd.

Schwartz, R.A. and Imberger, J., (1988), Flushing behaviour of a coastal marina, Proceeding 21st International Coastal Engineering Conference, Spain, 1988.

Standard Australia, 2021. AS/NZS 1170.2: Structural Design Actions Part 2: Wind Actions. Published by SAI Global.

URS 2015. Tantabiddi Boat Ramp: Sand bypassing Environmental Management Plan. Prepared for the Shire of Exmouth.

URS 2016. Tantabiddi Boat Ramp: Sand Bypass Dredging & Revetment Repair – Close Out Report. Prepared for the Shire of Exmouth.